

Synthesis of reference guidance strategy based on re-entry corridor

Relatore: *Ing. Cosimo Chiarelli*
Co-relatori: *Ing. Martins Sudars*
Prof. Lorenzo Casalino

Tesi di Laurea Magistrale
in Ingegneria Aerospaziale
orientamento Aeromeccanica e Sistemi:
Veronica Borriero
Matr. *S230973*

20 Luglio 2018

Acknowledgements

Ringrazio il mio relatore, l'Ing. Cosimo Chiarelli, per avermi dato la possibilità di svolgere presso l'azienda Thales Alenia Space questo lavoro di tesi, nonché mia seconda esperienza lavorativa, che mi ha insegnato a maturare e crescere in ambito lavorativo, affrontando problematiche nuove senza mai scoraggiarmi.

Ringrazio il mio co-relatore, l'Ing. Martins Sudars, per avermi sempre supportata e aiutata durante questo lavoro, indirizzandomi sempre verso la giusta via.

Ringrazio il mio co-relatore, prof Lorenzo Casalino, per aver avuto la pazienza di leggere e correggere la tesi, aiutandomi quindi a migliorare il mio lavoro.

Ringrazio la mia famiglia, mia madre, mio padre e mio fratello, per avermi pagato gli studi e per avermi sopportato per cinque anni nei momenti di nervosismo dovuti agli esami, per avermi cucinato pranzetti prelibati che mi tiravano su di morale.

Ringrazio tutti i miei compagni dell'università per aver reso le giornate di studio al Politecnico meno ansiose, riuscendo a portare allegria e felicità in quelle aule così cupe. Li ringrazio per avermi strappato un sorriso anche nei minuti prima di un esame, facendo scomparire tutta l'ansia in un secondo. Li ringrazio per tutte le colazioni mattine davanti a un cornetto e un cappuccino, per la compagnia durante i "deliziosi" pranzi a mensa, per le corse nei corridoi durante i cambi d'ora, per aver inventato il nuovo sport del "Lancio dell'evidenziatore", per avermi dato man forte durante gli esami. Siete stati degli amici stupendi, siete stati capaci di starmi vicina anche quando ero triste o agitata, dandomi la possibilità di crescere e migliorare. Cinque anni sono volati in un secondo e solo ora mi rendo conto che, senza di voi, tutto ciò sarebbe stato assai noioso. Anche se questo è l'inizio di una nuova vita, vi voglio avere sempre con me!

Ringrazio tutte le persone conosciute in Thales, i tesisti e i tirocinanti del gruppo Cactus, per aver condiviso insieme a me gioie, dolori, ansie e risate dovute alla tesi: sono stati sei mesi brevi ma intensi. Non dimenticherò mai le passeggiate insieme a voi, le pause caffè e tutti i discorsi senza senso che abbiamo fatto.

Ringrazio tutti i miei amici di infanzia, i miei amici del liceo, i miei amici del cosplay. Grazie per aver avuto la pazienza di aspettarmi e venirmi incontro quando, a causa dello studio, non potevo uscire. Grazie per aver reso divertenti i miei weekend, dandomi la possibilità di spegnere il cervello e dimenticarmi, almeno per qualche ora, di tutte quelle formule matematiche studiate per gli esami.

Ringrazio il mio ragazzo Alessandro Romanetto, per esserci sempre stato, per aver ascoltato in silenzio e senza mai andarsene i miei sfoghi, per avermi offerto la cioccolata consolatoria, per avermi tirato su di morale quando un esame non andava bene, per avermi aiutata nello studio, per avermi asciugato le lacrime, per essere venuto a Torino le sere per vedermi, anche se solo per qualche ora, per avermi fatto ridere e divertire, portandomi via dalla quotidianità dello studio. Sei una persona dolcissima e tenerissima, non cambiare mai!

E per ultimo ringrazio anche il Politecnico, che nonostante sia un luogo infernale, mi hai insegnato che tutto è possibile, che non bisogna mai arrendersi nonostante gli ostacoli sembrano insormontabili. Perché con tanta pazienza, forza di volontà e, forse, anche un po' di pazzia, si può arrivare ovunque si voglia. Nessun sogno è irrealizzabile, basta crederci, provare, cadere e rialzarsi, fino a quando non si raggiunge la meta tanto desiderata.

Veronica Borriero

Abstract

The Atmospheric re-entry concerns the dynamic and the kinematic of a body coming from the space, descending from a planet orbit, as satellites and entry space vehicles, or from eccentric hyperbolic orbits, as meteoroids. The dynamic considered is a 3-Dof model represented with a Simulink algorithm. This model is valid up to a Mach number equal to the Triggered Mach.

The work in this thesis is integrating re-entry Guidance, Navigation and Control algorithms for re-entry in a single simulation tool, including also the vehicle dynamics, for the design and testing of entry guidance and control solutions and for the generation of the steep and shallow trajectory. For the work I used two tools: Matlab and Simulink. The procedure is validated comparing the results with IXV data. The output of the model is a trajectory that satisfies the load, heat and range constraints .

The work was developed at the company *Thales Alenia Space* in Torino in *Strada Antica di Collegno*.

Contents

1. Introduction.....	1
1.1 The re-entry problem	1
1.2 Re-entry corridor	2
1.2.1 Corridor constrains	5
1.3 Vehicles Dynamics	8
1.4 GNC in re-entry	13
2. Control Algorithm: PID model	15
2.1 PID gains: first study	17
2.2 Vertical dynamic and PID gains	21
2.3 Scheduled PID gains: linear system and LQT technique.....	31
3. Guidance Algorithm: Space Shuttle.....	51
3.1 Pre-entry phase	52
3.2 Constant Heat-rate Phase.....	52
3.3 Constant Drag Phase	53
3.4 Transition Phase	54
3.5 Range prediction Algorithm for the Space Shuttle.....	56
4. New guidance algorithm: custom profile	69
4.1 Reference profile	69
4.2 Maximum and Minimum Range	76
4.3 EIP initial conditions	82
4.4 Range formulation Validation	86
4.5 Range correction	89
5. Results from the simulations.....	115
6. Conclusions.....	159

List of Figures

Figure 1: Effects of lift: skip-entry for Deltaglider, Lifting entry for Space Shuttle and Ballistic entry for Apollo.....	2
Figure 2: Re-entry corridor.....	2
Figure 3: Re-entry corridor in Altitude-Velocity domain.....	3
Figure 4: Re-entry corridor in Drag acceleration-Velocity domain.....	4
Figure 5: Angle of Attack and Mach number profile for the IXV vehicle.....	4
Figure 6: Ceiling constrain.....	5
Figure 7: Heat flux peak constrain.....	6
Figure 8 : Max Dynamics Pressure Constrains.....	7
Figure 9: Maximum g-load constrain.....	8
Figure 10: Summary of reference frame links (simplified).....	10
Figure 11: Environmental model US76.....	11
Figure 12: Conceptual flow chart for the Simulink Model.....	12
Figure 13: Behind view of the vehicle: on the left, the case of zero bank angle; on the right the case of non-zero bank angle.....	13
Figure 14: Navigation, Guidance and Control flow chart.....	14
Figure 15: PID model.....	16
Figure 16: IXV re-entry trajectory [RD].....	17
Figure 17: Re-entry trajectory for different KP , $KI=0.6$, $KD=550$	18
Figure 18: Re-entry trajectory for different KD , $KP=40$, $KI=0.6$	19
Figure 19: Re-entry trajectory for different KI , $KP=40$, $KD=550$	20
Figure 20: Vertical dynamics and forces.....	21
Figure 21: Vertical dynamics and velocity composition.....	22
Figure 22: Altitude control flow chart.....	23
Figure 23: Vehicle dynamics flow chart.....	23
Figure 24: Vertical dynamics for a re-entry vehicle.....	24
Figure 25: Vertical dynamic to reach the ceiling.....	25
Figure 26: Vertical dynamics with PID controller with all gains set to 1.....	26
Figure 27: Vertical dynamic with optimized PID gains for each iterations.....	27
Figure 28: Time response for the vertical dynamic with the reduced PID gains: $KP = 0.4139$, $KD = 10.3638$, $KI = 0,7988$	28
Figure 29: Time response with the PID gains obtained during the second optimization.....	29
Figure 30: Time response with the PID gains obtained during the third optimization.....	30
Figure 31: Vehicle closed loop structure.....	38
Figure 32: Flow chart for <i>Moerder-Calise (1985)</i> algorithm.....	41
Figure 33: Medium reference profile (curve red) and vehicle acceleration drag (curve blue) with PID gains of Table 15. The red points are the chosen points for the LQT technique.....	42
Figure 34: Dynamic pressure for a vehicle that follow the medium profile with a PID controller (PID gain of Table 15). The blue points are the chosen points for the LQT technique.....	43
Figure 35: Time response of a linearized system for two different initial conditions: the green curve has an initial dynamic pressure of 3513 Pa and the red curve has an initial dynamic pressure of 1505 Pa. The PID gains are equal to $KP = 120 * 100$ and $KD = 2400 * 1000$	44

Figure 36: Lower reference profile (curve red) and vehicle acceleration drag (curve blue) with PID gains of Table 15.	45
Figure 37: Dynamic pressure for a vehicle that follow the lower profile with a PID controller (PID gain of Table 15).	45
Figure 38: Sensitivity analysis for the lower trajectory.	46
Figure 39: Time response with different PID gains and an initial dynamic pressure equal to 4000 Pa.	47
Figure 40: Upper reference profile (curve red) and vehicle acceleration drag (curve blue) with PID gains of Table 15.	48
Figure 41: Dynamic pressure for a vehicle that follow the upper reference profile with a PID controller (PID gain of Table 15).	48
Figure 42: Sensitivity analysis for the upper trajectory.	49
Figure 43: Optimal PID gains.	50
Figure 44: Entry guidance Space Shuttle Drag-Velocity profile.	51
Figure 45: Constant Heat-rate phase and Constant Drag phase.	54
Figure 46: Reference profile and mathematical expressions for each phase.	56
Figure 47: Vehicle dynamics, PID controller and range prediction flow chart.	57
Figure 48: Constant Heat Rate phase with limit curves.	59
Figure 49 : Constant Drag phase with limit curves.	60
Figure 50: : Transition phase with limit curves.	61
Figure 51: Constant Heat Rate Range Correction Flow Chart.	64
Figure 52: Vehicle dynamic with two different velocity for following the Constant drag: the red curve starts the constant Drag Phase at a velocity equal to V_3 and the yellow curve starts the constant Drag Phase at a velocity equal to $V_3 + 300$	65
Figure 53: Constant Drag Range Correction Flow Chart.	66
Figure 54: Transition Range Correction Flow Chart.	67
Figure 55: Reference profile, profile after Range Correction and vehicle trajectory.	68
Figure 56: Reference Profile equidistant from the limits (red curve).	71
Figure 57: Reference Profile equidistant from the limits (red curve) and Reference Profile distant from the ceiling (blue curve).	72
Figure 58: Reference Profile equidistant from the limits (red curve) and Reference Profile distant from the g-load or the dynamic pressure limit (blue curve).	73
Figure 59: Reference Profile equidistant from the limits (red curve) and Reference Profile distant from the Heat Flux Peak limit (blue curve).	74
Figure 60: Example of lower and upper limitation for a reference profile.	76
Figure 61: Lower Reference profile and Drag Acceleration profile from the simulation with a PID controller and a pre-entry bank angle equal to 18°	77
Figure 62: Chosen of the Pre-entry Bank Angle and lower reference profile for the simulation with maximum range.	78
Figure 63: Identification of the Lower Reference Profile that gives the Maximum Range (blue curve) with an Initial Bank Angle of 18°	79
Figure 64: Identification of the first Upper Reference Profile that gives the Minimum Range (purple curve) with an Initial Bank Angle of 70° and the Profile obtained after the simulation (green curve).	80
Figure 65: Identification of the final Upper Reference Profile that gives the Minimum Range (purple curve) with an Initial Bank Angle of 70° and the Profile obtained after the simulation (green curve).	81
Figure 66: Eligible initial points (EIP location) to respect the Upper and Lower range limitations.	82
Figure 67: Bearing and Heading for the vehicle: in this picture the two angles have a positive value.	83

Figure 68: Velocity in axis ECI respect to the Altitude for the two situations.....	85
Figure 69: Velocity in wind axis respect to the Altitude for the two situations.	85
Figure 70: Velocity in wind axis respect to the Drag Acceleration for the two situations.	86
Figure 71: Reference profile with Spline and Straight Lines.	87
Figure 72: Reference Profile and Simulated profile for the range formulation validation.	88
Figure 73: Example of the reference curve translation.....	90
Figure 74: Example of upper and lower known coefficients for a reference profile represented with Spline.	93
Figure 75: Vehicle GNC flow Chart.	94
Figure 76: Reference Profile nodes and phases.	95
Figure 77: Straight Line Drag Acceleration Phase translation for the range correction. The behavior is only qualitative.....	96
Figure 78: <i>“Heat Rate Peak Phase Spline with the average values”</i> approach when the <i>H1, H2</i> and <i>H3</i> phases are all presented. The behavior is only qualitative.	98
Figure 79: Heat Flux Peak range correction flow chart.	99
Figure 80: Reference curve at the end of Heat Flux Peak Range correction. The behavior is only qualitative.	100
Figure 81: Phases and nodes of the reference profile when the Heat Flux Peak range correction ends.	101
Figure 82: S1, S2 and S3 Phase translation for the range correction. The behavior is only qualitative.....	102
Figure 83: <i>“Connection Phase straight line with the average values”</i> approach when the <i>C1, C2</i> and <i>C3</i> phases are all presented. The behavior is only qualitative.	103
Figure 84: <i>“Creation of S4-S5-S6 with a single straight line”</i> approach. The behavior is only qualitative....	104
Figure 85: Connection phase range correction flow chart.	105
Figure 86: Reference curve at the end of Connection Phase Range correction. The behavior is only qualitative.....	106
Figure 87: Straight Line Drag Acceleration Phase with the average values to build S1,S2,S3,S4,S5 and S6. The behavior is only qualitative.	107
Figure 88: Example of a new profile after the range correction.	108
Figure 89: Identification of <i>DaUL1 – VUL1</i> and <i>DaUL2 – VUL2</i>	109
Figure 90: Identification of a new Upper limitation and reference curve obtained after a range correction.	110
Figure 91: Identification of a new Upper limitation for the range correction.	110
Figure 92: Error Processing Parameters for the Straight Line Drag Acceleration Phase correction during the Heat Flux Peak Phase range correction.....	111
Figure 93: Error Processing Parameters for H1, H2, H3 Phase during the Heat Flux Peak Phase range correction.	111
Figure 94: Error Processing Parameters for S1, S2, S3 Phase correction during the Connection Phase range correction.	111
Figure 95: Error Processing Parameters for C1, C2, C3 Phase correction during the Connection Phase range correction.	111
Figure 96: Error Processing Parameters for S1, S2, S3, S4, S5, S6 Phase correction during the Straight Line Drag Acceleration Phase range correction.	112
Figure 97: Error Processing Parameters for the Transition Phase.....	112
Figure 98. Final reference profile (red curve) and contoured reference profile (blue curve)	113
Figure 99: Reference curves and simulated curves for the Heat load study.	114

Figure 100: Simulation with range correction for the case 1 and an initial position equal to $-1,7932^\circ$ as latitude and 195° as longitude.	117
Figure 101: Bank Angle for the case 1 and an initial position equal to $-1,7932^\circ$ as latitude and 195° as longitude, following the final reference profile obtained with the range correction.	118
Figure 102: Simulation with range correction for the case 2 and an initial position equal to $-1,7932^\circ$ as latitude and 195° as longitude.	119
Figure 103: Bank Angle for the case2 and an initial position equal to $-1,7932^\circ$ as latitude and 195° as longitude, following the final reference profile obtained with the range correction.	120
Figure 104: Simulation with range correction for the case 3 and an initial position equal to $-1,7932^\circ$ as latitude and 195° as longitude.	121
Figure 105: Bank Angle for the case 3and an initial position equal to $-1,7932^\circ$ as latitude and 195° as longitude, following the final reference profile obtained with the range correction.	122
Figure 106: Simulation with range correction for the case 4 and an initial position equal to $-1,7932^\circ$ as latitude and 195° as longitude.	123
Figure 107: Bank Angle for the case 4 and an initial position equal to $-1,7932^\circ$ as latitude and 195° as longitude, following the final reference profile obtained with the range correction.	124
Figure 108: Simulation with range correction for the case 5 and an initial position equal to $-1,7932^\circ$ as latitude and $194,3^\circ$ as longitude.	125
Figure 109: Bank Angle for the case 5 and an initial position equal to $-1,7932^\circ$ as latitude and $194,3^\circ$ as longitude, following the final reference profile obtained with the range correction.	126
Figure 110: Simulation with range correction for the case 1 and an initial position equal to $-3,071^\circ$ as latitude and 185° as longitude.	129
Figure 111: Bank Angle for the case 1 and an initial position equal to $-3,071^\circ$ as latitude and 185° as longitude., following the final reference profile obtained with the range correction.	130
Figure 112: Simulation with range correction for the case 2 and an initial position equal to $-3,071^\circ$ as latitude and 185° as longitude.	131
Figure 113: Bank Angle for the case 2 and an initial position equal to $-3,071^\circ$ as latitude and 185° as longitude., following the final reference profile obtained with the range correction.	132
Figure 114: Simulation with range correction for the case 3 and an initial position equal to $-3,071^\circ$ as latitude and 185° as longitude.	133
Figure 115: Bank Angle for the case 3 and an initial position equal to $-3,071^\circ$ as latitude and 185° as longitude, following the final reference profile obtained with the range correction.	134
Figure 116: Simulation with range correction for the case 4 and an initial position equal to $-3,071^\circ$ as latitude and 185° as longitude.	135
Figure 117: Bank Angle for the case 4 and an initial position equal to $-3,071^\circ$ as latitude and 185° as longitude, following the final reference profile obtained with the range correction.	136
Figure 118: Simulation with range correction for the case 5 and an initial position equal to $-3,071^\circ$ as latitude and 185° as longitude.	137
Figure 119: Bank Angle for the case 5 and an initial position equal to $-3,071^\circ$ as latitude and 185° as longitude, following the final reference profile obtained with the range correction.	138
Figure 120: Simulation with range correction for the case 1 and an initial position equal to IXV latitude and longitude.	140
Figure 121: Bank Angle for the case 1 and an initial position equal to IXV latitude and longitude, following the final reference profile obtained with the range correction.	141
Figure 122: Simulation with range correction for the case 3 and an initial position equal to IXV latitude and longitude.	142

Figure 123: Bank Angle for the case 3 and an initial position equal to IXV latitude and longitude, following the final reference profile obtained with the range correction.....	143
Figure 124: Simulation with range correction for the case 4 and an initial position equal to IXV latitude and longitude.....	144
Figure 125: Bank Angle for the case 4 and an initial position equal to IXV latitude and longitude, following the final reference profile obtained with the range correction.....	145
Figure 126: Simulation with range correction for the case 5 and an initial position equal to IXV latitude and longitude.....	146
Figure 127: Bank Angle for the case 5 and an initial position equal to IXV latitude and longitude, following the final reference profile obtained with the range correction.....	147
Figure 128: Simulation with range correction for the case 1 and an initial position equal to $-4,9786^\circ$ as latitude and 169° as longitude.	149
Figure 129: Bank Angle for the case 1 and an initial position equal to $-4,9786^\circ$ as latitude and 169° as longitude, following the final reference profile obtained with the range correction.....	150
Figure 130: Simulation with range correction for the case 2 and an initial position equal to $-4,2816^\circ$ as latitude and $175,1^\circ$ as longitude.	151
Figure 131: Bank Angle for the case 2 and an initial position equal to $-4,2816^\circ$ as latitude and $175,1^\circ$ as longitude, following the final reference profile obtained with the range correction.....	152
Figure 132: Simulation with range correction for the case 3 and an initial position equal to $-5,0764^\circ$ as latitude and $168,6^\circ$ as longitude.	153
Figure 133: Bank Angle for the case 3 and an initial position equal to $-5,0764^\circ$ as latitude and $168,6^\circ$ as longitude, following the final reference profile obtained with the range correction.....	154
Figure 134: Simulation with range correction for the case 4 and an initial position equal to $-5,0764^\circ$ as latitude and $168,6^\circ$ as longitude.	155
Figure 135: Bank Angle for the case 3 and an initial position equal to $-5,0764^\circ$ as latitude and $168,6^\circ$ as longitude, following the final reference profile obtained with the range correction.....	156
Figure 136: Simulation with range correction for the case 5 and an initial position equal to $-4,9786^\circ$ as latitude and 169° as longitude.	157
Figure 137: Bank Angle for the case 1 and an initial position equal to $-4,9786^\circ$ as latitude and 169° as longitude, following the final reference profile obtained with the range correction.....	158

List of Tables

Table 1: Initial conditions for re-entry guidance.	17
Table 2: Integrated error, maximum difference between vehicle acceleration drag and reference drag in the part 1 and in the part 2 of the reference profile and velocity at which the maximum difference occurs for different proportional gains.....	18
Table 3: Integrated error, maximum difference between vehicle acceleration drag and reference drag in the part 1 and in the part 2 of the reference profile and velocity at which the maximum difference occurs for different derivative gains.	19
Table 4: Integrated error, maximum difference between vehicle acceleration drag and reference drag in the part 1 and in the part 2 of the reference profile and velocity at which the maximum difference occurs for different integrative gains.	20
Table 6: Upper and lower limits using in the “ <i>Check Custom Bounds</i> ” optimization.....	26
Table 7: Response time for the vertical dynamics with an altitude control.....	27
Table 8: PID gains finding with first optimizations.	27
Table 9: New PID gains using for the second optimization.	28
Table 10: PID gains bounds for the second optimization.	28
Table 11: New PID gains finding with the second optimization.	29
Table 12: Upper and lower limits using in the “ <i>Check Custom Bounds</i> ” optimization for the third optimization.....	29
Table 13: PID gains obtained with the third optimizations	30
Table 14: Response time for the vertical dynamics with an altitude control.	30
Table 15: PID gains for the 3-Dof dynamic control.....	31
Table 16: Optimal PID gains for the lower trajectory.....	46
Table 17: Initial conditions for the LQT optimization.....	46
Table 18: Optimal PID gains for the upper trajectory.	49
Table 19: Optimal PID gains.....	50
Table 20: Integrated error for a vehicle that follow the medium reference profile with PID gains of Table 15 (column 1) and optimal PID gains (column 2).	50
Table 21: Drag form and Range prediction for the three phases of Space Shuttle re-entry.	58
Table 22: Chosen coefficient c_5 maximum add minimum for different velocity.....	62
Table 23: Derivative of the range for the three re-entry phase.....	63
Table 24: Terminal conditions for IXV 3-Dof dynamic simulation with range correction and PID controller.	68
Table 25: Maximum Range and Initial Bank Angle for the Lower Reference Trajectory.	79
Table 26: Minimum Range and Initial Bank Angle for the Upper Reference Trajectory.....	81
Table 27: Initial and final geographical coordinates.	84
Table 28: Initial conditions for two different situations.....	84
Table 29: Simulated Range, Analytic Range and Error for the Range Formulation Validation.	89
Table 30: Strategy for the Range correction.	91
Table 31: Time and Traveled range following the reference curves in Figure 97	114
Table 32: PID gains for the first simulation	116
Table 33: Initial coordinates for the first simulation.	116
Table 34: Final coordinates for the first simulation.	116
Table 35: Final values and errors for the case 1 in the first simulation.	118
Table 36: Final values and errors for the case 2 in the first simulation.	120

Table 37: Final values and errors for the case 3 in the first simulation.	122
Table 38: Final values and errors for the case 4 in the first simulation.	124
Table 39: Final values and errors for the case 5 in the first simulation.	126
Table 40: PID gains for the second simulation.	127
Table 41: Initial coordinates for the second simulation.	128
Table 42: Final coordinates for the second simulation.	128
Table 43: Final values and errors for the case 1 in the second simulation.	130
Table 44: Final values and errors for the case 2 in the second simulation.	132
Table 45: Final values and errors for the case 3 in the second simulation.	134
Table 46: Final values and errors for the case 4 in the second simulation.	136
Table 47: Final values and errors for the case 5 in the second simulation.	138
Table 48: Initial coordinates for the third simulation.	139
Table 49: Final coordinates for the third simulation.	139
Table 50: Final values and errors for the case 1 in the third simulation.	141
Table 51: Final values and errors for the case 3 in the third simulation.	143
Table 52: Final values and errors for the case 4 in the third simulation.	145
Table 53: Final values and errors for the case 5 in the third simulation.	147
Table 54: Initial coordinates for the fourth simulation.	148
Table 55: Final coordinates for the fourth simulation.	148
Table 56: Final values and errors for the case 1 in the fourth simulation.	150
Table 57: Final values and errors for the case 1 in the fourth simulation.	152
Table 58: Final values and errors for the case 3 in the fourth simulation.	154
Table 59: Final values and errors for the case 4 in the fourth simulation.	156
Table 60: Final values and errors for the case 5 in the fourth simulation.	158

List of Symbols

A State Matrix

a Speed of sound

$[a]_I$ Acceleration in ECI axis

B Control matrix

B_C Ballistic coefficient

BA Bank angle

C Observation matrix

c Constant term in Drag equation

C_D Drag coefficient

C_L lift coefficient

D Drag Force

D_a Drag acceleration

E Energy

e Drag acceleration error

\vec{F} Force vector

F_C Centrifugal force

f Added State Variable

$G(s)$ Low-Pass filter

g Gravitational acceleration

H Hamiltonian

H Performance output matrix

$H(s)$ PID compensator

h Altitude

\dot{h} Vertical velocity

\ddot{h} Vertical acceleration

I Identity matrix

$I_{XY} I_{YZ}$ Inertial moment

J Performance index

K Matrix PID gains
 K_D Derivative gain
 K_I Integrative gain
 K_P Proportional gain
 L Lift force
 lat Latitude
 $long$ Longitude
 L_V Lift vertical component
 M Mach number
 \vec{M}_B Angular moment
 m Mass
 N Cutoff frequency
 P Total impulse
 q Dynamic pressure
 \dot{q} Heat flux
 R Weight matrix
 R_D Desired range
 R_T Distance from the Earth center
 r Drag reference signal
 S_{ref} Reference surface
 s Range
 t Time
 u_m Maximum permissible deviations
 V Velocity
 \mathbf{V} Weight matrix
 x State vector
 y Output vector
 y_P Output proportional term
 z Performance output

α Angle of attack

γ Flight path angle

η Derivative term output

η_N Derivative term state variable

ρ Density

σ Bank angle

$\vec{\omega}$ Angular velocity

1. Introduction

1.1 The re-entry problem

The first goal of atmospheric re-entry is to land the vehicle on the ground safely, for this reason the vehicle must not burn, the trajectory must ensure descent, aerodynamic load limits must not be exceeded and the vehicle must have guidance capabilities to follow the reference trajectory. All these constraints are linked at the type of vehicle, initial conditions and if it is manned.

The re-entry starts when the vehicle reaches the EIP (Entry Interface Point) conditions and it gains sufficiently aerodynamic forces to control its trajectory. Usually the EIP Altitude is equal to 120 Km, where the atmosphere is sufficiently dense. Another parameter is the initial velocity: if it is low the lift isn't sufficiently to equilibrate the gravity force, so the vehicle accelerates, loses rapidly altitude until the aerodynamic forces become significant, in this case the vehicle overcomes the heat and load limits. For this reason the initial velocity must be controlled: in a lot of case is equal to 7500 m/s.

The second parameter is the initial flight path angle γ . If the angle is shallow, the generated drag is insufficient to slow the vehicle. In this case the vehicle isn't able to follow a path directing to the planet surface and rebounds out of the atmosphere, returning in the space. But if the angle is steep, the vehicle gains an excessive descent rate and drag force and the body is destroyed by the action of atmospheric re-entry due to excessive heat flux (the vehicle burns) or external load (the vehicle is disintegrated).

So the vehicle can reach the planet surface only if the angle with which impacts the atmosphere is within a tight range of value.

The vehicle can reach the Earth following three different scenarios: ballistic entry, lifting entry and skip entry.

The ballistic entry occurs when the lift-to-drag ratio L/D is low, typically lower than 0,5, this is the case of meteoroids, missiles or capsule, like vehicle as Apollo Command Module. The vehicle dynamic is function of the ballistic coefficient $B_C = \frac{m}{c_D S}$, the vehicle can't be controlled with lift and its re-entry trajectory is only function of the initial velocity and flight path angle, it's a straight path with significant heat flux and g-load.

In the case of lifting entry, where the $L/D \geq 0.5$, the vehicle generates lift to control the trajectory, to dissipate energy and to reach the landing site safety, for this reason the vehicle can be reused. The lift modulation happens with a bank angle control. This is the case of Space Shuttle.

The last re-entry configuration is the skip entry: it consists on impacting planet atmosphere at an angle such that the entry body rebounds out the atmosphere but it is kept in a trajectory that will enable it to enter atmosphere some time later, with reduced entry velocity. This is the case of Deltaglider.

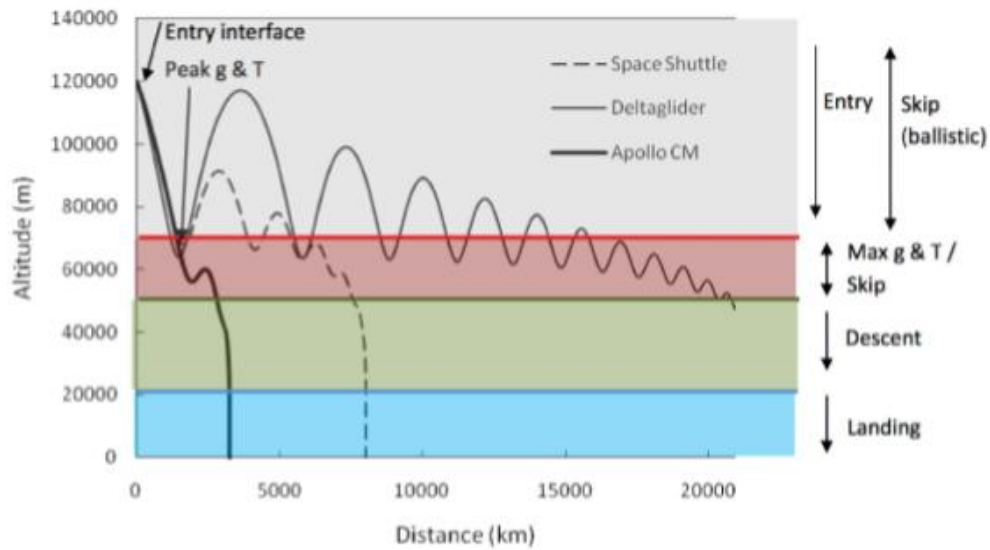


Figure 1: Effects of lift: skip-entry for Deltaglider, Lifting entry for Space Shuttle and Ballistic entry for Apollo.

1.2 Re-entry corridor

Atmospheric re-entry is one of the most difficult problems in the Aerospace field: the vehicle re-enters the Earth atmosphere with a high speed, so a big amount of kinetic energy is transferred into heat energy. But this isn't the only one problem: to reach the Earth surface the vehicle is subjected to high accelerations, therefore the maximum structural load can be exceeded.

The vehicle structure is not damaged with low drag acceleration, but in this case the vehicle doesn't produce enough aerodynamic force, it skips out of the atmosphere and it returns to space.

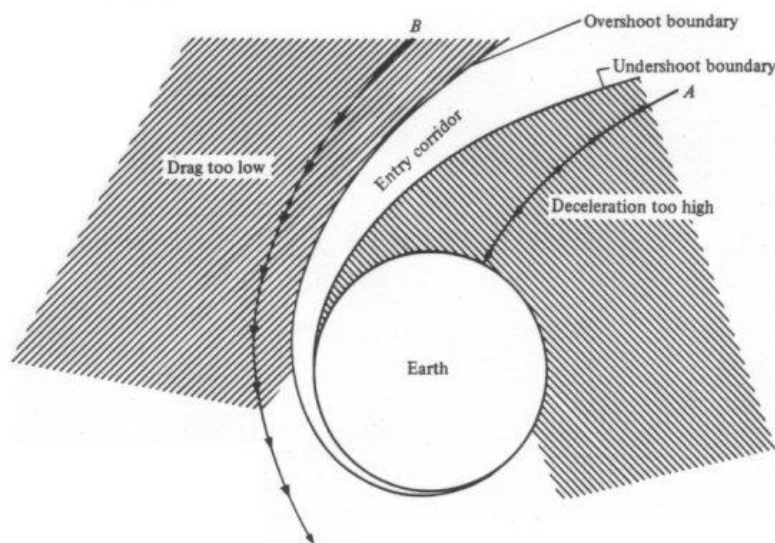


Figure 2: Re-entry corridor.

All these limits are represented in a plot named re-entry corridor, here there are all the drag acceleration-velocity combinations to keep the vehicle safe. The re-entry corridor can be also represents with other two

variables: altitude-velocity. I chose the first representation because the input control for the vehicle is a drag acceleration profile.

If the vehicle must perform a controlled re-entry, during the trajectory he must be able to product the aerodynamic force necessary to reach the chosen landing point.

For this reason the reentry problem can be split in two different problems:

- Do not exceed the structural and thermal limits of the vehicle
- Range control to reach the landing point

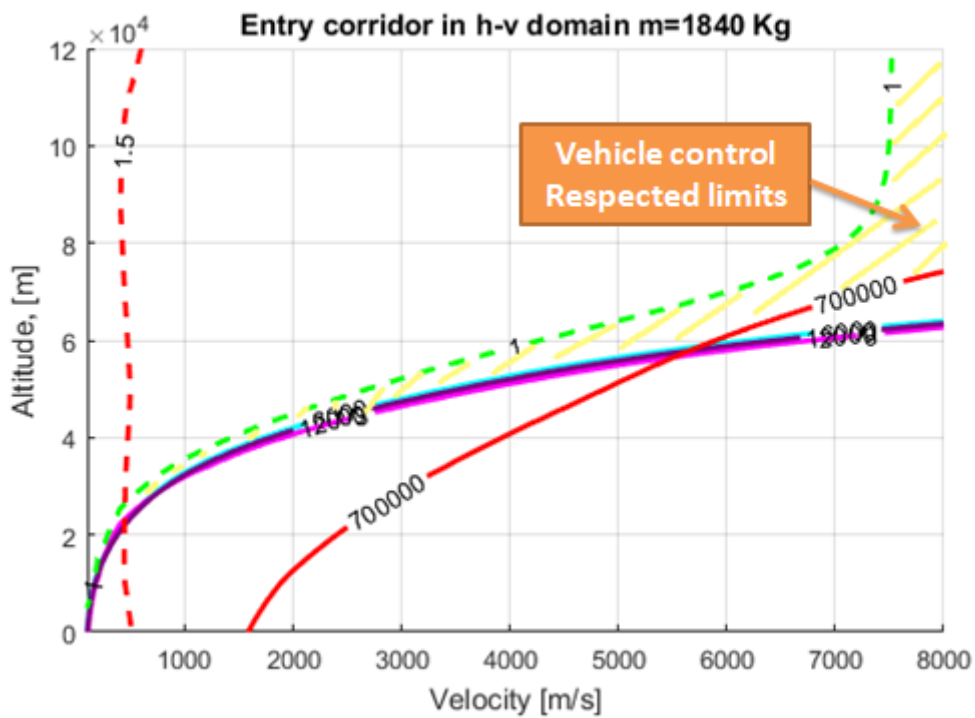


Figure 3: Re-entry corridor in Altitude-Velocity domain.

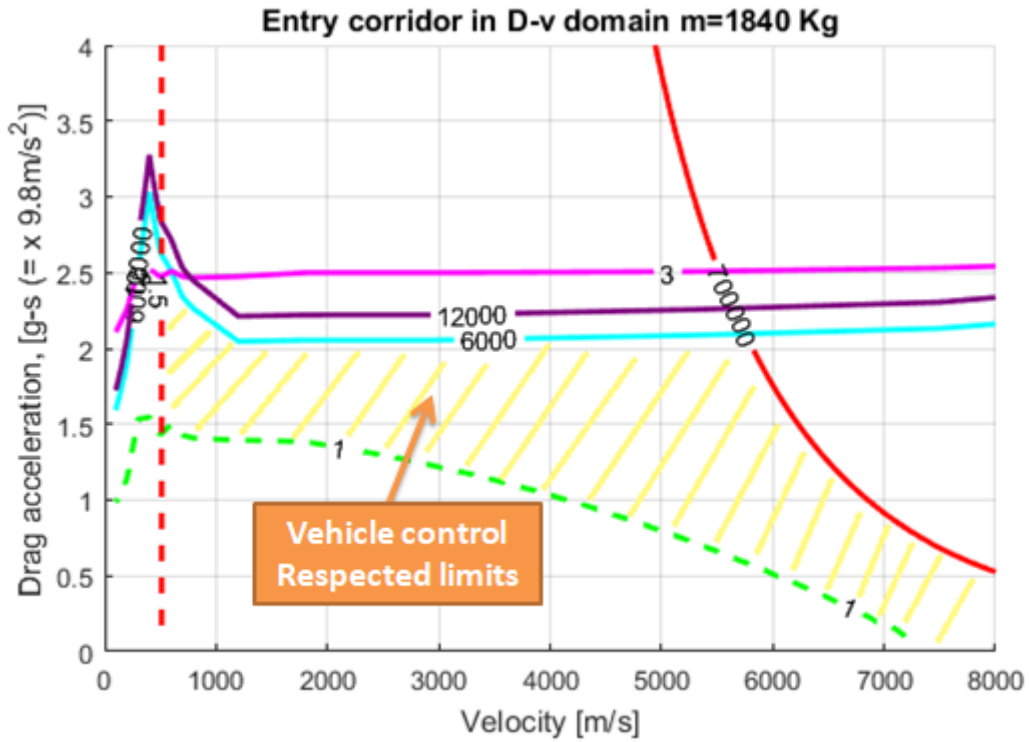


Figure 4: Re-entry corridor in Drag acceleration-Velocity domain.

The angle of attack is chosen for the minimization of the heat rate: in the first part of re-entry with an high Alpha trim , for example 40°, the heat is dissipated from a large area, so entered heat flux is lower and the TPS can be thinner, reducing costs and weights. Reached low Mach number the Alpha trim follows a linear profile, reducing its value, so the vehicle can increase the lift-to-drag and cross-range capability, improving the control and the static and dynamic stability.

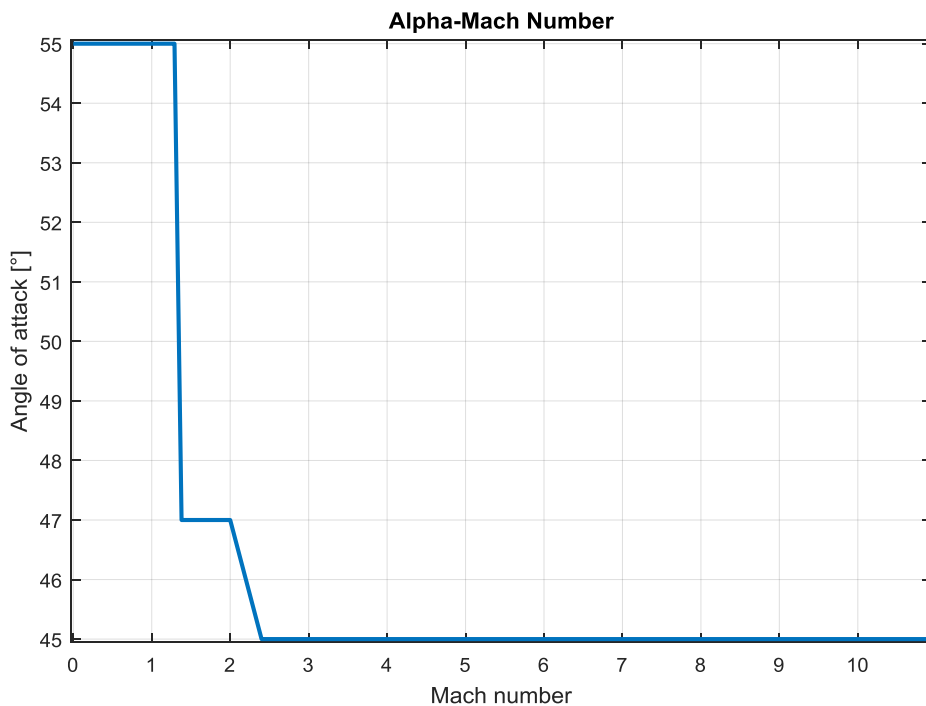


Figure 5: Angle of Attack and Mach number profile for the IXV vehicle.

1.2.1 Corridor constrains

The constrains can be divided in three different classes: path, stability and performance constrains. The stability constrain is linked with the dynamic equilibrium and it's repents by the Ceiling. The path constrains are linked with the vehicle safety: if they are overcame the vehicle suffers structural damage and the crew, where it is presented, risks irreversible damages. These constrains are the maximum heat flux, maximum aerodynamic acceleration and maximum dynamic pressure. The performance constrain is linked with the aerodynamic characteristics: in this case it's represented by the triggering Mach. Overcoming this Mach the aerodynamic changes because the vehicle opens the parachute and guidance and control low changes.

The ceiling constrain is linked with the vehicle capacity to generate a control action: when the vehicle is under the ceiling only a part of the lift balances the gravity and centrifugal force, so the remaining part of lift can be used for the bank angle control. If the vehicle overcomes the ceiling constrain there isn't available lift for the control, in this situation the vehicle can fly, but it's impossible control it. The ceiling equation is found setting the bank angle equal to zero and maintaining constant the flight path angle:

$$\left(\frac{1}{2}\rho V^2 S C_L\right) par_{ceiling} = m \left(9,81 - \frac{V^2}{r}\right) \quad (1)$$

If the vehicle flies in ceiling $par_{ceiling}$ is equal to 1, if the vehicle can be controlled $par_{ceiling}$ is lower than 1.

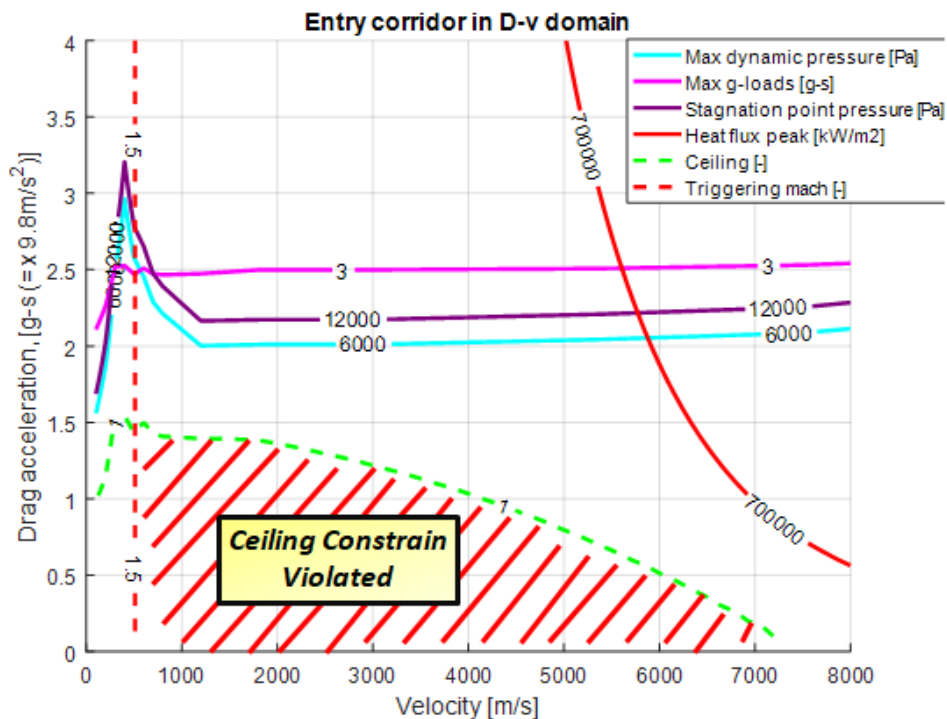


Figure 6: Ceiling constrain.

The heat load constrain is based on the heat absorbed during the unit of time, the heat flux is written using the DKR formulation, that analyses the conductive flux, but for a velocity higher than 9 Km/s, it's necessary

to introduce also the radiative heat, because this term is no longer negligible. The following formulation is for the conductive flux DKR:

$$\dot{q}_{max} = K \text{ catal} \frac{1}{\sqrt{R_N}} \left(\frac{\rho}{\rho_0}\right)^{\frac{1}{2}} \left(\frac{V}{V_0}\right)^{3,15} \quad (2)$$

In this equation R_N is the nose radius of the vehicle and V_0 and ρ_0 are respectively the velocity and the density at the sea level. K and catal are two coefficients. If the heat flux is bigger than \dot{q}_{max} the heat flux constrain is violated.

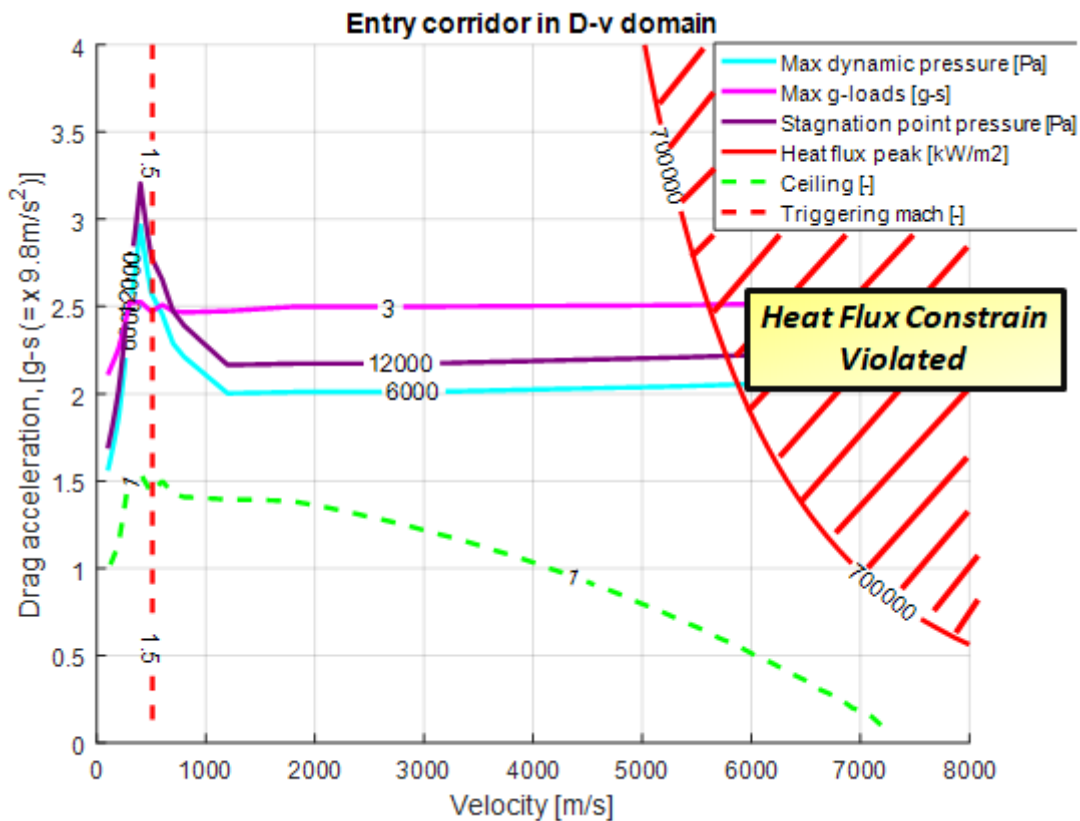


Figure 7: Heat flux peak constrain.

The dynamic pressure constrain is linked to the maximum load that the aerodynamic control surfaces can tolerate, so this is a structural constrain, written as function of velocity V and density ρ :

$$q_{max} = \frac{1}{2} \rho V^2 \quad (3)$$

This constrain is also linked with the maximum pressure at the stagnation point: in fact this pressure is equal to $q_{stag} = 1,85 q_{max}$.

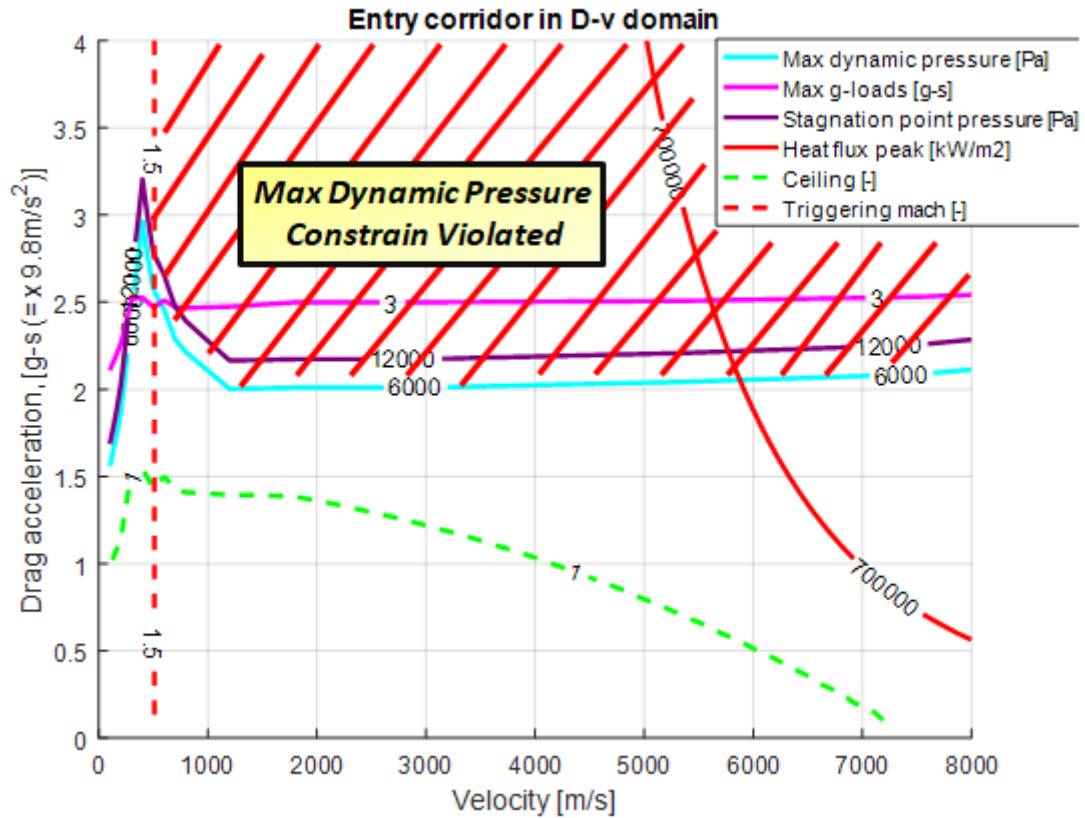


Figure 8 : Max Dynamics Pressure Constrains.

The maximum g-load constrain represents the maximum load constrain in the body normal direction, expressed like an acceleration. The load is given by the vector sum of lift force L and drag force D :

$$g_{max} = \frac{\sqrt{L^2 + D^2}}{m \cdot 9,81} \quad (4)$$

This constrain is linked to the structural vehicle limits but also to the maximum force that the vertebral column of man can bear without suffering irreversible damage.

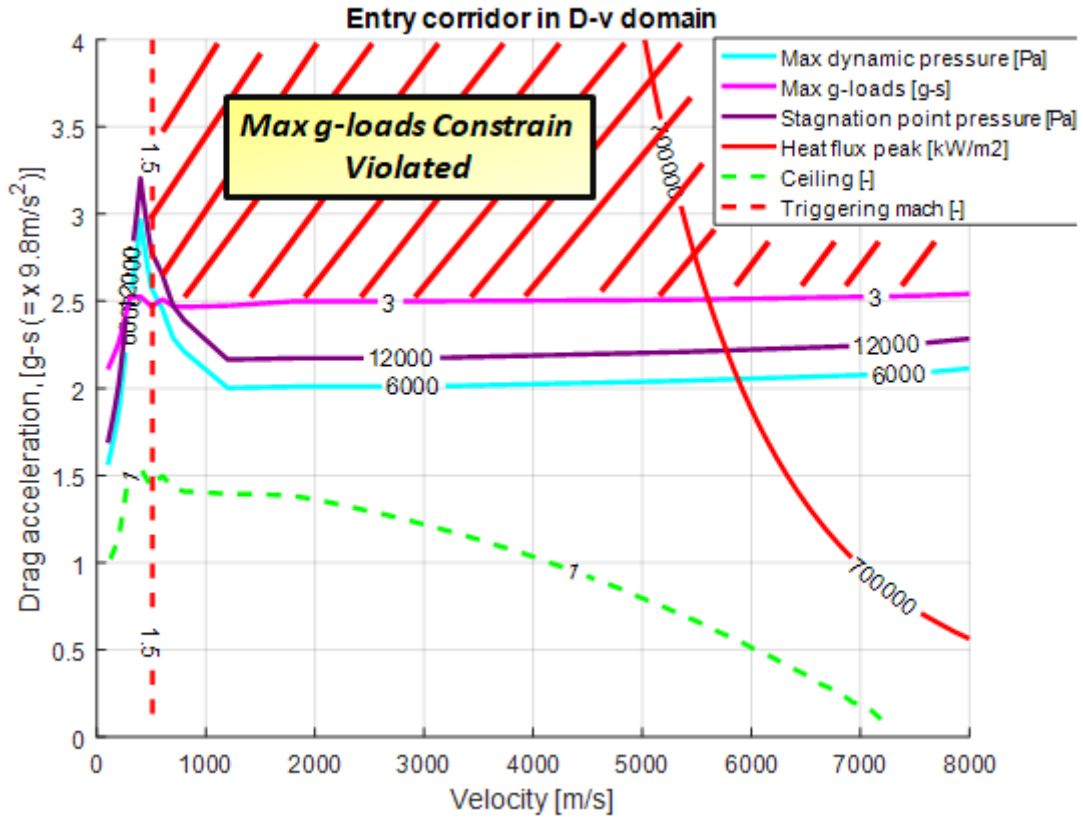


Figure 9: Maximum g-load constrain.

1.3 Vehicles Dynamics

The re-entry vehicle translation and rotational motion can be described with the Newtonian-Euler mechanics, using the dynamic and kinematic equation written in Earth Centered Earth Fixed (ECEF) reference frame, where the X-axis is aligned with Equatorial Plane, pointing to a Prime Meridian, the Z-axis is orthogonal to the X-axis, aligned with the Earth's rotation axis pointing towards north, the Y-axis completes the orthogonal right-handed reference frame:

$$\frac{d\vec{r}}{dt} = \vec{v}$$

$$\vec{F} = m \frac{d\vec{v}}{dt} + 2m\vec{\omega} \times \vec{v} + m\vec{\omega} \times (\vec{\omega} \times \vec{r})$$

$$\vec{\omega}_B = I^{-1}(\vec{M}_B - \vec{\omega}_B \times I \vec{\omega}_B)$$

$$\vec{M}_B = \vec{M}_{AB} + \vec{M}_{FB} + \vec{M}_{TB}$$

(5)

In these equations t is the independent variable, \vec{r} and \vec{v} are the position and velocity vectors, \vec{F} is the total force applied on the re-entry vehicle, m is the vehicle mass, $\vec{\omega}$ is the Earth angular velocity, $\vec{\omega}_B$ is the angular velocity of the vehicle, I is the inertial matrix, \vec{M}_B is the total moment applied on the vehicle equal

to the sum of the moments of forces and torques from the actuating surfaces, aerodynamics forces and thrusting forces. These equations characterizes the point-mass vehicle motion and attitude, but the translational motion is associated to a long period trajectory dynamics and the rotational motion is associated to a short-period oscillations. For this reason it's possible decouple these two dynamics : the guidance approach considers only the translational motion and the attitude control algorithm considers the short-period oscillation. In this thesis, the first aim is studying a guidance algorithm and the control closed loop is used to follow the reference trajectory, for this reason it's possible using only a long-period dynamic and then decoupling the dynamic: a three-degree of freedom (3-Dof) longitudinal dynamics is thus considered .

$$\frac{d\vec{r}}{dt} = \vec{v}$$

$$\vec{F} = m \frac{d\vec{v}}{dt} + 2m\vec{\omega} \times \vec{v} + m\vec{\omega} \times (\vec{\omega} \times \vec{r})$$

Now it's important understanding how this dynamic is implemented in the Simulink model: the equations are written in an Earth Centered Inertial (ECI) frame. This frame has its origin at the center of mass of the Earth, the X-axis is aligned with the spring equinox point, the Y-axis follows the right hand low and the Z-axis is the axis of Earth rotation. This frame is really convenient because it permits to write the dynamic equations in a Cartesian form. The forces change the total impulse $P=mv$:

$$\frac{dP}{dt} = F$$

$$m \frac{dv}{dt} + \frac{dm}{dt} v = F$$

The term $\frac{dm}{dt}$ is linked to the fuel consumption, staging, separation springs, but, in this case, these terms are neglected so $\frac{dm}{dt} = 0$. The equation can be rewriting in the following matter:

$$m \left. \frac{d^2R}{dt^2} \right|_I = m \left. \frac{dv}{dt} \right|_I = m[a]_I = [F]_I \quad (6)$$

R is the vehicle position in the ECI reference frame, v is the velocity written in the ECI reference frame and a is its acceleration (in ECI). $[F]_I$ is the sum of the aerodynamic forces, gravitational force and propulsion forces (in this case they are equal to zero), all written in the ECI reference frame. So with the Simulink model it is necessary to transform the parameters (as for example velocity, position and acceleration) from their initial reference system to the ECI reference system. Then integrating the Eq. (6) it's possible to obtain the new position, velocity and acceleration of the vehicle in the ECI reference frame, these values are used to compute, with interpolation, equations and transformations from different reference systems. The new forces establish a new dynamic in the vehicle.

In the Figure 10 are represented the simplified links between different reference frames: with a rotation matrix is possible changing reference frame, this matrix is written as function of the variables indicated above the arrows. These variables are finding with passage from previous reference frames.

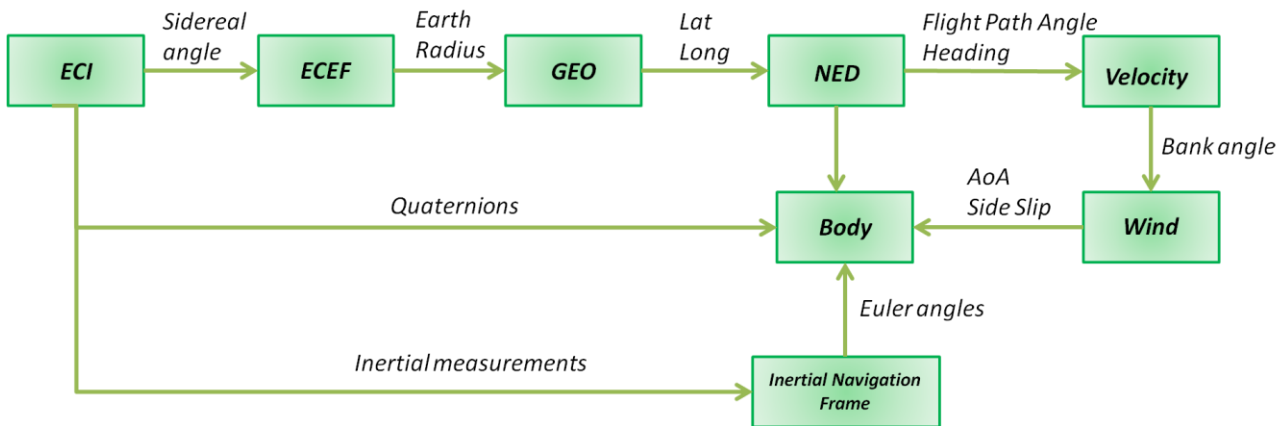


Figure 10: Summary of reference frame links (simplified).

In this flow chart are represented all the reference frames used in the Simulink model:

- **ECI:** inertial reference frame, used for writing the dynamic equations.
- **ECEF:** fixed reference frame respect to the Earth, with spherical coordinates.
- **GEO:** fixed system with Geographical coordinates (Latitude, Longitude, Altitude). The Altitude is used in the Atmosphere model US76 to evaluate, with interpolation from tables, the environmental variables as temperature, density, mole, sound velocity.
- **NED:** it's a body carried system, with the origin in the center of gravity CoG of the vehicle. The X-axis is directed to the North Pole, the Y-axis is directed at east and the Z-axis is directed down, perpendicular to the surface. It uses to find the flight path angle.
- **Velocity:** it's a body carried system, with the origin in the CoG of the vehicle. The X-axis is directed along the relative velocity vector, the Y-axis follows the right hand low and the Z-axis is contained in the vertical plane. It uses to define the bank angle, this angle enters in the GNC block.
- **Wind:** it's a body carried system, with the origin in the CoG of the vehicle. The X-axis is directed along the velocity vector relative to air, the Y-axis follows the right hand low and the Z-axis is contained in a plane defined by the bank angle. This reference system it uses for write the aerodynamic forces.
- **Body:** it's a body carried system, with the origin in the CoG of the vehicle. The X-axis is directed toward the nose vehicle, the Y-axis follows the right hand low and the Z- axis is directed toward the lower surface of the vehicle. This reference system it uses to express the propulsive force but also the aerodynamic forces. In fact many aerodynamic forces are written in wind axis, then they pass in Body axis and, at the end, they are written in the ECI reference frame, using the rotational matrix.

The gravity model is the J2 (WGS84), where the Earth is assimilated to a spheroid. The gravity force is written in the ECI reference frame.

The environmental mode follows the standard US76 where the atmosphere is tabulated: each altitude is associated at a density, pressure, speed of sound and temperature. For this reason knowing the altitude it's possible to use a simple interpolation, finding the desired values.

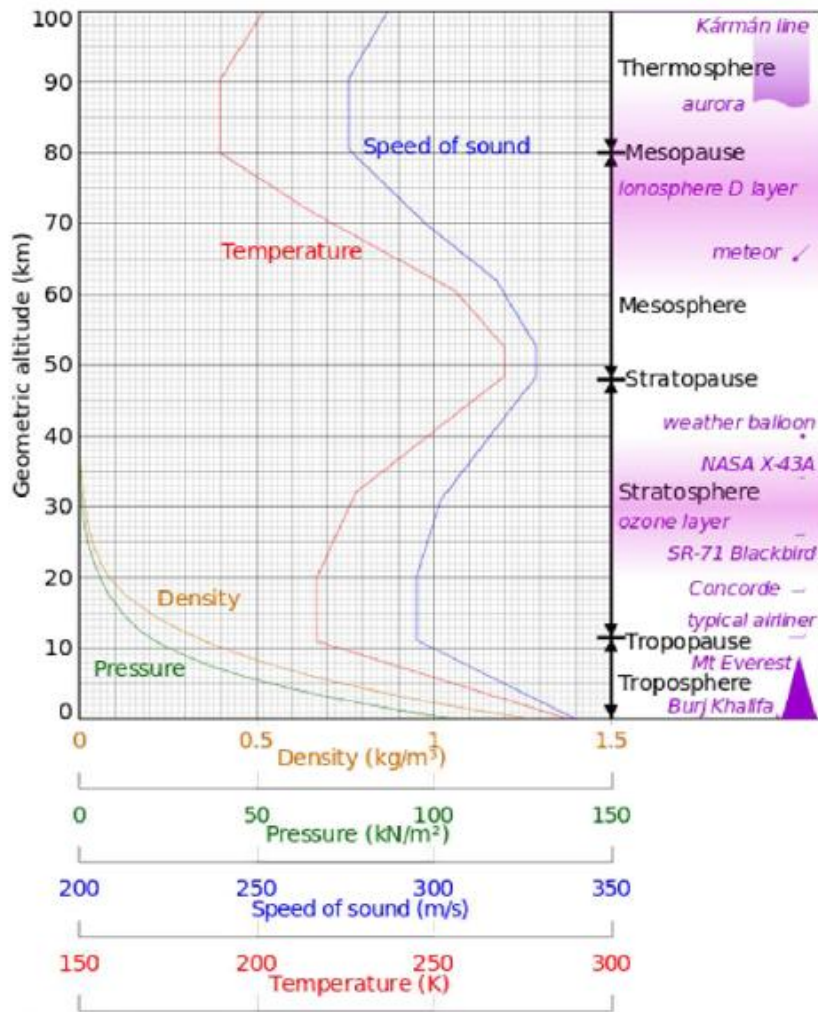


Figure 11: Environmental model US76.

Now, knowing all the used models, it's possible to define a conceptual flow chart to better understand the Simulink model.

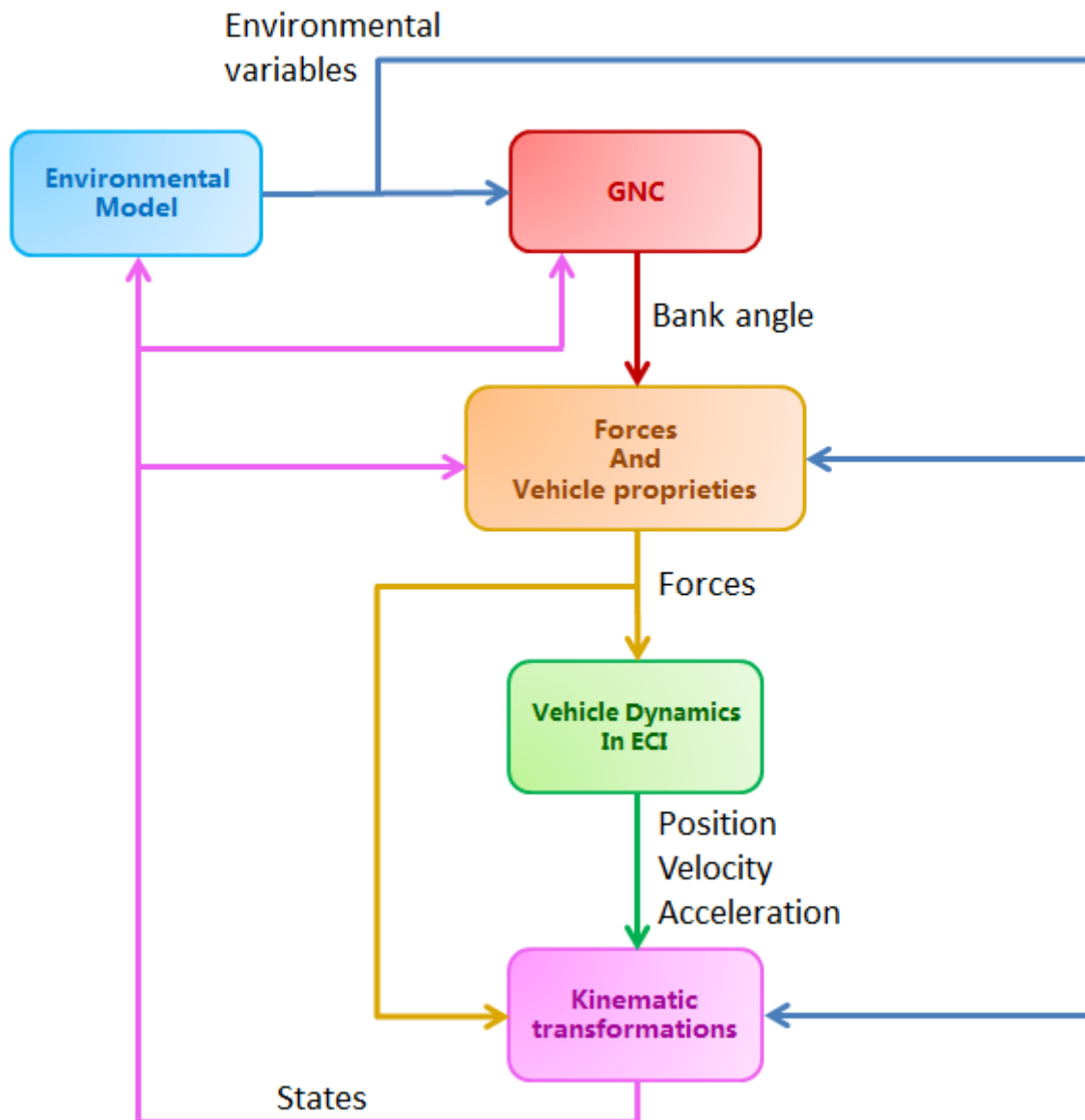


Figure 12: Conceptual flow chart for the Simulink Model

The Simulink model must integrate the equations of motion so it's necessary to choose the method: the method is a 4th-order Runge Kutta with a fixed step of 1. This step is the typical value for the 3-DOF system, based on experience.

1.4 GNC in re-entry

During the re-entry the vehicle must follow a certain trajectory and it must maintain a commanded attitude. This aim is reached thanks to the bank angle. The bank angle is the angle between the plane that contains the local vertical (defined as the direction of the gravity force) and velocity and the lift force: when the vehicle laterally rotates the lift vector is re-directed, reducing its vertical component and increasing its lateral component. With this procedure the vehicle can modify the rate of altitude change, the acceleration profile and the down range. In this matter the vehicle is guided from an initial point to a final point. The banking maneuver dissipates energy in a controlled matter but a lift lateral component is born, introducing a cross range deviation, this problem is solved with a bank angle reversals.

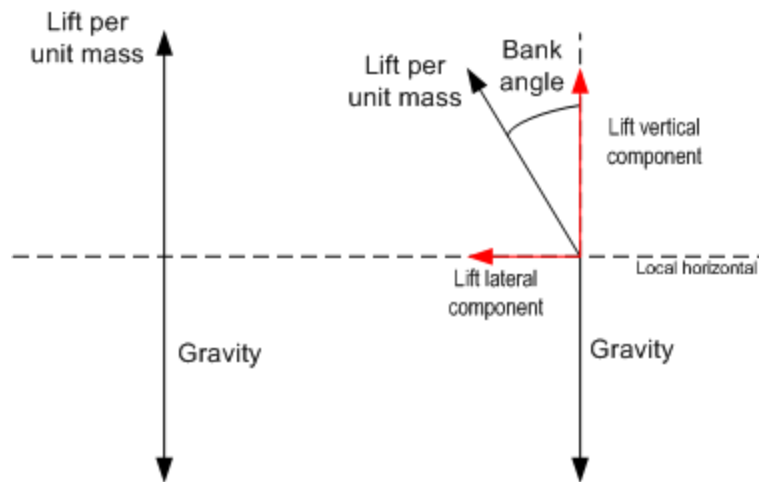


Figure 13: Behind view of the vehicle: on the left, the case of zero bank angle; on the right the case of non-zero bank angle.

In the case of re-entry vehicle, the banking maneuvers are selected by a GNC system, this system guides and controls the vehicle through its entry trajectory, from the EIP conditions to the TEAM conditions. Generally a GNC system is composed of three main functions: navigation, guidance and control.

The navigation system process the vehicles sensor output and estimates the vehicle state as altitude, velocity, angles. The guidance uses the state provided by navigation to produce reference commands and the control tracks this reference.

The vehicle rotation and the bank angle change are possible thanks to aerodynamic surfaces and small thrusters of the Reaction Control System (RCS): the maximum and minimum bank angle rates and the accelerations are limited by the RCS capabilities (thrust and specific impulse).

The behavior of a GNC system can be simulated with mathematical models:

- **Navigation:** the 3-Dof re-entry dynamics is described by equations of motion, a numerical propagation of the initial conditions can approximately provide the profile flown by the vehicle. In the model the sensor dynamic, like delays and uncertainties, aren't implemented.
- **Guidance:** drag acceleration and velocity are the two coordinates chosen to generate the reference profile. This profile must minimize the down range error, conduct the vehicle to TAEM condition and respect the re-entry corridor constrains.

- **Control:** the desired drag acceleration is compared with the vehicle drag acceleration, this error enters in a PID controller, and the output is the ratio between the vertical component of the lift and the lift module. This ratio is equal to the bank angle cosine. In the model the actuators dynamic, like delays and uncertainties, aren't implemented, only a rate limiter is inserted to create a realistic bank angle profile.

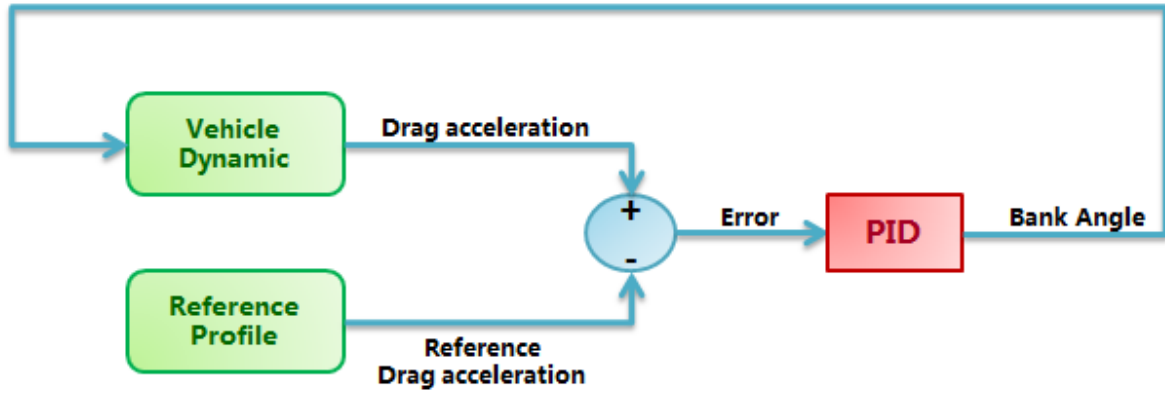


Figure 14: Navigation, Guidance and Control flow chart

2. Control Algorithm: PID model

In this chapter will be explained a typical control technique, the PID controller, and two different ways to find the optimal gains that allow to minimize the error between the reference Drag Acceleration signal and the vehicle Drag Acceleration.

PID is a type of controller used to follow a reference signal. It is composed by three different contributes: proportional, integrative and derivative.

The following expression shows the PID compensator formula with an high frequency filter in the derivative term:

$$H(s) = K_P + K_I \frac{1}{s} + D \frac{s}{\frac{s}{N} + 1} \quad (7)$$

The proportional term creates a correction proportional to the error between the actual and the desired value of the controlled variable; in this case the controlled variable is the drag acceleration in g-s. With this term the drag acceleration increases when it is too low and decreases when it is too high.

The integrative term creates a signal proportional to the integral of the error. With this term the error converge to zero, for this reason it is helpful during the stationary. This term creates a problem: if the error remains high, for example during command saturation, the integrative term keeps increasing. This fact creates an overcorrection when the saturation ends and the system diverges. This phenomenon is named wind-up. During the years a lot of different techniques are born as anti-wind up methods: one of this is the clamping. With clamping, when the output saturates and the output and input (in this case the input is the drag error) have the same sign, the integrative term remains constants.

The derivative term creates a signal proportional to derivate of the error; its action is linked to the speed of error increase or decrease. This term is effective during the transitory; it speeds up the response and decreases the oscillations. But this term is sensitive to noise: the noise creates an input signal with high frequency oscillations, the derivative term captures these oscillations and creates an overcorrection, proportional to the oscillation speed. To avoid this phenomenon a low pass filter is introduced in the PID, its aim is removing higher-frequency noise components.

The low pass filter has the following state-space formulation:

$$G(s) = \frac{N}{s + N} \quad (8)$$

N is the cutoff frequency, when this frequency is exceeded the output is damped . Using the PID, an approximate value can be found with an easy expression:

$$N = 20 \frac{K_P}{K_D} \quad (9)$$

A real value can be determined only knowing the real system, with its sensors and actuators, and the operative scenario with external disturbances.

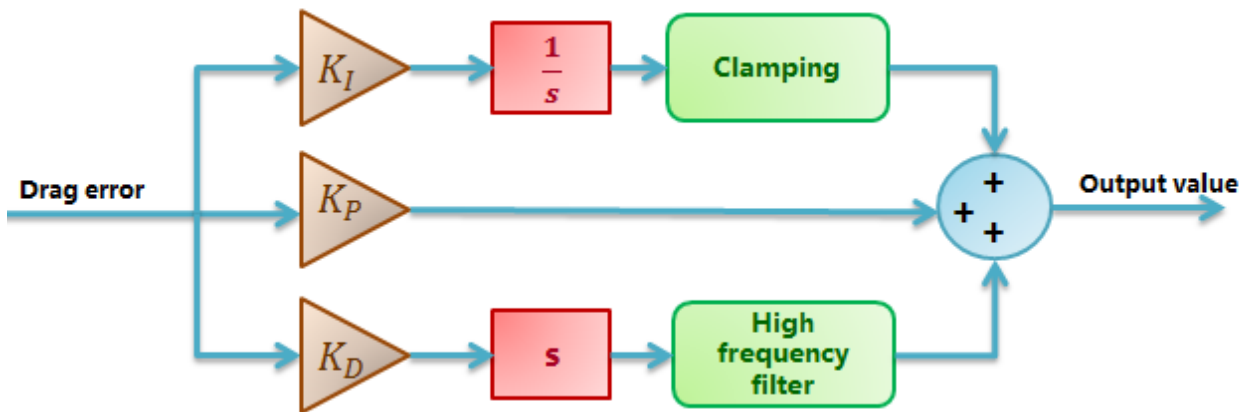


Figure 15: PID model

The output value represents the ratio between the lift vertical component and the lift module, for this reason it's necessary to insert a saturator because this value can only assume a value between 1 and -1. With a value of 1 the lift is directed along the vertical, the vehicle can reach the maximum down range and it's subjected to a low accelerations. With a value of -1 the lift vector is directed towards the Earth center, this means high accelerations and low down range

The link between PID output and bank angle is represented by the following expression:

$$\frac{L_V}{L} = \text{acos}(\sigma) \quad (10)$$

To avoid the acrobatic flight the bank angle can only assume in module a value between 0° and 90° , this operation is implemented in the model thanks to a saturator.

2.1 PID gains: first study

The first idea to test the system behavior with different gains is insert a reference trajectory and study how the vehicle follows it. The reference trajectory is based on IXV re-entry trajectory and it was approximated by straight lines going through seven points until a velocity of 3600 m/s where the reference drag acceleration reaches a constant value.

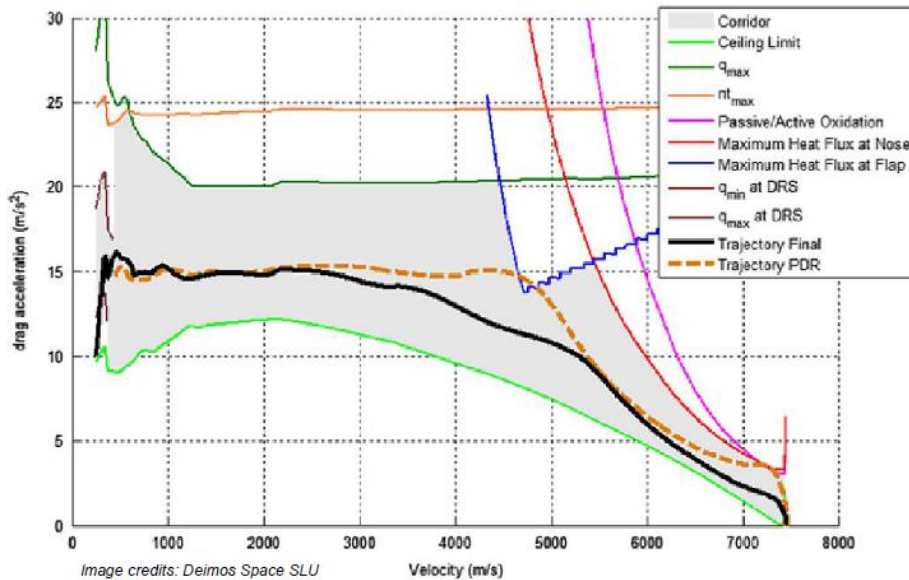


Figure 16: IXV re-entry trajectory [RD].

The vehicle used in the simulations has the same features of IXV: mass equal to 1840 Kg, wing surface of 7.25 m, scheduled Alpha, variable aerodynamic function of Mach and Alpha and initial conditions written in the Table 1.

Conditions	Value
Altitude	120000 m
Latitude	-4.48°
Longitude	173.48°
Velocity	7434,85 m/s
Heading	86.69°
Gamma	-1.2°

Table 1: Initial conditions for re-entry guidance.

For studying the gains three simulations have been made, in each simulation the analysed variable is the difference between the vehicle drag, obtained thanks to the control, and the reference drag. The reference profile has been split in two parts: the first part includes the velocities between 1000 m/s and 3500 m/s, the second part starts with a velocity equal to 3500 m/s and ends when the simulated acceleration drag intersects for the first time the reference drag profile.

In the first simulation the analysed variable is K_p , K_D and K_I are constant, the derivative gain is equal to 550 and the integrative gain is equal to 0.6. These values are chosen with a small sensitivity analysis to understand the effect of the PID gains on the trajectory.

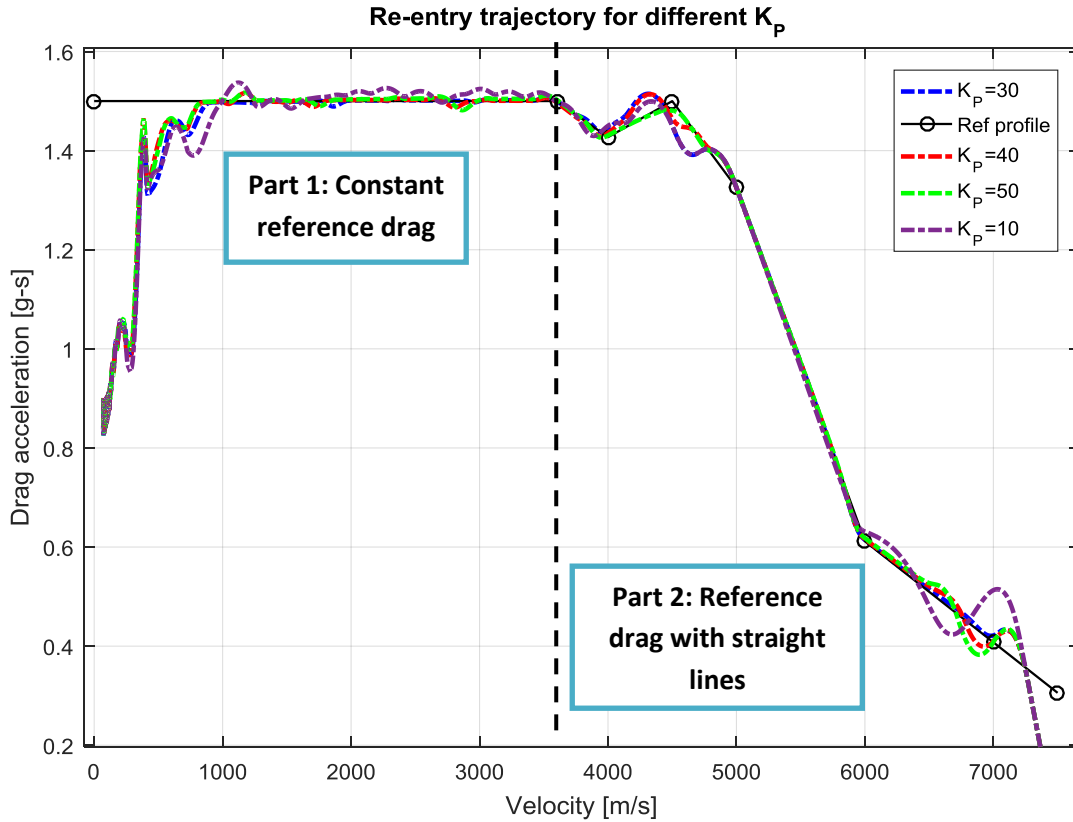


Figure 17: Re-entry trajectory for different K_p , $K_I=0.6$, $K_D=550$

K_p	10	30	40	50
Integrated error	113	101,8208	101,8612	103,2672

Part 1	Max error	0,1178	0,0653	0,0486	0,0517
	Velocity	7072 m/s	4583 m/s	7137 m/s	7132,8 m/s

Part 2	Max error	0,037	0,0079	0,0161	0,0169
	Velocity	1125 m/s	3524 m/s	1173 m/s	1181 m/s

Table 2: Integrated error, maximum difference between vehicle acceleration drag and reference drag in the part 1 and in the part 2 of the reference profile and velocity at which the maximum difference occurs for different proportional gains.

The proportional term, if it is chosen too high ($K_p=50$), degrades the system stability because it can create an overcorrection, the drag acceleration exceeds the commanded value and oscillates around the commanded position, but with appropriate values the error decreases and the system is more reactive ($K_p=30$). At the same time a low proportional term does not allow to reach the reference signal, this is the case of purple curve ($K_p=10$), where the PID output and the bank angle maintain limited value and the vehicle cannot being accurately controlled.

In the second simulation the analysed variable is K_D , K_P and K_I are constant, the proportional gain is equal to 40 and the integrative gain is equal to 0.6.

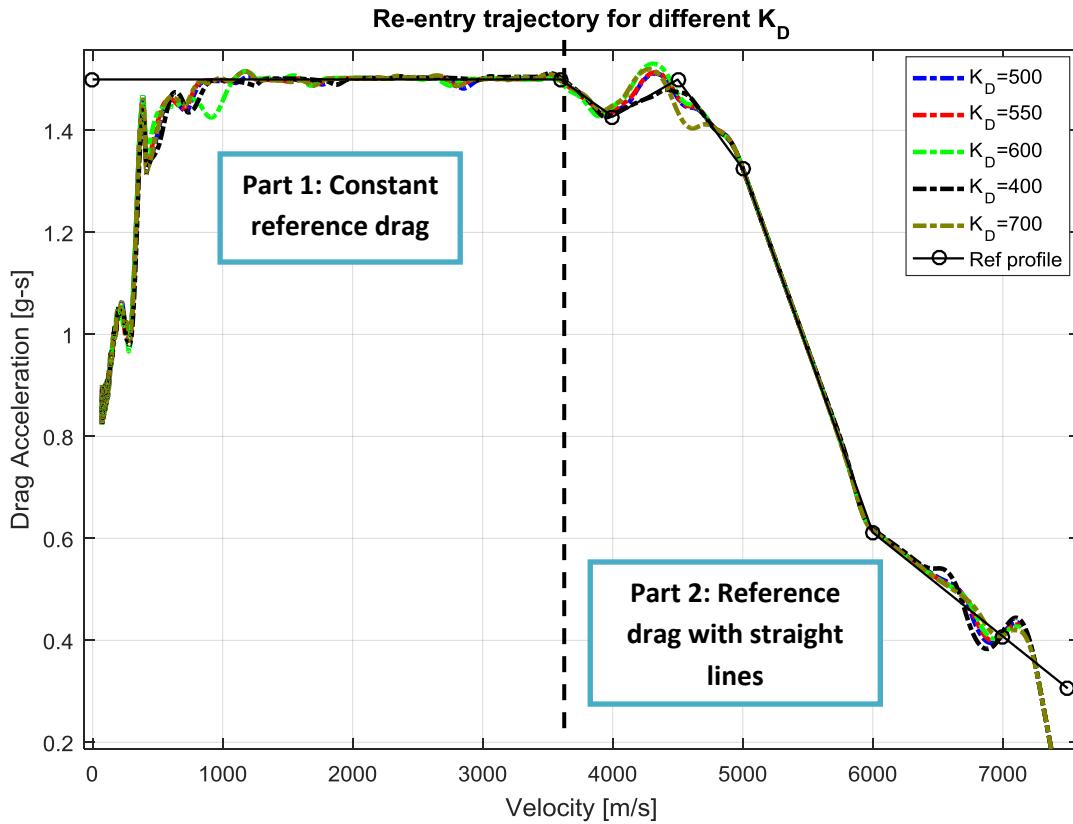


Figure 18: Re-entry trajectory for different K_D , $K_P=40$, $K_I=0.6$

K_D	40	50	55	60	70
Integrated error	104,5001	102,718	101,8612	103,1984	101,6566

Part 1	Max error	0,0599	0,0522	0,0486	0,0614	0,0156
	Velocity	7127,3 m/s	7132 m/s	7137,5 m/s	4269,4 m/s	4545 m/s

Part 2	Max error	0,0123	0,0177	0,0161	0,0494	0,0156
	Velocity	1250,4 m/s	2857,6 m/s	1173,1 m/s	1000 m/s	1177,3 m/s

Table 3: Integrated error, maximum difference between vehicle acceleration drag and reference drag in the part 1 and in the part 2 of the reference profile and velocity at which the maximum difference occurs for different derivative gains.

The derivative term must reconcile two different aspects: reducing the oscillations and following the reference profile. If the reference profile presents sudden curvature changes, an high derivative term doesn't allow following them ($K_D=600$). If the derivative term is too low the control action doesn't influence enough the system and the drag acceleration is characterized by oscillations and the dynamic isn't damped ($K_D=400$).

In the last simulation the analysed variable is K_I , K_D and K_P are constant, the derivative gain is equal to 550 and the proportional gain is equal to 40.

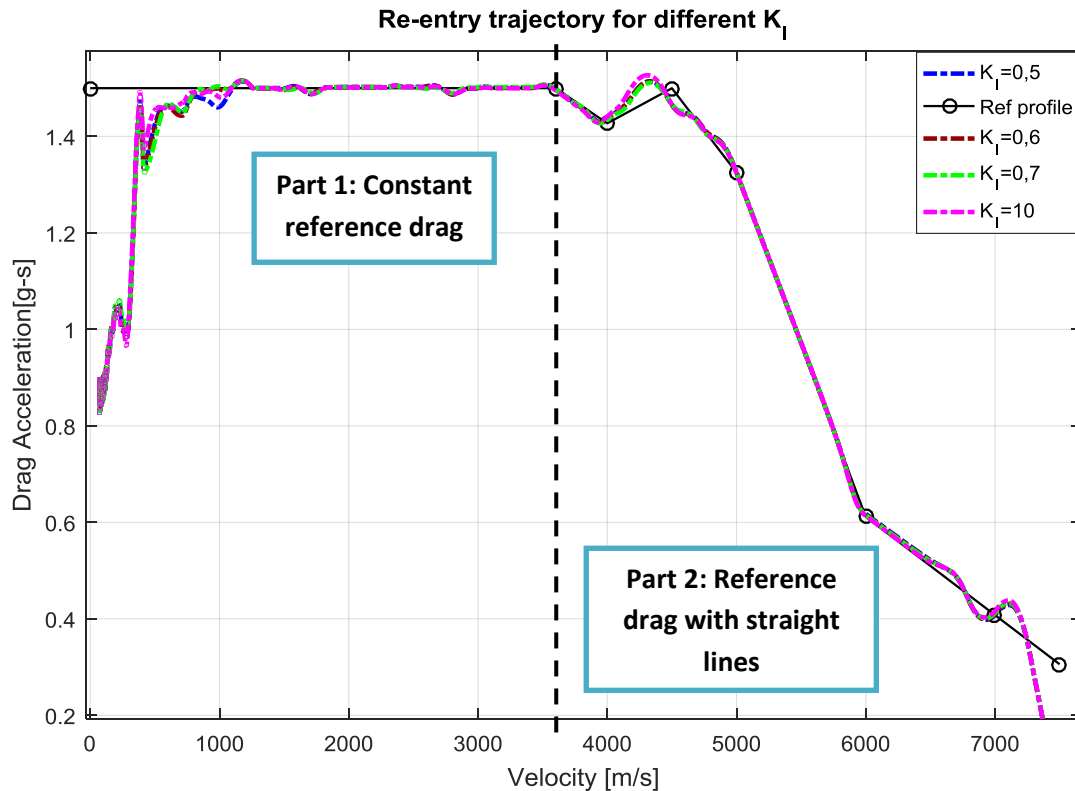


Figure 19: Re-entry trajectory for different K_I , $K_P=40$, $K_D=550$

K_I	0,5	0,6	0,7	10
Integrated error	102,3704	101,8612	1'1,6021	102,0465

Part 1	Max error	0,0391	0,0161	0,0151	0,0198
	Velocity	1000 m/s	1173 m/s	1184,9 m/s	1016 m/s

Part 2	Max error	0,0468	0,0468	0,0504	0,0577
	Velocity	7137,8 m/s	7137,8 m/s	7137 m/s	4270 m/s

Table 4: Integrated error, maximum difference between vehicle acceleration drag and reference drag in the part 1 and in the part 2 of the reference profile and velocity at which the maximum difference occurs for different integrative gains.

The integrative term is linked to the steady-state error, with appropriated values this error decreases and the system acquires a better behaviour in the stationary range, in particular the error is reduced following a constant reference acceleration drag ($K_I=0,7$). But this value must remain limited because the integrative gain is linked to the time, the control system takes time to decrease the integrative value when the error becomes small, for this reason the system overcorrects the acceleration drag and the system is characterized by peaks ($K_I=10$).

2.2 Vertical dynamic and PID gains

The PID gains choosing can be faced using a simplified model, this model studies the vertical dynamic: the aim is finding the optimal gains to reach and maintain a chosen altitude. This gains must minimize the oscillations and stationary error. This approach gives an idea about the order of magnitude of PID gains using in the 3-Dof dynamic model.

The vertical dynamic is represented by three forces:

- The lift force L it's an aerodynamic force perpendicular to the velocity vector, it's linked to the vehicle sustenance.
- The weight force mg : it's caused by the planet gravitational attraction, the force is directs towards the Earth center.
- The centrifugal force F_C : it's caused by the Earth sphericity, the force is directs towards the Earth radius in the opposite direction of the weight force.

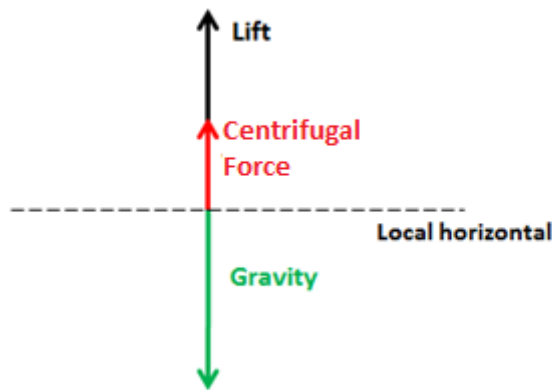


Figure 20: Vertical dynamics and forces.

If all the forces aren't in equilibrium, on the vehicle it's born an acceleration, this acceleration it's only a vertical acceleration and for this reason the vehicle changes altitude. The vertical dynamics is represented by the following equation:

$$m\ddot{h} = F_C - mg + L \quad (11)$$

Where:

$$F_C = m \frac{V^2}{R} \quad (12)$$

$$L = \frac{1}{2} \rho V^2 S_{ref} C_L \quad (13)$$

The longitudinal dynamic is characterized by a constant velocity . The atmospheric model is US76 and the gravity model is a spherical gravity model where the term g is maintained constant and equal to 9.81 m/s^2 . The lift coefficient is function of Mach and Alpha, the Mach number changes during the simulation because the altitude changes and the angle Alpha is constant and equal to 45° . Also the density changes because it's function of the altitude. In the centrifugal force F_C the term R represents the distance from the Earth center: for this reason if the altitudes changes, the centrifugal force change.

Input Parameters	Value
Wing surface	7,26 m
Alpha	45°
Mass	1840 Kg
Velocity	6500 m/s
Gamma	0°
Altitude	50000 m

Input Parameters for PID optimization .

When the vehicle is subjected to a vertical acceleration, a vertical velocity \dot{h} is born, this vertical velocity is made up with the longitudinal velocity, the flight path angle γ changes and the lift force changes directions. As first approximation the velocity module can be considered constant and equal to V , because \dot{h} is really small compared with the longitudinal velocity V . The changes in the flight path angle are inserted in the simulations because even just a small γ influences the dynamic. If the flight path angle is different from zero the lift is splitted in two components and only the vertical component $L \cos(\gamma)$ enters in the vertical dynamic.

So a new equation can be written:

$$m\ddot{h} = F_C - mg + L \cos(\gamma) \cos(\sigma) \quad (14)$$

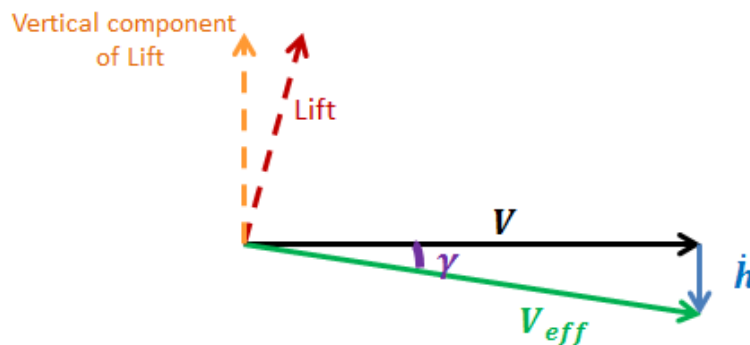


Figure 21: Vertical dynamics and velocity composition.

The last concept to explain is how the controller work. If the vehicle wants maintain an altitude it's necessary having the equilibrium between the forces. This equilibrium can be reached varying the bank angle. In this matter the vertical lift component changes, with the right bank angle the sum between vertical lift force, centrifugal force and weight force is equal to zero.

If the vehicle starts from an altitude and it wants to change altitude, the PID controller defines a law for the bank angle variation to arrive at the desired altitude, with a damped dynamics, and, reached the desired altitude, the PID controller imposes constant bank angle, this bank angle is the angle necessary to have the equilibrium. The PID input is the altitude error and the output is the ratio between vertical lift component and lift module. The bank angle is calculated from this ratio. It's important to insert a rate limiter so that the dynamics has a real behaviour. The rate limiter is set to 12°/s.

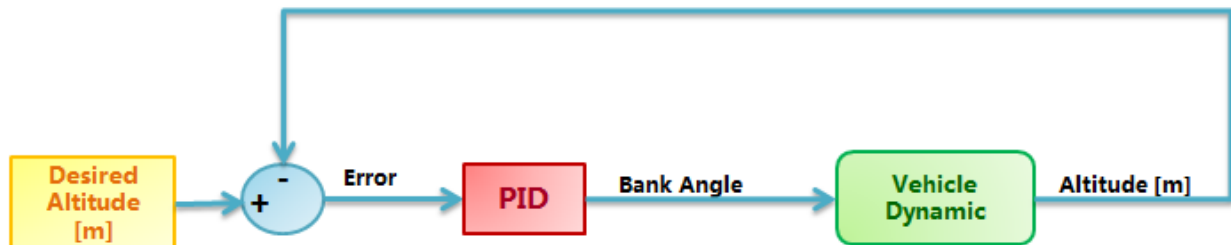


Figure 22: Altitude control flow chart.

If the vehicle must go down the error is negative, the output PID is negative and the cosine of the bank angle is negative: in this matter the lift is facing downwards. When the error decreases the bank angle increases and the lift vertical component decreases so that the dynamic becomes damped.

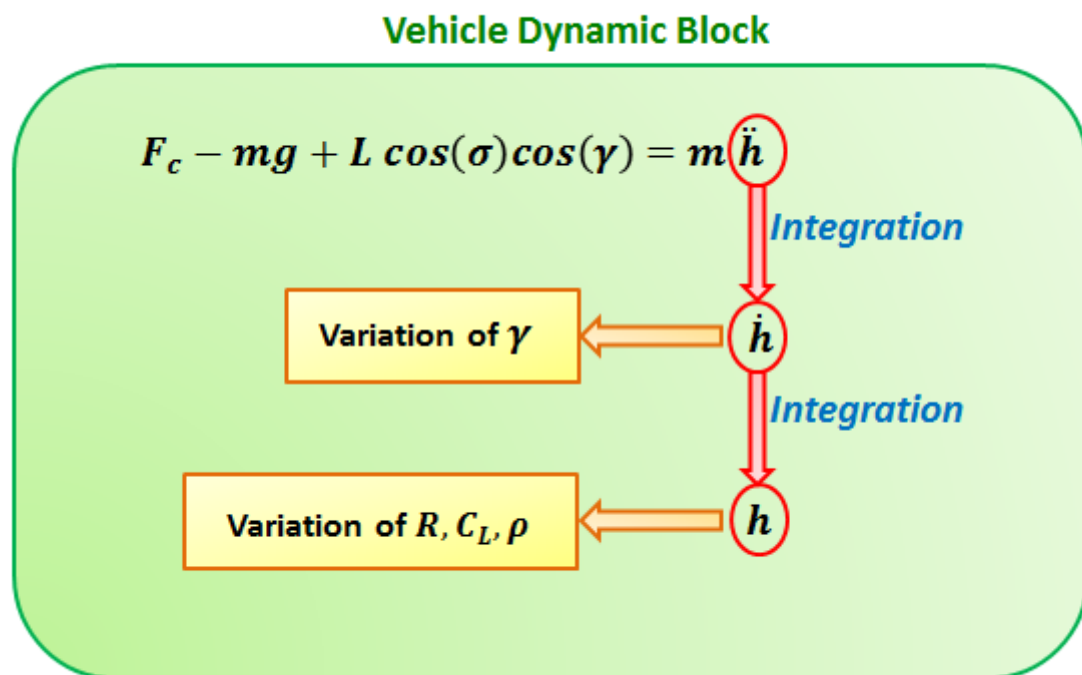


Figure 23: Vehicle dynamics flow chart.

To test the dynamic model, the vehicle is positioned at the ceiling: the ceiling is the maximum altitude at which the vehicle can fly because the developed lift equals the other forces. Going up in altitude the density is too low and the sum between lift and centrifugal force is less than the weight force. The ceiling is calculated for a bank angle and a flight patch angle null.

If the dynamic model is correct, the vehicle, in ceiling, must stay motionless, without altitude changing. In ceiling the dynamic equation becomes the following:

$$F_c + L - mg = 0 \quad (15)$$

From this equation it's possible calculating the ceiling air density and, subsequently, finding the corresponding altitude with a linear interpolation because, in the *Matlab* model, the atmosphere is tabulated.

In the first simulation the vehicle is placed 180 meters under the ceiling, in this case the ceiling is 71150 meters. The results are showed in the Figure 24.

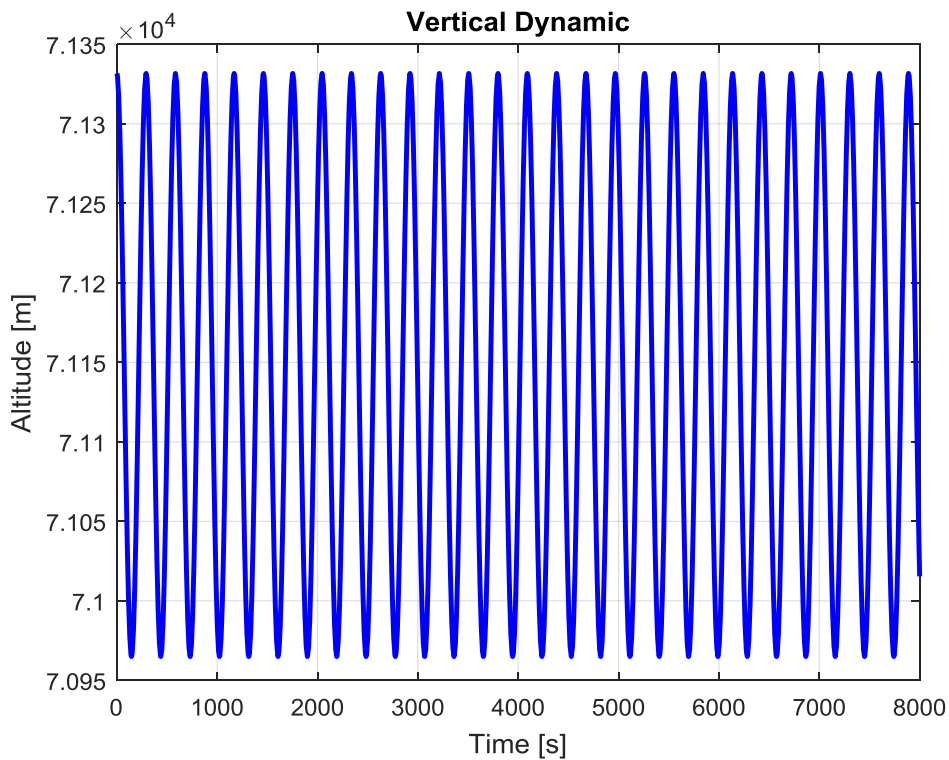


Figure 24: Vertical dynamics for a re-entry vehicle.

The results identifies a problem: the vehicle oscillates around the ceiling. This is due to an error in the dynamic: if the flight path angle changes, a small components of drag is directed along the vertical. This vertical component has a damping effect and the vehicle stabilizes at the ceiling. For this reason a new term is introduced in the equation:

$$F_c - mg + L \cos(\sigma) \cos(\gamma) - D \sin(\gamma) = m\ddot{h} \quad (16)$$

The Drag has the following expression, where the coefficient C_D is function of Mach and Alpha:

$$D = \frac{1}{2} \rho V^2 S_{ref} C_D \quad (17)$$

With this correction the vehicle reaches the ceiling and stabilizes themselves, as the Figure 25 shows.

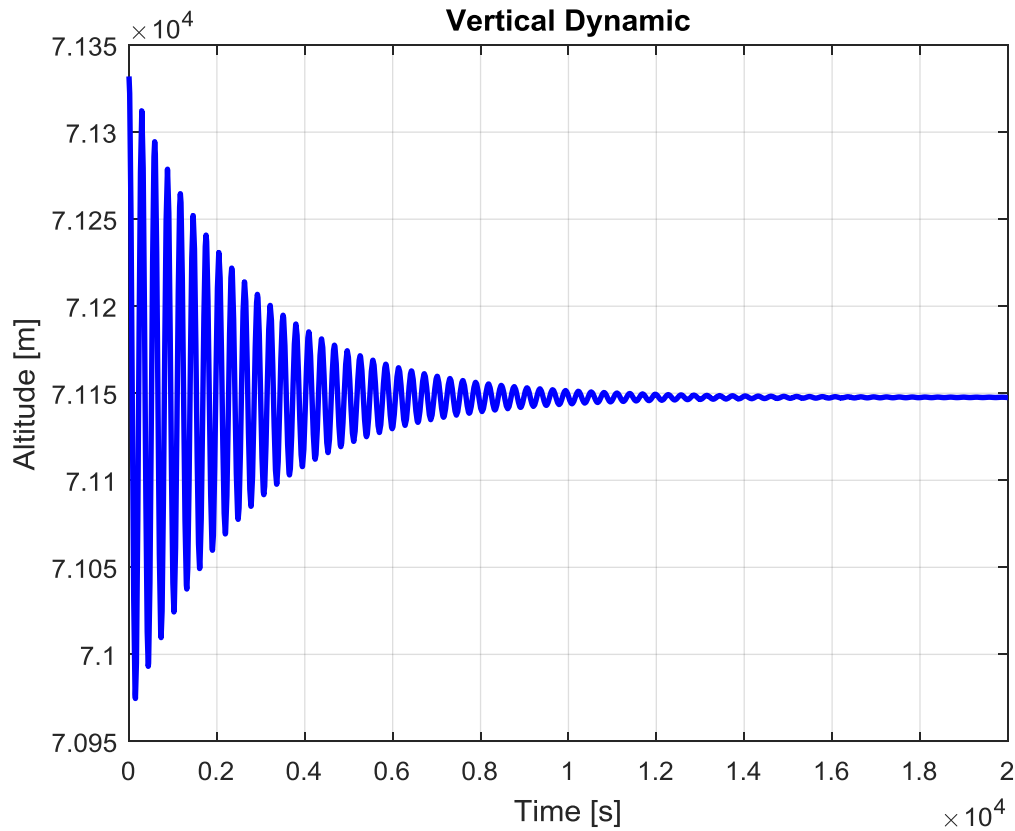


Figure 25: Vertical dynamic to reach the ceiling.

The next step is finding the optimal PID gains: the vehicle is positioned at an altitude of 50 Km and forced to reach the altitude of 60 Km. The climb maneuver develops greater oscillations because the aerodynamic forces are higher. For this reason the PID gains are optimized for this maneuver that has major loads.

As first attempt the PID gains are all chosen equal to 1, with N equal to 20. The result is an amplified dynamic, the vehicle diverges from the equilibrium condition going out the atmosphere.

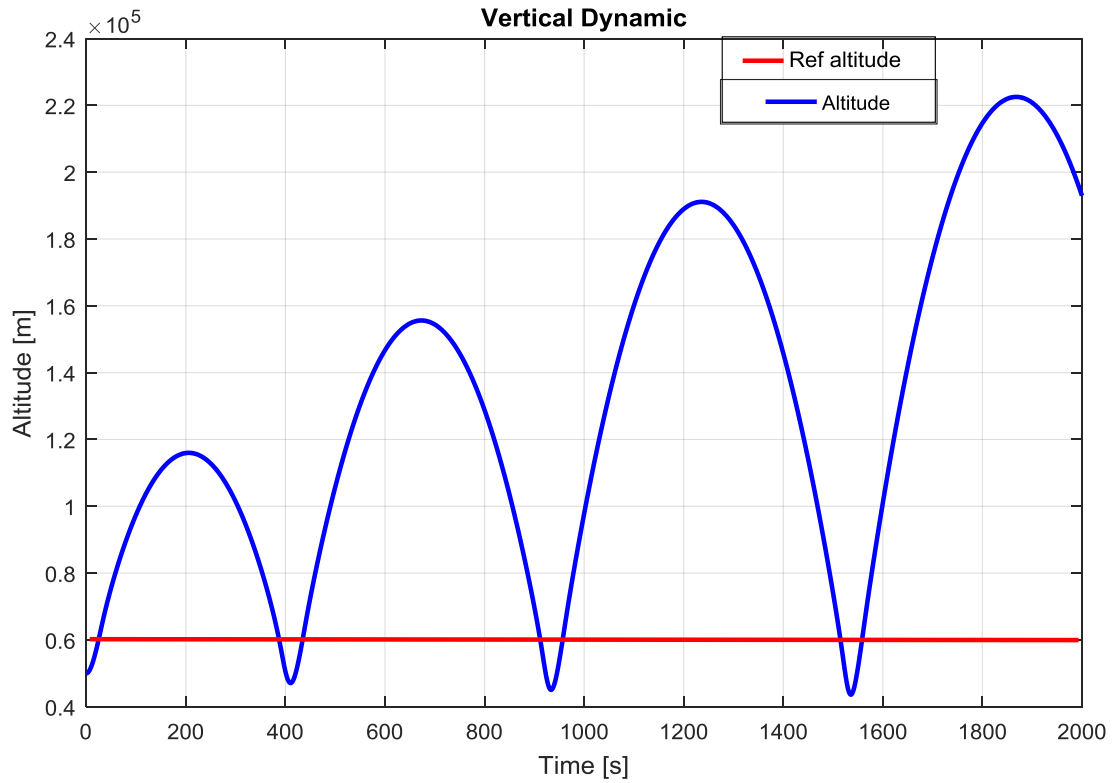


Figure 26: Vertical dynamics with PID controller with all gains set to 1.

To optimize the gains it's necessary used a Simulink tool :*"Check Custom Bounds"*. This tool checks that a signal satisfies upper and lower bounds during simulation. In this case the tested signal is the altitude. If the altitude doesn't respect the bounds the Simulink block changes parameters to optimize the model: the parameters are the PID gains. Each iteration the Simulink block testes the model and changes the parameters following an algorithm of minimization: the aim is that the response enters into the limits. The Matlab block uses the function *fmincon*, and the sequential quadratic programming algorithm (SQP) for *fmincon*. SQP is an iterative method for constrained nonlinear optimization: each iteration the algorithm solves an optimization sub problem, using a quadratic model of the objective subject to a linearization of the constraints. In this case the limits are given as combination of altitude-time, h_{rif} is the final altitude (60 Km) and h_i is the initial altitude (50 Km).

Time	0 s	100 s	300 s	600 s
Upper limit-Altitude	$h_{rif} + 5000$	$h_{rif} + 5000$	$h_{rif} + 500$	$h_{rif} + 50$
Lower limit-Altitude	h_i	$h_i + 7500$	$h_{rif} - 500$	$h_{rif} - 50$

Table 5: Upper and lower limits using in the *"Check Custom Bounds"* optimization.

After 11 iterations the optimization finishes and the results are showed in Figure 16: the curve represents the time response for each iterations, the final curve is the blue curve.

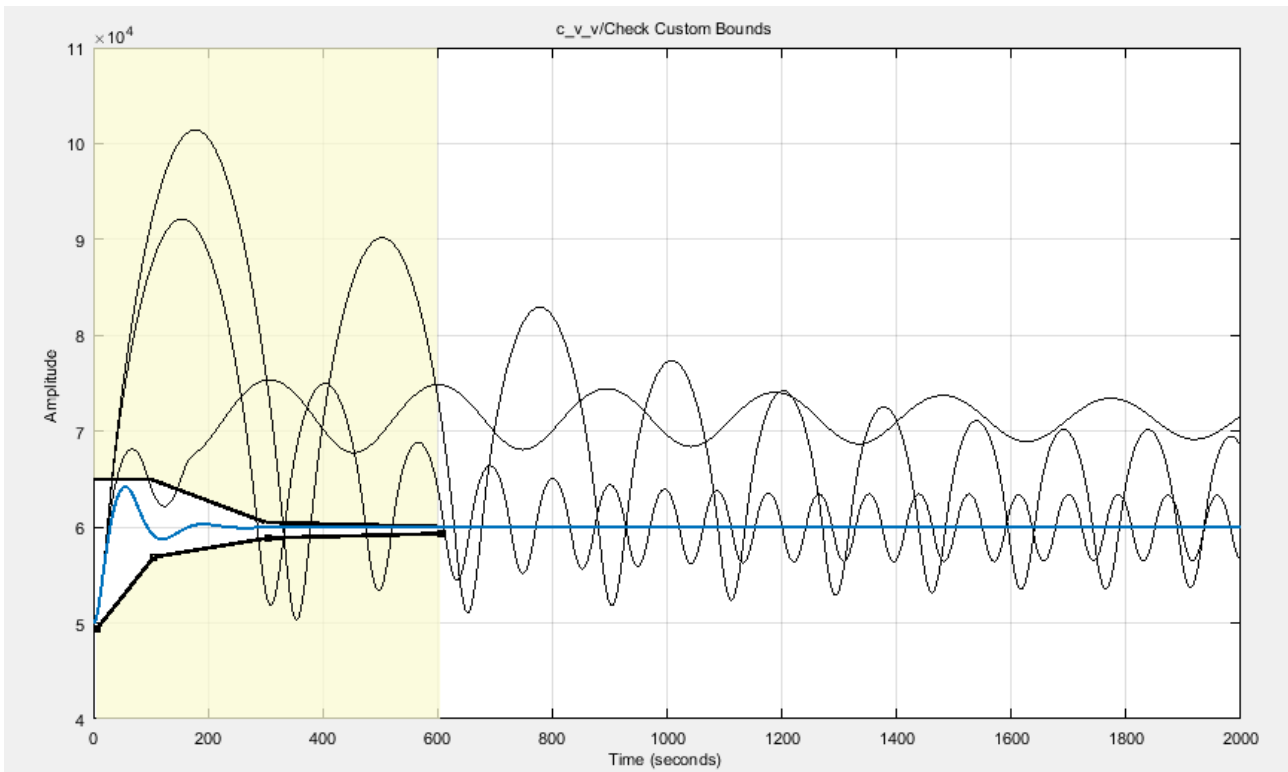


Figure 27: Vertical dynamic with optimized PID gains for each iterations.

The time response is characterized by three parameters:

- **Peak value:** it is the maximum percentage of deviation from the desired value.
- **Settling time:** it is time necessary to confine the answer in a band of amplitude $\pm 5\%$ respect to the final value.
- **Steady state error:** it's the difference between the desired value and the obtained value when the transitory it's ended.

<i>Peack value</i>	7%
<i>Settling time</i>	149,7 s
<i>Steady state error</i>	0,0035 m

Table 6: Response time for the vertical dynamics with an altitude control.

K_P	$4,14 \cdot 10^8$
K_I	$4,75 \cdot 10^7$
K_D	$1,036 \cdot 10^{10}$

Table 7: PID gains finding with first optimizations.

As the Table 8 shows the PID gain are really high, but the order of magnitude is different between the three gains. So the next step can be reducing the order of magnitude: the selected gains are written in Table 9.

K_P	0,4139
K_I	0,047
K_D	10,3638
N	0,7988

Table 8: New PID gains using for the second optimization.

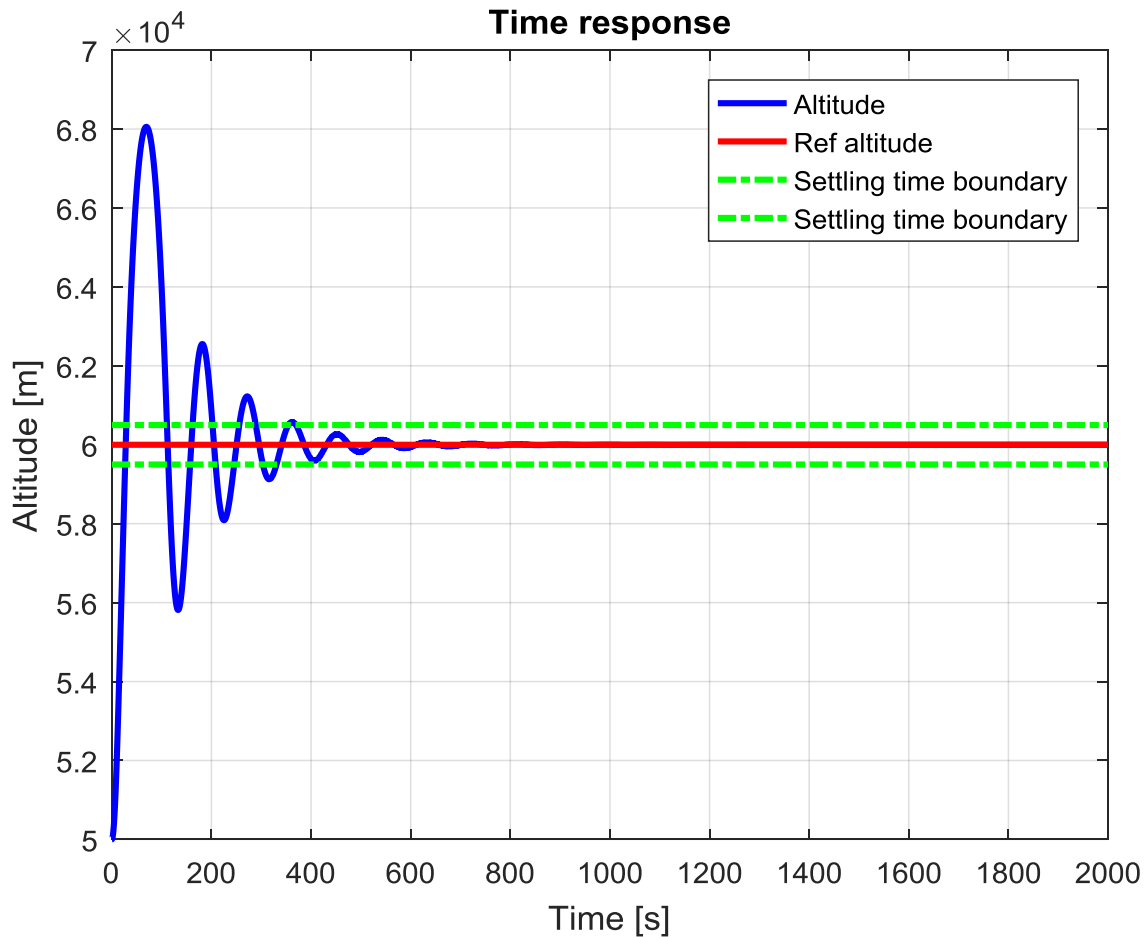


Figure 28: Time response for the vertical dynamic with the reduced PID gains:

$$K_P = 0.4139, K_D = 10.3638, K_I = 0.7988.$$

With new gains the response presents high oscillations, for this reason a second optimisation is necessary. In this optimization the PID gains values are limited and each value has a different scale variation:

	<i>Initial value</i>	<i>Max value</i>	<i>Min value</i>	<i>Scale</i>
K_P	0,4139	1	$-\text{inf}$	0,1
K_I	0,047	0,1	$-\text{inf}$	0,005
K_D	10,3638	100	$-\text{inf}$	1

Table 9: PID gains bounds for the second optimization.

After three iterations the optimization finishes and the PID gains values are changed:

K_P	0,44
K_I	0,0405
K_D	11,84
N	$20 \frac{K_P}{K_D}$

Table 10: New PID gains finding with the second optimization.

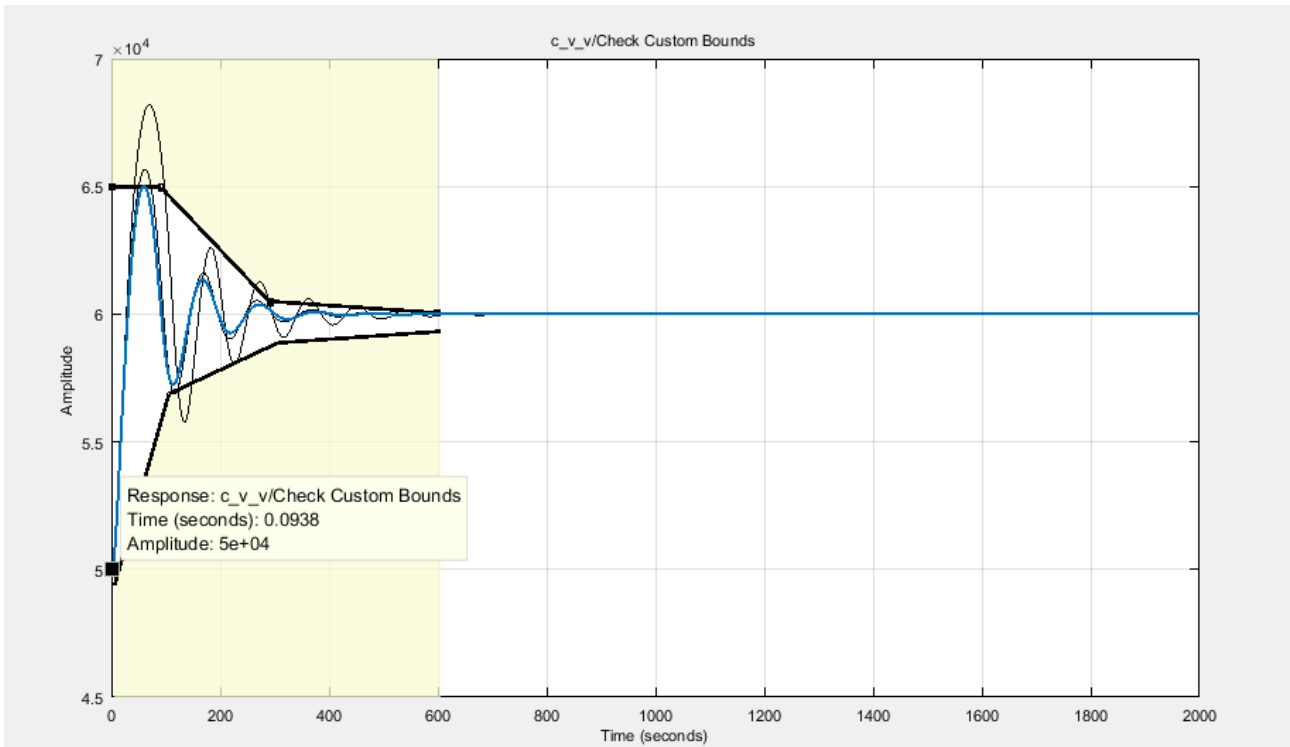


Figure 29: Time response with the PID gains obtained during the second optimization.

The better time response was obtained with high gains, for this reason the bounds are settled tangent at the curve obtained with high gains. The upper bound is settled to 64190 m for adjusting the peak value and then it's reduced for the settling time. The minimum is adjusted thanks to the lower bound settled to 58740 m.

Time	0	58 s	58 s	119 s	119 s	190 s
Upper limit: Altitude	64190	64190	60300	60300	60070	60070
Lower limit: Altitude	0	58740	58740	58740	58740	59930

Table 11: Upper and lower limits using in the "Check Custom Bounds" optimization for the third optimization.

After 4 iterations the model converges to a solution varying the PID gains and improving the time response, with a reduction of the peak value and the steady state error.

K_P	0,53
K_I	0,024
K_D	13,27
N	0,7692

Table 12: PID gains obtained with the third optimizations

<i>Peack value</i>	4,21%
<i>Settling time</i>	150,8 s
<i>Steady state error</i>	$9,46 \cdot 10^{-11} m$

Table 13: Response time for the vertical dynamics with an altitude control.

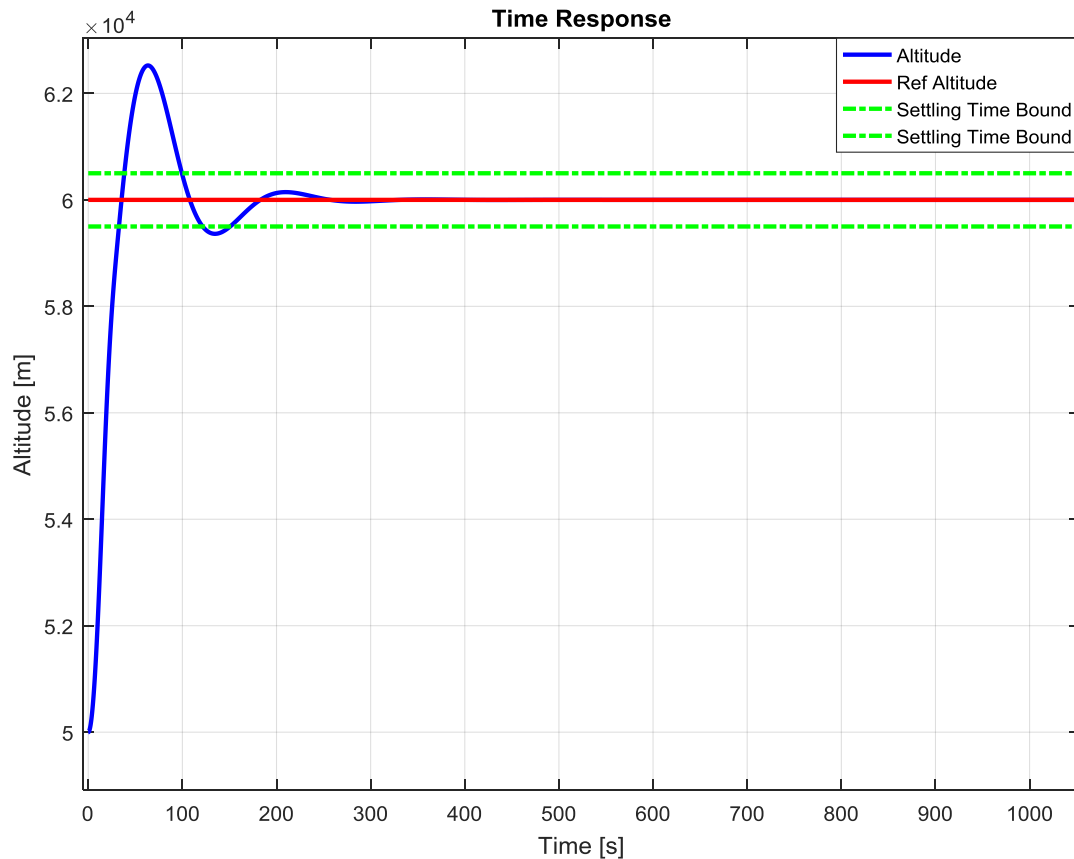


Figure 30: Time response with the PID gains obtained during the third optimization.

This gains must be used in the model with a 3-Dof dynamic where the control variable is the drag acceleration in g-s. This variable is lower in value than the altitude, in particular the two variable have two different order of magnitude. For this reason the choose gains must be increased before using them in the completed model.

K_P	50
K_I	2,4
K_D	1300
N	0,7692

Table 14: PID gains for the 3-Dof dynamic control.

2.3 Scheduled PID gains: linear system and LQT technique

The PID output is linked to the bank angle, the bank angle changes the vertical lift component. If the vehicle flies at low altitude, the lift force is greater, for this reason a smaller bank angle variation is necessary to reach the desired drag acceleration. So the PID gains decrease with altitude, keeping them constant would mean overcorrecting the error at low altitude and the vehicle drag acceleration would oscillate around the reference profile.

To study the PID gains variation it's possible to write the system as a liner system and then to study the behaviour at different dynamic pressures finding the optimal gains with an LQT technique.

Some simplifications in the 3-Dof dynamic are necessary for the system linearization:

- Earth is represented as a sphere
- Earth is non-rotating, which is allowed because the vehicle dynamic has a much higher frequency than the rotation of Earth. For this reason the frame can be assumed to be inertial
- The gravity field of the Earth is assumed to be spherical
- The vehicle trajectory is parallel to the equator

With these simplifications it's possible writing the dynamic in the ECI reference system:

$$\dot{V} = -\frac{D}{m} - g \sin \gamma \quad (18)$$

$$\dot{\gamma} = \left(\frac{V}{R_T} - \frac{g}{V} \right) \cos \gamma + \frac{L \cos \sigma}{mV} \quad (19)$$

$$\dot{R}_T = V \sin \gamma \quad (20)$$

A linearized system can be seen as an equilibrium trajectory. In this system is possible to identify state variables: these variables describe the system behaviour during the time when the system is perturbed by an external disturbance or by the pilot command. In this case the state variables are Velocity V , Flight path angle γ and distance from the Earth center R . Then we assume to create a small deviations from this equilibrium path: for this reason the state variables can be written as a sum of an equilibrium condition and a deviation. In this treatment the vehicle is not powered for this reason there isn't fuel consumption and the mass is constant.

$$V = V_0 + \Delta V \quad (21)$$

$$\gamma = \gamma_0 + \Delta \gamma$$

$$R_T = R_{T_0} + \Delta R_T$$

The bank angle is a variable using for the control (control variable), it's also written as a sum of a nominal state and a deviation:

$$\sigma = \sigma_0 + \Delta \sigma \quad (22)$$

The gravitational acceleration changes its value with the altitude, the used model is a spherical gravity model where the state variable is the distance from the Earth center. For this reason also the gravity acceleration can be written with a deviation:

$$\begin{aligned} g_0 + \Delta g &= \frac{\mu}{(R_{T_0} + \Delta R_T)^2} = \frac{\mu}{R_{T_0}^2 \left(1 + \frac{2\Delta R_T}{R_{T_0}}\right)} = \frac{\mu \left(1 - \frac{2\Delta R_T}{R_{T_0}}\right)}{R_{T_0}^2 \left(1 + \frac{2\Delta R_T}{R_{T_0}}\right) \left(1 - \frac{2\Delta R_T}{R_{T_0}}\right)} \\ &= \frac{\mu \left(1 - \frac{2\Delta R_T}{R_{T_0}}\right)}{R_{T_0}^2} \end{aligned} \quad (23)$$

Where the deviation is equal to $\Delta g = -2g_0 \frac{\Delta R_T}{R_{T_0}}$.

Substituting expression Eqs. (21)-(16) in Eqs. (18)-(19)-(20), neglecting higher-order terms as the product between deviations and the deviations pow, approximating the cosine of a deviation with 1 and the sine of a deviation with the deviation and subtracting the nominal states ($\dot{V}_0 = -\frac{D_0}{m} - g_0 \sin \gamma_0$, $\dot{\gamma}_0 = \left(\frac{V_0}{R_{T_0}} - \frac{g_0}{V_0}\right) \cos \gamma_0 + \frac{L_0 \cos \sigma_0}{mV_0}$, $\dot{R}_{T_0} = V_0 \sin \gamma_0$), the system becomes the following:

$$\Delta \dot{V} = -\frac{\Delta D}{m} + 2 \frac{g_0}{R_{T_0}} \sin \gamma_0 \Delta R_T - g_0 \cos \gamma_0 \Delta \gamma \quad (24)$$

$$\begin{aligned} \Delta \dot{\gamma} &= \left(-\frac{\dot{\gamma}_0}{V_0} + \frac{2 \cos \gamma_0}{R_{T_0}}\right) \Delta V + \left(\frac{2g_0}{R_{T_0}} - \frac{V_0^2}{R_{T_0}^2}\right) \frac{\cos \gamma_0}{V_0} \Delta R_T - \left(\frac{V_0^2}{R_{T_0}} - g_0\right) \frac{\sin \gamma_0}{V_0} \Delta \gamma \\ &\quad - \frac{L_0}{mV_0} \sin \sigma_0 \Delta \sigma + \frac{\cos \sigma_0}{mV_0} \Delta L \end{aligned} \quad (25)$$

$$\Delta \dot{R}_T = \sin \gamma_0 \Delta V + V_0 \cos \gamma_0 \Delta \gamma \quad (26)$$

Also the forces must be written as a function of state and control variables. Lift and drag are function of flight parameters as Mach number M , angle of attack α and altitude h :

$$\Delta D = \frac{\delta D}{\delta M} \Delta M + \frac{\delta D}{\delta \alpha} \Delta \alpha + \frac{\delta D}{\delta h} \Delta h \quad (27)$$

$$\Delta L = \frac{\delta L}{\delta M} \Delta M + \frac{\delta L}{\delta \alpha} \Delta \alpha + \frac{\delta L}{\delta h} \Delta h \quad (28)$$

To evaluate the partial derivatives, the aerodynamic forces are written as:

$$D = C_D q S_{ref} \quad (29)$$

$$L = C_L q S_{ref}$$

Where C_L and C_D are the aerodynamic coefficients function of Mach, Alpha and altitude, q is the dynamic pressure written as $q = \frac{1}{2} \rho V^2$ and function of velocity and altitude, S_{ref} is the reference area.

In this case the aerodynamic coefficients aren't function of the altitude, this means that $\frac{\delta C_L}{\delta h} = 0$ and $\frac{\delta C_D}{\delta h} = 0$. The angle of attack α is constant until a Mach of 2.4, then for lower Mach the angle of attack varies. The linearized model, in particular, is used until a Mach equal to 3, so the Angle of Attack is constant, this means that $\frac{\delta C_L}{\delta \alpha} = 0$ and $\frac{\delta C_D}{\delta \alpha} = 0$. For all these reasons the aerodynamic forces are only functions of Mach:

$$\frac{\delta D}{\delta M} = \frac{\delta C_D}{\delta M} q S_{ref} + \frac{\delta q}{\delta M} C_D S_{ref} \quad (30)$$

$$\frac{\delta L}{\delta M} = \frac{\delta C_L}{\delta M} q S_{ref} + \frac{\delta q}{\delta M} C_L S_{ref} \quad (31)$$

The Mach number is equal to the ratio between the velocity V and the speed of sound a :

$$M = \frac{V}{a} \quad (32)$$

Substituting the Eq. (32) in the partial derivative $\frac{\delta q}{\delta M}$ and in the deviation ΔM :

$$\frac{\delta q}{\delta M} = \frac{1}{2} \frac{\delta(\rho M^2 a^2)}{\delta M} = \rho_0 a_0^2 M_0 = \frac{\rho_0 V_0^2}{M_0} = \frac{2q_0}{M_0} \quad (33)$$

$$\Delta M = \Delta \left(\frac{V}{a} \right) = \frac{1}{a_0} \Delta V = \frac{M_0}{V_0} \Delta V \quad (34)$$

Summarising, the aerodynamic forces can be written as follow:

$$\Delta D = \left(\frac{M_0}{V_0} \frac{\delta C_D}{\delta M} + \frac{2C_D}{V_0} \right) q_0 S_{ref} \Delta V \quad (35)$$

$$\Delta L = \left(\frac{M_0}{V_0} \frac{\delta C_L}{\delta M} + \frac{2C_L}{V_0} \right) q_0 S_{ref} \Delta V \quad (36)$$

Now the equations of motion are linearized and so they can be written in a matrix form, this form is called state-space form:

$$\dot{x} = Ax + Bu \quad (37)$$

$$y = Cx \quad (38)$$

The states x are variables that describe the system during the time: they are indices of the energy stored in the system and its distribution. In this case the vehicle states are velocity, altitude and flight path angle. The input vector u contains the variables that destabilize the system. The output vector y contains the variables measured by the sensors. The matrix A describes the link between the states and the matrix B describes how the input influences the system. The input vector contains only a variable: the bank angle. In fact to change the drag acceleration following a reference signal the system uses the bank angle, for this reason this variable is a control variable.

To study the closed loop we need to linearize also the PID controller, but the choice is excluding the integrative term because this term is affected by the saturation, a non-linear phenomenon that occurs a lot of time during the simulations.

The input of the proportional term is the error e , the output of the proportional term is equal to the input. The error e is the difference between the reference drag acceleration and the vehicle drag acceleration.

To write the derivative term and the low pass filter is necessary introducing a new variable η : this variable is the output of the derivative term with low pass filter. The output is function of the error:

$$\frac{\eta}{e} = \frac{s}{\frac{s}{N} + 1} \quad (39)$$

The ratio $\frac{\eta}{e}$ is another new variable called η_N , remembering that a variable multiplied by the imaginary variable s is equal to the derivate of the variable the system becomes:

$$\dot{\eta}_N = -N\eta_N + Ne \quad (40)$$

In this case the state variable of the derivative term is η_N . But $\dot{\eta}_N = \eta_N s = \eta$ so we can write an second equation, where η is the output of the derivative term-low pass filter state space system:

$$\eta = -N\eta_N + Ne \quad (41)$$

The error is also function state variables: it's written as the difference between the reference signal r and the performance output z . The performance output is the tracked signal that the control system want to check following the reference signal r : in this case the performance output is equal to the drag acceleration in g-s and it's written as function of state variable ΔV .

$$e = r - z \quad (42)$$

$$z = Hx = \frac{\Delta D}{mg_0} \quad (43)$$

But we remember that in the system the real input isn't the bank angle but the $\cos \sigma$, so linearizing the bank angle the control input becomes:

$$u = \cos(\sigma_0 + \Delta\sigma) = \cos \sigma_0 - \sin \sigma_0 \Delta\sigma \quad (44)$$

In the $\Delta\dot{\gamma}$ equation appears the term $\Delta\sigma$ that it's written as $\Delta\sigma = -\frac{u}{\sin \sigma_0} + \frac{\cos \sigma_0}{\sin \sigma_0}$, substituting it in the $\Delta\dot{\gamma}$ equation remains a constant term equal to $-\frac{L_0}{m V_0} \cos \sigma_0$:

$$\begin{aligned} \Delta\dot{\gamma} = & \left(-\frac{\dot{\gamma}_0}{V_0} + \frac{2 \cos \gamma_0}{R_{T_0}} \right) \Delta V + \left(\frac{2g_0}{R_{T_0}} - \frac{V_0^2}{R_{T_0}^2} \right) \frac{\cos \gamma_0}{V_0} \Delta R_T - \left(\frac{V_0^2}{R_{T_0}} - g_0 \right) \frac{\sin \gamma_0}{V_0} \Delta \gamma \\ & + \frac{\cos \sigma_0}{m V_0} \Delta L + \frac{L_0}{m V_0} u - \frac{L_0}{m V_0} \cos \sigma_0 \end{aligned} \quad (45)$$

The effect of this constant term $-\frac{L_0}{m V_0} \cos \sigma_0$ in the dynamic can be studied introducing a new state variable f : this variable must stay constant and equal to 1, in this matter each step of integration a constant term is added to the $\Delta\dot{\gamma}$ equation.

But this approach is only theatrical, because if \dot{f} is equal to zero, the matrix A will have a null row and it will become not invertible. The matrix A must be invertible to apply the LQR technique used in the PID gain optimization: for this reason \dot{f} will be written as function of f :

$$f_0 = 1 \text{ Initial value for the state variable } f$$

$$\dot{f} = a_{66}f \rightarrow \Delta f \text{ Added equation that explains the variation law of } f \quad (46)$$

$$f_{new} = f_0 + \Delta f \cong f_0 \cong 1 \text{ New value for the state variable } f$$

The coefficient a_{66} is a small coefficient, equal to 10^{-15} , the matrix A becomes invertible and variation of f is neglected and doesn't influence the dynamic.

So the Eq. 45 becomes the following and in the last term appears f :

$$\Delta\dot{\gamma} = \left(-\frac{\dot{\gamma}_0}{V_0} + \frac{2 \cos \gamma_0}{R_{T_0}}\right) \Delta V + \left(\frac{2g_0}{R_{T_0}} - \frac{V_0^2}{R_{T_0}^2}\right) \frac{\cos \gamma_0}{V_0} \Delta R_T - \left(\frac{V_0^2}{R_{T_0}} - g_0\right) \frac{\sin \gamma_0}{V_0} \Delta \gamma + \frac{\cos \sigma_0}{m V_0} \Delta L + \frac{L_0}{m V_0} u - \frac{L_0}{m V_0} \cos \sigma_0 f$$

The augmented system is written joining all these elements:

$$\begin{Bmatrix} \Delta\dot{V} \\ \Delta\dot{\gamma} \\ \Delta\dot{R}_T \\ \dot{\eta}_N \\ \dot{f} \end{Bmatrix} = \begin{bmatrix} a_{11} & a_{12} & a_{13} & 0 & 0 \\ a_{21} & a_{22} & a_{23} & 0 & a_{26} \\ a_{31} & a_{32} & 0 & 0 & 0 \\ a_{51} & 0 & 0 & a_{55} & 0 \\ 0 & 0 & 0 & 0 & a_{66} \end{bmatrix} \begin{Bmatrix} \Delta V \\ \Delta \gamma \\ \Delta R_T \\ \eta_N \\ f \end{Bmatrix} + \begin{bmatrix} 0 \\ b_{21} \\ 0 \\ 0 \\ 0 \end{bmatrix} u + \begin{bmatrix} 0 \\ 0 \\ 0 \\ g_{51} \\ 0 \end{bmatrix} r \quad (47)$$

$$\begin{Bmatrix} y_P \\ \eta \end{Bmatrix} = \begin{bmatrix} c_{11} & 0 & 0 & 0 & 0 \\ c_{31} & 0 & 0 & c_{35} & 0 \end{bmatrix} \begin{Bmatrix} \Delta V \\ \Delta \gamma \\ \Delta R_T \\ \eta_N \\ f \end{Bmatrix} + \begin{bmatrix} 0 \\ 0 \end{bmatrix} u + \begin{bmatrix} f_{11} \\ f_{31} \end{bmatrix} r \quad (48)$$

The individual terms are the following:

$$a_{11} = -\frac{1}{m} \left(\frac{M_0}{V_0} \frac{\delta C_D}{\delta M} + \frac{2C_D}{V_0} \right) q_0 S_{ref}$$

$$a_{12} = -g_0 \cos \gamma_0$$

$$a_{13} = 2 \frac{g_0}{R_{T_0}} \sin \gamma_0$$

$$a_{21} = -\frac{\dot{\gamma}_0}{V_0} + \frac{2 \cos \gamma_0}{R_{T_0}} + \frac{\cos \sigma_0}{m V_0} \left(\frac{M_0}{V_0} \frac{\delta C_L}{\delta M} + \frac{2C_L}{V_0} \right) q_0 S_{ref}$$

$$a_{22} = -\left(\frac{V_0^2}{R_{T_0}} - g_0 \right) \frac{\sin \gamma_0}{V_0}$$

$$a_{23} = \left(\frac{2g_0}{R_{T_0}} - \frac{V_0^2}{R_{T_0}^2} \right) \frac{\cos \gamma_0}{V_0}$$

$$\begin{aligned}
a_{26} &= -\frac{L_0}{m V_0} \cos \sigma_0 \\
a_{31} &= \sin \gamma_0 \\
a_{32} &= V_0 \cos \gamma_0 \\
a_{51} &= -\frac{N}{m g_0} \left(\frac{M_0}{V_0} \frac{\delta C_D}{\delta M} + \frac{2 C_D}{V_0} \right) q_0 S_{ref} \\
a_{55} &= -N \\
a_{66} &= 10^{-15} \\
b_{21} &= \frac{L_0}{m V_0} \\
g_{51} &= N \\
c_{11} &= -\frac{1}{m g_0} \left(\frac{M_0}{V_0} \frac{\delta C_D}{\delta M} + \frac{2 C_D}{V_0} \right) q_0 S_{ref} \\
c_{31} &= -\frac{N}{m g_0} \left(\frac{M_0}{V_0} \frac{\delta C_D}{\delta M} + \frac{2 C_D}{V_0} \right) q_0 S_{ref} \\
c_{35} &= -N \\
f_{11} &= 1 \\
f_{31} &= N
\end{aligned} \tag{49}$$

In compact form the system can be written as follow:

$$\dot{x} = \begin{Bmatrix} \Delta \dot{V} \\ \Delta \dot{\gamma} \\ \Delta \dot{R}_T \\ \dot{\eta}_N \\ \dot{f} \end{Bmatrix} = Ax + Bu + Gr \tag{50}$$

$$y = \begin{Bmatrix} y_P \\ \eta \end{Bmatrix} = Cx + Du + Fr$$

When the loop is closed the input is written as a function of the output $y = \begin{Bmatrix} y_P \\ \eta \end{Bmatrix}$ using a matrix K , this matrix contains the PID gains: the closed loop is a controlled system, the gains are chosen to have a stable system with zero-based stationary error.

$$u = -Ky = [-K_P \quad -K_D] \begin{Bmatrix} y_P \\ \eta \end{Bmatrix} \tag{51}$$

Substituting Eq. (51) in Eq.

(50) the closed loop system acquires the following form:

$$\dot{x} = [A - BKC]x + [G - BKF]r = A_{CL}x + B_{CL}r$$

(52)

$$y = Hx$$

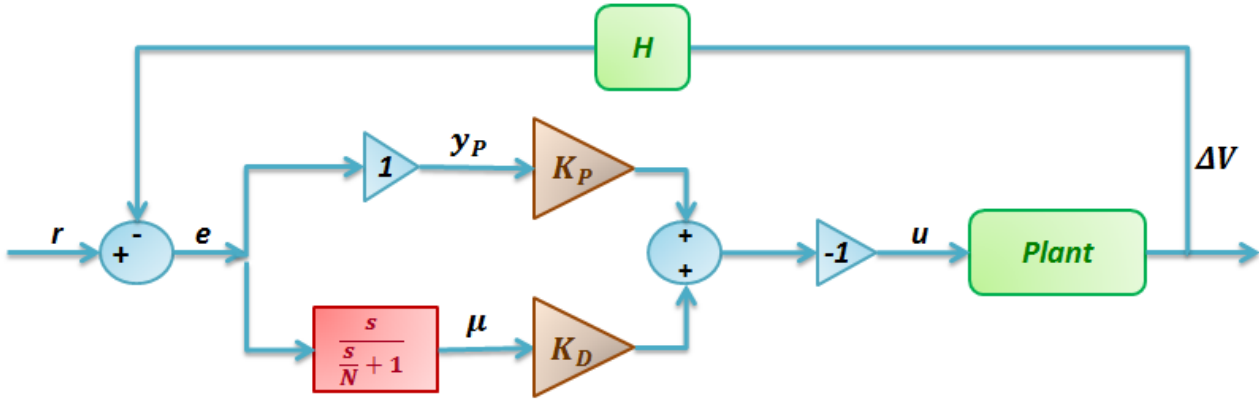


Figure 31: Vehicle closed loop structure.

It's really important to remember that the linear system works with infinitesimal order terms, for that reason the reference signal r is the difference between the acceleration drag in equilibrium conditions (initial condition) and the final desired drag both expressed in g-s.

The next step is the selection of the optimal PID gains: the system must have robustness proprieties, working well if there are disturbances or uncertainties, respecting the desired specifications and following a reference signal. The performance specifications are often given in terms of time-domain criteria and this criteria are related to the step response, for this reason the input signal $r(t)$ will be a step command with magnitude r . If the system has a good response for a step signal, it will have a good behaviour for all the other signals, because the step is the signal that causes the greatest aerodynamic ,structural and energetic stresses.

To define the PID gains can be used a technique named LQT: this technique works with a deviation system. Urging the system with a step input $r(t)$, the system answers with a dynamic and the states $x(t)$ can be seen as a sum between a steady-state value x_{ss} and his deviation during the time from this value $\delta x(t)$.

$$\left\{ \begin{array}{l} \delta x(t) = x(t) - x_{ss} \\ \delta y(t) = y(t) - y_{ss} = C\delta x(t) \\ \delta z(t) = z(t) - z_{ss} = H\delta x(t) \\ \delta u(t) = u(t) - u_{ss} = -KC\delta x(t) \\ \delta e(t) = e(t) - e_{ss} = (r - Hx(t)) - (r - Hx_{ss}) = -H\delta x(t) = -\delta z(t) \end{array} \right. \quad (53)$$

If the closed loop system is asymptotically stable, A_{CL} is non-singular and, at steady conditions, the dynamic equation is the following:

$$\dot{x}_{ss} = 0 = A_{CL}x_{ss} + B_{CL}r \rightarrow x_{ss} = -A_{CL}^{-1}B_{CL}r \quad (54)$$

The closed-loop dynamics of the state deviation are seen to be:

$$\begin{cases} \delta\dot{x}(t) = A_{CL}\delta x(t) \\ \delta y(t) = C\delta x(t) \\ \delta z(t) = H\delta x(t) = -\delta e(t) \\ \delta u(t) = -KC\delta x(t) \end{cases} \quad (55)$$

In this matter the step-response problem has been converted to a regular problem for the deviation system:

$$\delta\dot{x}(t) = A\delta x(t) + B\delta u(t) \quad (56)$$

The first objective of LQT technique is minimize the tracking error $e(t)$, this problem can be spilled in two different problems: regulating the error deviation $\delta e(t)$ to zero and making the steady-state error e_{ss} small. These problems are solved choosing the PID gains in K that minimize a performance index J written in the following matter:

$$J = \frac{1}{2} \int_0^{\infty} (\delta e^T \delta e + \delta u^T R \delta u) dt + \frac{1}{2} e_{ss}^T V e_{ss} \quad (57)$$

R and V are two weight matrix, their values are chosen with trade-off analysis for the optimization of the dynamic system behaviour. If the system is of type 1 (this happens when there is an integrator in the system) the steady-state error is automatically zero, so V is set equal to zero. In our case the linear system has only a PD controller, but the real dynamic system contains also the integrator term. For this reason the stationary behaviour is ignored setting V equal to zero. The matrix R is a square matrix with a dimension equal to the number of columns of B . This matrix can be selected equal to $R = r_{cost}I$, where r_{cost} is a constant number, this matrix is linked to the command influence, so if r_{cost} is big the system doesn't feel the influence of the command. To understand the order of magnitude of r_{cost} the maximum permissible deviations can be used:

$$r_{cost} = \frac{1}{u_m^2} \quad (58)$$

Where u_m is the maximum variation that the command can have. In our case the command u is linked to the bank angle, that can assume a value between 0 and 90°. For this reason u_m is chosen equal to $\frac{\pi}{2}$.

Remembering that the error deviation is linked to the state vector, the performance index can assume a second form:

$$J = \frac{1}{2} \int_0^{\infty} (\delta x^T H^T H \delta x + \delta u^T R \delta u) dt + \frac{1}{2} e_{ss}^T V e_{ss} \quad (59)$$

The matrix $H^T H$ is another weight matrix, named Q .

To simplify the problem is possible introduced a new matrix $P \geq 0$, that satisfies the Lyapunov equation g with a new performance index:

$$g \equiv A_{CL}^T P + P A_{CL} + C^T K^T R K C + Q \quad (60)$$

$$J = \frac{1}{2} \text{tr}(P X) + \frac{1}{2} e_{ss}^T V e_{ss} \quad (61)$$

The matrix X contains the initial deviations of the states:

$$X \equiv \delta x(0) \delta x^T(0) \quad (62)$$

$$\delta x(0) = x(0) - x_{ss} \quad (63)$$

At the initial time the vehicle is trimmed and all the states are equal to zero: the only exception is the added state f , it's initial value is 1.

$$x(0) = [\Delta V_0 \ \Delta \gamma_0 \ \Delta R_0 \ \eta_{N_0} \ f_0]^T = [0 \ 0 \ 0 \ 0 \ 1]^T \quad (64)$$

The LQT problem provides the determination of optimal gains in K , minimizing J with the constraint on P imposed by the Lyapunov equation.

The optimal solution can be determined with numerical algorithms of minimization: it is necessary to determine the Hamiltonian function and place the partial derivatives respect to S, P, K equal to zero:

$$H = \text{tr}(P X) + \text{tr}(g S) + \frac{1}{2} e_{ss}^T V e_{ss} \quad (65)$$

$$\frac{\delta H}{\delta S} = g = A_{CL}^T P + P A_{CL} + C^T K^T R K C + Q = 0 \quad (66)$$

$$\frac{\delta H}{\delta P} = A_{CL} S + S A_{CL}^T + X = 0 \quad (67)$$

$$\frac{1}{2} \frac{\delta H}{\delta K} = RKCSCT - B_{CL}^T PSC^T + B_{CL}(A_{CL}^{-1})^T (P + H^T V H) x_{ss} y_{ss}^T - B_{CL}^T (A_{CL}^{-1})^T H^T V r y_{ss}^T = 0 \quad (68)$$

Now to solve the problem can be used the *Moerder-Calise (1985)* iterative algorithm explained in Figure 32. It's important explained that K' is the matrix K finding solving the Eq. (62). The algorithm converge to a minimum of J and, when this happens, the difference between the performance index, calculated in two different iterations, is really small, tending to zero. So it's possible to set this difference with a chosen value, named *toll*, and stop the iterations when it's reached this value.

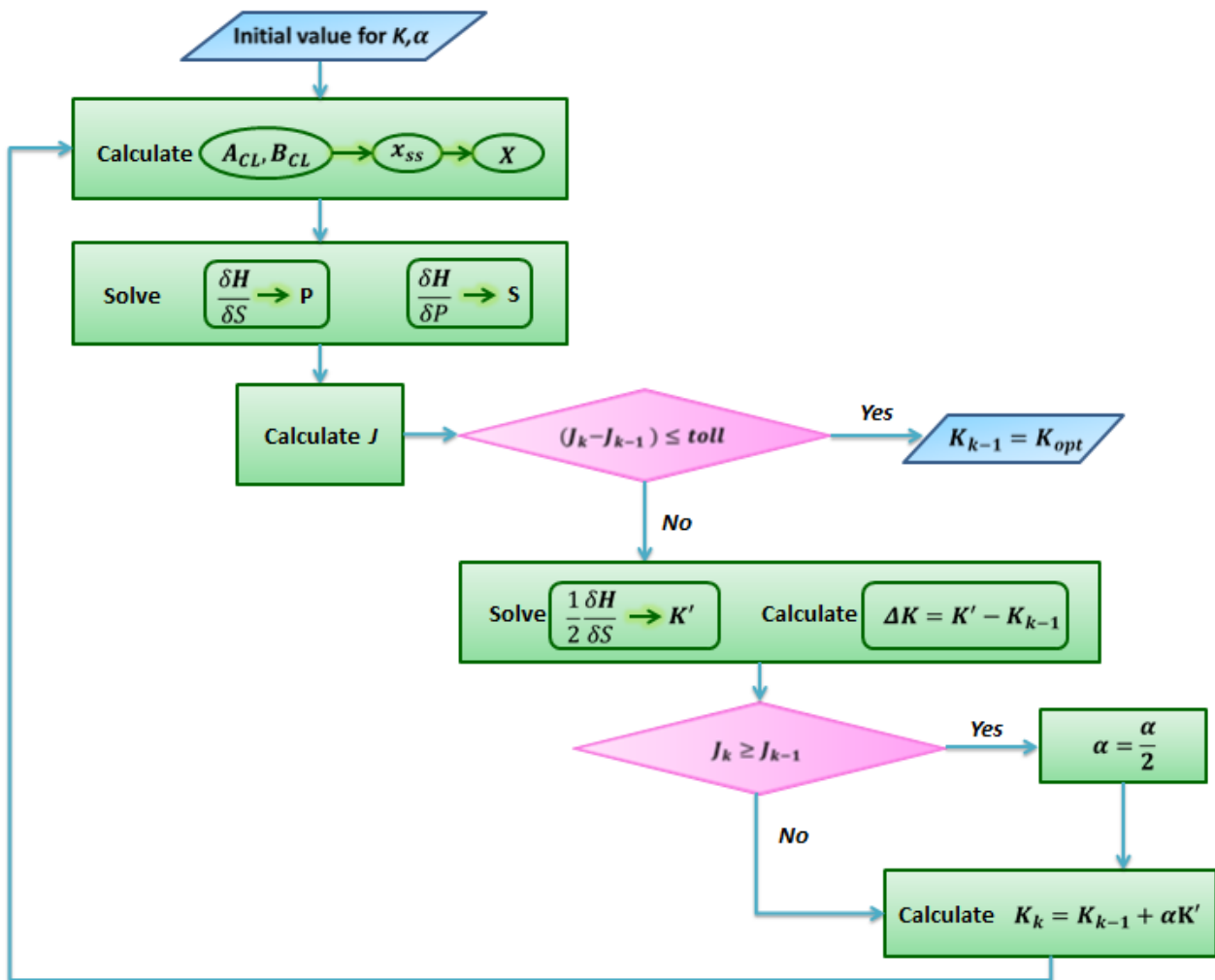


Figure 32: Flow chart for *Moerder-Calise (1985)* algorithm

The basic idea is that if α is sufficiently small the algorithm converge to a minimum: if the results give a performance index higher than the previous one, this means that α is too big and for this reason α is helved. Knowing α it's possible updating the value of K and continuing the iteration. Now we have a reference drag acceleration profile, the PID controller, with the gains found in the chapter 2.2, follows this profile, but the error between reference profile and real drag acceleration is really big, because the optimal

gains change with the dynamic pressure, if the dynamic pressure rises, the PID gains must decrease. So it's possible use the LQT technique for the optimisations of the gains as function of dynamic pressure:

- Chose a point from the drag acceleration profile, this point is seen as an equilibrium condition. The chosen point corresponds to the point that has a determinate dynamic pressure. From this point extrapolate the value of the lift, velocity, flight path angle, gravity acceleration, mass, Mach, C_L , C_D , distance from the Earth center, bank angle, acceleration drag, slope in C_L and C_D curves. These points are chosen to have a variation of the dynamic pressure of about 500 Pa between two following points, starting form a dynamic pressure of 1500, arriving at a dynamic pressure of 5000

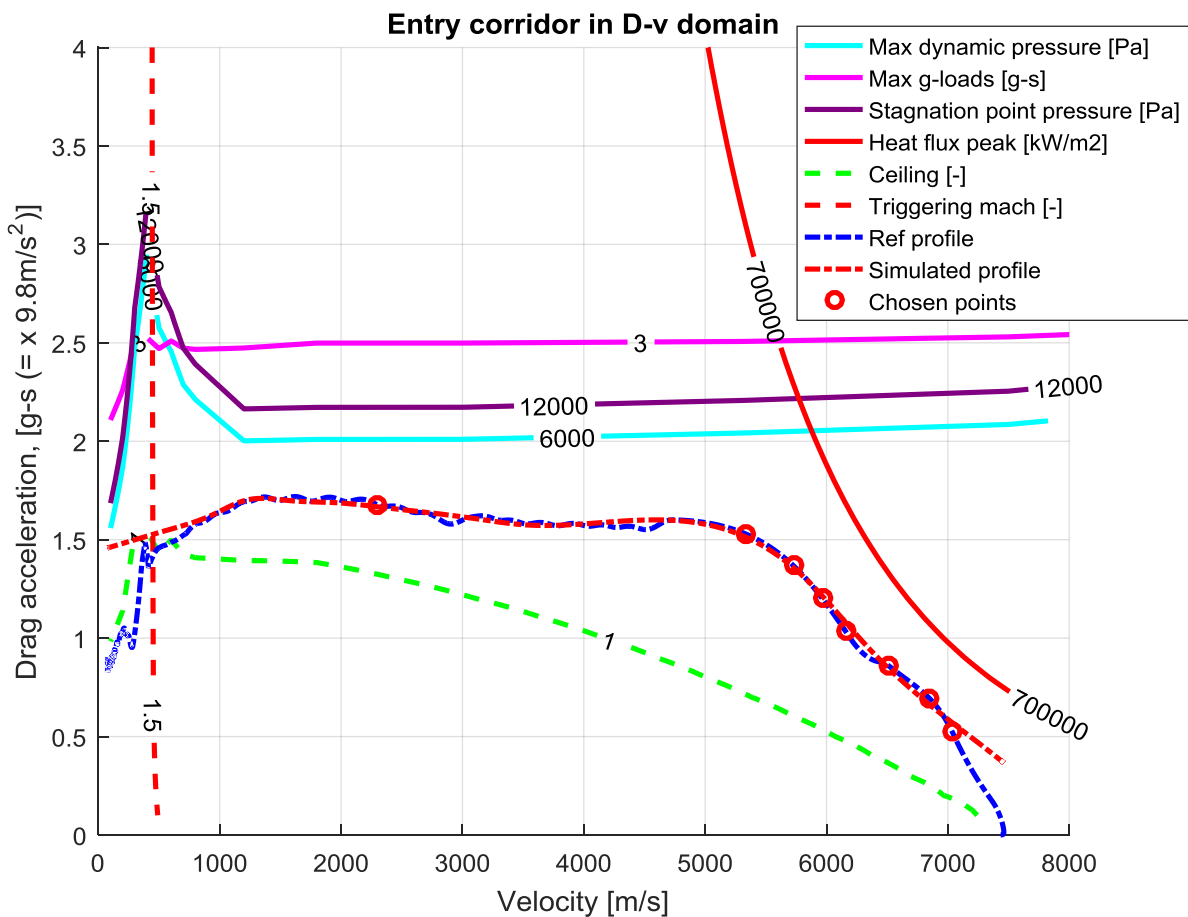


Figure 33: Medium reference profile (curve red) and vehicle acceleration drag (curve blue) with PID gains of Table 14. The red points are the chosen points for the LQT technique.

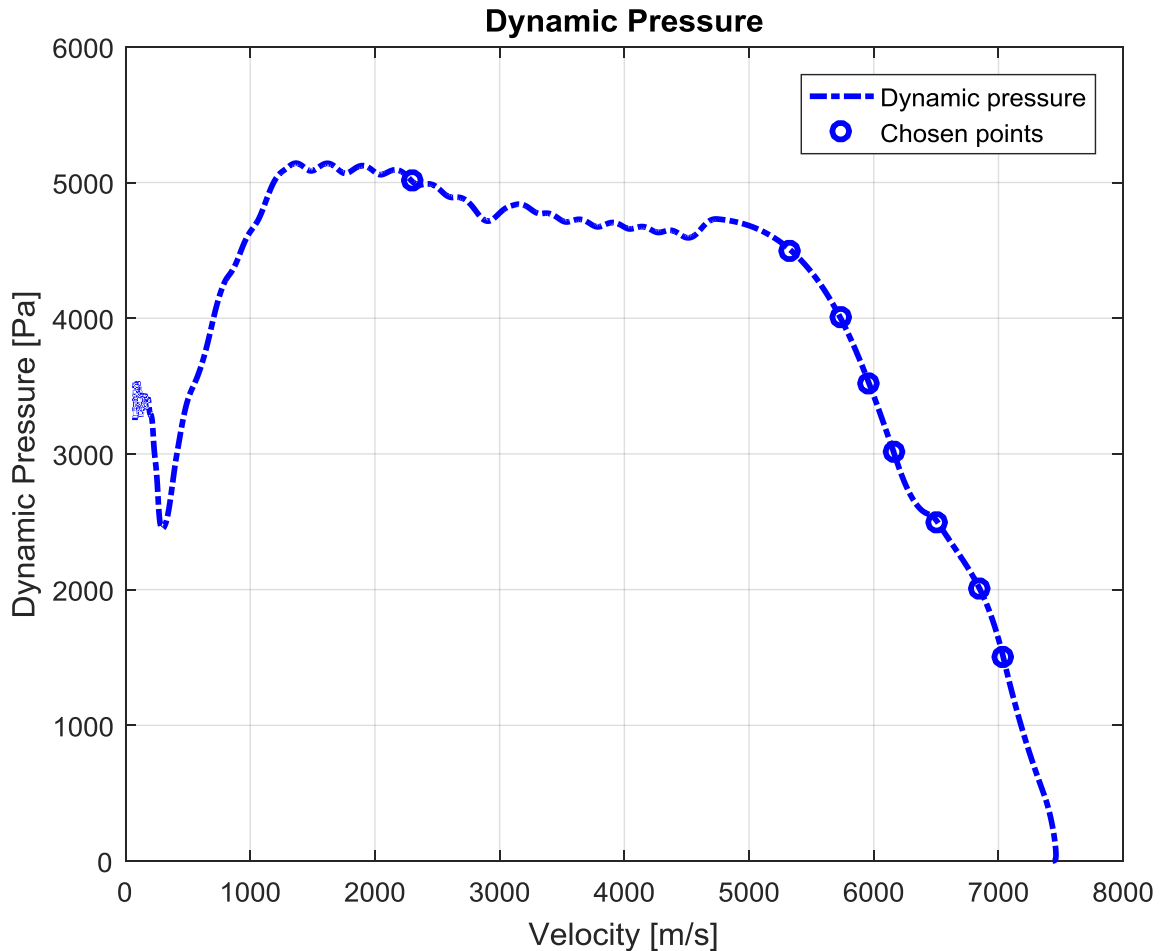


Figure 34: Dynamic pressure for a vehicle that follow the medium profile with a PID controller (PID gain of Table 14). The blue points are the chosen points for the LQT technique.

- Chose a reference drag acceleration r : this value is set equal to 0,1 for all the simulations.
- Chose the initial PID gains K_0 : these values are greater than the values found in the chapter 2.2 because, in the nonlinear dynamic is present the integrative term, but now, in the linear system this term is absent. Its function must be performed only by the other two terms, so they must give a stronger control action, making tend to zero the steady-state error. The initial values are chosen analysing the trajectory with the maximum range. This process will be explained in the next paragraph.
- Chose the initial value of α : in this case α is a vector. There is a value for the derivative term α_D and a value for the proportional term α_P . The α_P is smaller than α_D because the proportional gain is one order of magnitude less than the derivative gain. The α values are chosen analysing the first value of $\Delta K = [\Delta K_P, \Delta K_D]$: calculating K' using the initial conditions for a dynamic pressure of 1500 Pa and the PID gains K_0 , placing $\alpha_P = \frac{1}{\Delta K_P}$ and $\alpha_D = \frac{100}{\Delta K_D}$. In this matter in the first iterations the value K_P will change of 1 and the value K_D will change of 100. These value are used for a dynamic pressure of 1500 Pa, where, with the initial gains K_0 , the time response presents a good behaviour, with only one peak and absence of oscillations. If the dynamic pressure increases the behaviour with the initial gains K_0 changes a lot: the time response presents high oscillations, with lower settling time and steady-state error. For this reason to reduce the oscillations is necessary to

change more the PID gains: the initial values for α increases and the algorithm converges to a lower PID gains, because with each iteration the PID gains have a greater variation.

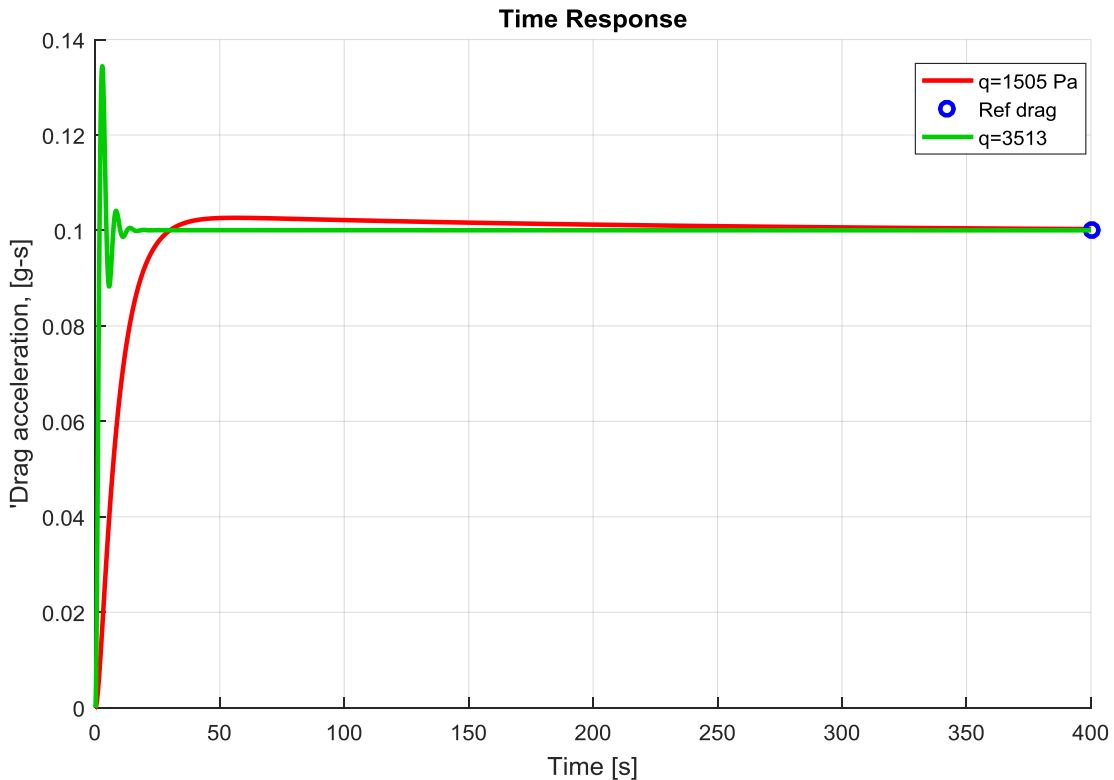


Figure 35: Time response of a linearized system for two different initial conditions: the green curve has an initial dynamic pressure of 3513 Pa and the red curve has an initial dynamic pressure of 1505 Pa. The PID gains are equal to $K_p = 120 * 100$ and $K_D = 2400 * 1000$.

- Chose the *toll* value: it is set equal to $5 * 10^{-10}$

It's necessary to choose the PID initial values: we know that with a lower pressure the gains must be high. The dynamic pressure is function of altitude and velocity, so if the vehicle loses altitude quickly, the vehicle will be at low altitude, where the density is high, with high speed and this will lead to high dynamic pressure. But if the vehicle loses velocity at high altitude, during the trajectory, the reached dynamic pressure will be lower: this condition is verified if the vehicle trajectory is near the ceiling. So when the vehicle is near the ceiling the PID gains will have their maximum value because a low dynamic pressure means low aerodynamic forces. So it's possible perform a sensitivity analysis, to find the PID gains that minimize the integrated error following a trajectory near the ceiling condition. K_p varies from 10 to 500 with a step of 10 and K_D varies from 100 to 5000 with a step of 100. The integrated error is calculated until reaching a dynamic pressure of 3700 Pa.

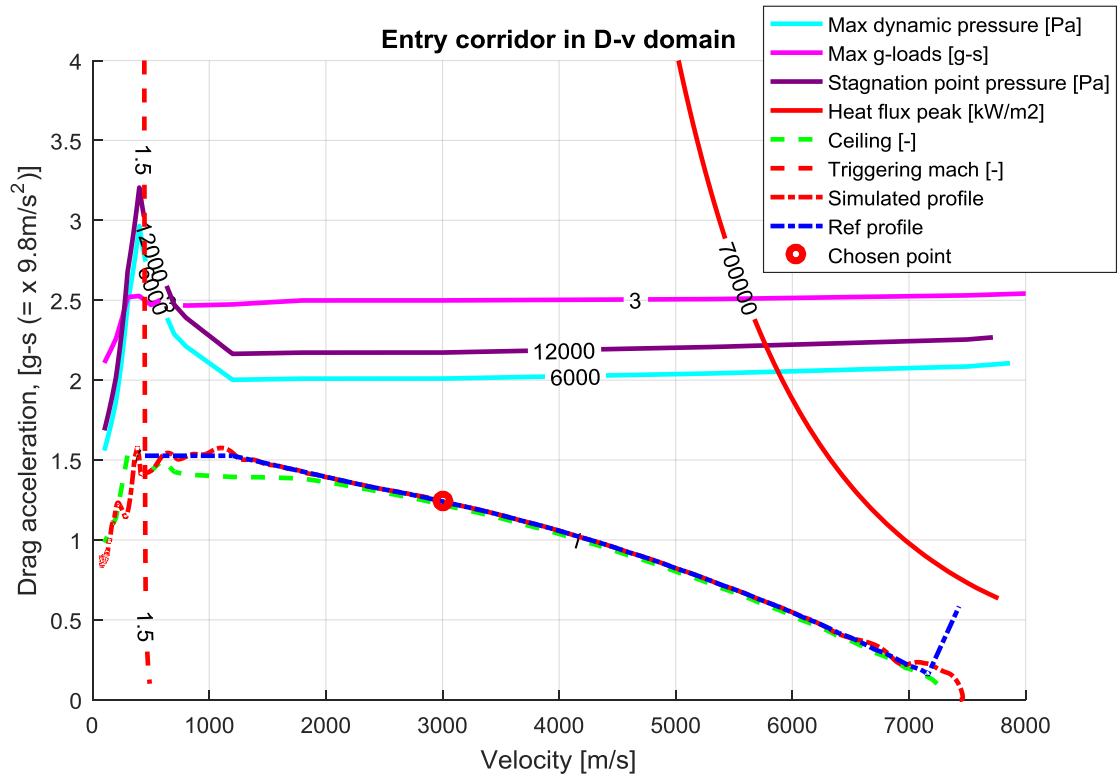


Figure 36: Lower reference profile (curve red) and vehicle acceleration drag (curve blue) with PID gains of Table 14.

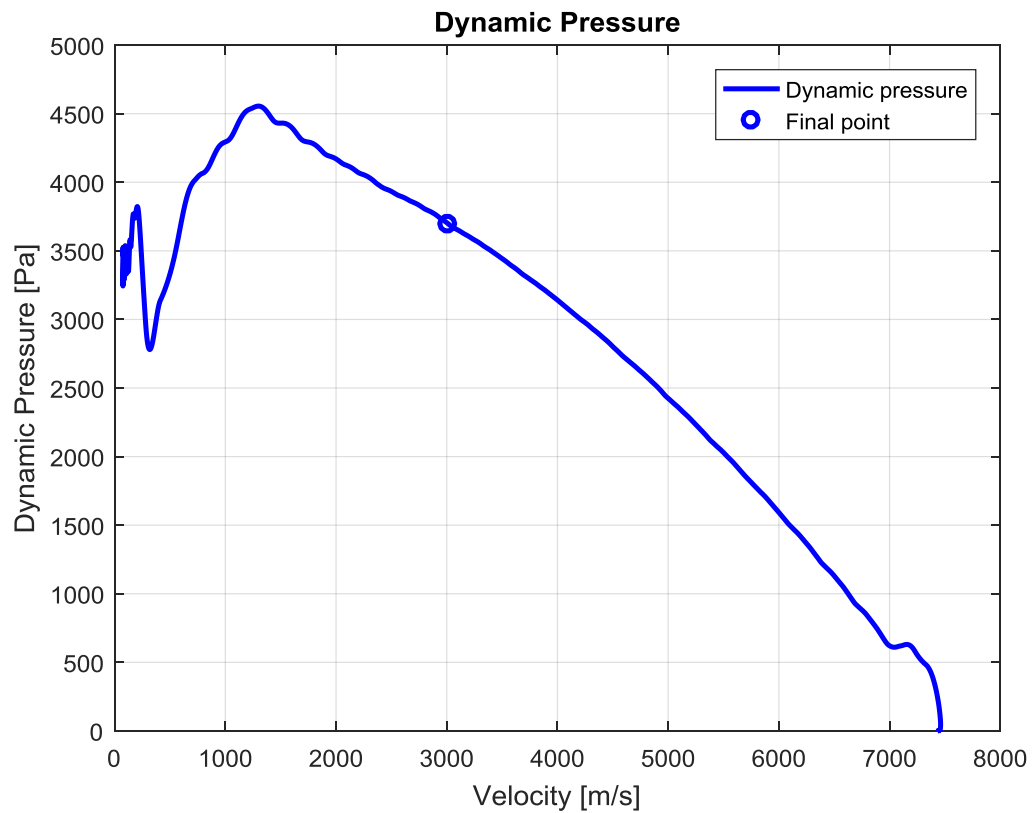


Figure 37: Dynamic pressure for a vehicle that follow the lower profile with a PID controller (PID gain of Table 14).

After the analysis we find the following integrated error distribution for each PID gains combination: the optimal PID gains are the gains that give the minimum integrated error.

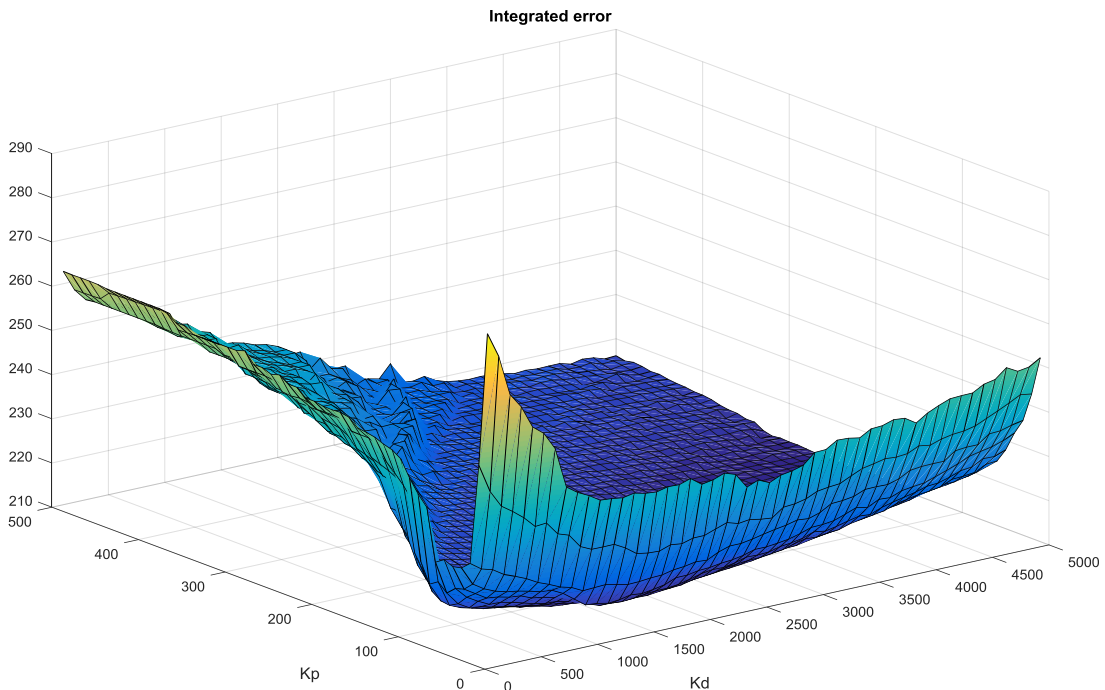


Figure 38: Sensitivity analysis for the lower trajectory.

K_P	K_D
120	2400

Table 15: Optimal PID gains for the lower trajectory.

These PID gains are the initial PID gains: with the LQT optimization for each chosen dynamic pressure will be find lower PID gains, if the dynamic pressure decreases. Finding the optimal gains their values are reduced before using them in the 3-Dof dynamic, for the reasons explained previously.

Dynamic Pressure [Pa]	K_{p0}	K_{D0}	α_p	α_D
1505,233	120*100	2400*1000	1/5e+10	1/5e+9
2008,078	120*100	2400*1000	1/1e+10	1/1e+9
2502,386	120*100	2400*1000	1/5e+9	1/5e+8
3013,382	120*100	2400*1000	1/1e+9	1/1e+8
3513,389	120*100	2400*1000	1/5e+8	1/5e+7
4011,477	120*10	2400*10	1/1e+8	1/1e+7
4503,342	120*10	2400*10	1/1e+5	1/1e+4
5012,983	120*10	2400*10	1/1e+5	1/1e+4

Table 16: Initial conditions for the LQT optimization.

As we can see in the Table 16, the initial PID gains, reached a dynamic pressure of 4000 Pa change their order of magnitude. This happens because with a $K_P = 120 * 100$ and a $K_D = 2400 * 1000$ the drag acceleration profile fluctuates excessively and the optimization brings to a PID gains too low unsuitable for the 3-Dof dynamic.

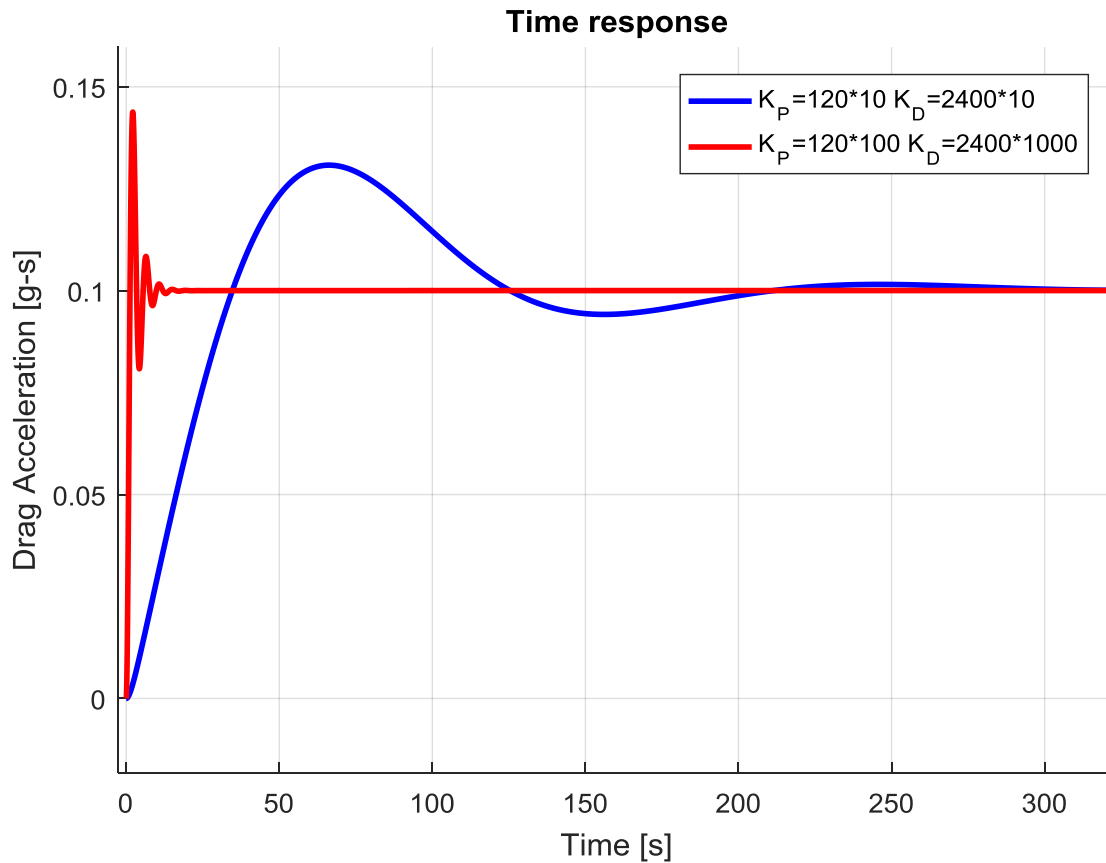


Figure 39: Time response with different PID gains and an initial dynamic pressure equal to 4000 Pa.

The idea of starting with a PID gains with a lower order of magnitude works good until a dynamic pressure of 5000. Over this value the linearized system doesn't represent correctly the real system, so the optimal PID gains are chosen using another sensitivity analysis: in this case the reference trajectory is the trajectory that follows the upper bounds, so the dynamic pressure acquires the maximum values. The sensitivity analysis is based on the integrated error between the reference profile and the simulated profile for velocities including between 5850 m/s and 957 m/s: in this region the dynamic pressure is higher than 5000 Pa.

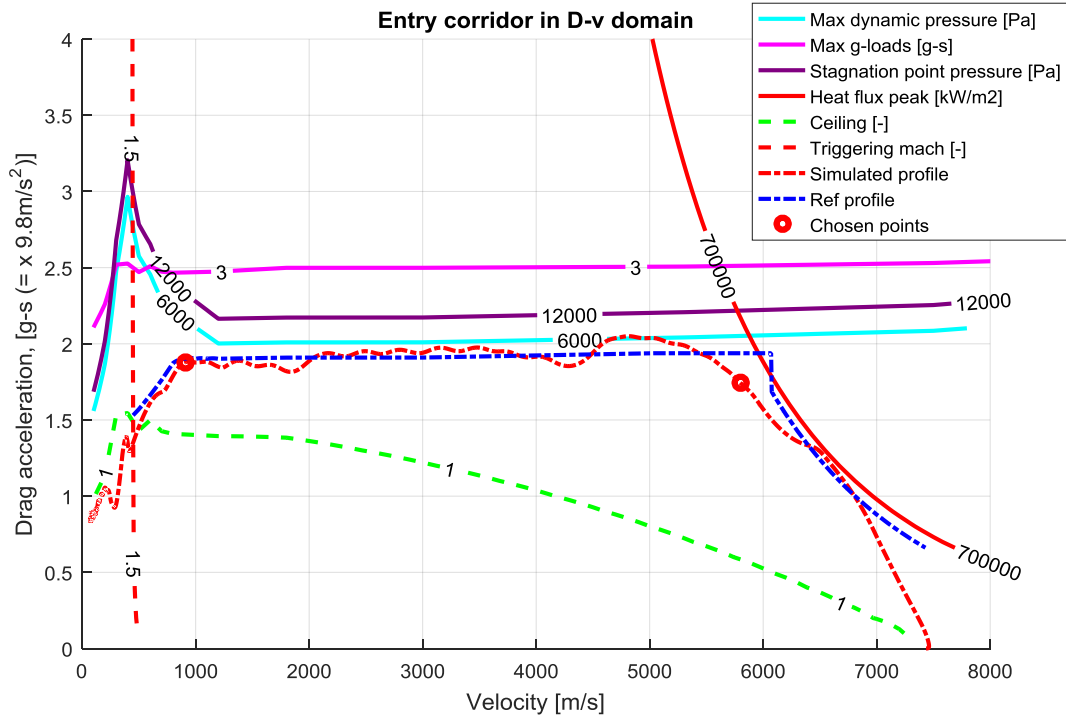


Figure 40: Upper reference profile (curve red) and vehicle acceleration drag (curve blue) with PID gains of Table 14.

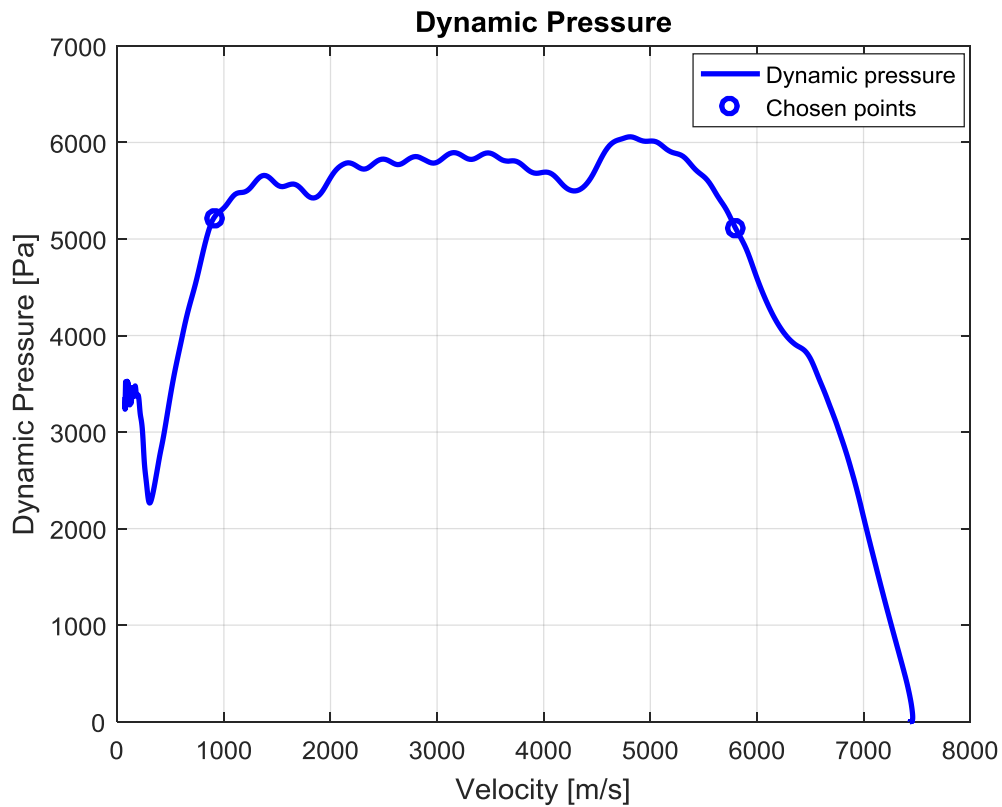


Figure 41: Dynamic pressure for a vehicle that follow the upper reference profile with a PID controller (PID gain of Table 14).

In the sensitivity analysis for the upper bound K_P varies from 10 to 120 with a step of 10 and K_D varies from 100 to 2400 with a step of 100. The results are shown in the Figure 42: the optimal gains are the gains that give the minimum integrated error.

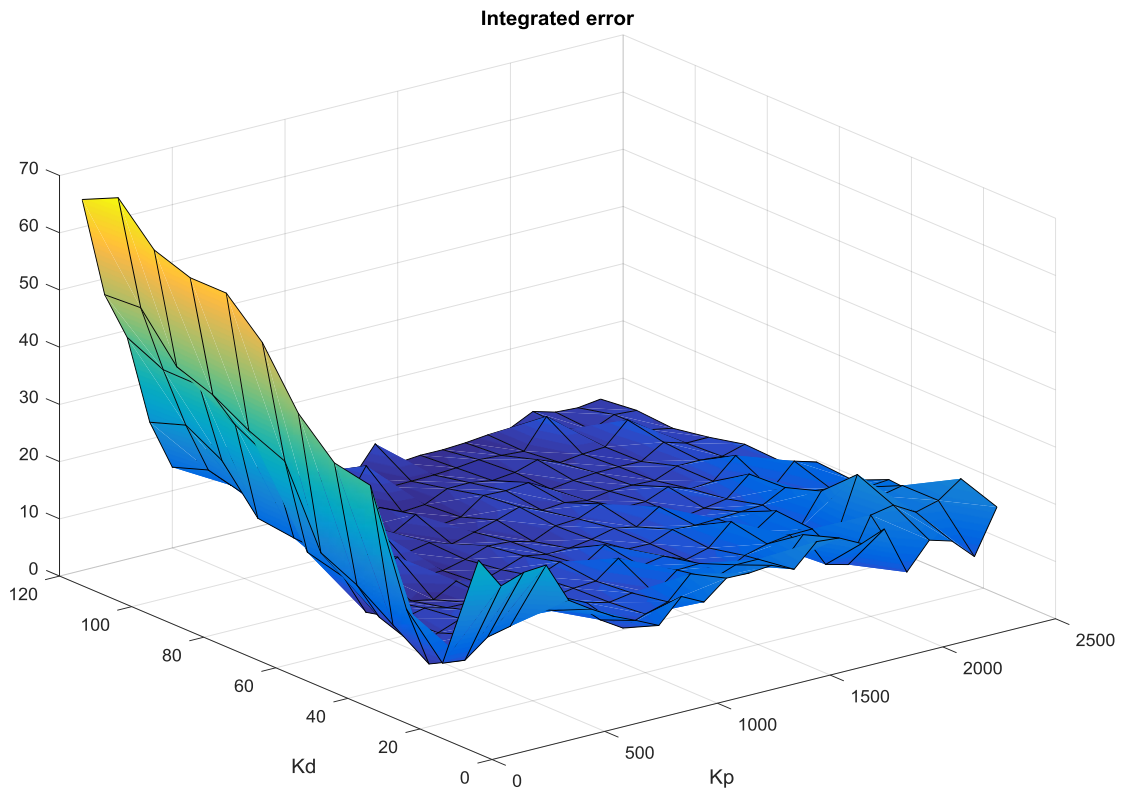


Figure 42: Sensitivity analysis for the upper trajectory.

K_P	K_D
110	1100

Table 17: Optimal PID gains for the upper trajectory.

Now it's possible create a table where the PID gains are function of the dynamic pressure: for the 3-Dof simulations, with a linear interpolation where the input is the dynamic pressure, the optimal PID gains are extrapolated, in this matter the integrated error decreases and the vehicles is able to follow better the reference profile.

Dynamic Pressure [Pa]	K_P	K_D
0	120	2400
1505,233	119,9895	2399,114
2008,078	119,943	2395,575
2502,386	119,871	2391,16
3013,382	119,1325	2356,232
3513,389	117,1894	2313,516
4011,477	115,4586	2006,827
4503,342	114,7672	1691,535
5012,983	110	1100
5500	110	1100
5900	110	1100

Table 18: Optimal PID gains.

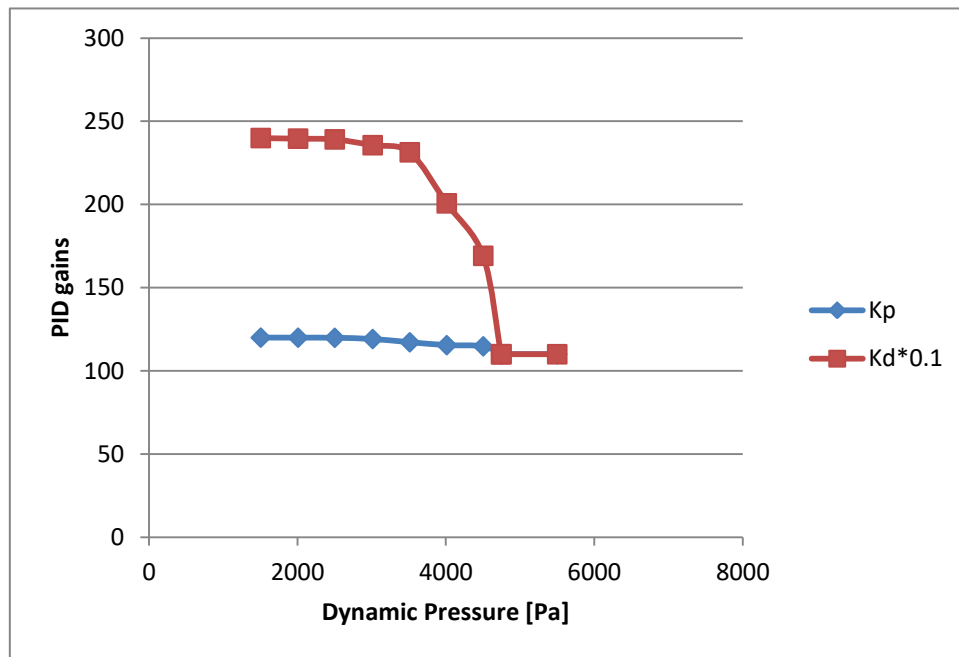


Figure 43: Optimal PID gains.

	Integrated Error Initial gains	Integrated Error Optimal gains
Lower profile	328,2003	323,6122
Upper profile	343,3069	342,4845
Medium profile	262,2189	261,0466

Table 19: Integrated error for a vehicle that follow the medium reference profile with PID gains of Table 14 (column 1) and optimal PID gains (column 2).

3. Guidance Algorithm: Space Shuttle

The Space Shuttle was a partially reusable low Earth orbital spacecraft system, the presence of wing guarantees an high lift-to-drag ratio that allows many abort options and a grate cross-range capacity, affording more return-to-Earth opportunities. The shuttle vehicle re-enters the Earth atmosphere with a velocity of 28000 Km/h at an altitude of 122 Km and at a distance of 7600 Km from the runway, until arriving in the terminal area guidance(a distance about 90 Km and 24 Km altitude from the runway). During this interval its important designing a control system that safely decelerates the Space Shuttle, respecting the crew and vehicle constrains. For this reason an optimal trajectory is chosen and each segment is designed to satisfy unique constraints during the flight. The surface temperature constrains resided at high velocity, in the case of space shuttle until a velocity of 5 Km/s. As the vehicle penetrates deeper into the atmosphere the upper limit is redefined by the vehicle control system capacity creating drag acceleration and the maximum dynamic pressure allowed. If the vehicle flies to close to the overshoot boundary it will not have enough drag acceleration to reach the landing site and could possibly skip back into the orbit.

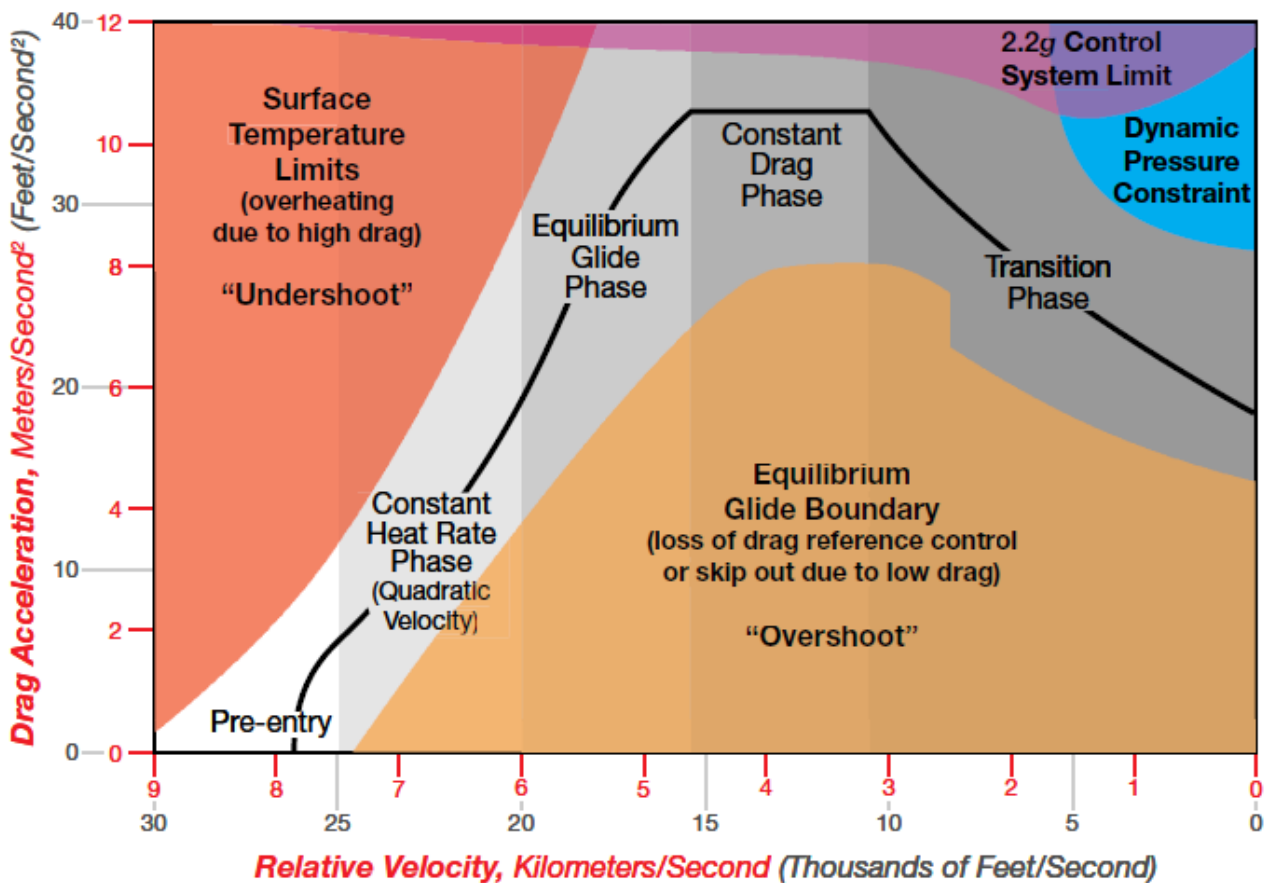


Figure 44: Entry guidance Space Shuttle Drag-Velocity profile.

In the Figure 44 is qualitatively represented a reference profile with all the different phases: in the next paragraphs will be explained how to create the reference profile inspired to the Space Shuttle Phases.

3.1 Pre-entry phase

When the orbiter is in atmospheric flight, it is piloted by varying the forces it generates while moving through the atmosphere, the forces are determined primarily by the dynamic pressure. If the vehicle is at high altitude the dynamic pressure is insufficient, for this reason is useless driving it using the aerodynamic surfaces, when the vehicle reaches 478.8 Pa the first aerodynamic surface, the ailerons, becomes effective and the pre-entry phase ends. During this phase the vehicle flies with a constant bank angle and the RCS jets are used for doing small attitude corrections. The pre-entry bank angle is chosen with a simulation: knowing the initial reference profile, the vehicle is forced following this trajectory varying the pre-entry bank angle. The bank angle takes value from 10° to 80°, with a step of 5°, knowing the desired range, the pre-entry bank angle which leads to the minor range error is chosen.

3.2 Constant Heat-rate Phase

The guidance phase is required to protect the structure and the interior from the blast furnace of plasma building up outside of the vehicle. The blast furnace is due to the high velocity impact of the vehicle with the air in the atmosphere. If the temperatures reach elevated value the vehicle can't be reusable because the structure suffers damage, but also the internal instrumentation is heat sensitive, for this reason it's essential equips the vehicle with a Thermal Protection System (TPS). But also this system has a maximum temperature, if this temperature is exceeded the TPS loses effective. So it's important maintaining the vehicle at a safe temperature, this heating limit is identified by the heat flux boundary in the re-entry corridor.

The TPS is designed to radiate heat, if the heating environment is in equilibrium, the heat transferred into the Space shuttle \dot{q} is equal to the expelled radiate heat and there isn't an heat flux into the vehicle.

$$\dot{q} = K \text{ catal} \frac{1}{\sqrt{R_N}} \left(\frac{\rho}{\rho_0}\right)^n \left(\frac{V}{V_0}\right)^m \quad (69)$$

To define the re-entry trajectory a first strategy is identify a reference profile with constant heat-rate, this heat rate is equal to the medium flow that entered in the Space Shuttle in the time unit. In the first approximation the heat rate is posed equal to 500000 KWat. The drag profile with constant heat-rate is represent by a quadric drag-velocity segment:

$$D_a = c_1 + c_2 V + c_3 V^2 \quad (70)$$

The reference drag acceleration is expressed in m/s^2 , c_1 , c_2 and c_3 are three constants and the Velocity V is expressed in Km/s .

To define this profile the first step is identify three velocity: V_1 is equal to the velocity at the EIP conditions, V_3 is the final point of the constant Heat-rate phase, in this case is equal to 5000 m/s , this value is taken from IXV profile, V_2 is the average between V_1 and V_3 . From the Eq. (69, knowing the velocity and the heat flux, it's possible to calculate the density and, with an interpolation, to obtain the altitude and the Mach value. The Mach number is used in the aerodynamic database to finding the aerodynamic coefficient C_D , with an interpolation. Now is possible calculating the drag acceleration for the three points using the following relation:

$$\frac{\rho}{\rho_0} = \frac{D_a m}{\frac{1}{2} V^2 S C_D \rho_0} \quad (71)$$

With these three pairs of points, we will obtain the coefficients values for a drag reference profile with constant heat-rate:

$$c_1 = \frac{D_{a2} - \frac{V_2}{V_1} D_{a1} + (V_2 V_1 - V_2^2) c_3}{1 - \frac{V_2}{V_1}}$$

$$c_2 = \frac{D_{a1} - c_1 - c_3 V_1^2}{V_1} \quad (72)$$

$$c_3 = \frac{D_{a3} - \left(1 - \frac{V_3}{V_1}\right) \frac{D_{a2} - \frac{V_2}{V_1} D_{a1}}{1 - \frac{V_2}{V_1}} - \frac{V_3}{V_1} D_{a1}}{\frac{(V_2 V_1 - V_2^2)}{1 - \frac{V_2}{V_1}} \left(1 - \frac{V_3}{V_1}\right) - V_3 V_1 + V_3^2}$$

3.3 Constant Drag Phase

After the Constant Heat Rate phase, the Space Shuttle enters in the Equilibrium Glide Phase, this phase is necessary for connecting the Heat Rate Phase and the Constant Drag Phase, increasing the decelerations. But in this case, the decelerations are gained with the Constant Heat Rate Phase, so the Equilibrium Glide Phase isn't necessary.

During the Constant Drag Phase the drag-velocity reference profile is computed to maintain constant the drag acceleration, for this reason its form is really simple:

$$D_a = c_4 \quad (73)$$

This constrains the accelerations on the vehicle structure and the maximum load accelerations for crew members confined to a sit positions during re-entry with normal accelerations direct along their spine. This reference profile also constrains the maximum dynamic pressure exercised on the vehicle. During this phase the velocity is rapidly reduced and kinetic energy is removed from the vehicle.

In the algorithm the first step is identified the initial and final velocity for this phase, the final velocity V_4 is sets equal to 2000 m/s and the initial velocity is equal to V_3 . For each velocity included between V_3 and V_4 with a step of 100 m/s is computed the difference between the drag acceleration for the upper boundary and the drag acceleration for the lower boundary of the re-entry corridor. The lower boundary is always the ceiling, the upper boundary is the minimum drag acceleration between the maximum dynamic pressure drag and the g-load limit drag. Then each velocity is associated to a difference between drag accelerations: to compute the reference profile it's taken the velocity at which the drag difference is minimum and, for this velocity, it's computed the average drag acceleration between the upper and lower limit.

Now it's necessary creating the union between the Constant Drag Phase and the Constant Heat Rate Phase: with an interpolation it's finding the velocity at which the drag acceleration for the constant Heat Rate profile is equal to the Constant drag c_4 , this velocity will be the new V_3 .

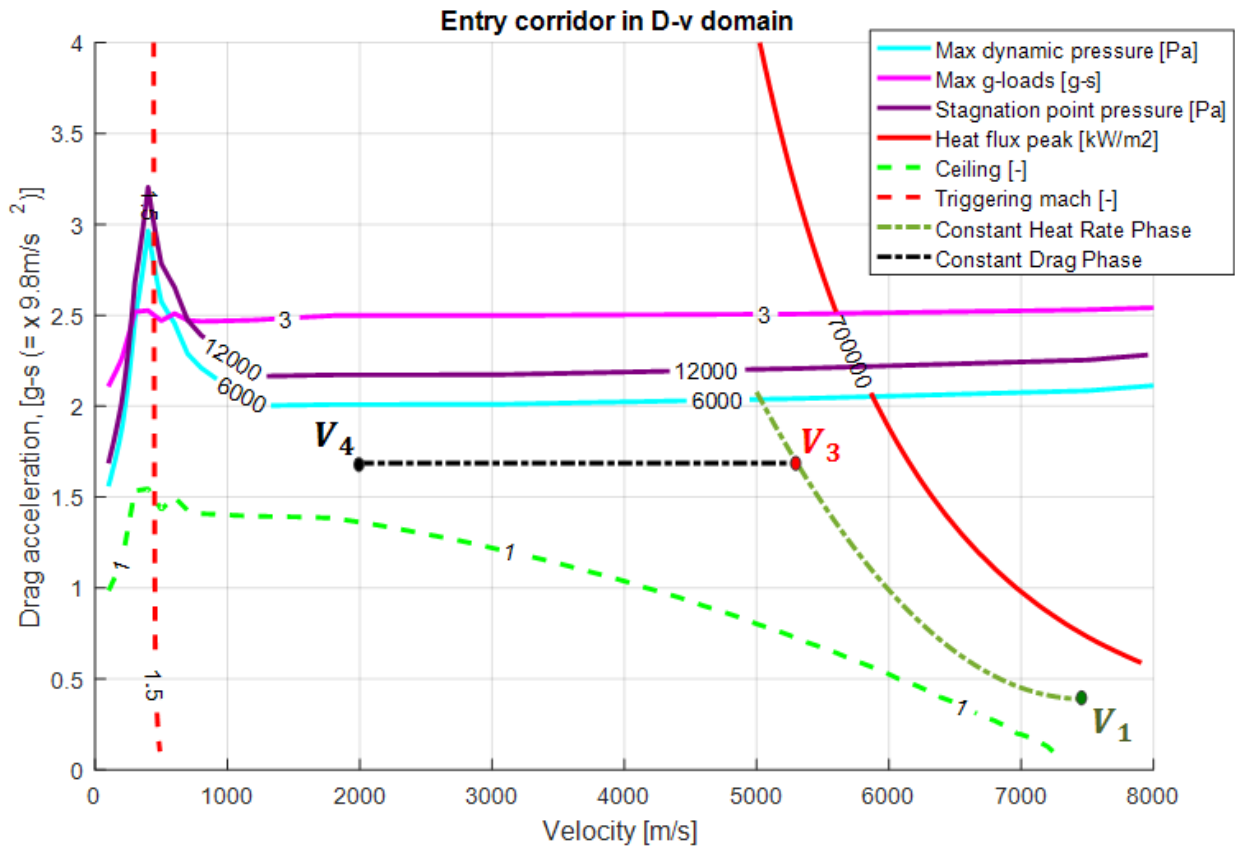


Figure 45: Constant Heat-rate phase and Constant Drag phase.

3.4 Transition Phase

The last phase is a linear drag-energy reference acceleration, with this phase the guidance system removes final trajectory-range errors and reduces the angle of attack, dissipating a great deal of energy.

The independent variable is now the energy because at low altitude and velocity the drag-velocity formulation becomes inaccurate for the range prediction.

The new formulation is the following:

$$D_a = D_{aF} + c_5(E - E_F) \tag{74}$$

$$E = g h + \frac{1}{2} V^2$$

D_{aF} and E_F are respectively the drag acceleration and the energy for the TEAM conditions: in this case the TEAM altitude is equal to 26 Km. Reaching the final conditions the vehicle opens the parachute, and that

occurs when the Mach number reaches the value of 1.5. So knowing the Mach number and the altitude is possible to calculate the TEAM velocity and subsequently the TEAM energy E_F . With a series of interpolations using the aerodynamic database and the atmospheric model, it's possible to determine the final drag acceleration D_{aF} in m/s^2 . Now it's important to verify that the final point respects some conditions:

- It must be within the limits of the re-entry corridor: the acceleration drag D_{aF} must be greater than the acceleration drag in ceiling for the final velocity V_F
- It must be lower or equal to the constant acceleration drag c_4

If one of these conditions isn't respected, the final altitude is changed: in particular if the Mach number doesn't change (the final Mach number isn't an independent variable, it's imposed by the parachute's characteristics) and the final drag acceleration must increase, the altitude decreases. It's chosen the final altitude corresponding to the average acceleration drag between c_4 and the drag acceleration in ceiling.

Knowing the final conditions and the initial conditions for the Transition Phase (the initial drag acceleration is equal to c_4 and the initial velocity is equal to V_4) it's possible to calculate the parameter c_5 :

$$c_5 = \frac{c_4 - D_{aF}}{E_4 - E_F} \quad (75)$$

E_4 is the energy of the final point in the Constant Drag Phase.

The next problem is calculating all the points of the Transition Phase: for doing this operation two different vectors are created, one for the velocity (from V_F to V_4 with a step of 100 m/s) and one for drag acceleration (from D_{aF} to D_{a4} with a step of 0.1 g-s). For all the velocity-drag acceleration combinations it's calculating the Energy and finally all these values enter in the Eq. (74), where $c_{5_{Ref Profile}}$ is the coefficient found with Eq. (75). If the selected point belongs to the curve of the Transition Phase Reference Profile, the equation gives as results zero otherwise the result is different from zero. So the final result is a matrix, where the rows are linked to the velocity and the columns are linked to the drag acceleration, with an interpolation, entering in the matrix with the number zero, it's possible to find, for each velocity, the drag acceleration that solves the Eq. (74): this procedure gives the drag-velocity reference profile for the Transition Phase.

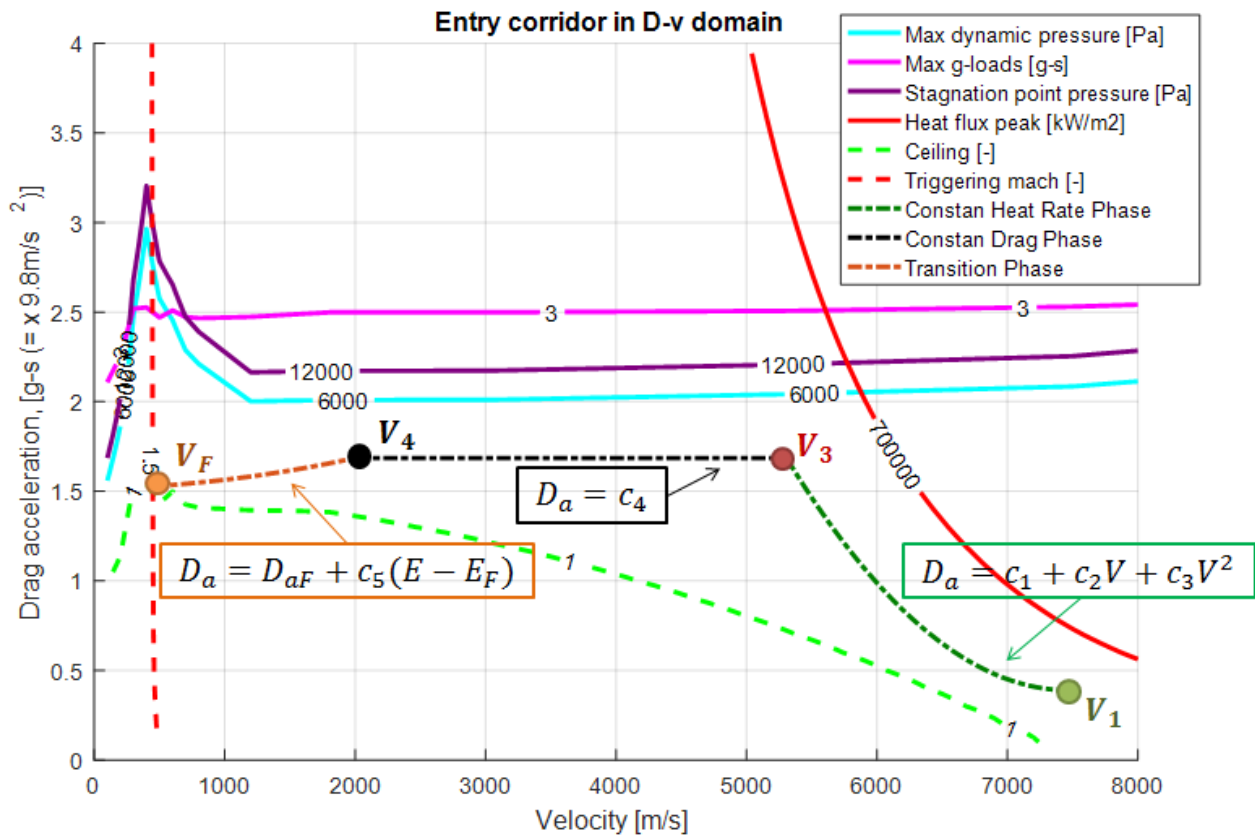


Figure 46: Reference profile and mathematical expressions for each phase.

3.5 Range prediction Algorithm for the Space Shuttle

The profile found in the chapter 3 is the initial reference profile that respects the boundaries, but if the vehicle follows this profile, using the PID controller, the range cannot be controlled. To obtain a determined range is necessary changing the reference profile, in this matter, following the new profile is possible, from an initial point, to arrive at a chosen final point.

The strategy for changing the profile is based on the range prediction: following the initial profile the vehicle will travel a certain nominal range, this range can be different from the desired range (the desired range is given by the distance between the vehicle position and the final desired position). The difference between the desired range and the nominal range gives a range error. Knowing this range error is possible shifting each part of the reference profile, obtained a new profile that respects the range constrain. This operation must be accomplished during the dynamic simulation because, knowing the position of the vehicle and its dynamic behavior in each time instant, it's possible obtaining the optimal reference profile to minimize the range error. So the reference profile is shifted at each simulation step.

In this chapter we explain how calculate the nominal range, knowing the phase mathematical expression and how translate the reference curve to minimize the range error at the end of the simulation.

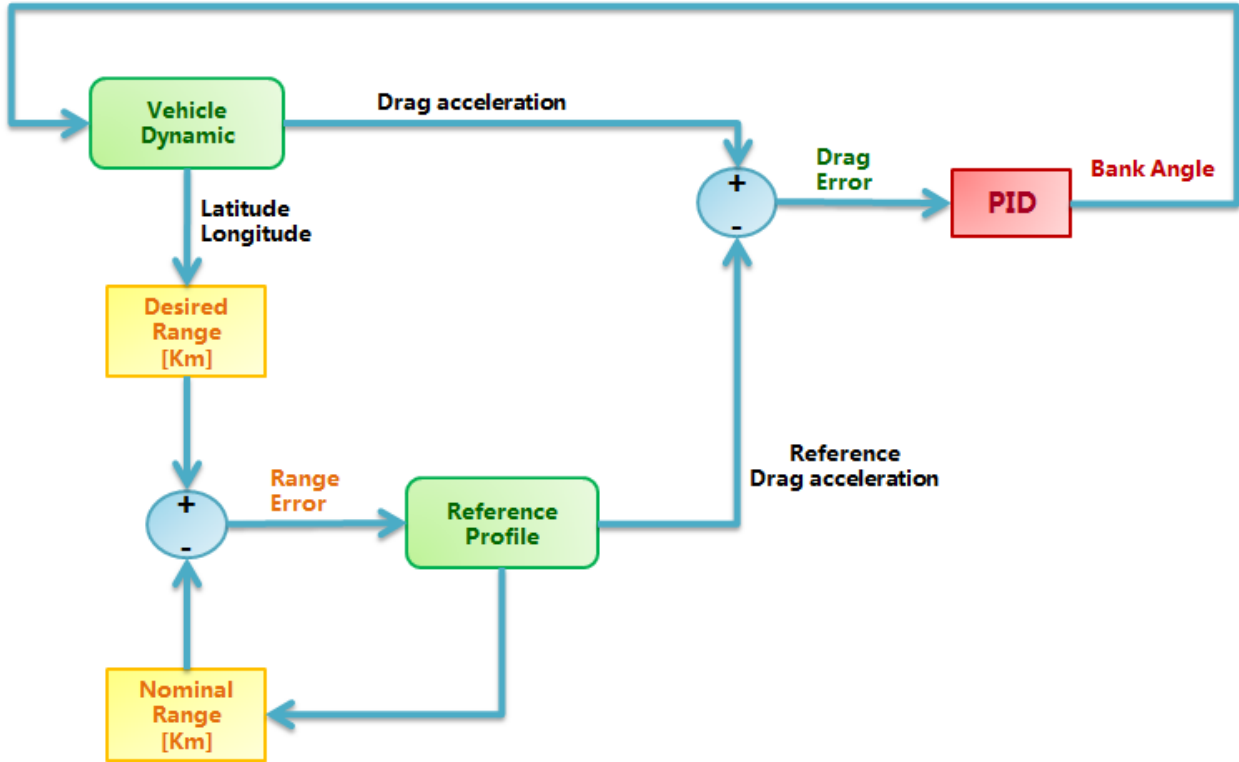


Figure 47: Vehicle dynamics, PID controller and range prediction flow chart.

The first step is understanding how calculating the desired and nominal range:

- The desired range R_D is the distance between two points expressed with a latitude and a longitude. Considering a spherical Earth, with radius equal to R_T , and approximating the distance with an arc of a circle, the range is calculating with the following formulation:

$$R_D = R_T [\cos^{-1} [\sin(lat) \sin(lat_F) + \cos(lat) \cos(lat_F) \cos(long - long_F)]] \quad (76)$$

- The nominal range is the range obtained if the vehicle follows the reference profile. This range can be calculated using approximated formulations, as velocity integral:

$$s = \int \frac{V \cos \gamma}{-D - g \sin \gamma} dV \quad (77)$$

If the angle γ is small, the integral is simplified:

$$s = - \int \frac{V}{D} dV \quad (78)$$

Substituting the drag expression $D(V)$ for each re-entry phase in the Eq. (78) it's possible finding the range prediction equation with a simple integration. For the last phase, when the angle γ increases, using a drag

function of velocity brings to an inaccurate range prediction ,for this reason the drag is expressed as a function of the energy and the range equation becomes the following:

$$s = - \int \frac{\cos\gamma}{D} dE \cong - \int \frac{1}{D} dE \quad (79)$$

The range prediction equations are summarised in Table 20:

Phase	Drag segment form	Range prediction equation
Constant Heat Rate	$D_a = c_1 + c_2V + c_3V^2$	$Q = 4c_3c_1 - c_2^2$ <p>if $Q > 0$</p> $s_1 = -\frac{1}{2c_3} \log \left[\frac{c_1 + c_2V_3 + c_3V_3^2}{c_1 + c_2V + c_3V^2} \right] + \frac{c_2}{c_3\sqrt{Q}} \left(\arctan \left[\frac{2c_3V_3 + c_2}{\sqrt{Q}} \right] - \arctan \left[\frac{2c_3V + c_2}{\sqrt{Q}} \right] \right)$ <p>if $Q < 0$</p> $s_1 = -\frac{1}{2c_3} \log \left[\frac{c_1 + c_2V_3 + c_3V_3^2}{c_1 + c_2V + c_3V^2} \right] + \frac{c_2}{c_3\sqrt{Q}} \left(\log \left[\frac{2c_3V_3 + c_2 - \sqrt{-Q}}{2c_3V_3 + c_2 + \sqrt{-Q}} \right] - \log \left[\frac{2c_3V + c_2 - \sqrt{-Q}}{2c_3V + c_2 + \sqrt{-Q}} \right] \right)$
Constant Drag	$D_a = c_4$	$s_2 = \frac{V^2 - V_4^2}{2c_4}$
Transition	$D_a = D_{aF} + c_5(E - E_F)$	$s_3 = \frac{E - E_F}{D_a - D_{aF}} \log \left[\frac{D_a}{D_{aF}} \right]$

Table 20: Drag form and Range prediction for the three phases of Space Shuttle re-entry.

With these equations is possible translated the reference profile, but the profile must never overcome the re-entry corridor limits. So it's necessary identifying the limit curves.

For the Constant Heat Rate Phase a velocity vector must be created, with values ranging from V_1 to $V = 5000 \text{ m/s}$ with a step of 1 Km/s . A second vector is also required, this vector contains different c_1 values, from the initial c_1 , taken from the initial reference profile, to $c_1 + 100$, in this vector there are 500 values. Now for each velocity, chosen a c_1 value, it's calculating the drag acceleration with the Constant Heat rate formulation and the drag acceleration for the Heat flux boundary. If the difference between the two values is equal or greater than zero, the chosen c_1 is the coefficient for the upper limit curve. For the lower limit the procedure is the same: the c_1 vector goes from the initial c_1 to $c_1 - 100$ and the iteration will stop when the difference between the drag acceleration with the Constant Heat rate formulation and the drag acceleration for the ceiling boundary is equal or lower than zero. With this method the curve only moves but doesn't change its form because the coefficients c_2 and c_3 doesn't change their values.

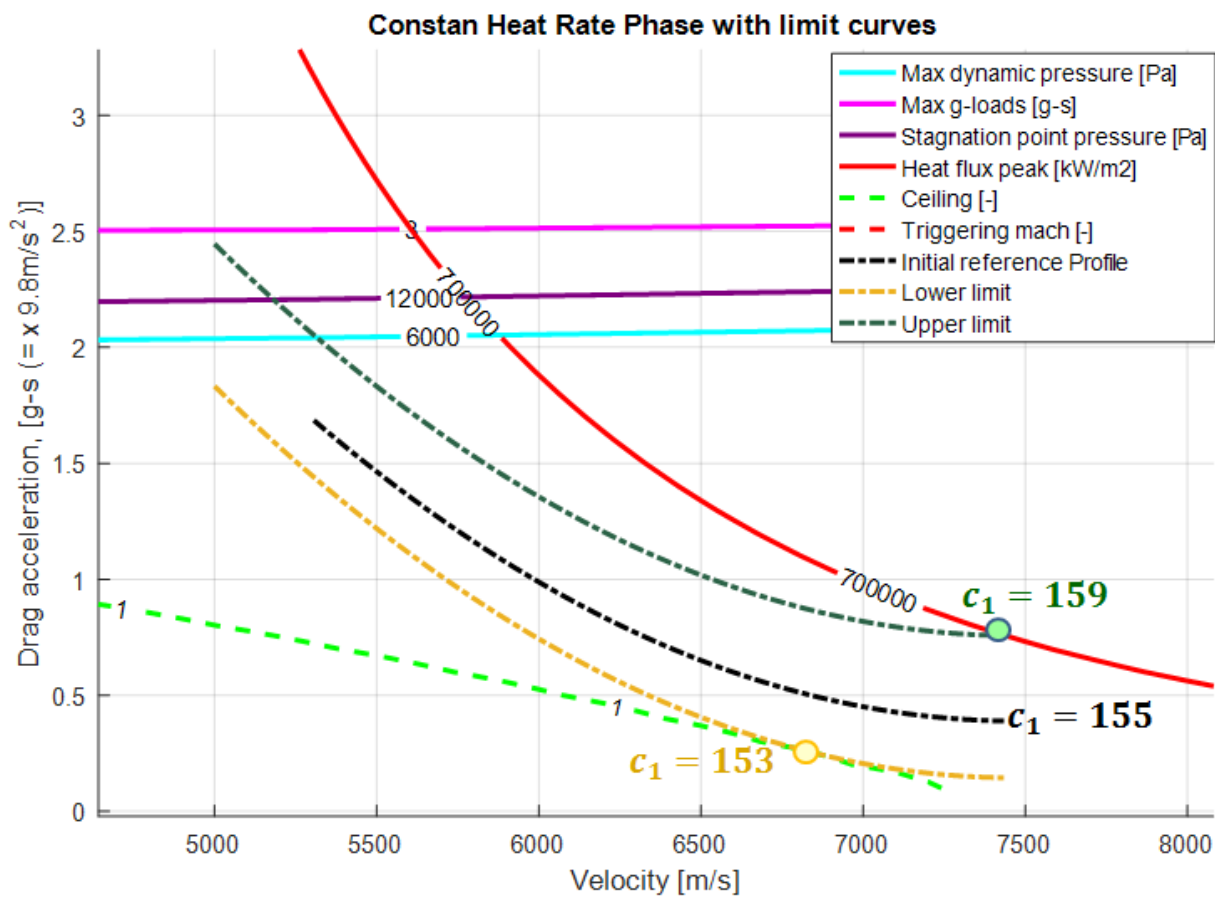


Figure 48: Constant Heat Rate phase with limit curves.

The three profiles in Figure 48 are found using a $c_2 = -0,04$ and a $c_3 = 2,71e - 6$, changing the c_1 value. The points highlighted with a dot are the points where the reference profile meets the limits. If the c_1 is lower than 159 the profile never intersects the upper Heat flux limit. At the same way if the c_1 is greater than 153 the reference profile never intersects the lower ceiling limit. The eligible value for c_1 are included between 159 ($c_{1maximum}$) and 153 ($c_{1minimum}$).

For the Constant Drag the situation is more simpler: for the velocities including between V_3 and V_4 is taken the maximum drag and the minimum drag. The maximum drag is the minimum value between all the drag of the g-load limit and dynamic pressure limit. The minimum drag is the maximum value between all the drag of the ceiling limit. Then the upper limit for c_4 is posed equal to the maximum drag decreasing of 0,1 and the lower limit for c_4 is posed equal to the minimum drag incremented of 0,1. But for the lower limit is

necessary another control: the constant drag mustn't be lower than the drag of the final point: so if the lower drag overcomes the final point, the lower limit for c_4 is changed and posed equal to D_{aF} .

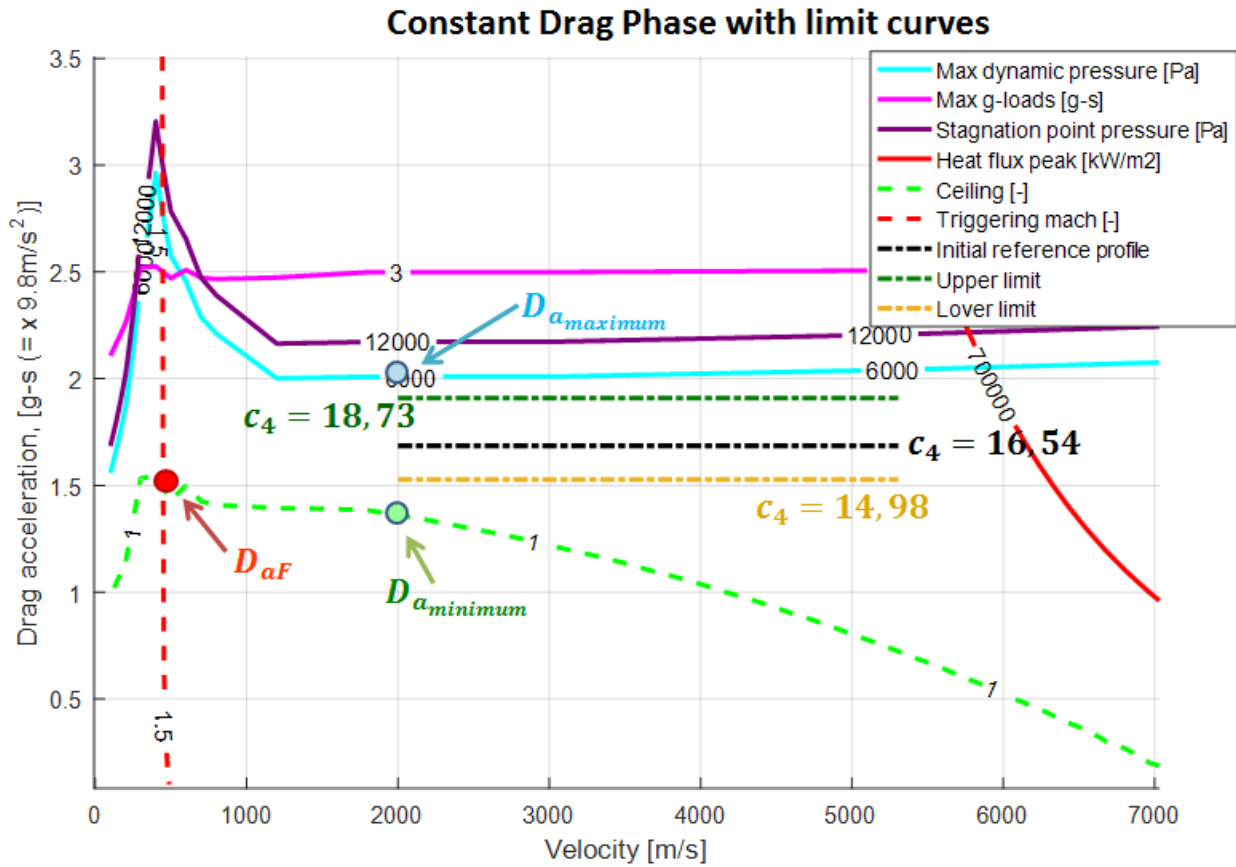


Figure 49 : Constant Drag phase with limit curves.

The upper profile ($c_{4_{maximum}}$) in Figure 49 is finding decreasing the $D_{a_{maximum}}$ of 0,1 and the lower profile ($c_{4_{minimum}}$) corresponds to a drag equal to D_{aF} because the final drag D_{aF} is greater than $D_{a_{minimum}} + 0,1$. The c_4 value can't overcome the two limits.

The Transition phase is probably the most difficult phase to analyze: first three vectors must be created. The first vector contains different values of c_5 , in this case the first value is $1e-9$ and the last value is $5e-6$. The second vector contains velocity, from V_F to V_4 . The third vector contains drag acceleration in m/s^2 .

The procedure is the following: we take a c_5 and a velocity, from the two vectors, and, for each drag acceleration, it's obtained the altitude and then the energy E . All this value are used in the (74):

$$D_{aF} - D_{a_{chosen}} + c_{5_{chosen}}(E_{chosen} - E_F) = par$$

If the drag-velocity combination belongs to the curve with $c_{5_{chosen}}$ as coefficient, par is equal to zero, in the other case par is different. Each $c_5 - Velocity$ combination is associated to a vector, in the vector there are the values of par , found with the previous equation. The par vector dimension is equal to the dimension of the *Drag Acceleration* vector. With an interpolation is possible found the zero of this vector and then finding the drag acceleration that completes the triad of values that gives as result $par = 0$.

The final results are two vectors, one with c_5 and one with velocity, and a matrix of drag acceleration where the rows are associated with a velocity and the columns are associated with a c_5 .

Selecting a row, it's possible to enter with the maximum drag equal to the c_4 upper limit and searching the last position that has an acceleration drag lower than c_4 upper limit: this position will correspond at the c_5 upper limit. With this procedure we obtain a vector where for each velocity the $c_{5_{maximum}}$ is identified. If all the drag accelerations in a row are lower than c_4 upper limit, the $c_{5_{maximum}}$ becomes the biggest value of the vector c_5 .

For the lower limit the situation is a bit different: decreasing the c_5 we will obtain curves similar to horizontal lines passing for the final point $D_{aF} - V_F$. That means that the lower value for c_5 will be zero. But with this coefficient there would be numerical problems so the lower limit is a really small number near to zero: in this case the number is $c_5 = 1e - 9$.

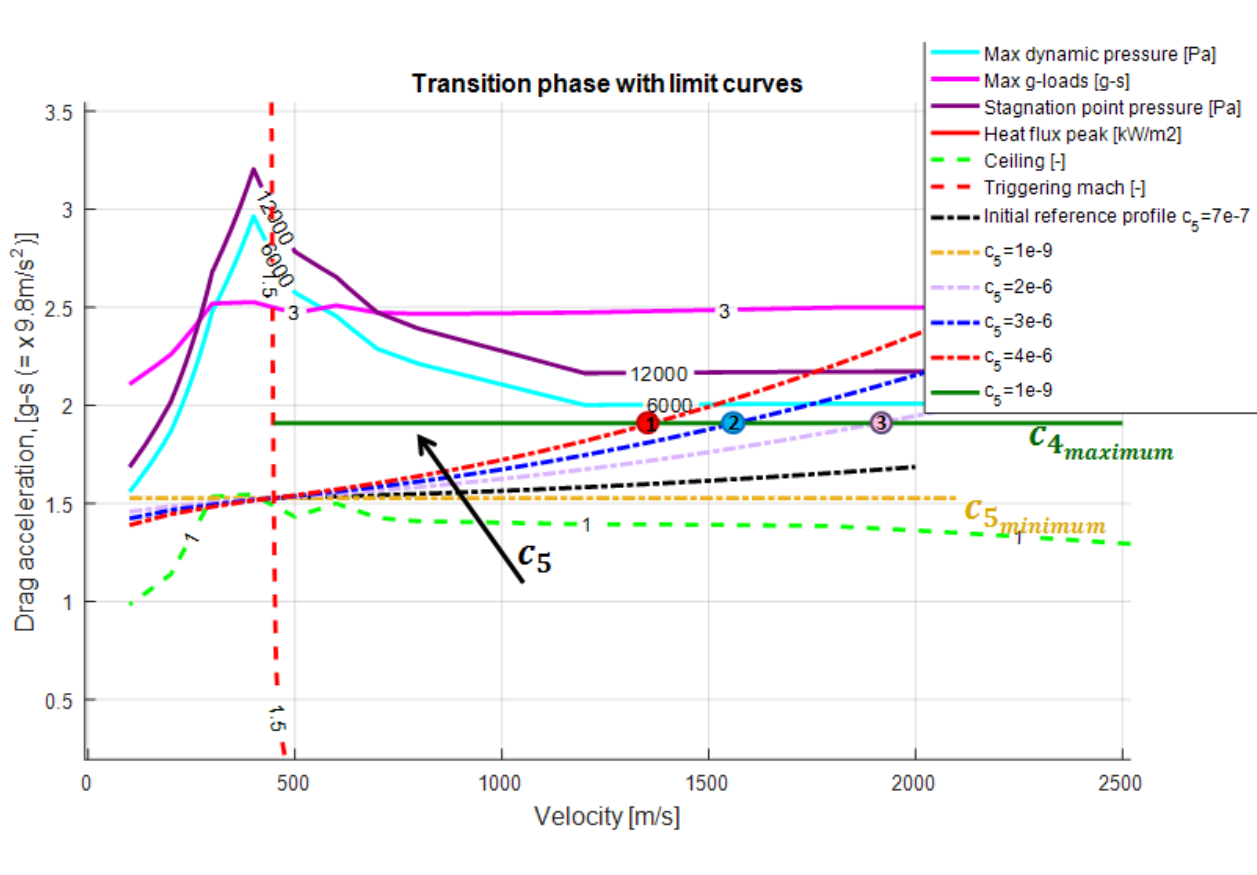


Figure 50: : Transition phase with limit curves.

The Figure 50 represents a qualitative behaviour for choosing the c_5 coefficient. For each velocity the chosen coefficient is that associated at the curve that intersects the line with a drag equal to $c_{4_{maximum}}$: the intersection is represented with a circle. For all the velocity that have a value lower than the velocity in the red point 1 the chosen $c_{5_{maximum}}$ is equal to $4e-6$ (this is the maximum coefficient in the c_5 vector). In this matter it's possible creating a vector where each velocity is associated to an $c_{5_{maximum}}$.

Velocity	$C_{5_{maximum}}$	$C_{5_{minimum}}$
1930 m/s	$2e^{-6}$	$1e^{-9}$
1600 m/s	$3e^{-6}$	$1e^{-9}$
1400 m/s	$4e^{-6}$	$1e^{-9}$
1000 m/s	$4e^{-6}$	$1e^{-9}$

Table 21: Chosen coefficient c_5 maximum add minimum for different velocity.

The next step is the determination of a strategy for changing the reference profile for doing the range correction: if the errors are small, it is possible link the variation of the constant term with the range error, using the approximation for the derivative of range with respect to drag:

$$\frac{ds}{dD_a} = \frac{ds}{dc} \frac{dc}{dD_a} = \frac{ds}{dc} \quad (80)$$

Explained the Eq.(80 is really easy: c is the constant term in the Constant Drag phase and in the Constant Heat Rate phase, so deriving the acceleration drag respects to a constant term, the result is 1. Now for small time intervals, if the range error is small, it's possible writing ds as the difference between the nominal and the desired range Δs :

$$\Delta c = \frac{dD_a}{ds} \Delta s \quad (81)$$

For the transition phase the question is a bit different: in the range equation appears the term c_5 , so it's possible to calculate mathematically the derivate ds_3/dc_5 .

$$\Delta c_5 = \frac{dc_5}{ds_3} \Delta s \quad (82)$$

The derivative of range with respect to drag can be finding with a mathematical derivation:

Phase	Drag segment form	Derivative of range
Constant Heat Rate	$D_a = c_1 + c_2V + c_3V^2$	$\frac{ds_1}{dD_a} = -\frac{s_1}{D_{a3}}$
Constant Drag	$D_a = c_4$	$\frac{ds_2}{dD_a} = -\frac{(V_3^2 - V_4^2)}{2c_4^2}$

Transition	$D_a = D_{aF} + c_5(E - E_F)$	$\frac{ds_3}{dc_5} = \frac{1}{c_5} \left[-s_3 + \frac{E - E_f}{D_a} \right]$
-------------------	-------------------------------	---

Table 22: Derivative of the range for the three re-entry phase.

In the Table 22 the value s_1 represents the current range of Constant Heat Rate Phase and D_{a3} is the acceleration drag of the Constant Heat Rate final point. The parameters V_3 and V_4 are respectively the initial and the final velocity of Constant Drag Phase that has a value equal to c_4 . In the transition Phase E and D_a are the Energy and the acceleration Drag at the current Velocity V , s_3 is the current range in the Transition Phase, c_5 is the current constant parameter of the Transition Phase and E_F is the Energy of the final point.

As we can see, with these form formulations, the derivative of range is always negative: this mean that if the error range is positive (with the reference profile we obtain a range too low), the reference profile steps down and the coefficient c decreases. A reference profile that steps down is a profile with a lower drag acceleration, so the vehicle loses altitude more slowly and the range increases.

Now the next step is to explain the strategy for the range correction: this correction starts when the Pre-entry phase ends. During this phase the vehicle follows the initial reference profile. In the pre-entry phase is necessary choosing the initial Bank Angle, this angle is selected after a series of simulations. Each simulation uses a different Initial Bank Angle, taken from a vector that has 11 equidistant values, from the value 10° to the value 70° . For each simulation is saved the range to go and the Bank Angle selected is the Bank Angle that guarantees the minimum difference between the desired range and the simulated range to go.

Ended the Pre Entry Phase, the range correction is divided in three parts: the Constant Heat Rate Range Correction, the Constant Drag Range Correction, the Transition Range Correction. Each Phase ends reached a determinate velocity: the Constant Heat Rate Range Correction ends 300 m/s before having reached the intersection velocity between the Constant Heat Rate Phase and the Constant Drag Phase and the Constant Drag Range Correction ends reached the V_4 . Now we can analyse each Range Correction Phase.

For the Transition Phase and the Constant Drag Phase the nominal Range is calculated. Then the nominal range for the Constant Heat Rate Phase is calculated, from the actual velocity to the final Velocity of this phase. Finally the total nominal range is subtracted to the desired range. The range is expressed in Km. This difference is used for the correction of the Constant Drag Phase, using the Eq.(81: the result is the variation of the coefficient c_4 . This variation is summed to the old c_4 to obtained a new value: $c_{4_{new}} = \Delta c_4 + c_{4_{old}}$. Then is necessary controlled if the $c_{4_{new}}$ respects the re-entry corridor boundary: this operation is doing with a saturator, where the upper and lower limits are the values found in the Figure 49. This new curve will give a new range, this range is summed with the Transition Phase Range and the Constant Heat Rate Phase Range and then subtracted to the desired range, the result is a range error, used for the Constant Heat Rate Range Correction passing through the Eq. (81. This Δc_1 value must be limited to avoid an excessive variation of the reference curve, that conduces to an oscillation of the reference profile: the limit is posed to 0,4. Like for the Constant Drag Phase, we can calculate the new coefficient: $c_{1_{new}} = c_{1_{old}} + \Delta c_1$. This coefficient is limited with the value finding in Figure 48. Each iteration is necessary recalculating the intersection velocity $V_{3_{new}}$ between the new Constant Drag Phase and the new Constant Heat Rate phase, this intersection is finding with an interpolation: it's created a vector with 1000 elements from V_1 to $V = 1000$, and for each velocity is calculated the drag acceleration using the Constant Heat Rate formulation, the interpolation occurs between the Constant Drag value and this new vector. The velocity $V_{3_{new}}$ will be used for the nominal range s_1 and for the D_{a3} .

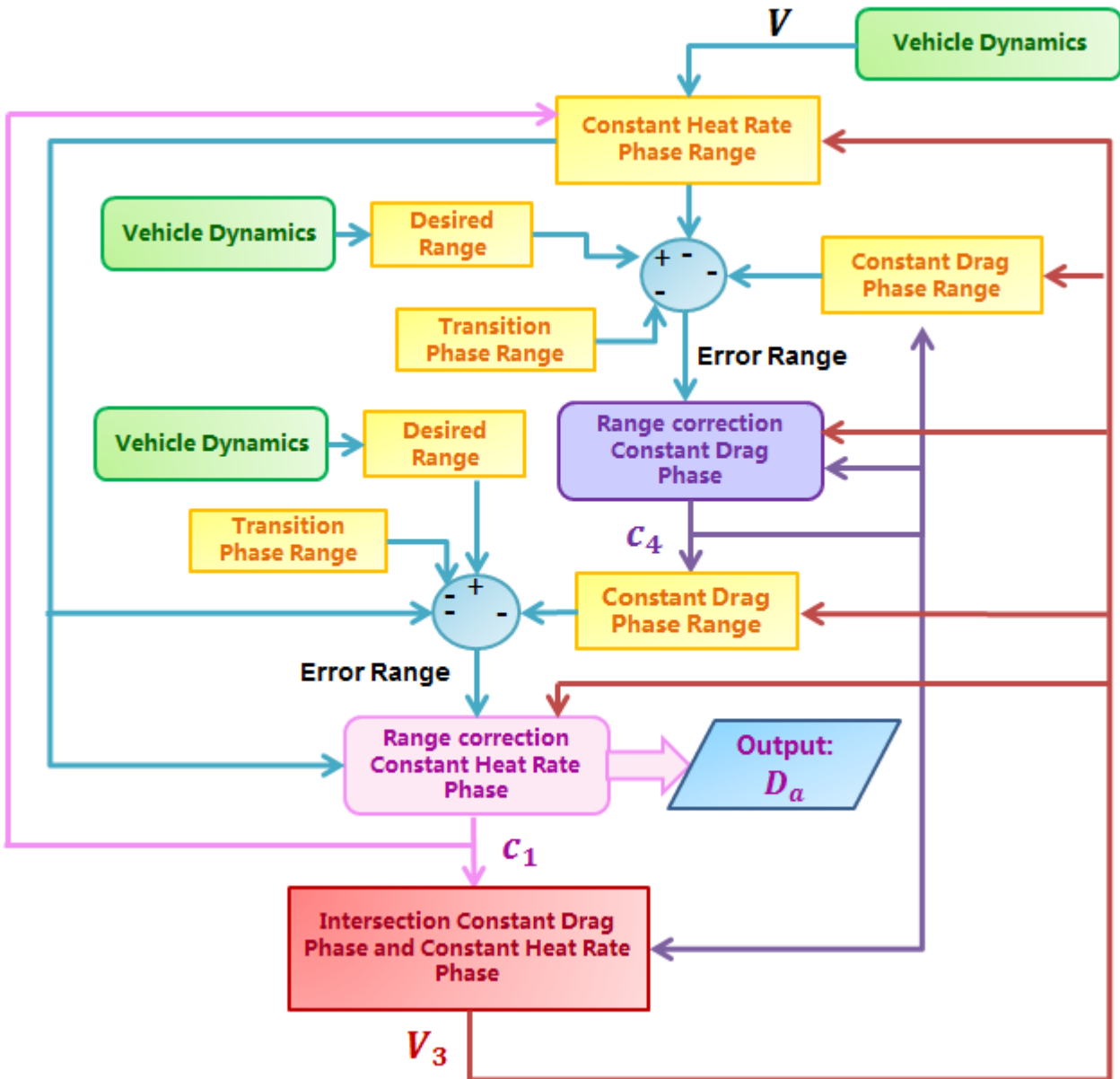


Figure 51: Constant Heat Rate Range Correction Flow Chart.

Reached the velocity $V_{3_{new}} + 300$ the Constant Drag Range Correction starts: the motivation because the velocity isn't set equal to $V_{3_{new}}$ for the change is really simple. The reference profile for passing from the Constant Heat Rate Phase to the Constant Drag Phase performs an abrupt change of curvature, the vehicle isn't able so follow this change and deviates too much from the reference profile and this behaviour produces a pick and oscillation in the vehicle dynamic.

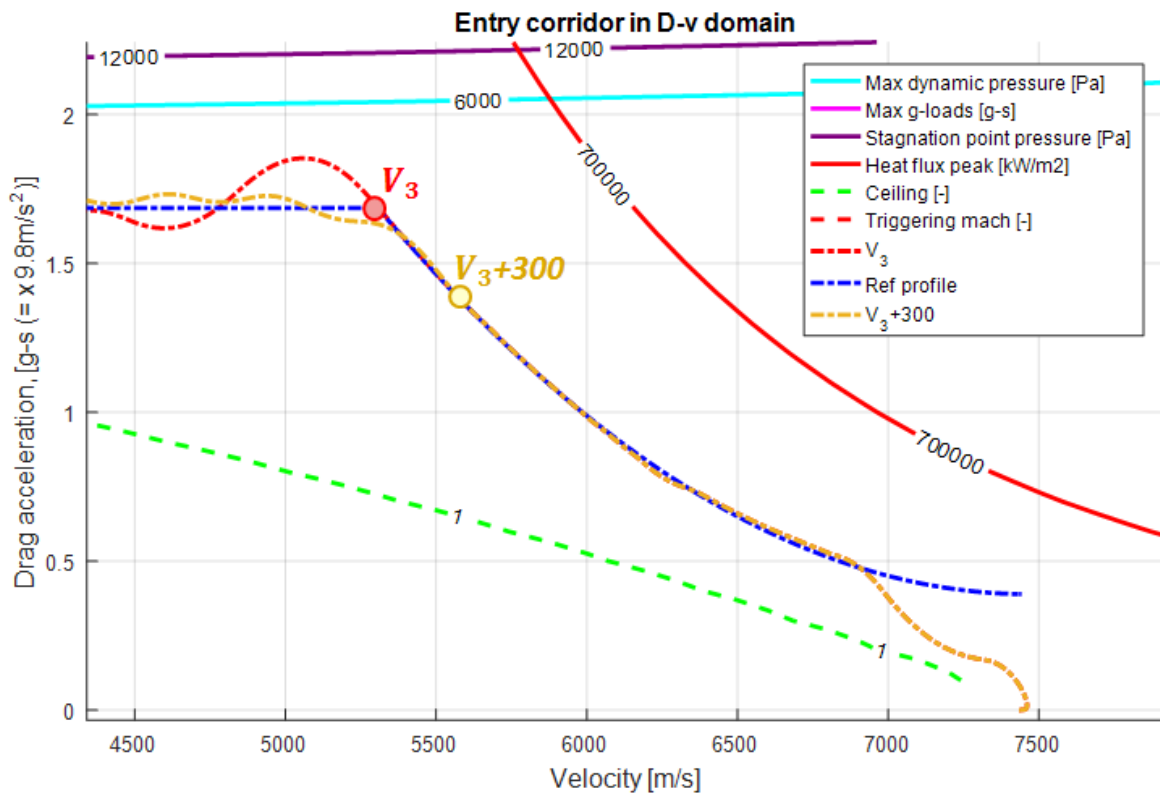


Figure 52: Vehicle dynamic with two different velocity for following the Constant drag: the red curve starts the constant Drag Phase at a velocity equal to V_3 and the yellow curve starts the constant Drag Phase at a velocity equal to $V_3 + 300$.

The initial value for the Constant Drag phase is equal to the c_4 finding in the previous range correction phase. During the Constant Drag Range Correction the first step is calculating the error range: also in this case the Transition Phase curve doesn't change. The error range enters in the Eq. (81 and the output is the Δc_4 that must be limited: is maximum value in module is equal to 0.0005. This value is summed to the old value, $c_{4_{new}} = c_{4_{old}} + \Delta c_4$, and, then, it's saturated with the limits finding in Figure 49. This phase finishes when the vehicle reaches the velocity V_4 .

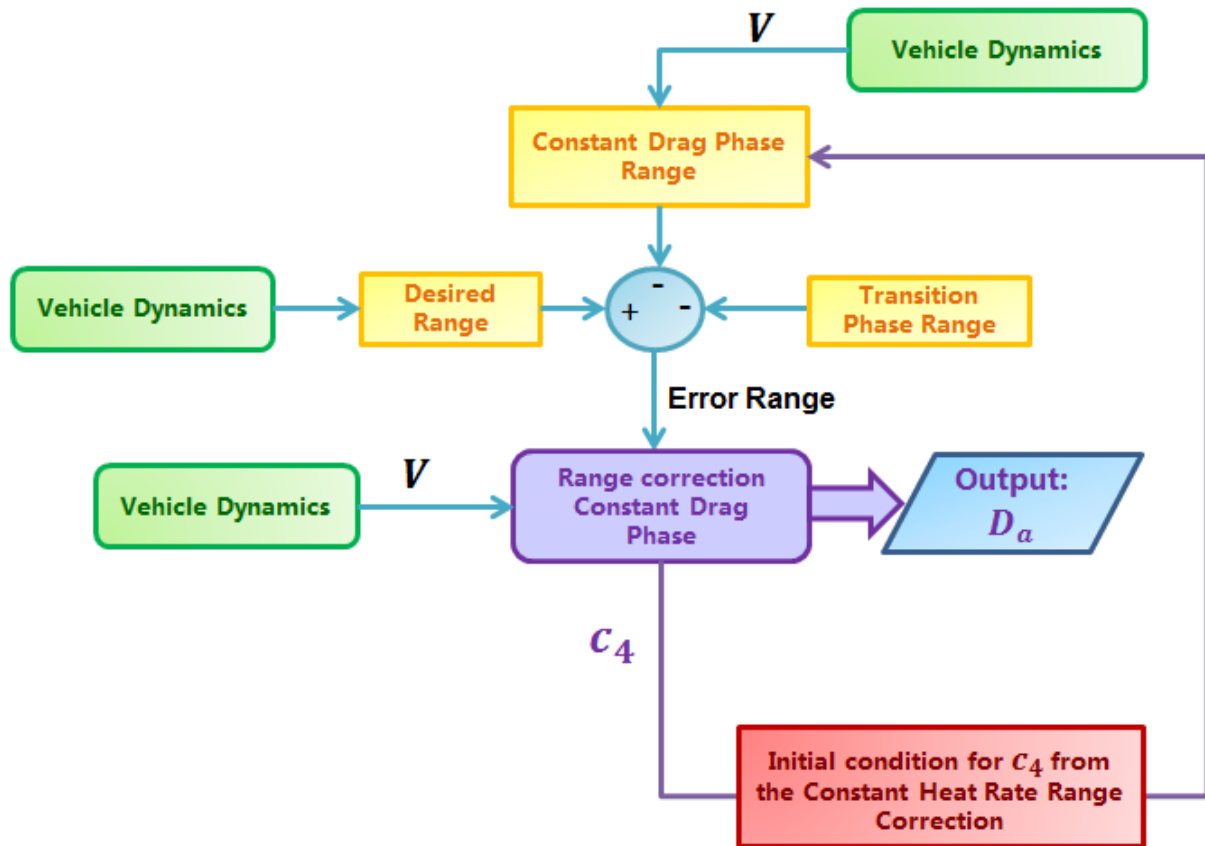


Figure 53: Constant Drag Range Correction Flow Chart.

The initial condition for c_5 is equal to the coefficient that allows linking the Constant Drag Phase final point and the Transition Phase final point. The last Phase provides only the correction of the Transition Phase curve: the error range is given by the difference between the nominal range, calculated from the vehicle actual point, and the desired range. This error, using the Eq. (82), permits the calculation of Δc_5 , that must be limited (the maximum value in module is $2e-8$, this value is equal to the step in the c_5 vector) with a saturator. Using this value it's calculated the new parameter $c_{5_{new}} = c_{5_{old}} + \Delta c_5$. This parameter is saturated: the lower limiter is the same for all the velocities and equal to $c_{5_{minimum}}$, finding in the Figure 50, the upper limit is found with an interpolation, using the $c_{5_{maximum}}$ vector. Now, entering in the drag acceleration matrix (we talk about this matrix in page 60) with the $c_{5_{new}}$ and the actual velocity, is possible obtaining the drag acceleration and then, with a second interpolation, the Energy value for the actual point, these value will be used in the next iteration for calculating the nominal range and the range derivative.

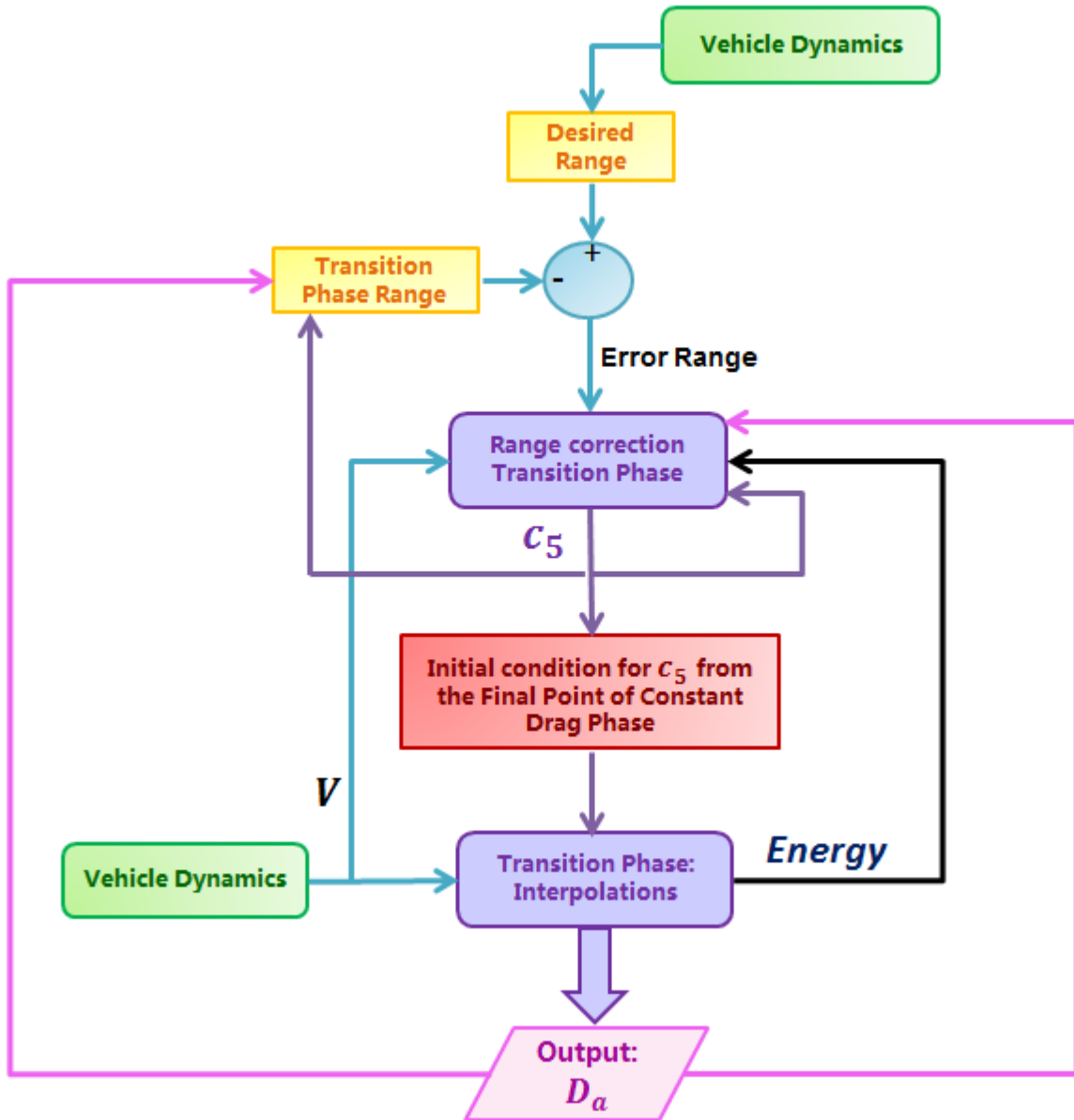


Figure 54: Transition Range Correction Flow Chart.

From each iteration the output is the desired drag acceleration at the current velocity that allows the range correction. The vehicle has its drag acceleration, the difference between the two values (Vehicle Drag Acceleration and Desired Drag Acceleration) is associated with a bank angle, thanks to the PID controller. This bank angle gives the aerodynamic forces that permit to follow the desired drag profile, arriving in the selected final point.

To test the algorithm we use the IXV data, the initial conditions from the Table 1 and PID control gains function of Dynamic Pressure. The results are the following:

Conditions	Nominal	Actual	Guidance Error
Velocity	448.5836 m/s	449.2017 m/s	0.1378%
Altitude	26 Km	26.6 Km	2.3567%
Latitude	3.2721°	3.2673	0.1480%
Longitude	-123.1265°	-123.1313	0.0039%
Range	7103.1 Km	7105.3	2.2387 Km

Table 23: Terminal conditions for IXV 3-Dof dynamic simulation with range correction and PID controller.

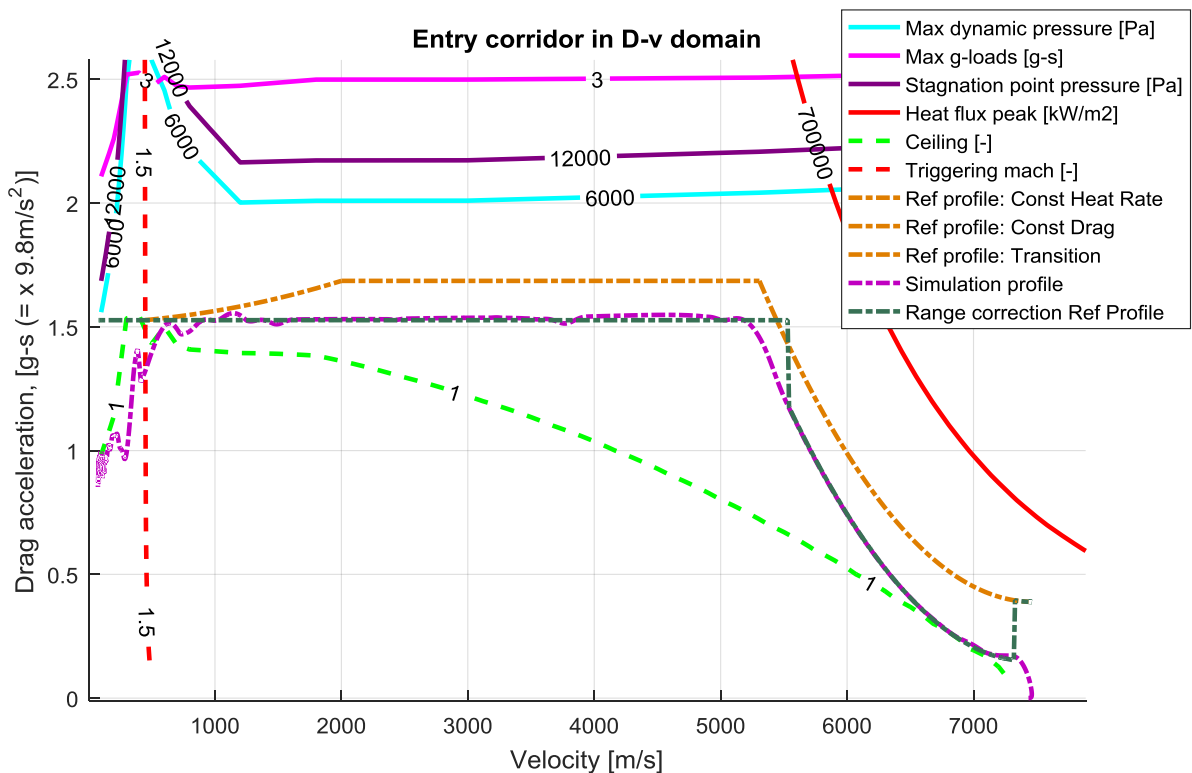


Figure 55: Reference profile, profile after Range Correction and vehicle trajectory.

As we can see in the Figure 55 the reference profile obtained with the Range correction doesn't present discontinuity or oscillations and the final range requirement is respected. But there is a problem: the range chosen is the maximum range reached with this algorithm, the profile has a small freedom to change because of the rigid geometry of each phase. So, for example, we can't choose a trajectory near the ceiling. For this reason it's necessary implements a new strategy for the generation of the initial reference profile and for the range correction. This strategy will use Straight Lines and Splines.

4. New guidance algorithm: custom profile

In this chapter we explain the new strategy for determinate the initial reference profile and the strategy for doing the range correction.

The new reference profile can be created using Spline: a Spline is a function defined piecewise by polynomials. In mathematics, a piecewise function is a function defined by multiple sub-function each sub-function applying to a certain interval of the main function's domain. With the Spline interpolation, it's possible to guarantee the function continuity and the derivative continuity in each node of the chosen interval. In this case the chosen Spline type is a cubic Spline with a not-a-knot end condition, that means that the third derivate is continuous. So chosen a series of point, each interval is described with this function:

$$A(x - x_0)^3 + B(x - x_0)^2 + C(x - x_0) + D \quad (83)$$

Where A , B , C and D are four coefficients and x_0 is the first value of the chosen interval. With this interpolation, a series of four points will be described with three different equations, each equation will have different coefficients where D will be equal to the first value of a couple of points.

In the guidance algorithm the series of point includes 14 couples of points expressed as Drag Acceleration-Velocity. These are the points where the initial reference profile must pass to respect the re-entry corridor limits. The variable x is equal to the velocity and the spline equation gives as result the Drag acceleration in m/s^2 .

4.1 Reference profile

To create an initial reference profile it's important define the re-entry corridor limit that must have the greater importance. Five different possibilities are identified:

- Reference profile equidistant from the limits
- Reference profile distant from the Ceiling
- Reference profile distant from the Constant Heat Flux limit
- Reference profile distant from the g-load limit
- Reference profile distant from the Dynamic Pressure limit

The two final options will be really similar. In all the cases the logic is the same to create the velocity vector:

- The velocity interval where the upper limit it the Heat Flux is described by four nodes: v_6, v_7, v_8, v_9 . The node v_9 corresponds to the initial velocity at the EIP conditions and the node v_6 is the velocity where the upper limit is no longer the Heat Flux limit. The other nodes are chosen to have all the points equidistant. This Phase will be named *Heat Flux Peak Phase*.
- The transition phase is described with four node v_1, v_2, v_3, v_4 : the final node v_1 is the final point corresponding to the TEAM condition and the initial node velocity v_4 corresponds at the point where the aerodynamic flow passes from the hypersonic field to the transonic field. This phenomenon can be seen from the limit curves, because, increasing compression phenomena and

shock waves, the dynamic pressure limit curve changes its curvature and the limit values increase. But if the aerodynamic field is characterised by constant coefficients this phenomena doesn't occur so the initial point is chosen equal to the Velocity which corresponds to a Mach number equal to 3. The other nodes are chosen to have all the points equidistant. This Phase will be named *Transition Phase*.

- Knowing the initial velocity of the Transition phase v_4 and the final velocity of the Heat flux limit Spline v_6 , it's possible to find the average speed v_5 between these two velocities. Then the interval between v_4 and v_5 is divided in 6 parts of same length and other 5 velocities are chosen: $v_{r1}, v_{r2}, v_{r3}, v_{r4}, v_{r5}$. In this phase a lot of points are chosen because with the Spline Interpolation, if the desired profile is similar to a straight curve, the interpolation gives as result a curve profile with oscillation between the node. So, augmenting the nodes, this phenomenon is attenuated. This Phase will be named *Straight Line Drag Acceleration Phase*.
- The Phase for the velocities including between v_5 and v_6 will be named *Connecting Phase*.

Now, knowing the velocity vector, it's necessary to create the Drag acceleration vector: the five cases will take separately in consideration.

- **Reference profile equidistant from the limits:** for creating this profile it's necessary to chose a law for the Drag Acceleration generation; in this case, in each node, the Drag acceleration will be the mean value between the upper and lower limit Drag Acceleration, the lower limit is always the ceiling and the upper limit is the smaller value between the dynamic pressure limit and the g-load limit:

$$D_{aNode} = \frac{D_{aupper} + D_{alower}}{2} \quad (84)$$

For doing this operation has been created a vector contained the Drag Acceleration mean value for each velocity and then, with an interpolation, entered with the nodal velocity, it's obtained the nodal Drag Acceleration. Arriving at the velocity v_4 the logic changes: the curve it's written as the Transition Phase for the Space shuttle, so it's necessary finding the coefficient c_5 that verifies the following equation, where E_1 and D_{a1} are the energy and the Drag Acceleration of the final point and E_4 and D_{a4} are the energy and the Drag Acceleration of the initial point of the Transition Phase:

$$D_{a4} = D_{a1} + c_5(E_4 - E_1)$$

The other points D_{a2} and D_{a3} are calculated, in Matlab with two cycles *for*, finding the Nodal Velocity- Nodal Drag acceleration combination that satisfies the Transition Phase Equation, exactly how we did for the Space Shuttle.

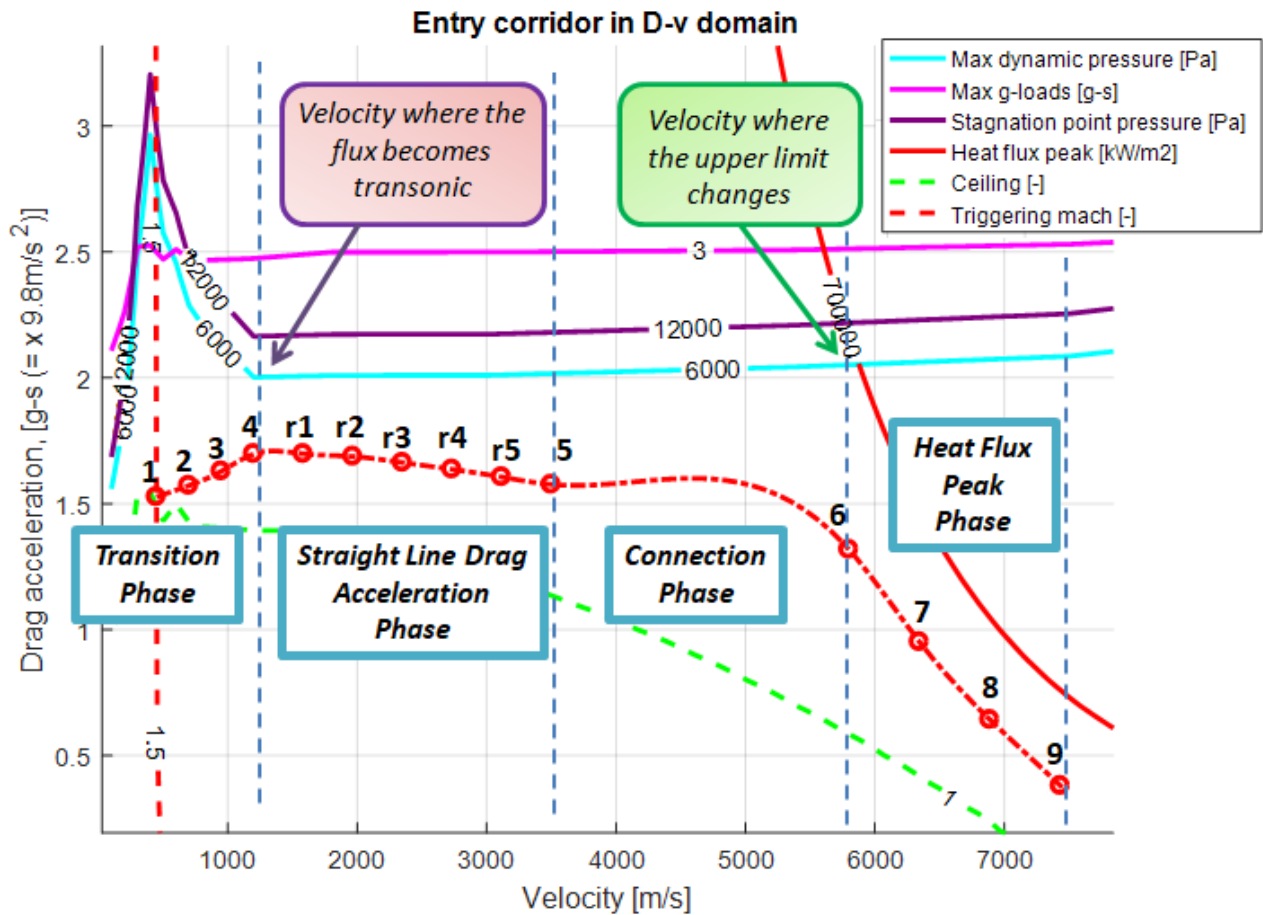


Figure 56: Reference Profile equidistant from the limits (red curve).

- **Reference profile distant from the ceiling:** the first step is redefine the Drag Acceleration D_{a4} , this drag is positioned in the middle between the Upper limit Drag acceleration in v_4 and the node 4 belonged to the "Reference profile equidistant from the limits". Then the second step will be to create an horizontal line, for the Straight Line Drag Acceleration Phase, where all the nodes have the same value of Drag Acceleration. But with this operation the coefficient D will be equal to zero, bringing to numerical problem during the range correction. For this reason the nodal Drag Acceleration will have a value lower than 0.001 with respect to the previous node, except for the node r_1 , that has an Drag Acceleration lower than 0.005 respect to the Drag Acceleration of the node 4. Knowing the new D_{a4} it's possible to find a new value for c_5 and then writing the law for the *Transition Phase*, where the final point is the same of the precedent case. The reference curve *Heat Flux Peak Phase* maintains the same form of the reference curve for the profile equidistant from the limits, but it gets up of a value equal to half of the difference between the Drag Acceleration of the Heat Flux limit at the velocity v_9 and the Drag Acceleration of the node 9 belonging to the reference profile equidistant from the limits. This difference is calculated in the node 9 because this is the point where the re-entry corridor is narrower. The last step is to create the Connection Phase with the Spline Equation. This trajectory is also known as step trajectory.

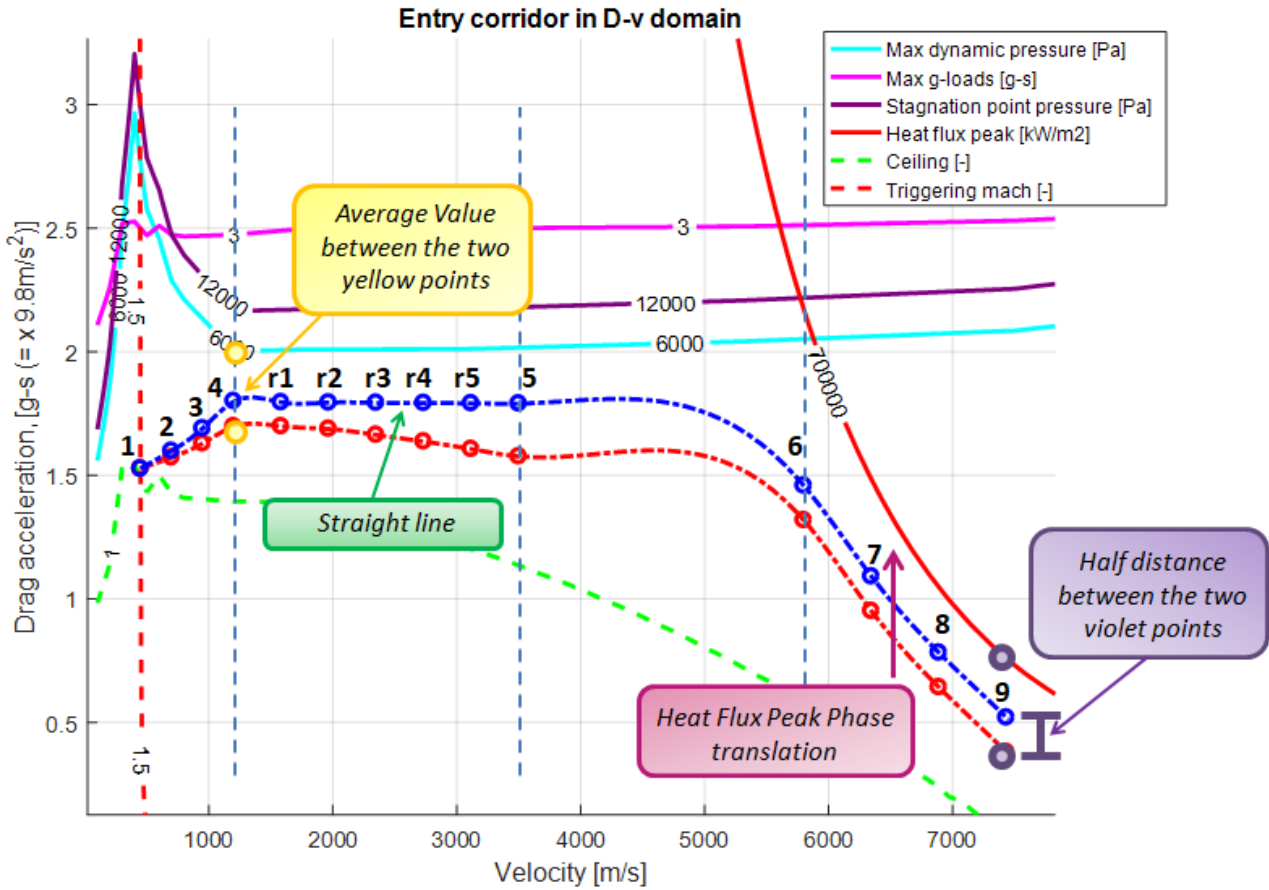


Figure 57: Reference Profile equidistant from the limits (red curve) and Reference Profile distant from the ceiling (blue curve).

- **Reference profile distant from the g-load limit or from the Dynamic Pressure limit:** the reference profile is the same for the two cases. The first step is translating the node 4, which is placed at a Drag Acceleration greater than 0,001 with respect to the acceleration drag of the final point (node 1). Chosen the new node 4, it's possible determinate all the other nodes for the Straight Line Drag Acceleration Phase: the nodal Drag Acceleration will have a value lower than 0.01 with respect to the previous node. Finding all the nodes it's necessary to verify that they aren't lower than the ceiling value: if this happens the nodal Drag Acceleration is posed equal to the ceiling Drag Acceleration. The procedure to finding the Transition Phase is always the same: knowing the initial and the final point it's possible calculate the coefficient c_5 and then, with an Interpolation, finding the Drag Acceleration for the node 2 and 3. The Drag Acceleration for the node 6 it's finding doubling the distance between the Drag Acceleration for the node 5 and the Drag Acceleration for the node 6, both belonging to the reference profile equidistant from the limit. So if in the reference profile equidistant from the limit $D_{a5} - D_{a6} = dif$, now in this new reference profile $D_{a5} - D_{a6} = dif * 2$. The new node 6 has a limit value, in fact it mustn't be lower than the average value between the Drag Acceleration in ceiling and the Drag Acceleration of the reference profile equidistant from the limits, both calculated at the velocity v_6 . The node 9 it's posed halfway between the Drag Acceleration in ceiling calculated at the velocity v_9 and the node 9 from the reference profile equidistant from limits. Now, with a proportion, it's possible finding the distance of the others nodes from the previous node:

$$(D_{a6_{old}} - D_{a9_{old}}) \div (D_{a6_{new}} - D_{a9_{new}}) = (D_{a6_{old}} - D_{a8_{old}}) \div (D_{a6_{new}} - D_{a8_{new}})$$

$$(D_{a6_{old}} - D_{a9_{old}}) \div (D_{a6_{new}} - D_{a9_{new}}) = (D_{a6_{old}} - D_{a7_{old}}) \div (D_{a6_{new}} - D_{a7_{new}})$$

In this problem the unknown value is the difference $(D_{a6_{new}} - D_{a8_{new}})$ and $(D_{a6_{new}} - D_{a7_{new}})$, with the subscript *new* are represented the values belonging to the Reference profile distant from the g-load limit or from the Dynamic Pressure limit and with the subscript *old* are represented the values belonging to the Reference profile equidistant from the limits. Finding this difference and using the old nodal values it's possible calculating D_{a7} and D_{a8} . This trajectory is also known as shallow trajectory.

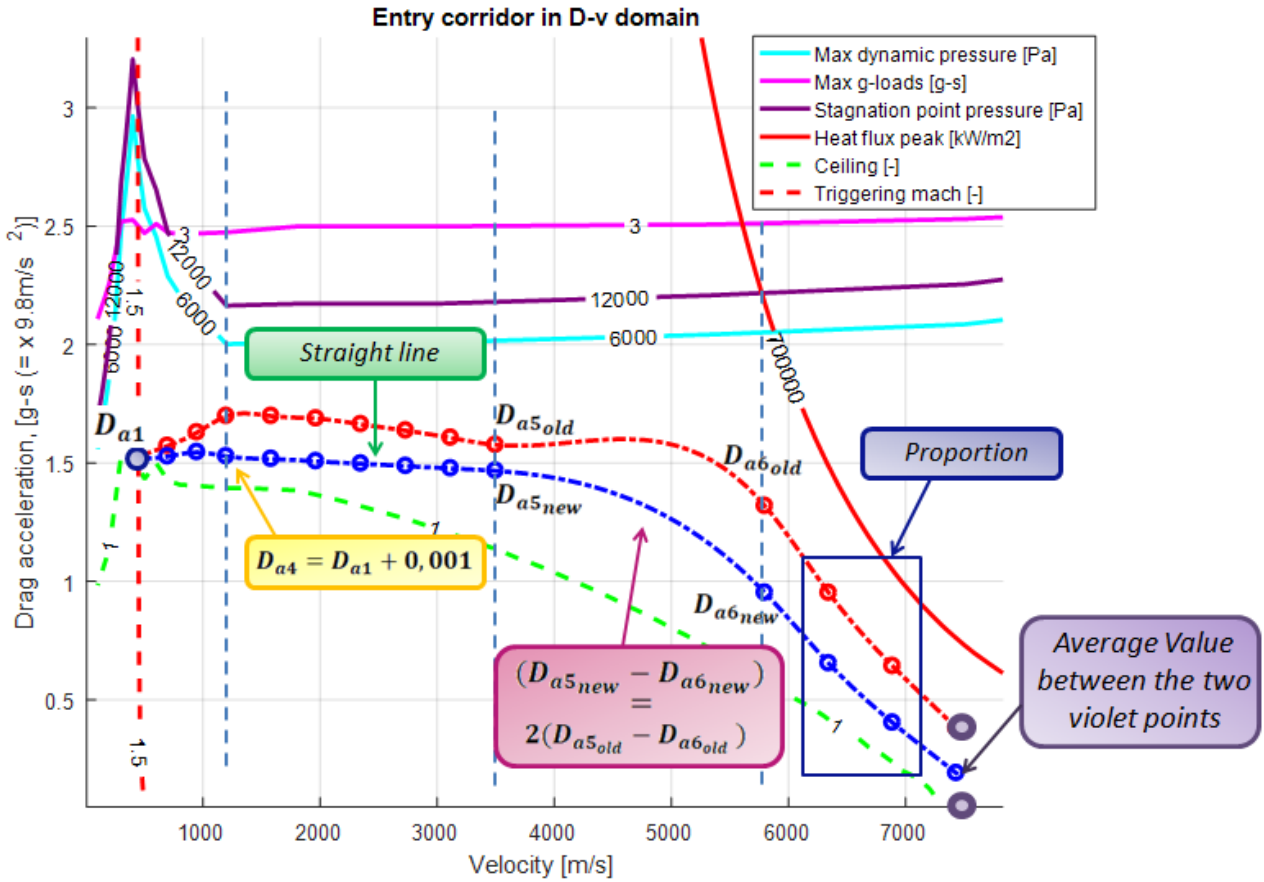


Figure 58: Reference Profile equidistant from the limits (red curve) and Reference Profile distant from the g-load or the dynamic pressure limit (blue curve).

- **Reference profile distant from the heat flux peak limit:** in this reference profile the Transition Phase and the Straight Line Drag Acceleration Phase have the same form of the Reference Profile distant from the Ceiling. The different phase is the Heat Flux Peak Phase, where all the nodes are equidistant from the ceiling: the distance is equal to the Drag Acceleration of the reference profile equidistant from limits at the velocity v_9 .

Then it's necessary identify a limit distance: it's calculated a quarter of the difference between the Drag Acceleration for the upper limit and for the ceiling at the velocity v_4 and a quarter of the difference between the Drag Acceleration for the upper limit and for the ceiling at the velocity v_9 , than it's taken the minimum between the two distance and if this value it's lower than 0.1, the lower limit is raised by this distance and not by 0.1. This operation is doing to avoid that with 0.1 the new lower limits overcomes the initial reference profile when the re-entry corridor is strict.

For the upper limitations the situation is different: if the limitation is not stringent the maximum value is set 0,1 g-s below the upper limit and the limit distance is set equal to the half of the difference between the Drag Acceleration of the upper limit and the Drag acceleration of the reference profile equidistant from limits at the velocity v_4 , for the velocities between v_6 and v_4 , and equal to the quarter of the difference between the Drag Acceleration of the upper limit and the Drag acceleration of the ceiling at the velocity v_9 , for the velocities between v_6 and v_9 .

If the limitation is stringed each case must be analyzed individually:

- For the reference profile distant from the Heat Flux, for the velocities between v_6 and v_9 , the upper limit is set 0,2 g-s below the upper limit. In this case the limit distance is equal to the half of the difference between the Drag Acceleration of the upper limit and the Drag acceleration of the reference profile equidistant from limits at the velocity v_4 .
- For the reference profile distant from the g-load, if the minimum lower limit is the g-load in the re-entry corridor, for the velocities between v_6 and v_4 , the maximum upper limit is set 0,15 g-s below the upper limit. In this case the limit distance is equal to the quarter of the difference between the Drag Acceleration of the upper limit and the Drag acceleration of the ceiling at the velocity v_9 .
- For the reference profile distant from the Dynamic Pressure, if the minimum lower limit is the Dynamic Pressure in the re-entry corridor, for the velocities between v_6 and v_4 , the maximum upper limit is set 0,15 g-s below the upper limit. In this case the limit distance is equal to the half of the difference between the Drag Acceleration of the upper limit and the Drag acceleration of the reference profile equidistant from limits at the velocity v_4 .
- For the reference profile equidistant from limits all the limitation are set 0,1 g-s below the upper limit. In this case the limit distance, for the velocities between v_4 and v_6 , is equal to the half of the difference between the Drag Acceleration of the upper limit and the Drag acceleration of the reference profile equidistant from limits at the velocity v_4 . For the velocities between v_6 and v_9 , the limit distance is equal to the quarter of the difference between the Drag Acceleration of the upper limit and the Drag acceleration of the ceiling at the velocity v_9 .

Then it's necessary evaluate the limitation for the transition phase: the lower limit, as we had already seen with the algorithm based on the Space Shuttle model, is the curve with c_5 equal to zero, an horizontal line passed for the final Drag acceleration and parallel to the X-axis. The maximum c_5 value is the coefficient belonging at the curve that links the final Drag Acceleration and the couple of points with a velocity equal to the average velocity between v_1 and v_4 and the Drag Acceleration equal to the upper limitation for the point with the velocity equal to v_4 . Knowing the maximum and the minimum c_5 it's possible finding a vector where there are 500 equidistant value of c_5 .

Then it's created a velocity vector and, with two *for* cycles and interpolations, it's finding the combination of Drag Acceleration-Velocity- c_5 that solves the equation $D_{aF} - D_{a_{chosen}} + c_{5_{chosen}}(E_{chosen} - E_F) = par$, with *par* equals to zero. The final result is a matrix of Drag Acceleration, a vector of velocity and a vector of c_5 . Entered in the matrix with the maximum Drag Acceleration (this drag is equal to the Drag Acceleration for the limitation in the point 4), it's possible finding, with an interpolation, for each velocity between v_1 and v_4 , the maximum allowed value for c_5 . For the lower limit it's taken the second value of the vector, because a c_5 equal to zero will lead numerical problems in the range correction algorithm.

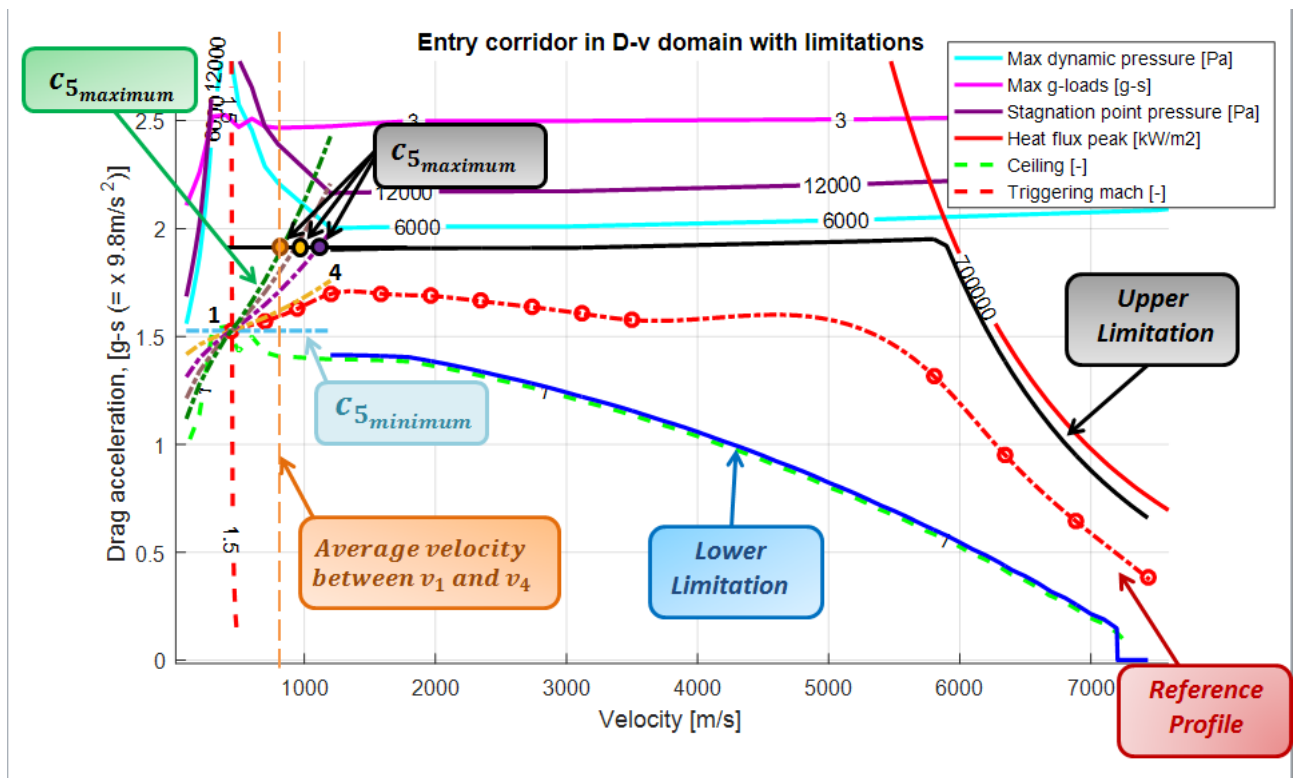


Figure 60: Example of lower and upper limitation for a reference profile.

4.2 Maximum and Minimum Range

The user selects the initial and final point expressed with latitude and longitude. For arriving at the final point the vehicle must run across a certain range. But because of the re-entry corridor limits a maximum and a minimum range exists. The desired range must be contained between these two range values.

The maximum range is travelled when the vehicle flies near the ceiling, but it's important that the vehicle never overcomes the ceiling curve because if that happens the vehicle becomes uncontrollable. So it's necessary chose the limit curve: the first idea is choosing a Drag Acceleration reference profile equal to the lower limitation (blue curve in 61) until the vehicle reaches a velocity equal to v_{r3} . Then for the velocities

between v_1 and v_4 the Drag acceleration reference profile is an horizontal line with a value equal to the final Drag Acceleration D_{a_1} . The section included between v_4 and v_{r3} has a reference profile represented by a straight line passing for two points: the first point has a velocity equal to v_4 and a Drag Acceleration equal to D_{a_1} , the second point has a velocity equal to v_{r3} and a Drag Acceleration equal to the Drag of the lower limitation at the velocity v_{r3} . But using this reference profile, the vehicle, trying to following the reference with a PID controller, went to the ceiling, behaviour that we want to avoid.

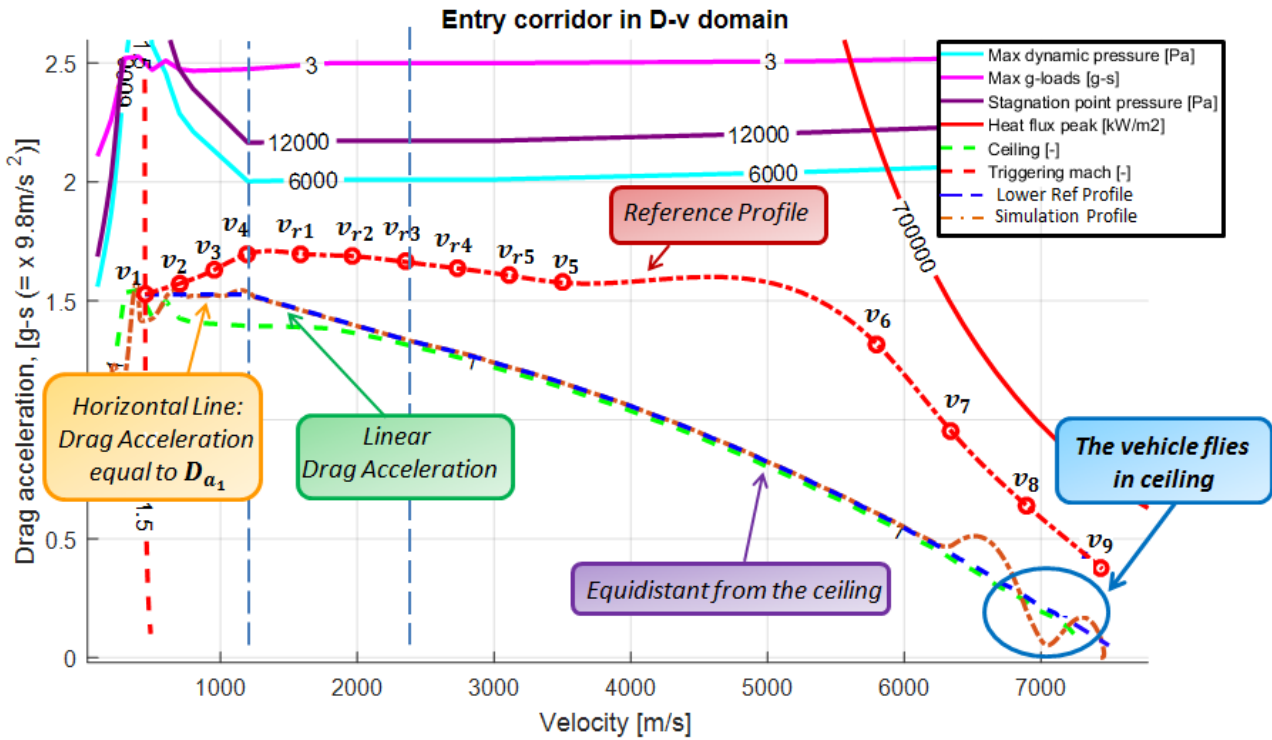


Figure 61: Lower Reference profile and Drag Acceleration profile from the simulation with a PID controller and a pre-entry bank angle equal to 18°.

So it's necessary to impose a different reference profile for the first part of the flight: this new profile must maintain the highest Drag Acceleration so the vehicle gains the necessary dynamic pressure for not going in ceiling.

The procedure is the following:

- The vehicle, at the velocity v_9 , can fly in ceiling but, when it goes out from this situation, the vehicle mustn't return in ceiling during the Pre-Entry Phase. So it's necessary to choose an appropriate initial Bank Angle: with a low angle the vehicle returns in ceiling in the Pre-Entry Phase.
- With a PID controller the vehicle follows the lower reference trajectory.
- It identifies the velocity V_1 : at this velocity finishes the Pre-Entry Phase. $D_{a_{V_1}}$ is the Drag Acceleration of the reference profile (in red in figure 61) at the velocity V_1 .
- Following the reference profile the vehicle can return in ceiling, because its dynamic pressure is too low. When the vehicle comes out again from the ceiling it's identified the velocity V_2 : at this velocity the vehicle will have a Drag Acceleration equal to $D_{a_{V_2}}$.
- It's identify the new velocity $V_{1/10}$ equal to V_1 minus a tenth of the difference between V_1 and V_2 .
- The new lower reference profile for the velocity between V_1 and $V_{1/10}$ will be equal to a straight line passed for $V_1 - D_{a_{V_1}}$ and for a second couple of point $V_{1/10} - D_{a_{V_{1/10}}}$, where $D_{a_{V_{1/10}}}$ is the Drag Acceleration of the lower reference profile at the velocity $V_{1/10}$, finding with an interpolation.

Following this new profile the vehicle doesn't return in ceiling.

- This procedure it's done with different initial Bank Angle, from the first Bank Angle equal to 18° to a last Bank Angle equal to 70°. The first Bank Angle that guarantees that the vehicle doesn't return in ceiling, during the Pre-Entry Phase, will be the chosen Bank Angle.
- In certain situations with all the Bank Angle the vehicle doesn't return in ceiling nor in the Pre-Entry Phase nor after. This means that it develops the necessary dynamic pressure right away and it's not necessary to create a new lower reference profile. The initial Bank Angle will be equal to 18°, intact with a low angle the maximum range will be bigger.
- In other situations with all the Initial Bank angle the vehicle re-enters in ceiling during the Pre-entry Phase. In this case the Initial Bank Angle is chosen equal to 18°: but it must be clear that the aircraft will travel a very high range but at the expense of controllability.

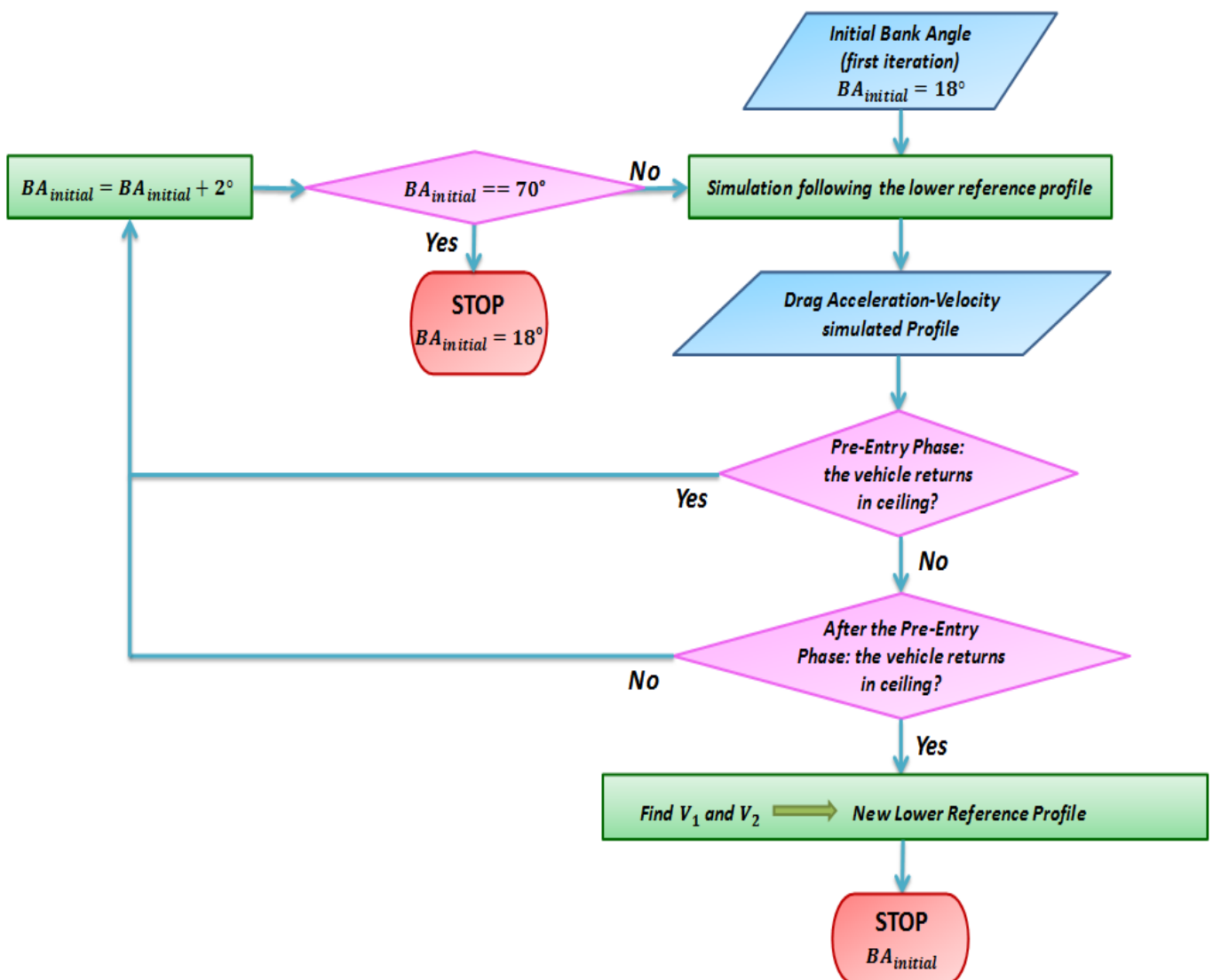


Figure 62: Chosen of the Pre-entry Bank Angle and lower reference profile for the simulation with maximum range.

There are two cases where the initial bank angle is set equal to 18°: the vehicle never returns in ceiling and the vehicle always returns in ceiling during the Pre-Entry Phase. The difference is that with the second case the range is really high: the vehicle can go even 9046 Km, but in the first part of the flight it's uncontrollable. In the first case the maximum range remains content.

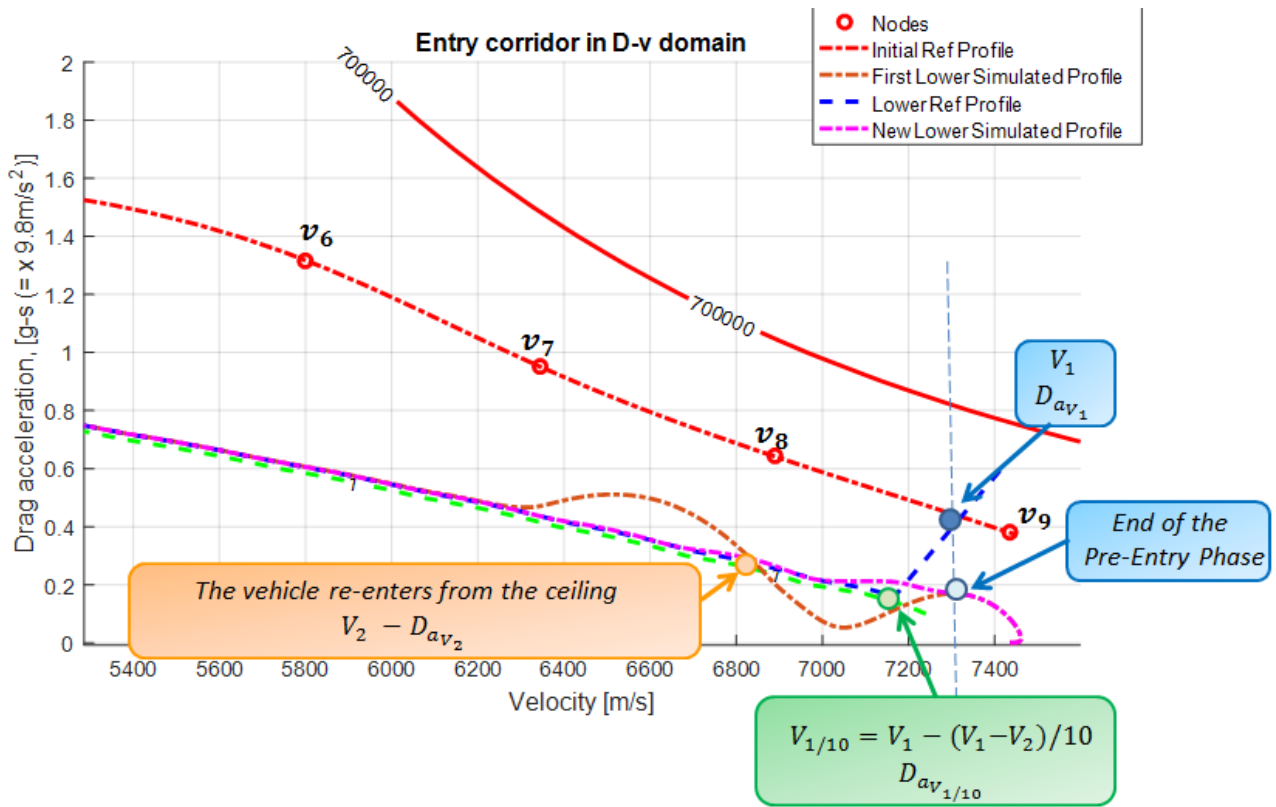


Figure 63: Identification of the Lower Reference Profile that gives the Maximum Range (blue curve) with an Initial Bank Angle of 18°.

Following the blue curve in Figure 63 the vehicle has a trajectory represented by the purple curve: this trajectory is obtained with an Initial Bank Angle equal to 18°. The range obtained following the lower reference Trajectory is the maximum range obtainable.

Initial Bank Angle	Maximum Range
18°	7634 Km

Table 24: Maximum Range and Initial Bank Angle for the Lower Reference Trajectory.

The blue curve in Figure 63 will be also the new lower limitation in the Re-Entry corridor, during the range correction algorithm. After to reach the velocity V_1 , the reference profile doesn't change form.

For finding the Minimum Range the vehicle must fly with the higher available Drag Acceleration: in the Heat Flux Peak Phase, in the Straight Line Drag Acceleration Phase and in the Connection Phase the profile is equal to the upper limitation finding in the Chapter 4.1, in the Transition Phase the reference profile is found using the maximum c_5 value .

The Pre-Entry Bank Angle is set equal to 70° for all the cases except for the Reference Profile distant from the Heat Flux Peak limit where the Bank angle is set equal to 60°. This chose is done because with a lower Bank Angle the vehicle reaches the reference profile at lower speeds and therefore there are less chances of exceeding the limit.

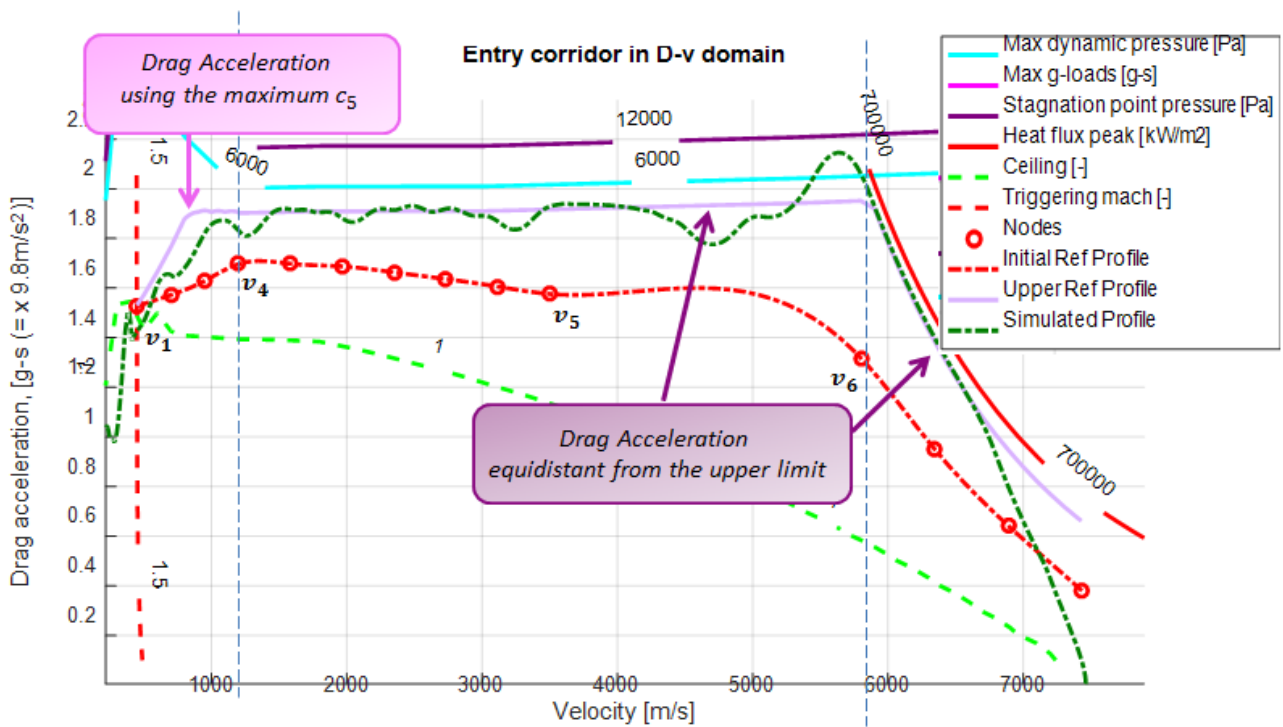


Figure 64: Identification of the first Upper Reference Profile that gives the Minimum Range (purple curve) with an Initial Bank Angle of 70° and the Profile obtained after the simulation (green curve).

Using this reference profile the vehicle overcomes the limits because the PID controller isn't able to follow the sudden change of curvature of the reference profile at the velocity v_6 . To avoid this behaviour the upper reference profile is changed: there are identified two velocities. The first velocity V_T is equal to the average velocity between v_6 and v_7 and the second velocity V_R is equal to v_6 minus a third of the difference between v_6 and v_5 . For the velocities between V_T and V_R the upper reference profile is represented by a constant Drag Acceleration equal to the Drag Acceleration of the upper limitation at the velocity V_R . Using this shrewdness the vehicle can follow the reference profile without exceed the limits of the Re-entry Corridor.

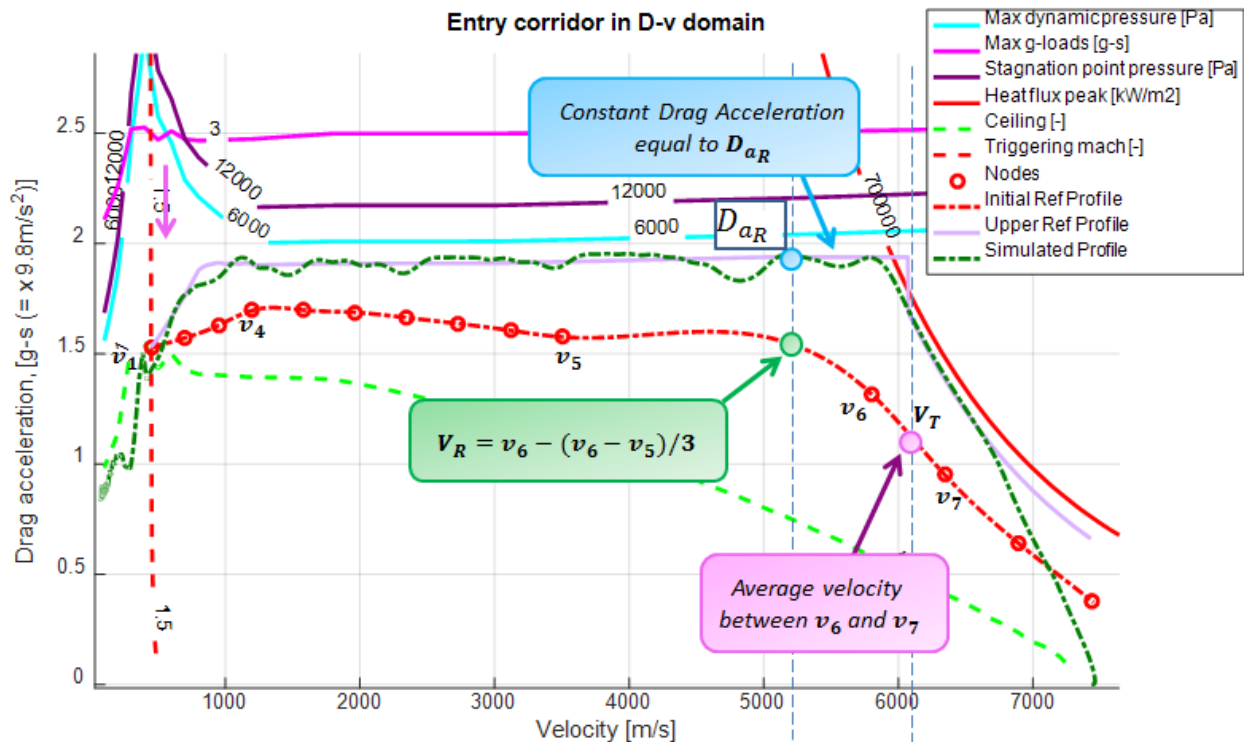


Figure 65: Identification of the final Upper Reference Profile that gives the Minimum Range (purple curve) with an Initial Bank Angle of 70° and the Profile obtained after the simulation (green curve).

Following the purple curve in Figure 65 the vehicle has a trajectory represented by the green curve: this trajectory is obtained with an Initial Bank Angle equal to 70°. The range obtained following the lower reference Trajectory is the minimum range obtainable.

Initial Bank Angle	Maximum Range
70°	4631 Km

Table 25: Minimum Range and Initial Bank Angle for the Upper Reference Trajectory.

These two profiles allow to find the maximum and minimum range, overcoming these values the vehicle doesn't respect the re-entry corridor limits. So it's necessary verify that the initial and final points, chosen by the user, are linked by a range contained between the two minimum and maximum values.

Now with a *Matlab* script it's possible identify, chosen the final coordinates, all the initial point that respect the upper range limitation and the lower range limitation. The output are two curves: the couples of coordinates internal to the two curves represent the eligible initial points.

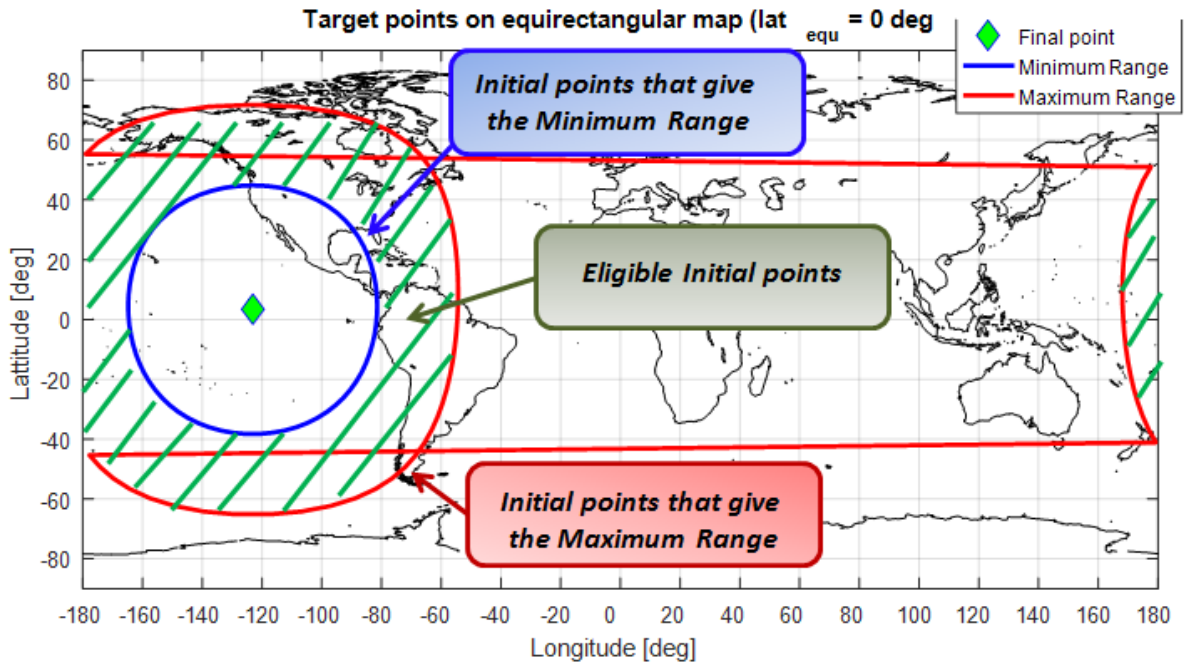


Figure 66: Eligible initial points (EIP location) to respect the Upper and Lower range limitations.

With this procedure it's then possible to determine the shallow trajectory (figure 63) and the steep trajectory (figure 65), these two trajectories are really important not only for determining the maximum and minimum range but also for understanding the maximum and minimum loads to sizing the vehicle systems.

4.3 EIP initial conditions

Knowing the initial and final point it's necessary to set up the initial Heading: the heading is the angle between the North and the Body X-axis.

With a formulation, using a four-quadrant inverse tangent, considering the Earth as a sphere, it's possible to find the Bearing, the angle between the North and the line passing from the Target and the centre of the vehicle:

$$Bearing = atan2(\sin(long_f - long_i) * \cos(lat_f), \cos(lat_i) * \sin(lat_f) - \sin(lat_i) * \cos(lat_f) * \cos(long_f - long_i)) \quad (85)$$

For having the vehicle aligned with the target it's necessary that the initial Heading will be equal to the Initial Bearing. So with the Eq. 85 it's also possible to find the initial Heading.

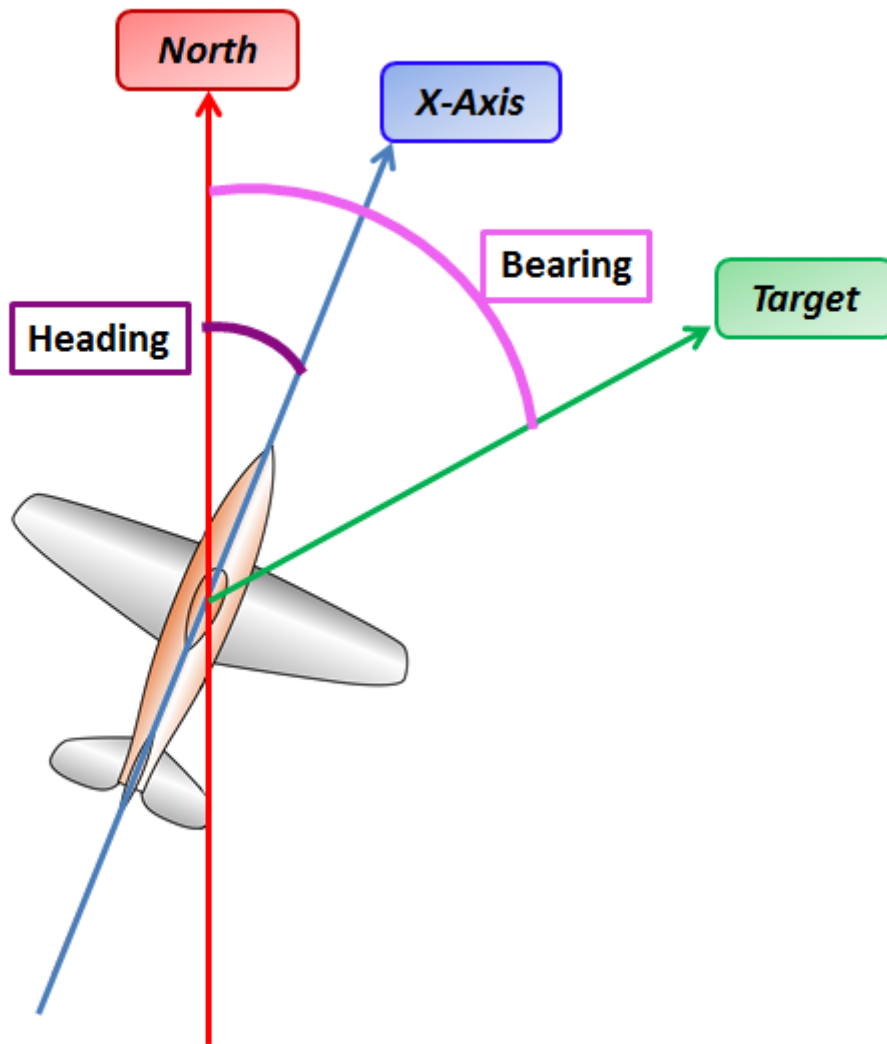


Figure 67: Bearing and Heading for the vehicle: in this picture the two angles have a positive value.

During the simulation the lateral controller has the task to keeping aligned the X-axis and the axis passing through the target.

The initials conditions are chosen by the user that must be aware about the vehicle dynamic: in fact if the vehicle has to fly in a direction opposite to the Earth rotation it's necessary have a larger velocity.

The vehicle velocity in a rotating system (in this case the reference system is expressed in wind axis) is given by the sum of two contributes: the velocity respect to an inertial system and a second contribute gives from the product between the angular velocity of the rotating system and the distance from the inertial system. In this case the inertial system is the ECI reference system and the angular velocity is the Earth angular velocity, because the vehicle angular velocity is neglected.

$$V_{Wind} = V_{ECI} - \omega_{Earth} \times r_{ECI} \quad (86)$$

We can take two different final points, positioned at the same latitude but at an opposite longitude respect to the initial point

	Latitude	Longitude
Initial point	-4,48°	173°
Final point A	3,27°	236,87°
Final point B	3,27°	110°

Table 26: Initial and final geographical coordinates.

To reach the point B the vehicle flies in the opposite direction to the Earth's rotation, while the point A is situated in a direction in agreement with the Earth rotation.

We impose then the vehicle starts with an initial velocity in wind axis equal to 7434,85 m/s, in the two situations the term $\omega_{Earth} \times r_{ECI}$ in module is the same but changes the sign: for the situation A this term is positive, for the situation B this term is negative. This means that, if in the two situations the initial velocity is the same but the term $\omega_{Earth} \times r_{ECI}$ has opposite sign, the V_{ECI} in A is biggest then the V_{ECI} in B.

	V_{Wind}	V_{ECI}	$\omega_{Earth} \times r_{ECI}$
Final point A	7434,851589 m/s	7906,423603 m/s	472,4138881 m/s
Final point B	7434,851589 m/s	6963,393705 m/s	472,4138881 m/s

Table 27: Initial conditions for two different situations

The V_{ECI} will be used as initial condition in the integral dynamic block in Simulink, this initial condition gives the initial forces, so if the velocity V_{ECI} is low also the forces will be low. The forces will then be decomposed into aerodynamic, gravitational and propulsive forces, but if the resultant is low also the single forces will be low. This will mean that such forces will not be enough to keep the vehicle in high orbit, so the vehicle, unable to decelerate, penetrates deeply into the atmosphere and reaches low altitude with high velocity, where it gains an high dynamic pressure. High dynamic pressure means high aerodynamic forces but also high Drag Acceleration: the vehicle will overcome the limit of the re-entry corridor.

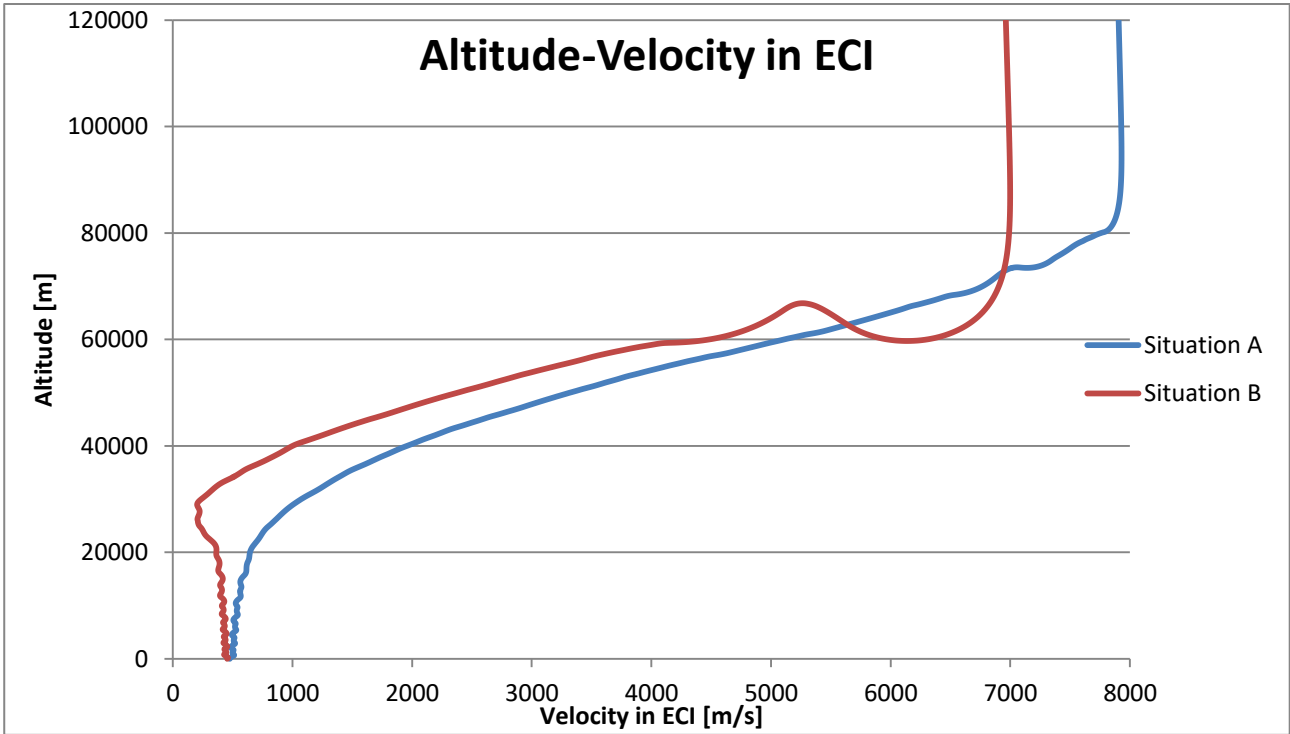


Figure 68: Velocity in axis ECI respect to the Altitude for the two situations.

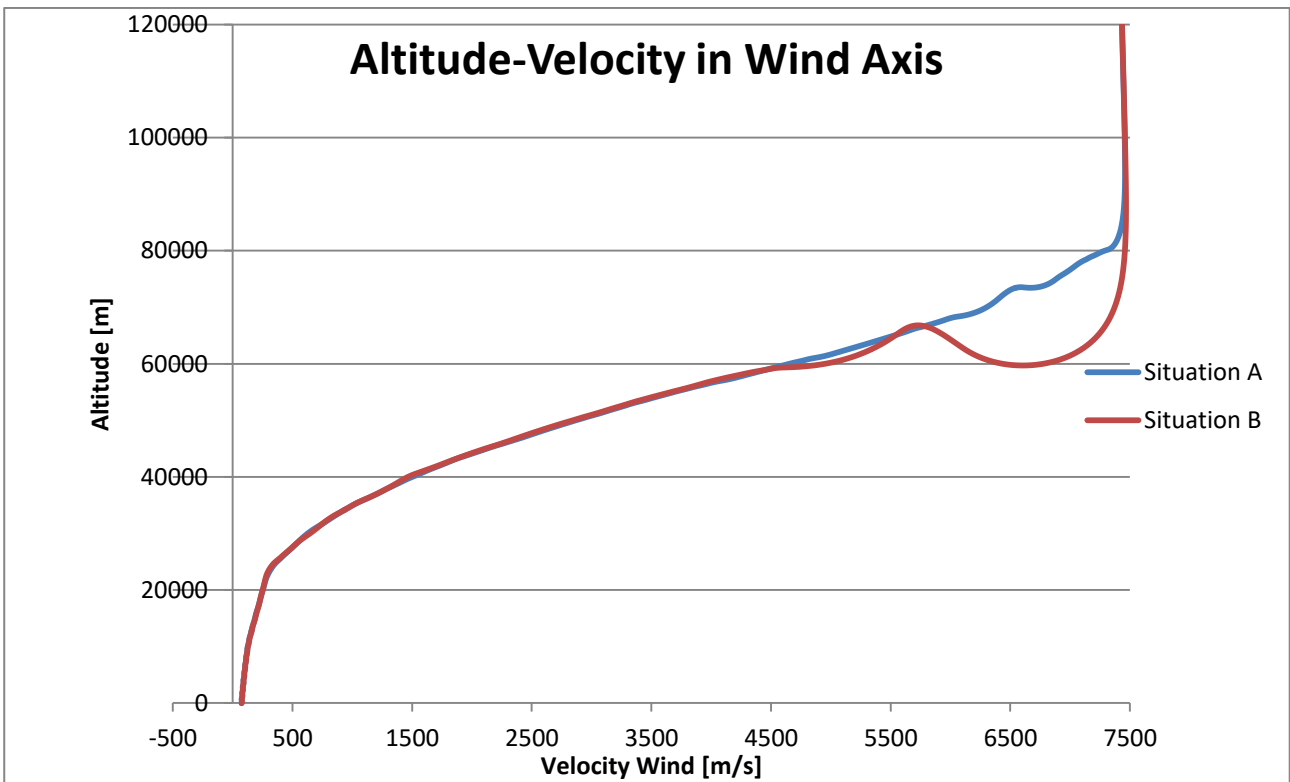


Figure 69: Velocity in wind axis respect to the Altitude for the two situations.

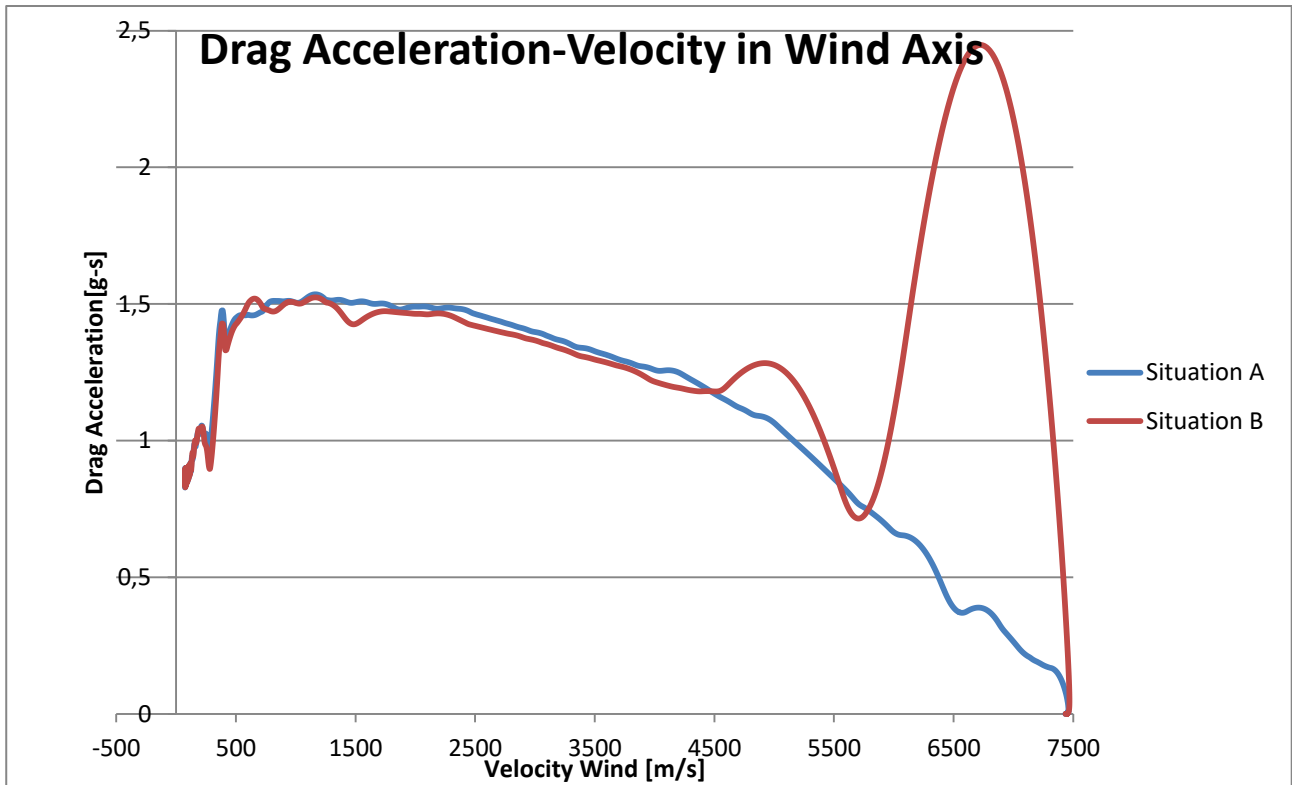


Figure 70: Velocity in wind axis respect to the Drag Acceleration for the two situations.

After this analysis we have understand that it's really important choosing with cognition the initial conditions because not all the combinations lead to results.

4.4 Range formulation Validation

Now, defined the initial profile, it's necessary calculating the range obtained following the profile. A first elucidation it's necessary: for simplifying the problem the profile is written connected the nodes in the Connection Phase and Straight Line Drag Acceleration Phase with Straight Line. For this reason the equation changes form:

$$D_a = AV + B \tag{87}$$

In the Eq. 87, A and B are two coefficients (B is the known term), V is the velocity, D_a is the Drag Acceleration .

The coefficients A and B are found using the formulation of a Straight Line passing through two points:

$$A = \frac{D_{af} - D_{ai}}{V_f - V_i} \tag{88}$$

$$B = D_{ai} - AV_i$$

With the subscript i we identify the initial node, and with f the final node.

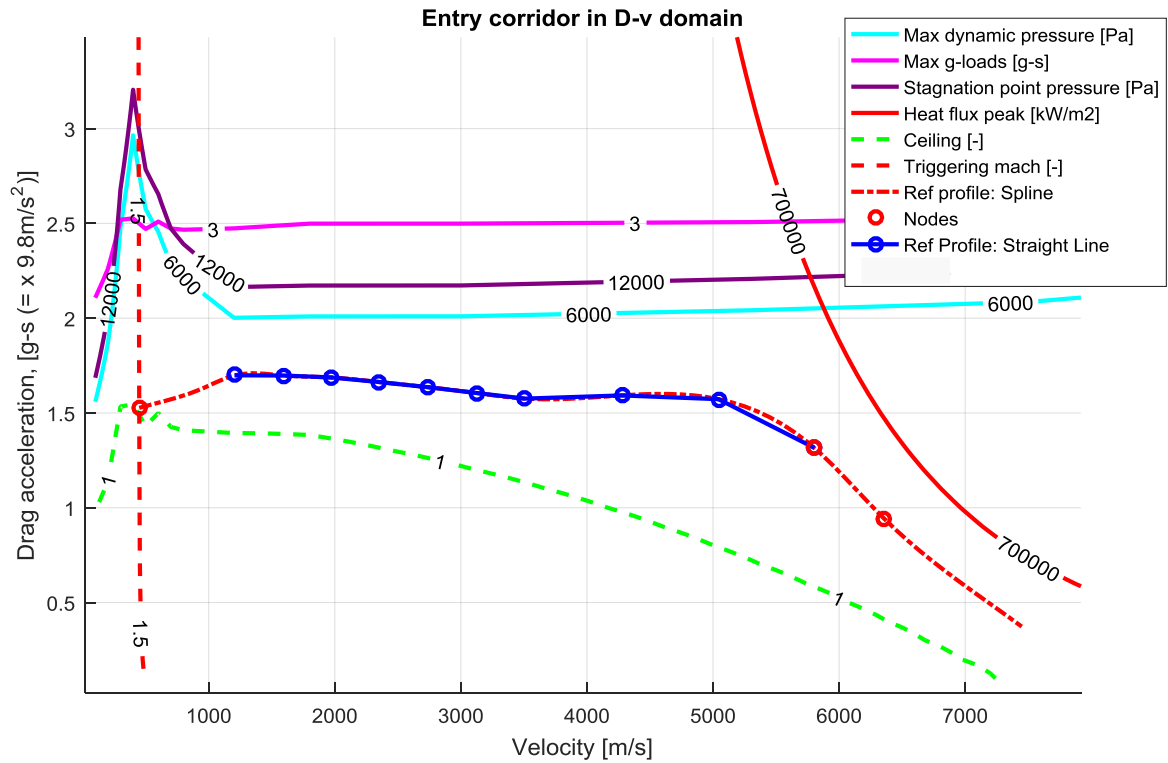


Figure 71: Reference profile with Spline and Straight Lines.

As we can see in Figure 71, the Straight Lines in the Connection phase don't match perfectly the Spline lines but with this approximation the equation is easier. The Connection Phase is divided in three parts.

The range s is calculated starting from an integral:

$$s = - \int_{V_i}^{V_f} \frac{V}{D_a} dV \quad (89)$$

The integral is solved with the Matlab command *integral*: this command numerically integrates the function using global adaptive quadrature and default error tolerances equal to $1e-10$.

For the Transition Phase the range is function of the Energy and the solution is an exactly solution :

$$s = - \int_{E_i}^{E_f} \frac{1}{D_a} dE = \log\left(\frac{D_{a_i}}{D_{a_f}}\right) c_5 \quad (90)$$

Now it's necessary to compare the range found with the formulations and the range obtained with a simulation. So a simulation runs and the range is saved for each Phase. Then it's calculated the analytic range from the initial velocity to the final velocity for each Phase. The comparison starts when the Simulated profile intersect the Reference profile, for this reason the initial point doesn't coincide with a node.

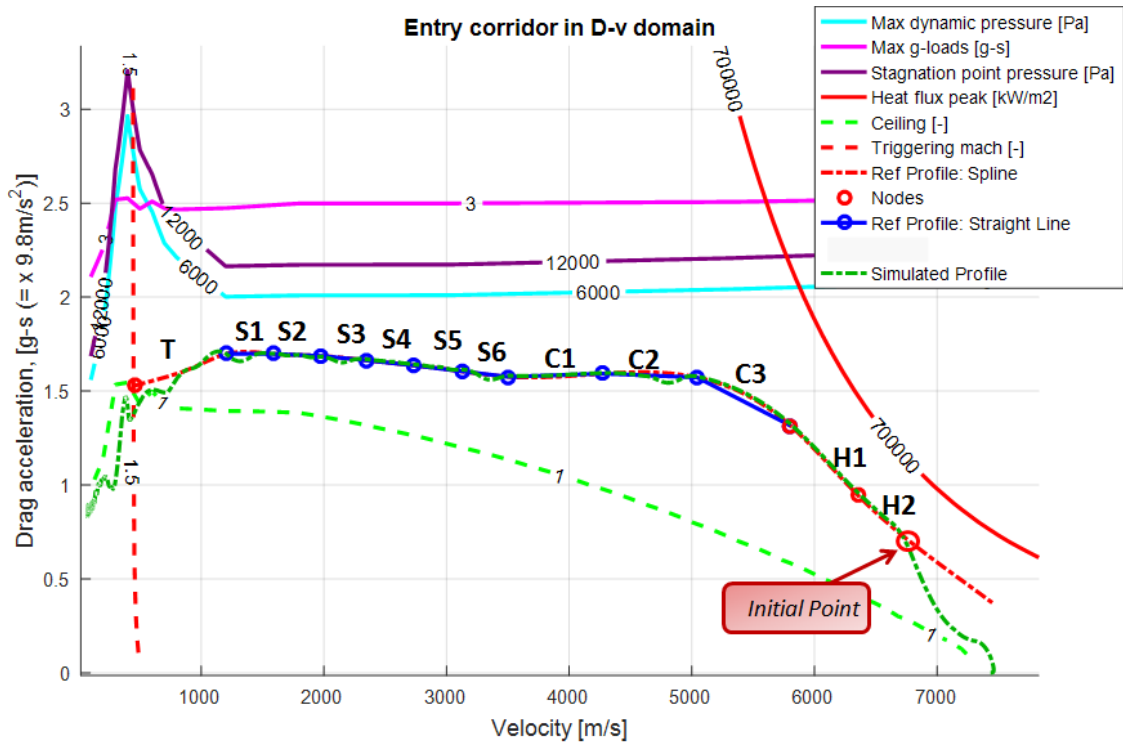


Figure 72: Reference Profile and Simulated profile for the range formulation validation.

Phase		Simulate Range [Km]	Analytic Range [Km]	Error [Km]	Error %
Transition	T	42,7554466	44,1819544	-1,426507799	3,336435268
Straight Line	S1	32,89296535	30,9472501	1,945715248	5,915292911
	S2	40,32463001	38,9741073	1,350522713	3,349126111
	S3	48,60518599	47,80695546	0,798230534	1,642274415
	S4	57,39981795	57,17090024	0,228917715	0,398812616
	S5	69,42797092	69,02536755	0,402603365	0,579886406
	S6	78,73593231	77,71891585	1,017016458	1,291680212
Connection	C1	188,3844625	188,4122512	-0,027788668	0,01475104
	C2	223,7321286	225,1176	-1,385471443	0,619254576
	C3	277,0385858	286,285997	-9,247411195	3,337950621
Heat Flux Peak	H1	294,5909762	297,9261362	-3,335159954	1,132132422
	H2	278,0465588	283,3409609	-5,294402054	1,904142269

Total Range	1631,934661	1646,908396	-14,97373508	0,917545012
--------------------	-------------	-------------	--------------	-------------

Table 28: Simulated Range, Analytic Range and Error for the Range Formulation Validation.

As we can see from the Table 29, the final error is really small, 0.9%, so the model can be used for the Range Correction.

4.5 Range correction

Also in this case the first aim is going from an initial point to a final point, so the range obtained following the reference profile must be equal to the desired range. If the two ranges are different a range correction is necessary, exactly as in the case of Space Shuttle Algorithm.

In this case the first operation is to translate the reference curve to obtain a range as close as possible to the desired range. With this operation the form of the Reference curve doesn't change: the nodes from the point 4 to the point 9 are translated by the same distance, than the Transition Phase is recreated connecting the final point (node 1), that doesn't move, with the new point 4.

The translation distance is equal to one tenth of the minimum difference between the initial reference profile and the upper limitation, if the curve must go up. This difference is calculated for all the velocities including between v_4 and v_9 . If the curve must go out the consider distance is equal to the minimum between two values:

- The minimum difference between the Drag acceleration from the initial reference profile and the Drag Acceleration from the lower limitation
- The difference between the Drag Acceleration for the point 4 and the final Drag Acceleration (point 1)

Taken the minimum value, the considered distance is equal to one tenth.

The reference profile must go up if the desired range is lower than the simulated range and it must go out if the desired range is bigger than the simulated range. The simulated range is obtained following the reference profile with a Pre-Entry Bank Angle equal to 44°.

The simulation is towed after one of the two end conditions has been reached:

- 10 iterations have been completed and the reference profile has reached the upper or lower limitation: this profile will be the new reference profile, the error range isn't equal to zero but it has been minimized.
- The difference between the desired range and the Simulated Range changes sign: the new reference profile that minimize the range error is obtained with an interpolation, where it's possible to find the translation distance that gives as result for the range error zero.

The translated profile will be the new Reference Profile.

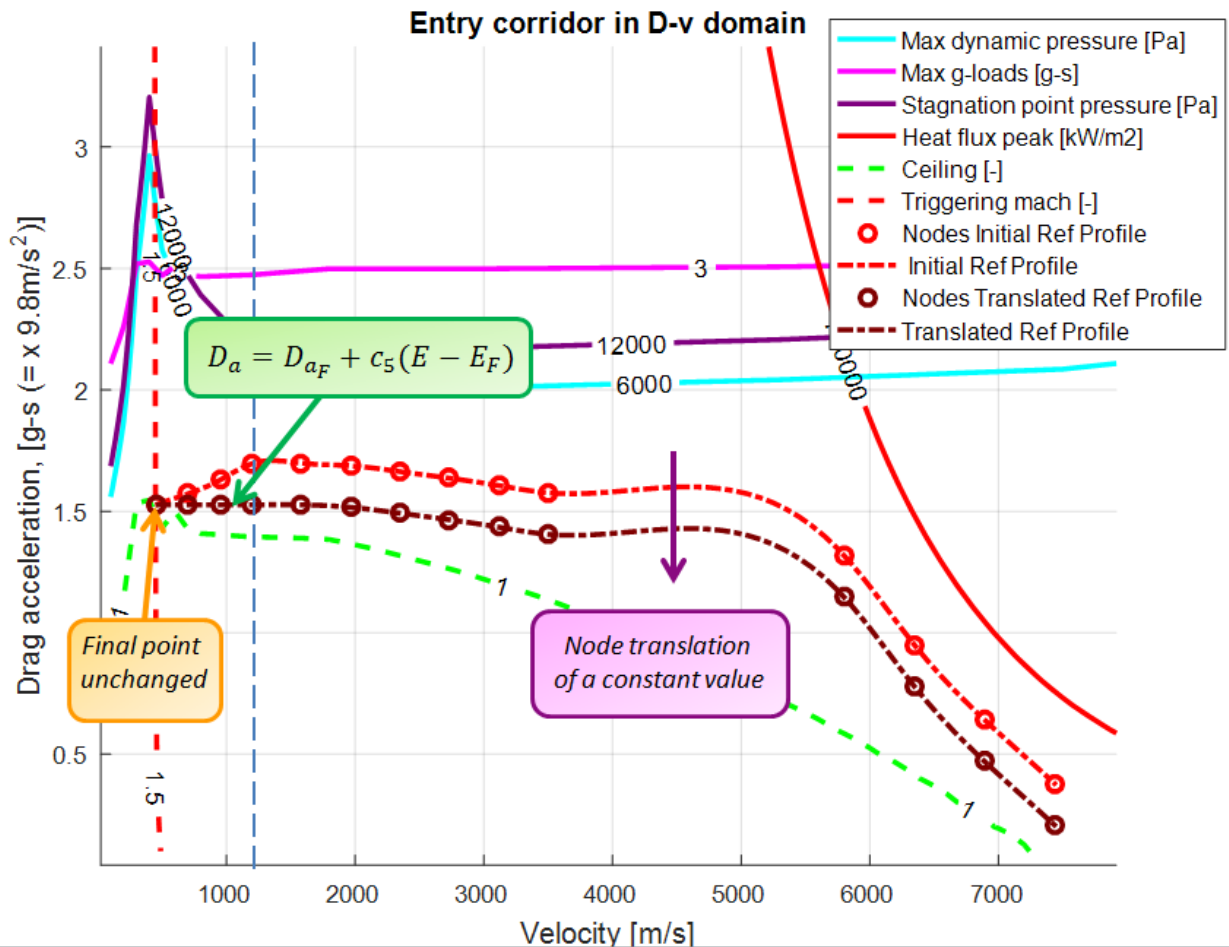


Figure 73: Example of the reference curve translation.

The second step is choose the Pre-Entry Bank Angle. The strategy is the following:

- Create a vector with different Pre-Entry Bank Angle values, from the bank angle chosen for the lower profile (Chapter 4.2) to the bank angle chosen for the upper profile (70° or 60°), with a step of 2°.
- Test the system behavior for each Pre-Entry Bank Angle, following the Reference Profile and saved the Total simulated range.
- Choose the Bank Angle that gives the minimum difference between the desired range and the simulated range. This will be the new Pre-Entry Bank Angle.

Now it's possible redefine the new lower reference profile with the new $V_1, D_{\alpha_{V_1}}, V_{1/10}$ and $D_{\alpha_{V_{1/10}}}$ using the new Pre-Entry Bank Angle.

In a lot of cases, the translated profile doesn't give a range error equal to zero so it's necessary create a law for the range correction. If the range error is restrained, it's possible link the ratio between range error Δs and variation of constant term with the derivate of the range respect to the known term:

Phase	Drag segment form	Known term	Variation of Known Term
Spline	$D_a = A(V - V_f)^3 + B(V - V_f)^2 + C(V - V_f) + D$	D	$\Delta D = \frac{dD}{ds} \Delta s$
Straight Line	$D_a = AV + B$	B	$\Delta B = \frac{dB}{ds} \Delta s$
Transition	$D_a = D_{aF} + c_5(E - E_F)$	c_5	$\Delta c_5 = \frac{dc_5}{ds} \Delta s$

Table 29: Strategy for the Range correction.

So if the reference curve is translated of the value written in the last column in Table 30, the range error tends to zero.

The derivative for the Spline is found numerically using a product of three different derivatives:

$$\frac{dD}{ds} = \frac{dD}{dD_a} \frac{dD_a}{dV} \frac{dV}{ds} \quad (91)$$

The first derivative $\frac{dD}{dD_a}$ is equal to 1. The derivative $\frac{dD_a}{dV}$ can be found analytically and it is equal to:

$$\frac{dD_a}{dV} = 3A(V - V_f)^2 + 2B(V - V_f) + C \quad (92)$$

The last derivative can be found using approximations :

$$-ds = -\frac{V}{D_a} dV$$

So:

$$\frac{dV}{ds} = \frac{D_a}{V} \quad (93)$$

The value of D_a and V are the Drag Acceleration and the Velocity calculated in the current point and for the successive phases they are the value calculated for the initial node of each phase.

The derivative for the Straight Line is calculated analytically, with an exact formulation:

$$\frac{ds}{dB} = -\frac{1}{A^2} \log(AV + B) - \frac{B}{A^2(AV + B)} + \frac{1}{A^2} \log(AV_f + B) - \frac{B}{A^2(AV_f + B)} \quad (94)$$

Also in this case V is the current velocity or the initial velocity for the next phases.

For the Transition Phase the range derivative is equal to the derivative found in the Space Shuttle Algorithm:

$$\frac{ds}{dc_5} = \frac{1}{c_5} \left[-s + \frac{E - E_f}{D_a} \right] \quad (95)$$

In this case the range s , the Drag Acceleration D_a and the Energy E are the values at the current point.

But the curve, with the translation derived from the range correction, can't overcome the limitations found in the Chapter 4.1, so it's necessary identify an algorithm to limit the known value:

- For each Phase is identified an initial and final velocity V_i and V_f . If the Phase is the current Phase the initial velocity is the current velocity. For these two velocities, it is found, with interpolations, the Drag Acceleration belonged to the upper and lower limitation ($D_{a_{i_{lower}}}, D_{a_{f_{lower}}}, D_{a_{i_{upper}}}, D_{a_{f_{upper}}}$).
- The variable to be found is the known term of the curve passed for the Drag Acceleration belonged to the upper limitation for the two velocities and the known term of the curve passed for the Drag Acceleration belonged to the lower limitation for the two velocities. The other coefficients stay the same.

The formulations for the known term D of the Spline are the following:

$$\begin{aligned} D_{i_{lower}} &= D_{a_{i_{lower}}} - A(V_i - V_f)^3 - B(V_i - V_f)^2 - C(V_i - V_f) \\ D_{f_{lower}} &= D_{a_{f_{lower}}} \\ D_{i_{upper}} &= D_{a_{i_{upper}}} - A(V_i - V_f)^3 - B(V_i - V_f)^2 - C(V_i - V_f) \\ D_{f_{upper}} &= D_{a_{f_{upper}}} \end{aligned} \quad (96)$$

The formulations for the known term B of the Straight Line are the following:

$$\begin{aligned} B_{i_{lower}} &= D_{a_{i_{lower}}} - V_i A \\ B_{f_{lower}} &= D_{a_{f_{lower}}} - V_f A \\ B_{i_{upper}} &= D_{a_{i_{upper}}} - V_i A \\ B_{f_{upper}} &= D_{a_{f_{upper}}} - V_f A \end{aligned} \quad (97)$$

- If the analyzed Phase is the current Phase the limit coefficient is the coefficient found for the current velocity (V_i), in fact we want that the reference curve, at the current velocity, can reach the limitation.

- For the other phases, if the curve goes up, the analyzed coefficients are the coefficients with the subscript *upper*: it's taken the lower coefficient between $B_{i_{upper}}$ and $B_{f_{upper}}$ for the Straight Line and the lower coefficient between $D_{i_{upper}}$ and $D_{f_{upper}}$ for the Spline. With the chosen coefficient all the points between V_i and V_f don't overcome the limitations. if the curve goes down the analyzed coefficients are the coefficients with the subscript *lower*: it's taken the bigger coefficient between $B_{i_{lower}}$ and $B_{f_{lower}}$ for the Straight Line and the lower coefficient between $D_{i_{lower}}$ and $D_{f_{lower}}$ for the Spline. With the chosen coefficient all the points between V_i and V_f don't overcome the limitations.
- These limit values are calculated only if certain situations are checked: if the values ΔD or ΔB are negative, the curve will goes down and only the values with the subscript *lower* will be calculated. If the values ΔD or ΔB are positive, the curve will goes up and only the values with the subscript *upper* will be calculated. These value are calculated each step of simulation.

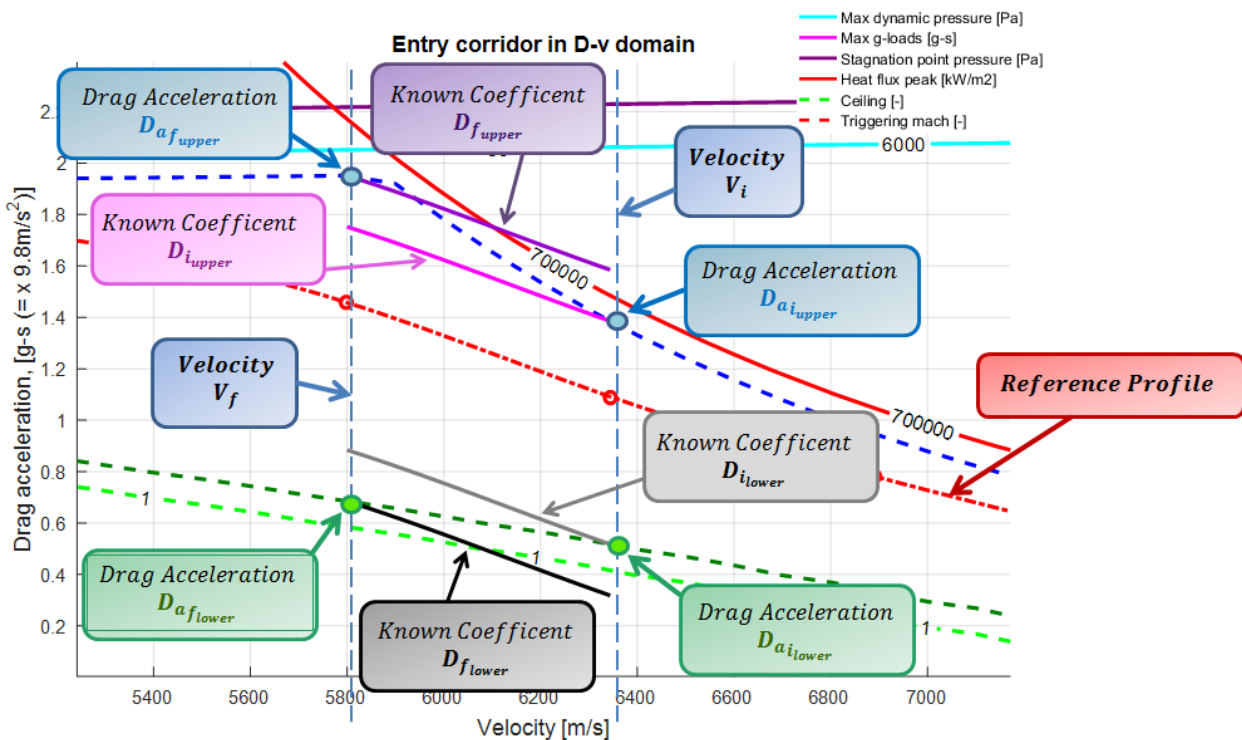


Figure 74: Example of upper and lower known coefficients for a reference profile represented with Spline.

For the Transition Phase the maximum and the minimum value for c_5 is found in Figure 60, using the same procedure of the Space Shuttle Algorithm.

The algorithm aim is the same explained for the Space Shuttle: the range error, given by the difference between the desired range (distance between final point and actual point) and the nominal range (range obtained following the reference profile), must be brought to zero, this operation is made translating the reference profile. Then the vehicle must follow the reference profile (expressed as combination of Drag Acceleration-Velocity): the difference between the Reference Drag Acceleration and the vehicle Drag Acceleration enters in a PID controller, the output is the Bank Angle necessary to bring the Drag Acceleration error to zero.

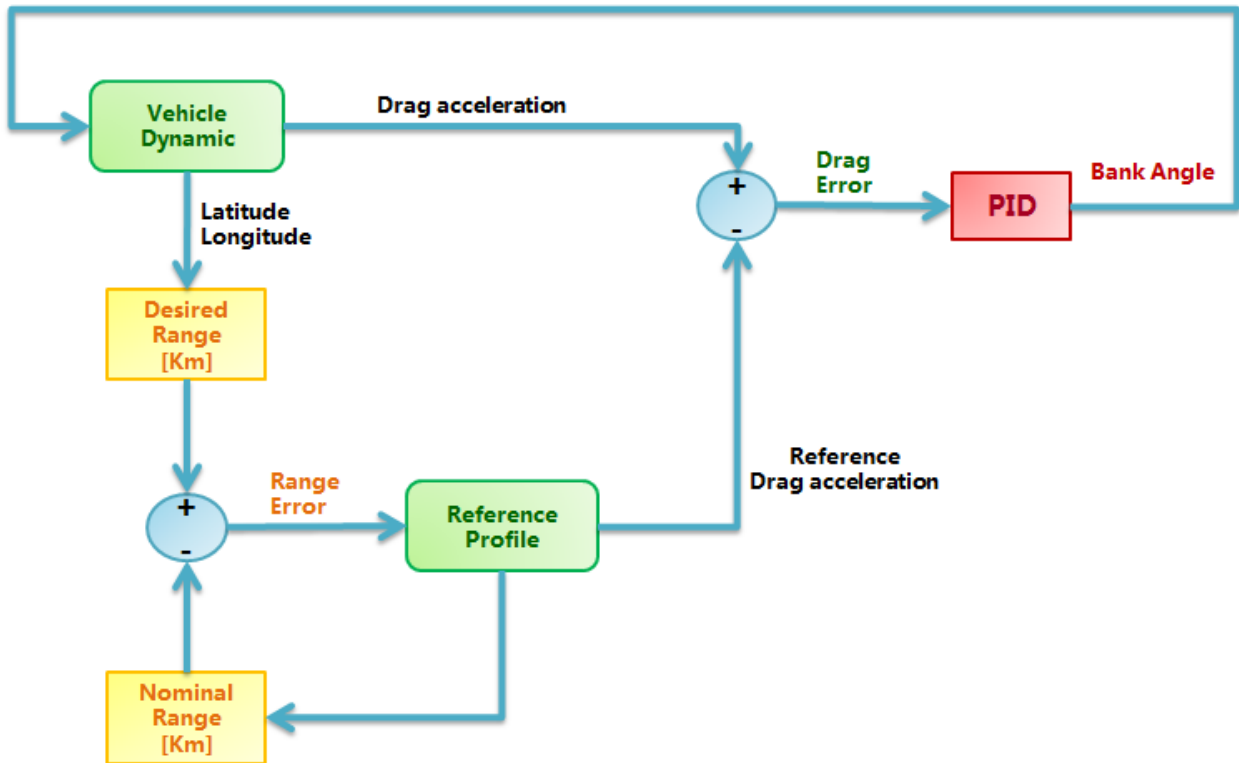


Figure 75: Vehicle GNC flow Chart.

The last step is to identify a procedure to translate, during the simulation, the reference profile. Respect to the Space Shuttle Algorithm, in this algorithm, a new is introduced: the range correction and then the translation of the reference profile is done every two simulation steps, using a Triggered Subsystem. This solution is been adopted to reduce the simulation time. Without the Triggered Subsystem the simulation Elapsed time is 115 seconds, using the Triggered Subsystem this time will decrease, reaching a value of 24 seconds.

Until a Dynamic Pressure of 478.8 Pascal the vehicle is in Pre-Entry Phase, using the Initial Bank Angle finding previously. Reached the necessary Dynamic Pressure a new Phase starts: the *Heat Flux Peak Phase*.

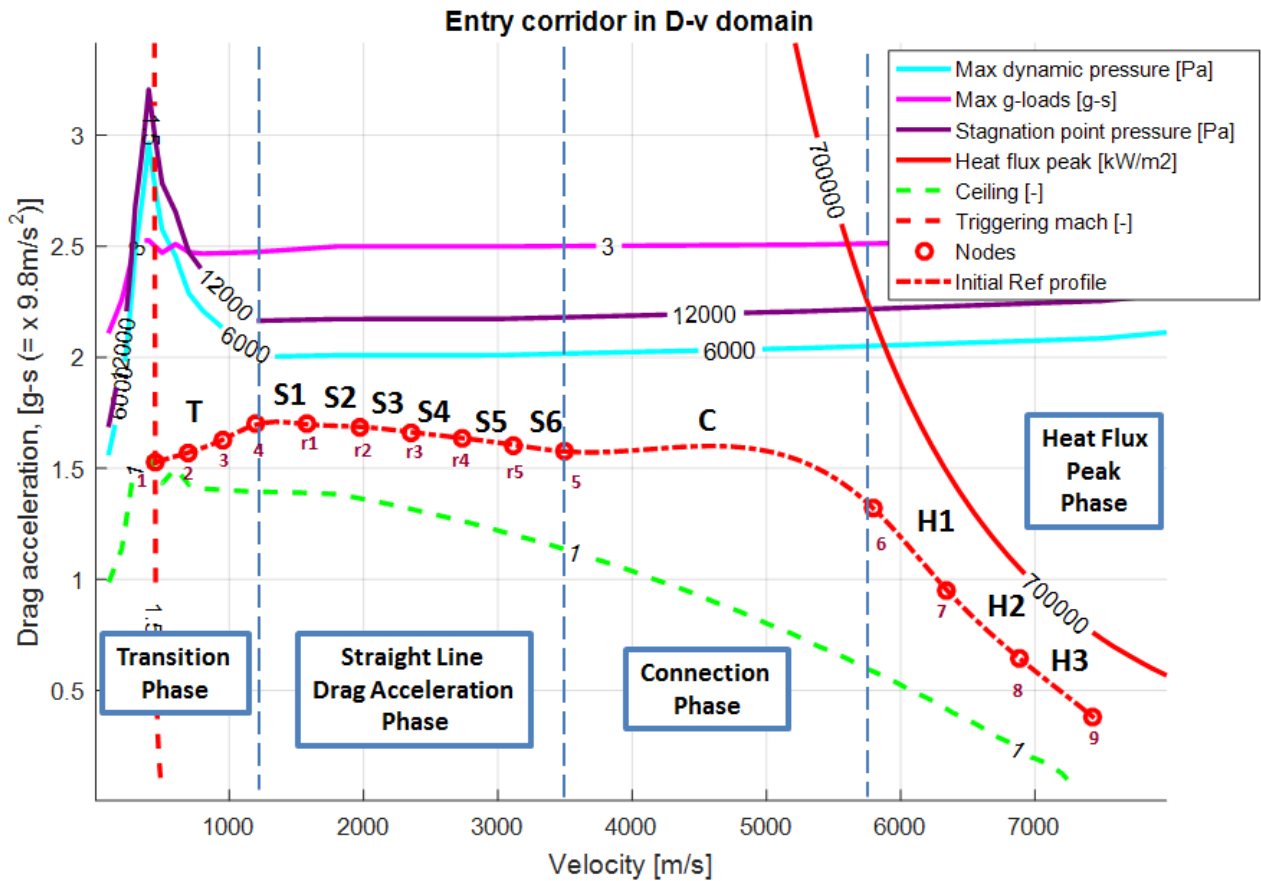


Figure 76: Reference Profile nodes and phases.

The Heat Flux Peak Phase is divided in three segments: *H1*, *H2* and *H3*. Each segment is included between two nodal velocity. *H1* is includes between v_6 and v_7 , *H2* is includes between v_7 and v_8 , *H3* is includes between v_8 and v_9 . The strategy for the range correction is the following:

- The straight Line Drag Acceleration Phase is translated by a value proportional to the range error given by the difference between the desired range and the nominal range (each simulation step only the Transition Phase Range will stay unchanged, the other phases are translated so the range changes). All the nodes, included between v_4 and v_5 , will be translated of the same value, until a limit value is reached. This limit value is equal to the Drag Acceleration belonging to the upper limitation for the velocity v_4 , if the curve goes up, and equal to Drag Acceleration belonging to the reference curve for the velocity v_1 (final point), if the curve goes down.

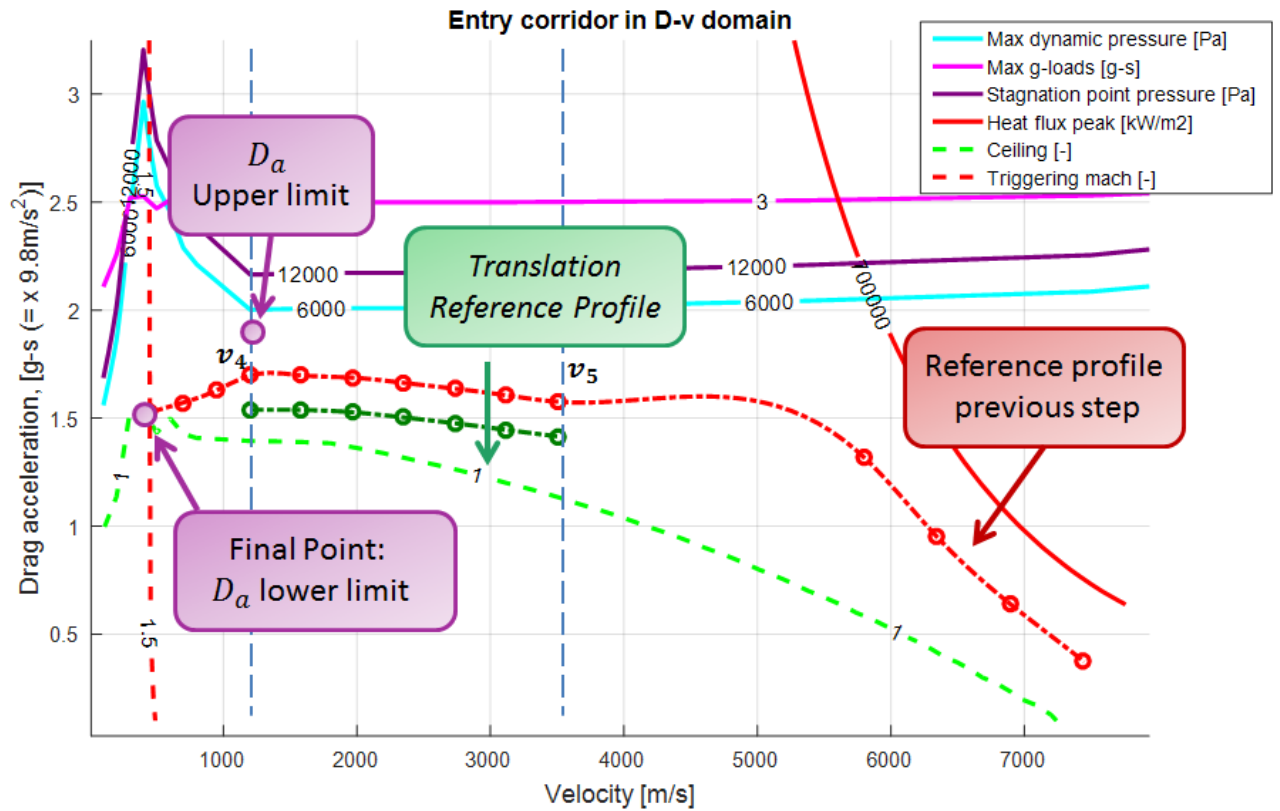


Figure 77: Straight Line Drag Acceleration Phase translation for the range correction. The behavior is only qualitative.

- Knowing the new Spline Equations for the Straight Line Drag Acceleration Phase it's possible to calculate a new range and then a new range error Δs . For the calculation of the range error the Straight Line Drag Acceleration Range is given by the curve just found. The *H1*, *H2*, *H3* and *Connection Phase* ranges are given by the old reference profile found with the previous step. This error will be used for the translation of the last part of the Heat Flux Peak Phase *H1*. The translation consists in identifying the variation of the known term in the equation of the spline to make the range error tends to zero. Remembering that the Spline equation for the Phase *H1* is the following:

$$D_{a_{H1}} = A_{H1}(V - v_6)^3 + B_{H1}(V - v_6)^2 + C_{H1}(V - v_6) + D_{H1}$$

The variation of the Known term will be given by the following expression:

$$\Delta D_{H1} = \frac{dD_{H1}}{ds} \Delta s$$

This new curve will give a new range value. In this equation the derivate $\frac{dD_{H1}}{ds}$ is calculated as function of the initial and final nodal Drag Acceleration and velocity. If the current velocity doesn't belong to the interval between v_6 and v_7 , the initial nodal velocity corresponds to the velocity v_7 and the final nodal velocity to the velocity v_6 . If the current velocity belongs to this interval the initial nodal velocity is the current velocity. The curve can't overcome the limit value for the know term found previously.

- The same procedure will be done for the Phase $H2$ and $H3$, finding new value for D_{H2} and D_{H3} . The difference is that $H1$ range will be calculated using the new translated profile. The $H2$ range is calculated using the new translated profile when the considered Phase is the $H3$ Phase. When the current velocity changes phase, the previous phases will no longer be considered. This means that if the current velocity belongs to the phase $H2$, the phase $H3$ isn't considered. When the current velocity belongs to the phase $H1$, the phases $H2$ and $H3$ aren't considered. The curves can't overcome the limit value for the know term found previously.
- At the end of this operation we have obtained three curves $H1$, $H2$ and $H3$. But the nodes of these three curves aren't connected. So it's necessary created a new curve for the Heat Rate Peak Phase: this operation is performed in the block "*Heat Rate Peak Phase Spline with the average values*". It's calculated the nodal Drag Acceleration for each phase belonging to the *Heat Rate Peak Phase*, than for two nodes that have the same velocity, it's found the average Drag Velocity between the two nodal Drag Acceleration: this will be the new node for the Spline. The first node is always the Drag Acceleration at the current velocity for the translated reference curve. The last node is the Drag Acceleration at the velocity v_6 for the translated curve $H1$ ($D_{av6_{new}}$). But to build a Spline it's necessary have four nodes, so when the phase $H3$ ends, it's necessary creates new nodes. These new nodes have as velocity v_5 and v_{r5} and as Drag Acceleration the Drag Acceleration $D_{av5_{new}}$ and $D_{avr5_{new}}$ given by the following relation:

$$D_{av5_{old}} - D_{av6_{old}} = D_{av5_{new}} - D_{av6_{new}}$$

$$D_{avr5_{old}} - D_{av6_{old}} = D_{avr5_{new}} - D_{av6_{new}}$$

$D_{av5_{old}}$ $D_{av6_{old}}$ $D_{avr5_{old}}$ are the Drag Acceleration for the selected velocity (v_5 v_6 v_{r5}) belonging to the reference profile found at the previous iteration

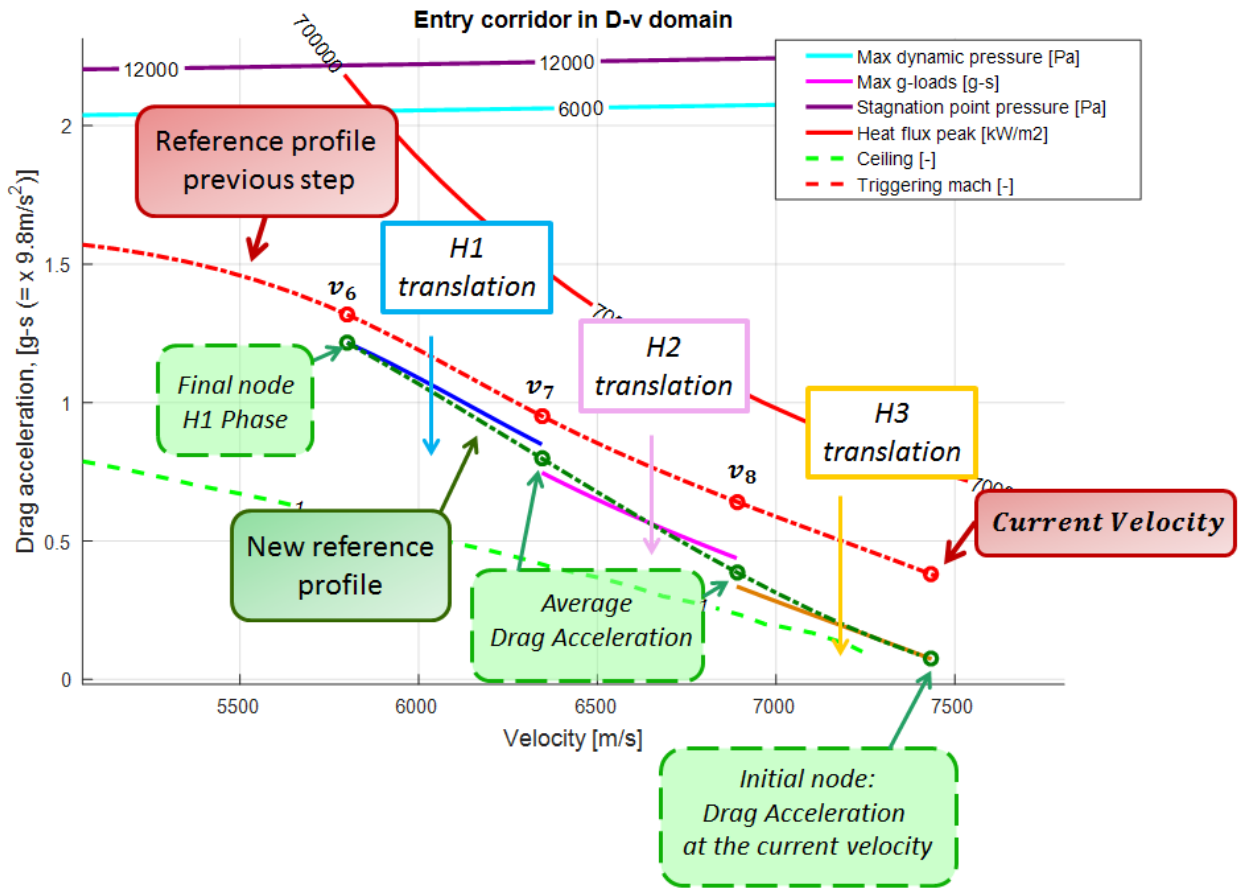


Figure 78: "Heat Rate Peak Phase Spline with the average values" approach when the H1, H2 and H3 phases are all presented. The behavior is only qualitative.

- The last Phase to generate is the Connection Phase: It's taken the initial and final node of H1 and the initial and final node of S6. These four nodes are used for generate the Spline Equation of the Connection Phase.
- When the Phase H3 or H2 ends the part of the algorithm referred to this trait isn't considered and the next trait becomes the new current trait.

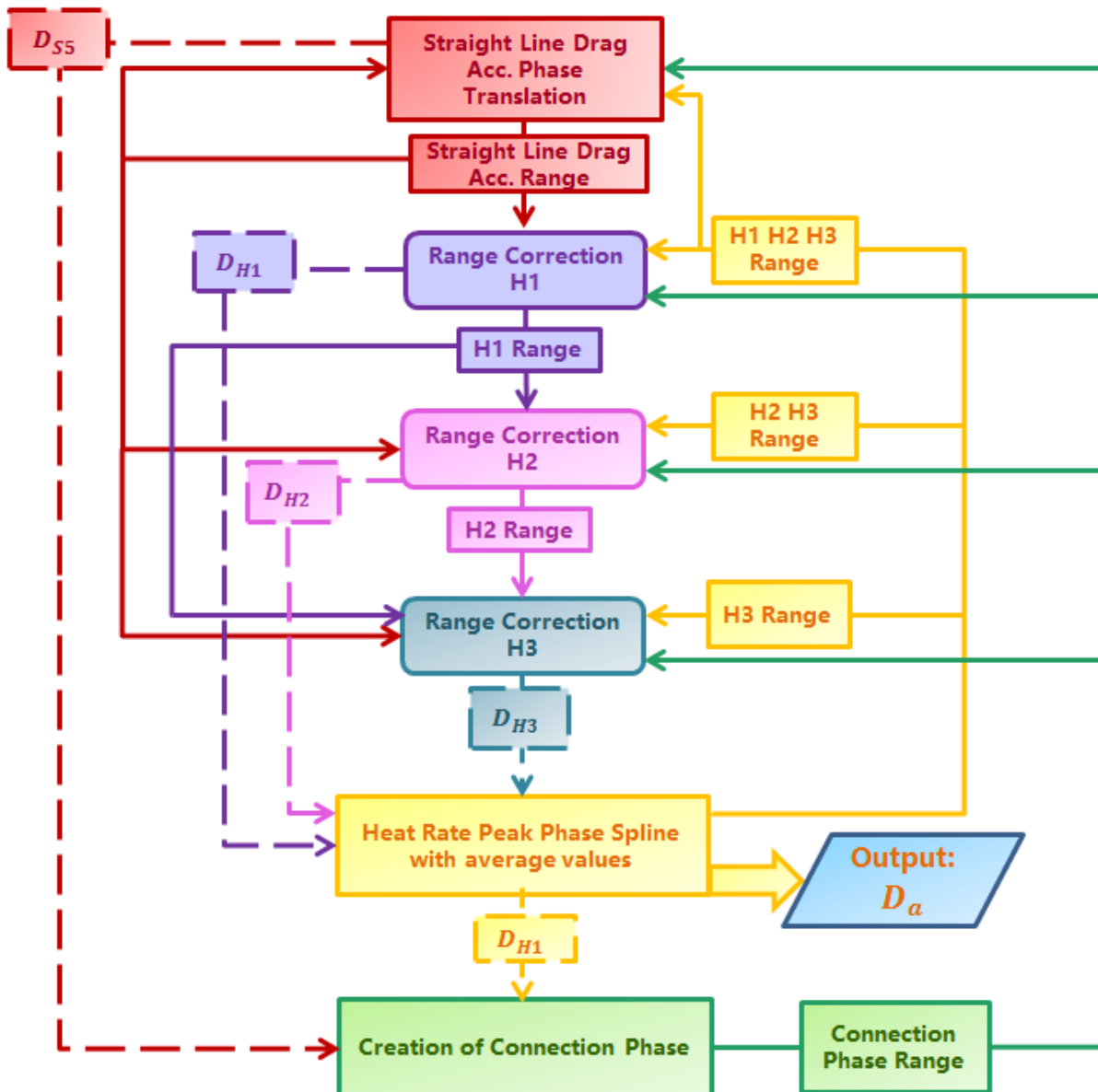


Figure 79: Heat Flux Peak range correction flow chart.

Finished the Heat Flux Peak Phase, the reference curve has the following form:

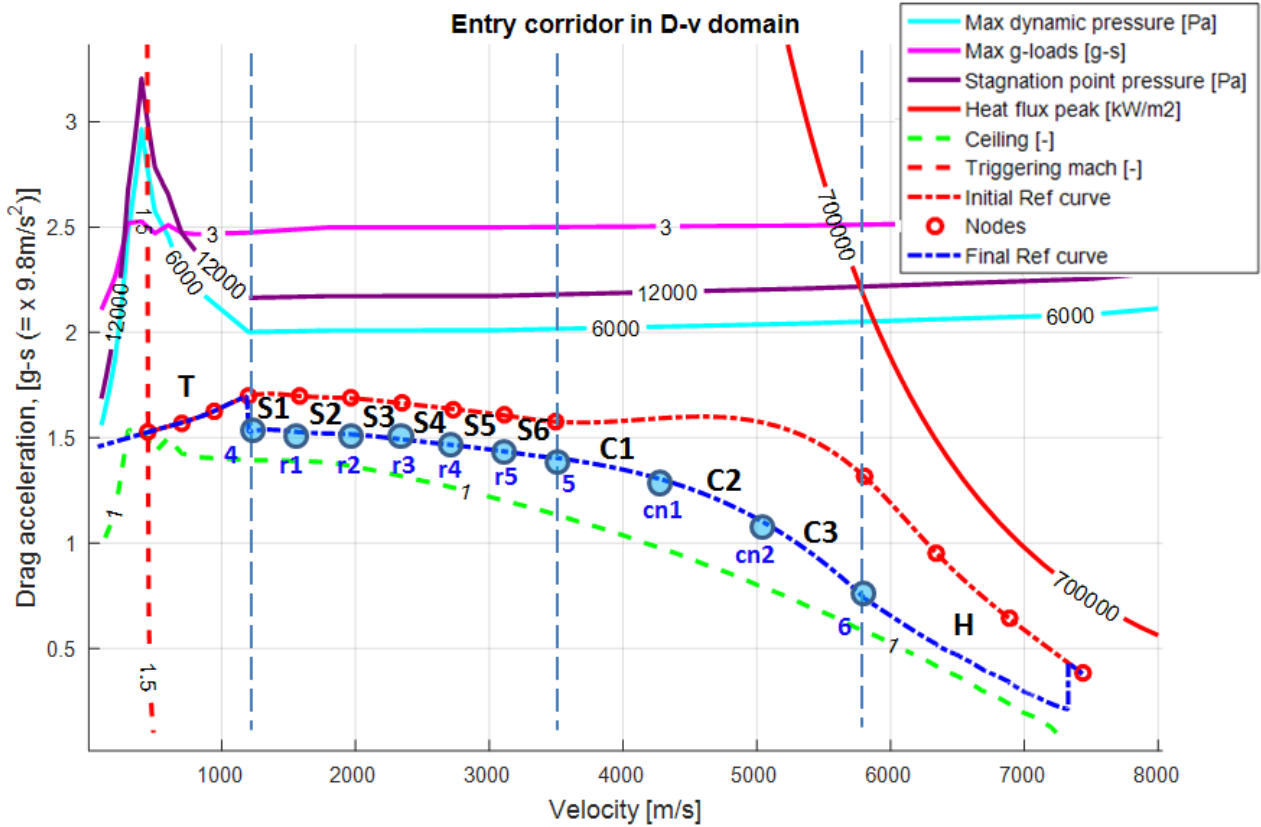


Figure 81: Phases and nodes of the reference profile when the Heat Flux Peak range correction ends.

The algorithm for the range correction follows the following steps:

- After reaching the velocity v_6 the Connection Phase Range correction starts. The error range is given by the difference between the desired range and nominal range. In the nominal range enters six contributes. The first contribute is the Transition Phase range that is always the range given by the first reference profile (this curve is never changed). Other three contributes are $S1, S2$ and $S3$ range found at the previous step. Another contribute is the range given by the Straight Line reference curve that contains the $S4, S5$ and $S6$ phase. The last three contributes are $C1, C2$ and $C3$ range calculated with the reference curve of the previous step. The first three parts of the Straight Line Drag Acceleration Phase ($S1, S2, S3$) are translated by the same value, this value is proportional to the error range. Exactly as for the Heat Flux Peak range correction, this curve can be translated until the node 4 reached a limit value: the upper limit coincides with the Drag Acceleration for the upper limitation at the velocity v_4 , the lower limit is the Drag Acceleration of the final point (D_{a_1}).

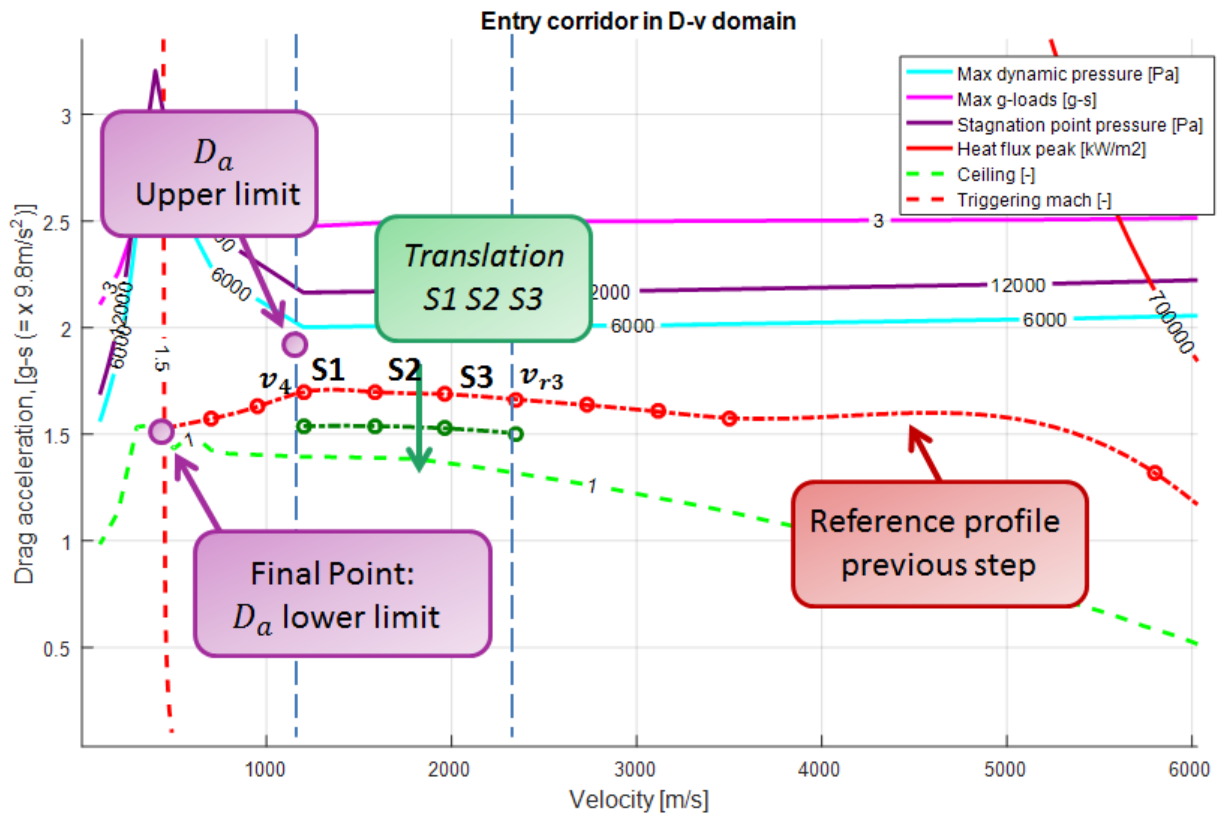


Figure 82: S1, S2 and S3 Phase translation for the range correction. The behavior is only qualitative.

- Knowing the new Straight Line Equations for the S1, S2 and S3 phases, it's possible to calculate a new range and then a new range error Δs . For the calculation of the range error the S1, S2 and S3 range is given by the curves just found. The C1, C2, C3 and S4, S4, S5 (remembering that these three phases are represented with an single equation) ranges are given by the old reference profile found with the previous step. This error will be used for the translation of the last part of the Heat Connection Phase C1. The translation consists in identifying the variation of the known term in the equation of the straight line to make the range error tends to zero. Remembering that the straight line equation for the Phase C1 is the following:

$$D_{aC1} = A_{C1}V + B_{C1}$$

The variation of the known term will be given by the following expression:

$$\Delta B_{C1} = \frac{dB_{C1}}{ds} \Delta s$$

This new curve will give a new range value. In this equation the derivate $\frac{dB_{C1}}{ds}$ is calculated as function of the initial and final nodal velocity. If the current velocity doesn't belong to the interval between v_5 and v_{cn1} , the initial nodal velocity corresponds to the velocity v_{cn1} , and the final nodal velocity to the velocity v_5 . If the current velocity belongs to this interval the initial nodal velocity is the current velocity. The curve can't overcome the limit value for the know term found previously.

- The same procedure will be done for the Phase C2 and C3, finding new value for B_{C2} and B_{C3} . The difference is that C1 range will be calculated using the new translated profile. The C2 range is calculated using the new translated profile when the considered Phase is the C3 Phase. When the current velocity changes phase, the previous phases will no longer be considered. This means that if the current velocity belongs to the phase C2, the phase C3 isn't considered. When the current velocity belongs to the phase C1, the phases C2 and C3 aren't considered. Also in this case the initial and final velocity are the nodal velocity, if the current phase isn't the considered phase for the range correction. If the range correction is applied to the current phase, the initial velocity is the current velocity. The curves can't overcome the limit value for the know term found previously.
- At the end of this operation we have obtained three curves C1, C2 and C3. But the nodes of these three curves aren't connected. So it's necessary created a new curve for the Connection Phase: this operation is performed in the block "Connection Phase Straight Line with the average values". It's calculated the nodal Drag Acceleration for each phase belonging to the Connection Phase, than for two nodes that have the same velocity, it's found the average Drag Velocity between the two nodal Drag Acceleration: this will be the new node for the straight line. The first node is always the Drag Acceleration at the current velocity for the translated reference curve. The last node is the Drag Acceleration at the velocity v_5 for the translated curve C1. Knowing all the nodal velocity and the new nodal Drag Acceleration is finding the new Straight Line equations.

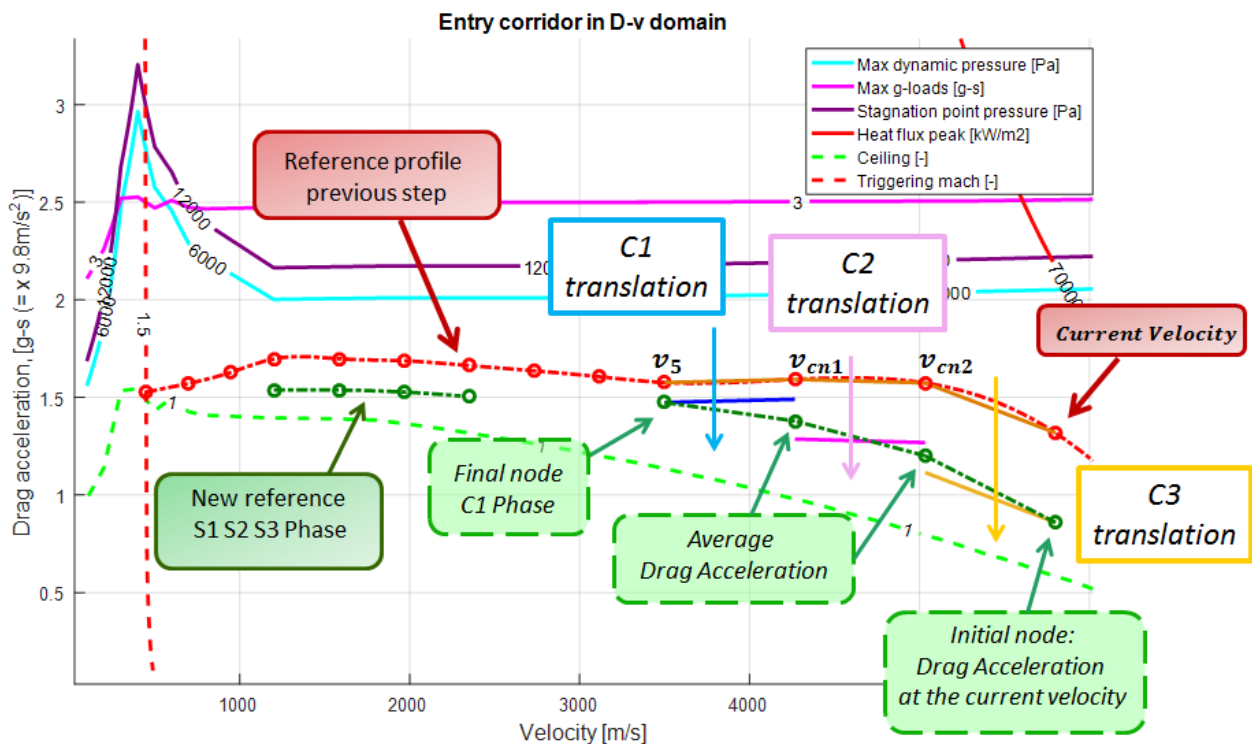


Figure 83: "Connection Phase straight line with the average values" approach when the C1, C2 and C3 phases are all presented. The behavior is only qualitative.

- The last phase to generate are S4, S5, S6 phases. They are represented with a single equation. To write the straight line equation, it's taken the final node of C1 and the initial of S3.

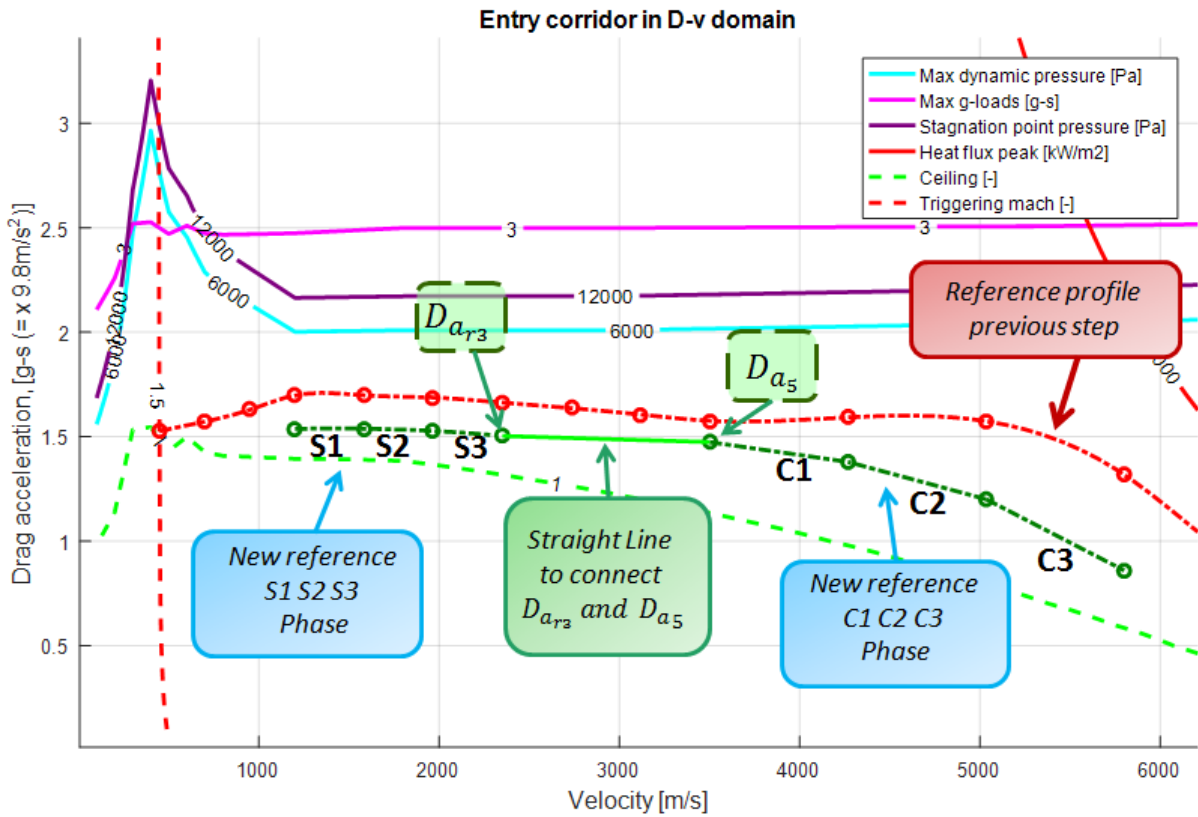


Figure 84: "Creation of S4-S5-S6 with a single straight line" approach. The behavior is only qualitative.

The algorithm is also explained by the flow chart in Figure 85:

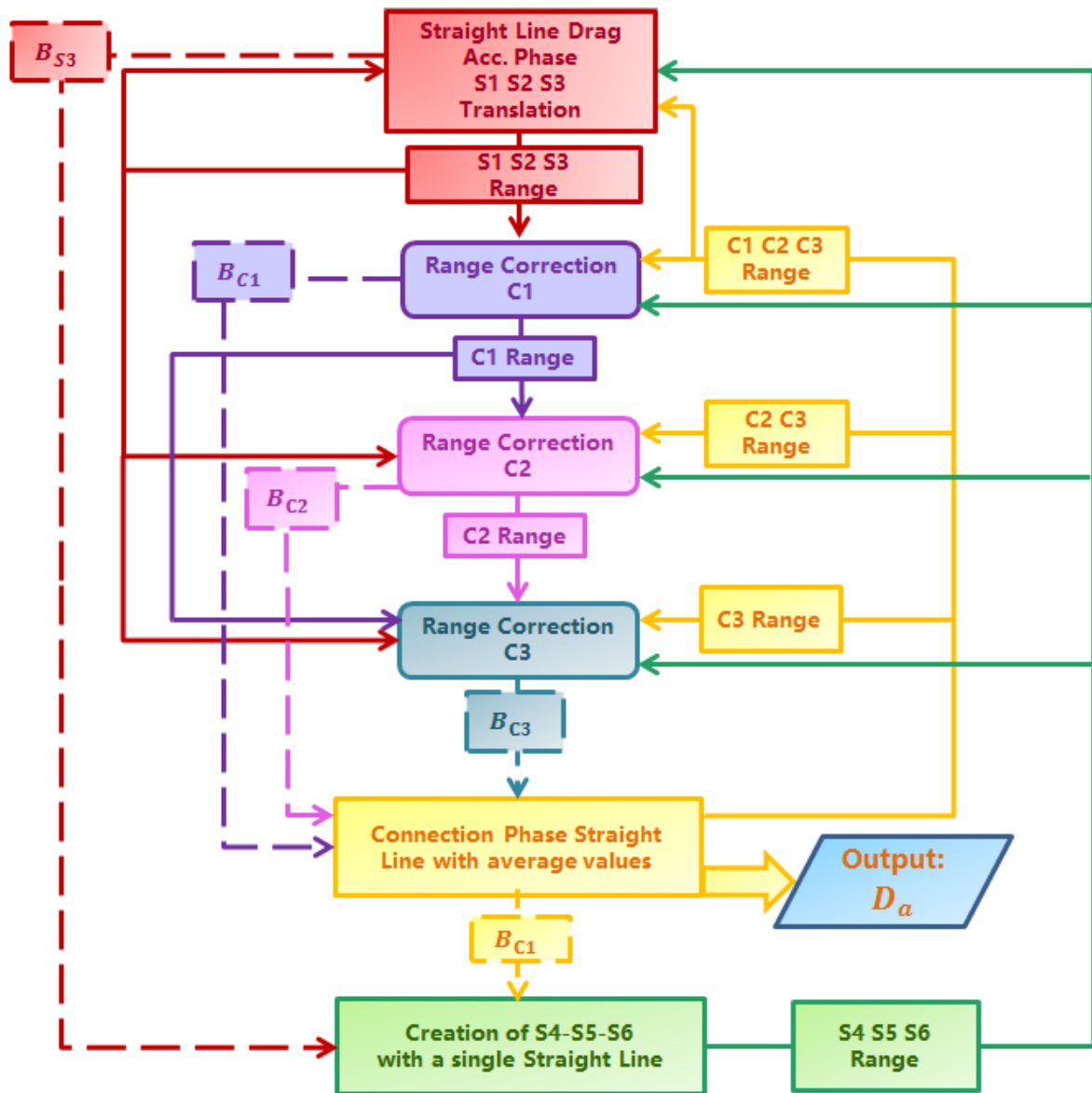


Figure 85: Connection phase range correction flow chart.

Ended this phase the new reference profile is the following:

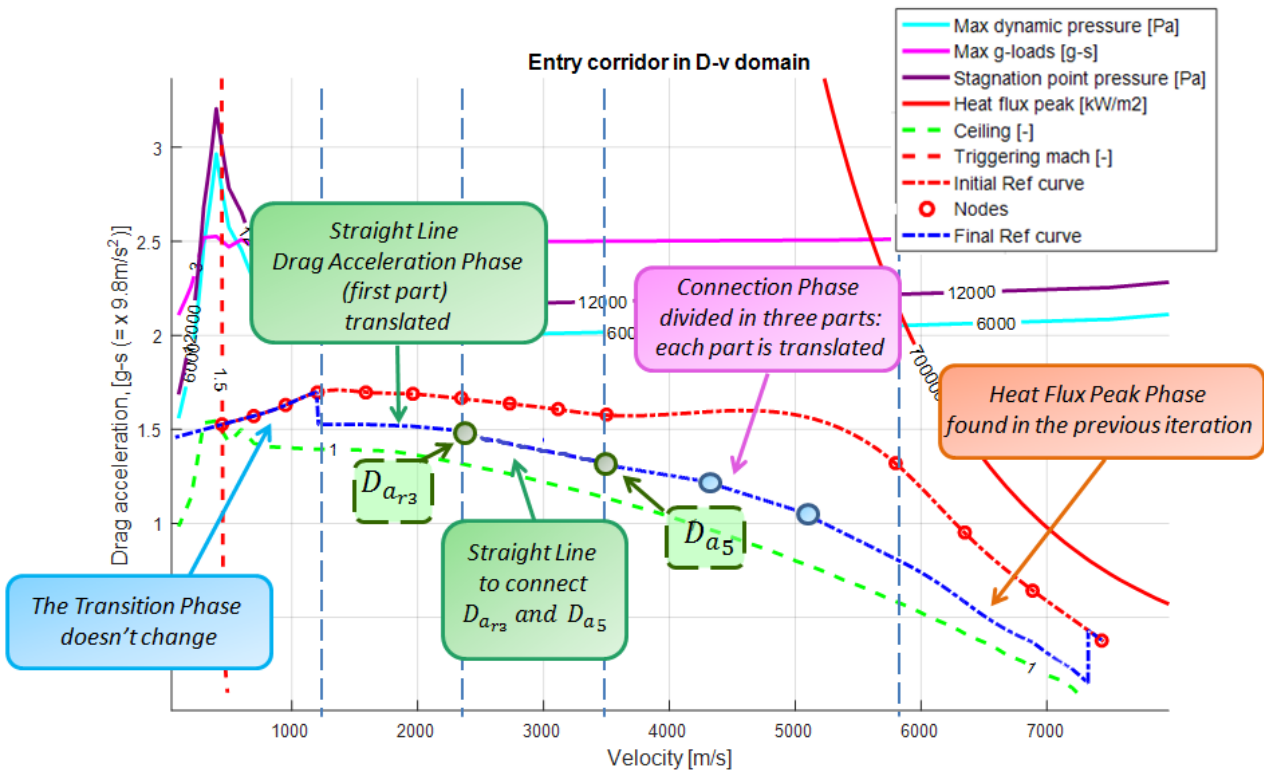


Figure 86: Reference curve at the end of Connection Phase Range correction. The behavior is only qualitative.

The Straight Line Phase has an approach similar to the other phases. We have six parts S_1, S_2, S_3, S_4, S_5 and S_6 , all represented by the equation of the straight line. The error range, obtained by the difference between the desired range and the nominal range (the nominal range is given by the sum of the range belonging to the reference profile of the previous step), is used to correct the first part S_1 , changing B_{S_1} . We must remember that the equation to change B_{S_1} , knowing the error range, is the following:

$$\Delta B_{S_1} = \frac{dB_{S_1}}{ds} \Delta s$$

$$B_{S_1_{new}} = B_{S_1_{old}} + \Delta B_{S_1}$$

With a new B_{S_1} , the S_1 phase will be associated to a new nominal range and, then, to a new range error. This new range error enters in the S_2 and B_{S_2} changes. The procedure is the same for all the phases until you reach the S_6 phase. The range derivative respect to the known term is calculated using the nodal velocity: only for the current phase the initial nodal velocity is the current velocity. When a phase finishes, this phase will not be considered for calculating the range error.

The new known value can't overcome the upper and lower limit found previously. The only node that follows a different law is the node 4: its minimum Drag Acceleration is equal to the final drag acceleration ($D_{a_{v1}}$). So the curve can be translated up to a minimum value of B_{S_1} for which node 4 assumes a Drag Acceleration equal to $D_{a_{v1}}$.

Exactly as for the other phases, the six curves will have nodes that don't coincide. So it's necessary to create new nodes. The first node is always the Drag Acceleration of the phase $S1$ at the velocity v_4 , the last node is the Drag Acceleration at the current velocity, the other nodes are given by the average Drag Acceleration between the nodal Drag Accelerations belonging to two nearby phases calculated (for the two nodes the velocity is the same).

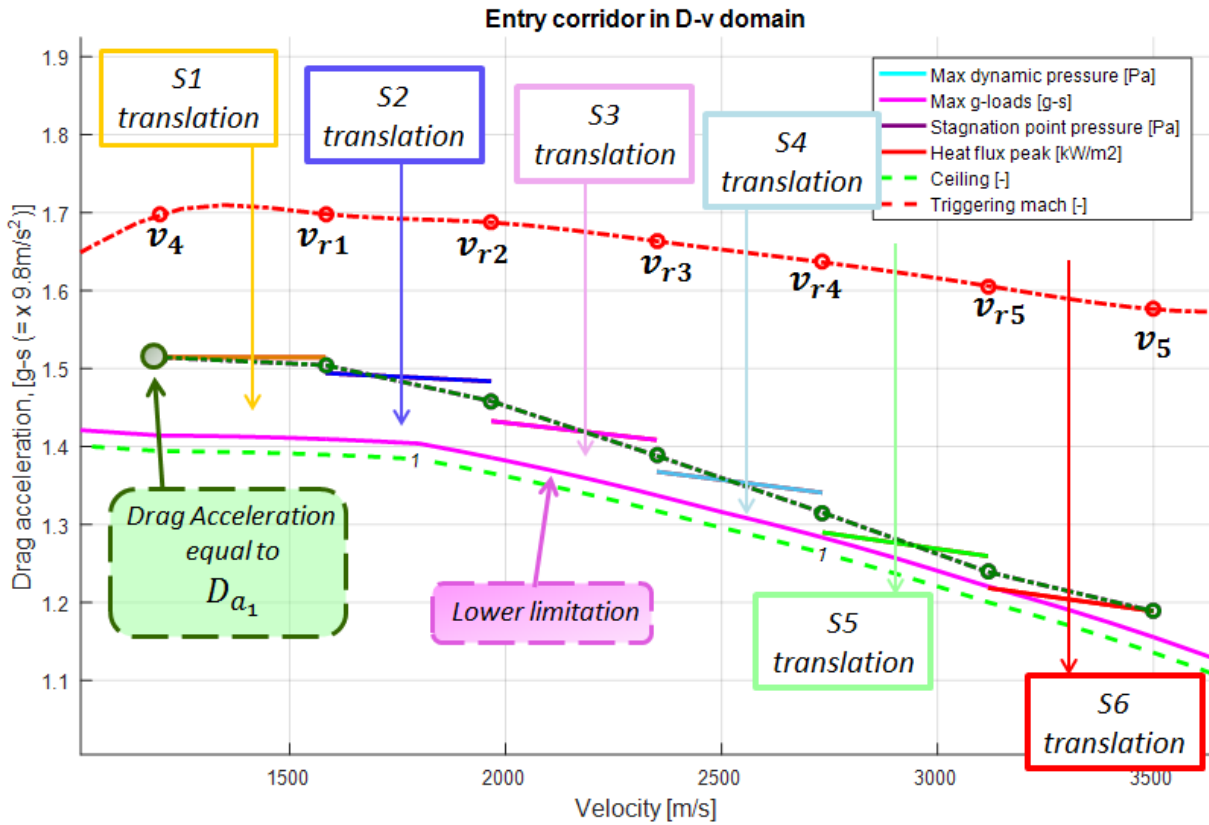


Figure 87: Straight Line Drag Acceleration Phase with the average values to build S1,S2,S3,S4,S5 and S6. The behavior is only qualitative.

When the vehicle reaches a velocity equal to v_4 the Transition Phase starts. The algorithm for the Transition Phase range correction is equal to the algorithm used with the Space Shuttle approach in Chapter 3.5.

Ended all the phases the obtained reference profile permits to minimize the range error, respecting the requirement.

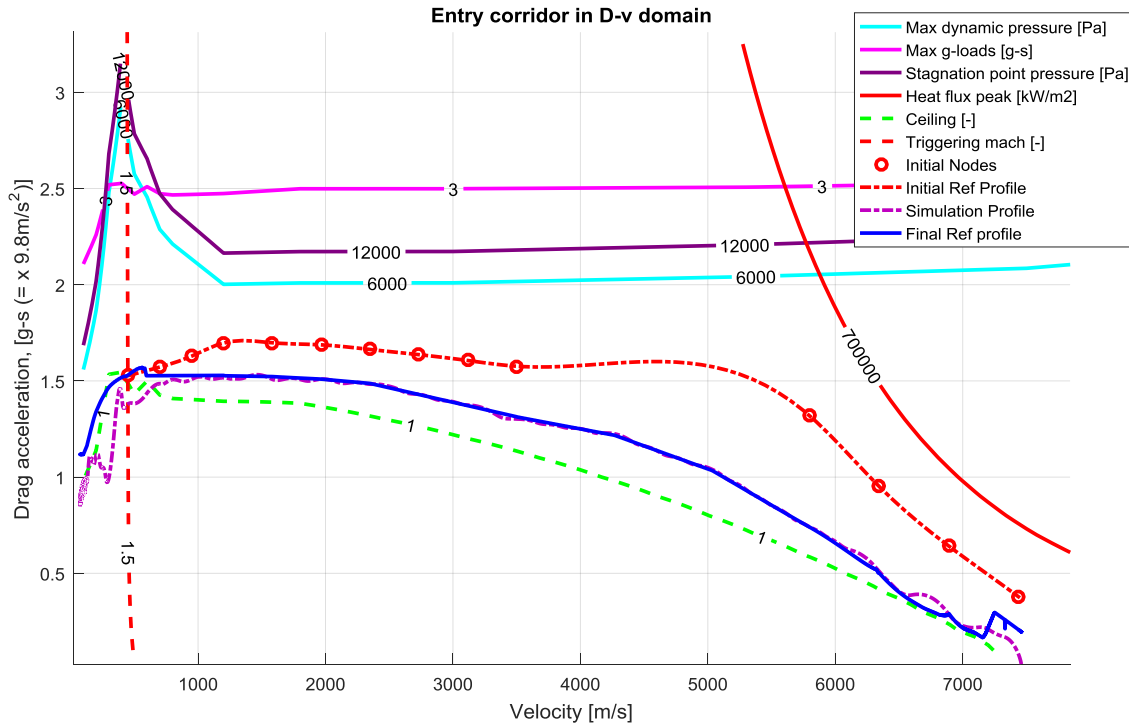


Figure 88: Example of a new profile after the range correction.

We have explained the functioning of the range correction algorithm, but we must remember that the formulas in the last column of Table 29 give a realistic result only if the error range is small. So it's necessary to use only a part of the error range in each range correction block. To choose the error range portion is possible identify different error processing parameters:

- Use a *constant gain* that reduce the error range that enters in the algorithm.
- Use *saturation* that identifies a maximum and a minimum value for the range error
- Use a *variable gains*. This strategy is based on the percentage of travelled range in each phase respect to the total travelled range $Range_{tot}$ following the initial reference profile. This percentage is used to define a variable gain which allow to choose the range portion that enters in the range correction algorithm. If the selected phase is the current phase the percentage is calculated from the current velocity to the final velocity of the phase. The first step is saved the travelled range as function of the velocity, following the initial reference profile. For this reason we have two vectors: the first vector contain the velocity values, the second vector contains the range values travelled until at the selected velocity. Then with an interpolation it is found the range travelled at a certain velocity: this procedure is done for the nodal velocity. The percentage of range travelled in each phase will be equal to the variable gain:

$$Gain_{variable} = \frac{Range_{Final\ Node} - Range_{Initial\ Node}}{Range_{tot}} \quad (98)$$

- Use *limit curves*. This strategy is used when the reference profile must go up. When the vehicle follows the upper limitation with the maximum Bank angle it will have a certain Drag Acceleration-Velocity combination. This combination will be the maximum possible combination. For all the other cases (lower reference profile or lower Bank Angle), for a certain Velocity, the Drag

Acceleration will be lower. So even if the reference profile overcomes this maximum combination, the simulated profile will be always the same. For this reason the new reference profile, during the range correction, is forced to follow the Drag Acceleration-Velocity combination found with the upper limitation simulation. This operation is done because the reference profile translates thanks to the range correction algorithm, this translation gives a certain nominal range, but the vehicle, reached the maximum Drag Acceleration-Velocity combination, can't reach the reference profile. So the desired range doesn't change a lot and the error range decreases little. This behaviour can produce overcorrections, because the reference profile can't be reached. For this reason the strategy is the following:

- Save the Drag Acceleration-Velocity combination for a simulation where the reference profile is the upper limitation.
- Identify the point (Drag Acceleration-Velocity) $D_{a_{UL1}} - V_{UL1}$ where the simulated profile, found with the upper limitation as reference profile, intersects the initial reference profile chose for the second simulation. Until this velocity the reference profile doesn't translate with the range correction.
- Identify a second point $D_{a_{UL2}} - V_{UL2}$: here the simulated profile, found with the upper limitation as reference profile, meets the upper limitation.
- For all the velocity included between the first point and the second point, the reference profile can translate, during the range correction, only following the simulated profile, found with the upper limitation as reference profile.

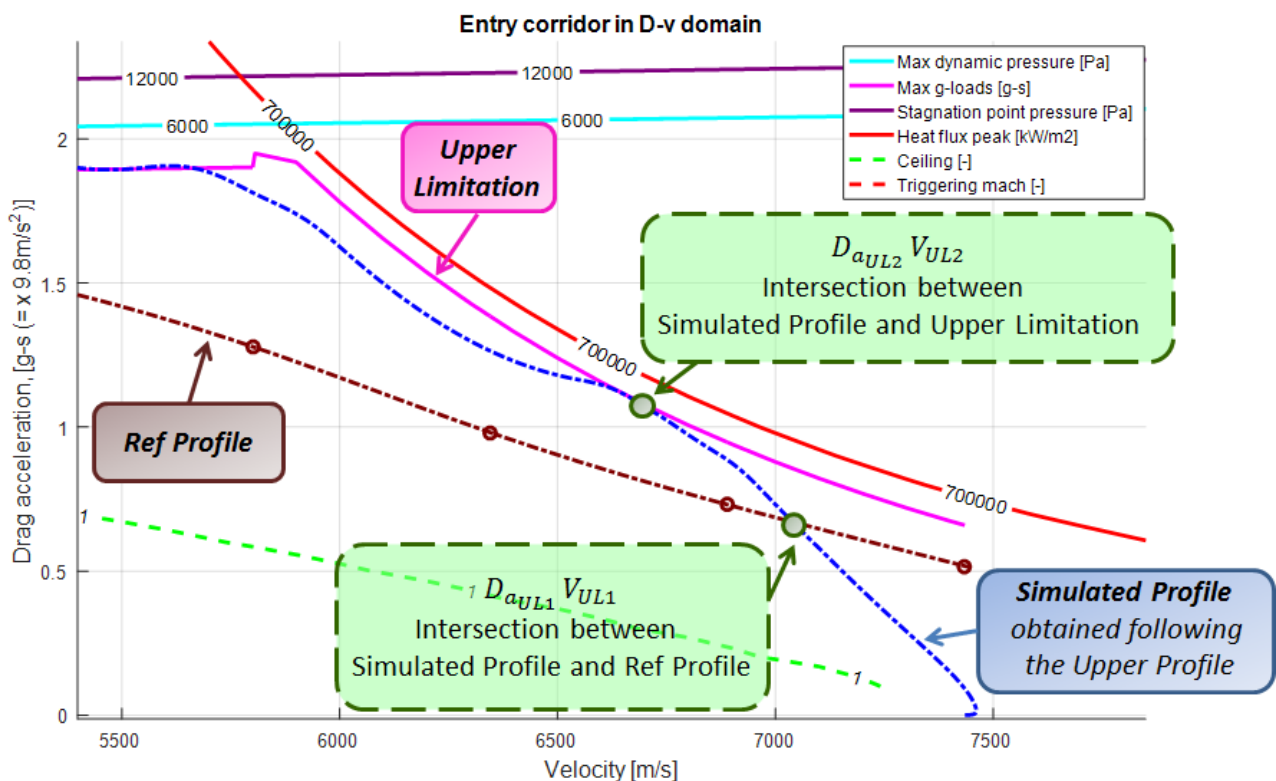


Figure 89: Identification of $D_{a_{UL1}} - V_{UL1}$ and $D_{a_{UL2}} - V_{UL2}$.

- Use of *saturator* for the variation of known term. In this way the movement of the reference profile is limited in each simulation step.

In the Heat Flux Peak Phase range correction the error processing parameters are the following:

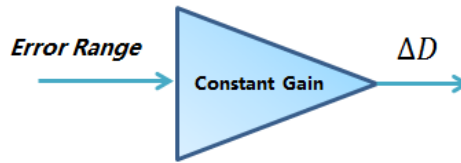


Figure 92: Error Processing Parameters for the Straight Line Drag Acceleration Phase correction during the Heat Flux Peak Phase range correction.

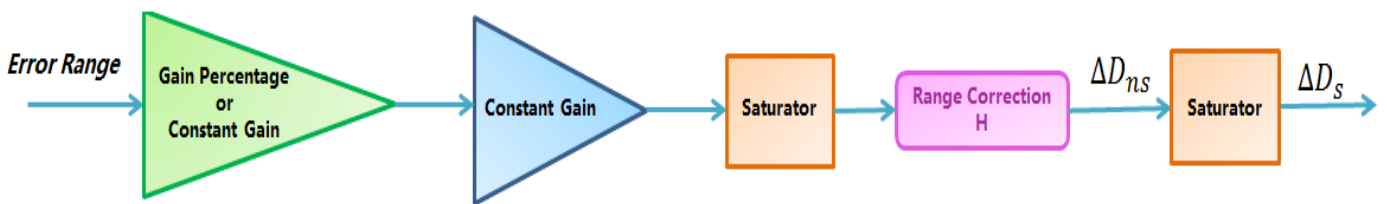


Figure 93: Error Processing Parameters for H1, H2, H3 Phase during the Heat Flux Peak Phase range correction.

In the Connection Phase range correction the error processing parameters are the following:

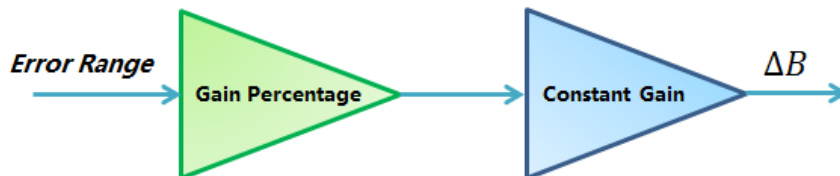


Figure 94: Error Processing Parameters for S1, S2, S3 Phase correction during the Connection Phase range correction.

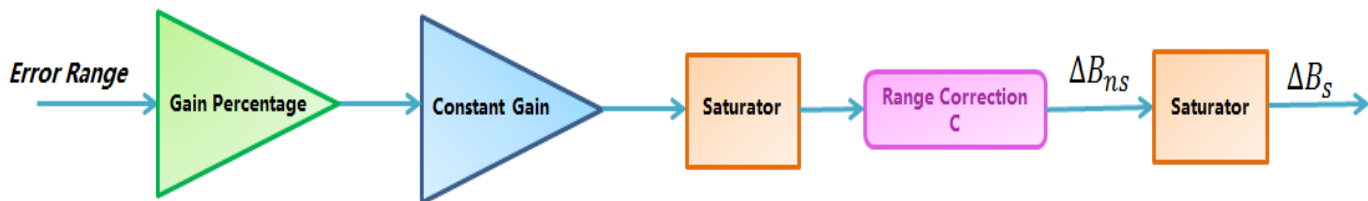


Figure 95: Error Processing Parameters for C1, C2, C3 Phase correction during the Connection Phase range correction.

In the Straight Line Drag Acceleration Phase range correction the error processing parameters are the following:

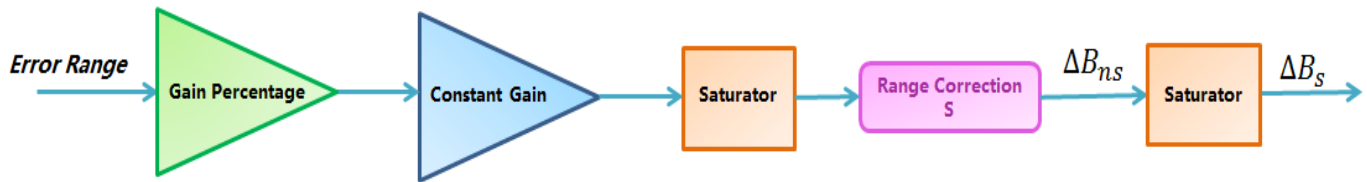


Figure 96: Error Processing Parameters for S1, S2, S3, S4, S5, S6 Phase correction during the Straight Line Drag Acceleration Phase range correction.

In the Transition Phase range correction the error processing parameters are the following:

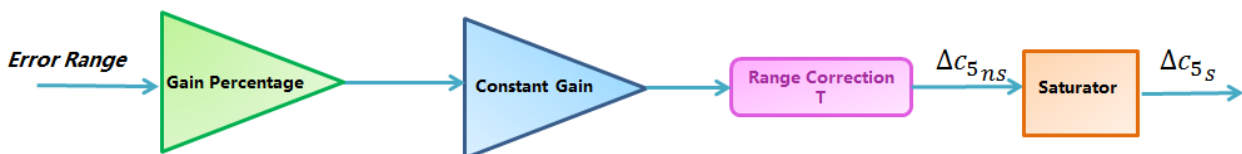


Figure 97: Error Processing Parameters for the Transition Phase.

The values of these gains can be chosen using a sensitivity analysis, in fact, with these gains, the problem is really not linear and the linear optimisation technique can't be used. For each case it is necessary to change the gains, to have, at the end of the simulation, the minimum range error.

As we can see from the Figure 88, the new reference profile presents some discontinuities near the nodes (the first derivative or the second derivative aren't continuous). This is due to the fact that the range equations are resolved with approximate mathematical models, so the algorithm is not able to define with precision the exactly translation of the reference profile. The algorithm becomes more precise when the range error is reduced and this happens with a phase ends. For this reason the translation becomes more marked near the nodes. When there are the discontinuities in the reference profile the vehicle presents oscillations because the vehicle dynamics isn't able to follow sudden changes in the reference profile curvature. For this reason to avoid oscillation it's created a new reference profile taking as new nodes the Drag Acceleration value near the old nodes, so a contoured profile is created where there are no discontinuities. This operation is only done if the error range is reduced.

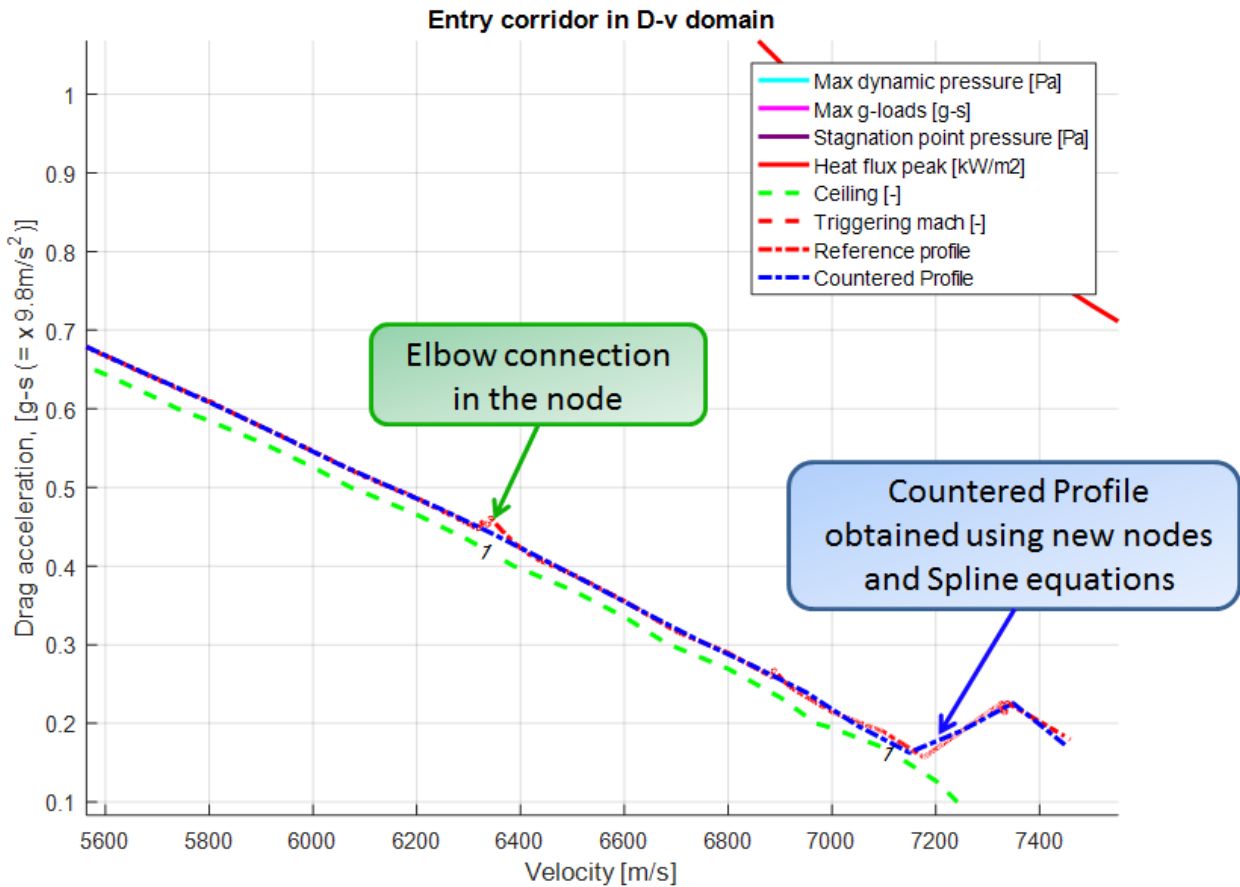


Figure 98. Final reference profile (red curve) and countered reference profile (blue curve)

For the same reason described above, if the initial range error is really small (less than 1 Km), the algorithm isn't able to reduce it, because the range equations aren't exactly, but approximate formulation. So the result is that the range error, at the end, increases. For this reason, in certain cases, as reference profile, it's taken the translated profile, found in Figure 73, without doing the range correction.

The final consideration is verify if the final Heat load absorbed during the simulation respect the permitted limitations. If the vehicle flies at high altitude, following a reference profile with a low Drag Acceleration the Heat Flux is reduced but it takes more time to go down. For this reasons the Integrated Heat Load increases. The consequence is that in the vehicle penetrates a greater quantity of heat, risking to damage the internal equipment or protective thermal layers. If the Integrated Heat Load overcomes the limit value it's necessary to translate the reference profile. In fact if the Drag Acceleration increases, the integrated Heat Load decreases.

This reasoning is been validated with a simulation: an initial reference profile is considered and it's saved the Integrated Heat Load. Then all the nodes are translated of an equal value, for increasing the Drag Acceleration, the Integrated Heat Load is saved after the simulation. This procedure is done three times, three reference profile are obtained, each distant from the previous one 0.2 g-s.

5. Results from the simulations

The simulation must be stopped when the vehicle reaches the Triggered Mach, in fact overcoming this Mach number, the dynamic changes and the algorithm loses its validity. So it's necessary introduces in the Simulink algorithm a block named *stop*.

The second consideration is that the vehicle dynamic is really sensible to the aerodynamic changes, so the PID gains impact differently on the vehicle dynamic based on the value of aerodynamic coefficients. In certain cases the model found in chapter 2.3 leads to a damped dynamic, because the value of aerodynamic coefficients remain content. In other cases, with the same dynamic pressure, these PID gains create oscillations in the dynamic response, because, for example, the aerodynamic coefficients increase. For this reason the PID gains model is only a first approximation of optimal model and in each case, making different simulation, with a sensitivity analysis, it's possible to correct this model, by halving, for example, the gains reached a given dynamic pressure. In other cases the best choice was inserting constant gains if the dynamic behaviour gives constant pressure for most of the simulation .

The second value to be corrected is the integrative gain: in chapter 2.3 we have said that the K_I is a constant gain. But this gain is subjected to many non-linearity, as the anti-wind up phenomenon. For this reason it's impossible, using the classic linear optimization techniques, to find an optimal gain or a law for the gain variation. For this reason the approach used in this thesis was to select a constant gain for each case, with sensitivity analysis.

The error processing parameters have instead been chosen visibly evaluating which part of the curve you had to go to change in case the range error was not under 10 km.

There are also other requirement linked to the final error, over the maximum range error of 10 Km:

- Final Velocity error: lower than 0.2%
- Final Altitude error: lower than 3%

After making these considerations, the algorithm has been tested for four different initial positions, each linked to a particular flight condition. The simulations has been done with all the five initial references profile:

- The case 1 is reference profile equidistant from the limits
- The case 2 is reference profile distant from the Ceiling
- The case 3 is reference profile distant from the Dynamic Pressure limit
- The case 4 is reference profile distant from the g-load limit
- The case 5 is reference profile distant from the Constant Heat Flux limit

The first simulation wants to give a range really similar to the minimum range. The vehicle will fly near the upper limitation. The PID gains are chosen constant for all the simulations and for all the five cases:

K_P	30
K_I	0,5
K_D	550
N	0,7692

Table 31: PID gains for the first simulation

During the Heat Flux Peak Phase range correction only constant gains are used. This first gain is equal to 0.2 for case 5, equal to 1 for case 3 and equal to 0.7 for all the other cases. The second constant gain in the Heat Flux Peak Phase range correction is equal to 1. The error Processing Parameters for the Straight Line Drag Acceleration Phase correction during the Heat Flux Peak Phase range correction is set equal to 1/10 for the case 1 and 2, and equal to 1/100 for all the other cases.

For the case 1, 2 and 4 is used the upper limitation described in Figure 90.

The error Processing Parameters for S_1 , S_2 , S_3 Phase correction during the Connection Phase range correction are chosen equal to 1/100 and the error Processing Parameters for C_1 , C_2 , C_3 Phase correction during the Connection Phase range correction are chosen equal to 1/10.

The error Processing Parameters for S_1 , S_2 , S_3 , S_4 , S_5 , S_6 Phase correction during the Straight line Drag Acceleration Phase range correction are equal to 1/20.

The saturator for the range error is set equal to *inf*.

The initial point is the following:

	Latitude [°]	Longitude [°]
Case 1	-1,7932	195
Case 2	-1,7932	195
Case 3	-1,7932	195
Case 4	-1,7932	195
Case 5	-1,7932	194,3

Table 32: Initial coordinates for the first simulation.

The final point is always the same:

	Latitude [°]	Longitude [°]
Final Point	3,2721	-123,1265

Table 33: Final coordinates for the first simulation.

For the case 1 the results are the following:

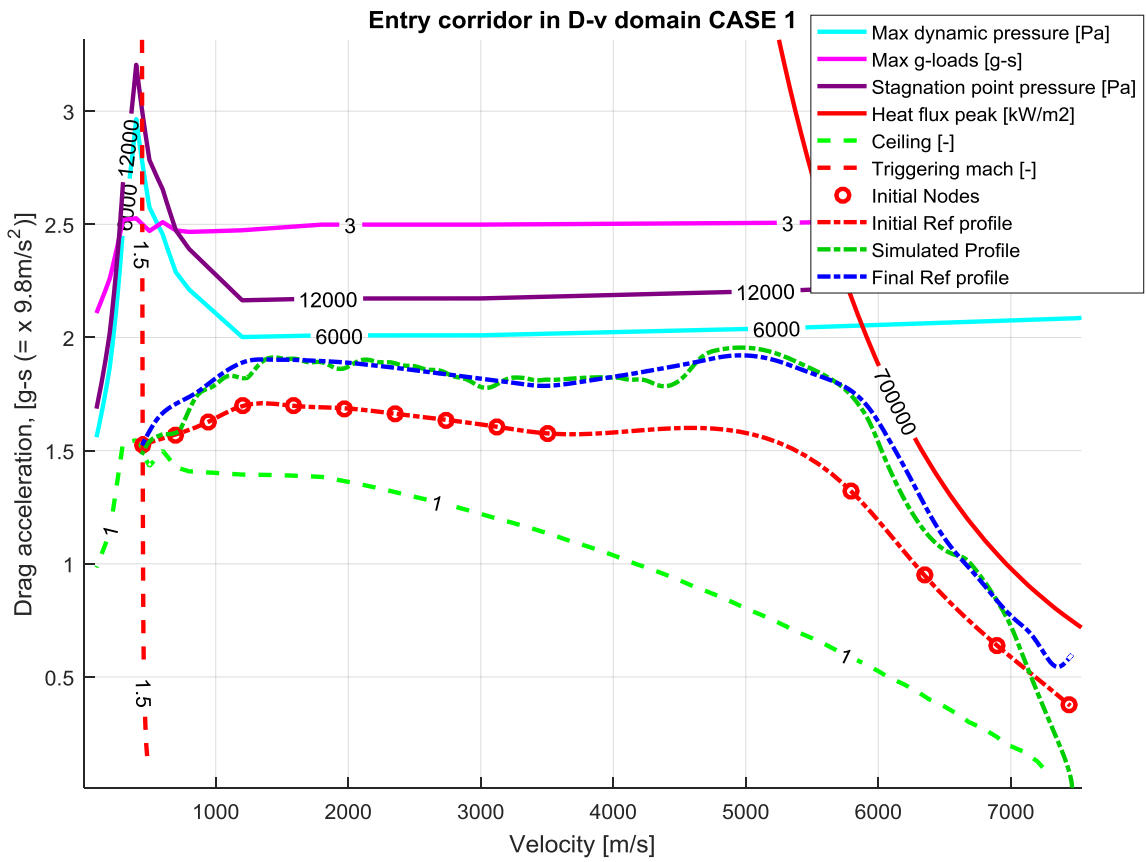


Figure 100: Simulation with range correction for the case 1 and an initial position equal to $-1,7932^\circ$ as latitude and 195° as longitude.

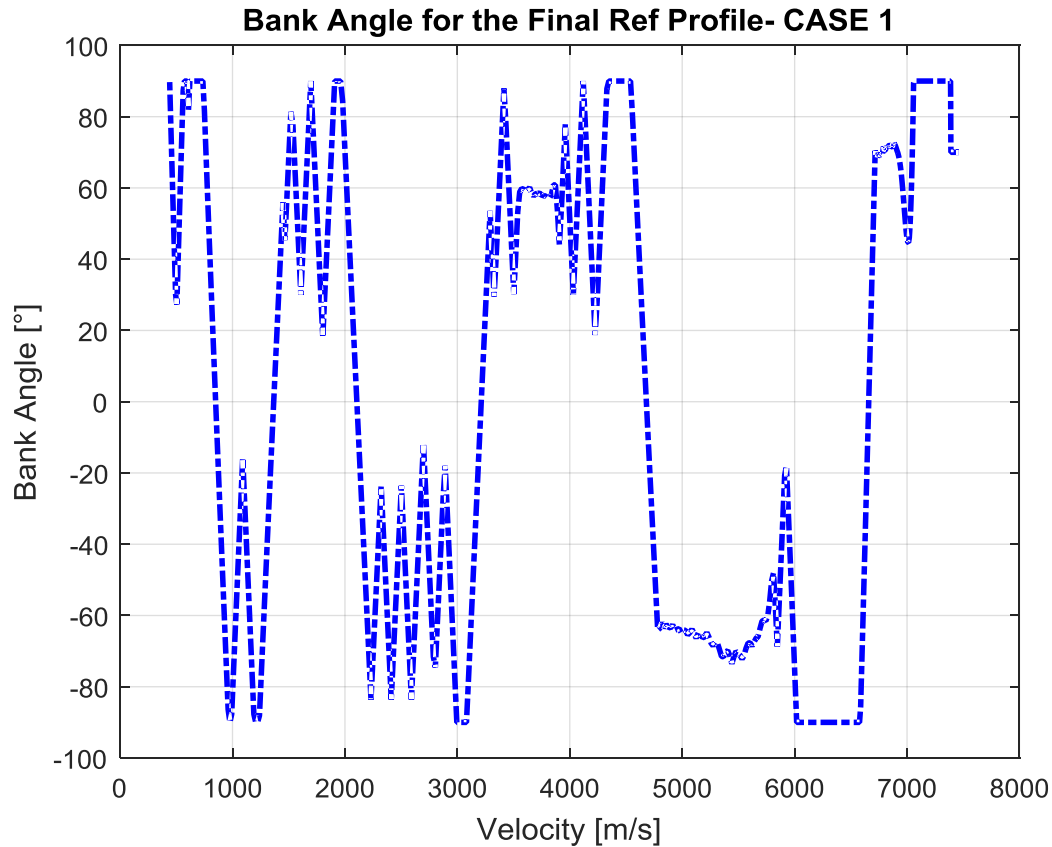


Figure 101: Bank Angle for the case 1 and an initial position equal to $-1,7932^\circ$ as latitude and 195° as longitude, following the final reference profile obtained with the range correction.

Conditions	Nominal	Actual	Guidance Error
Velocity	448.5836 m/s	448.7414 m/s	0.0352%
Altitude	26 Km	26.2 Km	0.5993%
Latitude	3.2721°	3.2717°	0.0112%
Longitude	-123.1265°	-123.0804°	0.0375%
Range	4693.4 Km	4698.8 Km	5.1266 Km

Table 34: Final values and errors for the case 1 in the first simulation.

The results in Table 34 respect the specifications about the maximum error, the vehicle is guided until the final point without violating the re-entry corridor constrains. The problem is that in the Bank Angle profile there are a lot of oscillations that must be eliminated with a post-processing work. Probably these oscillations can be avoided inserting a new PID gain law.

For the case 2 the results are the following:

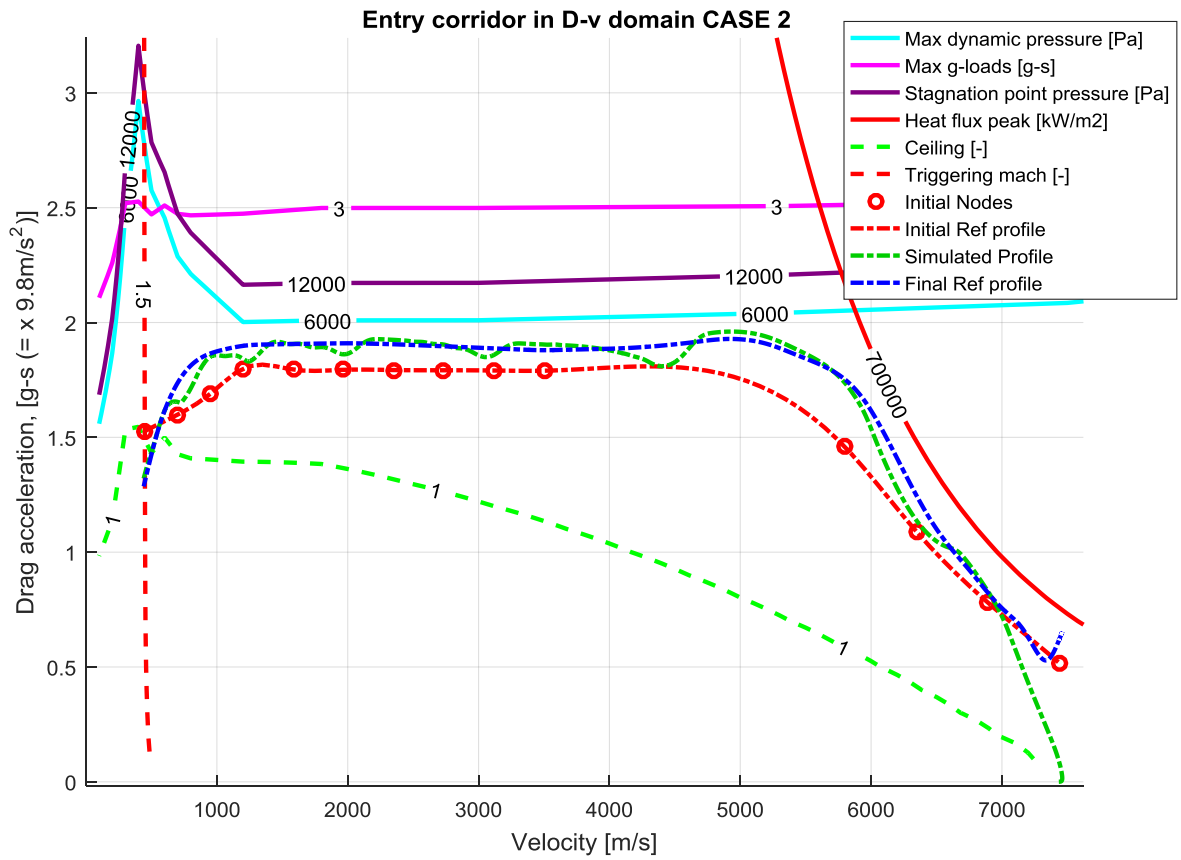


Figure 102: Simulation with range correction for the case 2 and an initial position equal to $-1,7932^\circ$ as latitude and 195° as longitude.

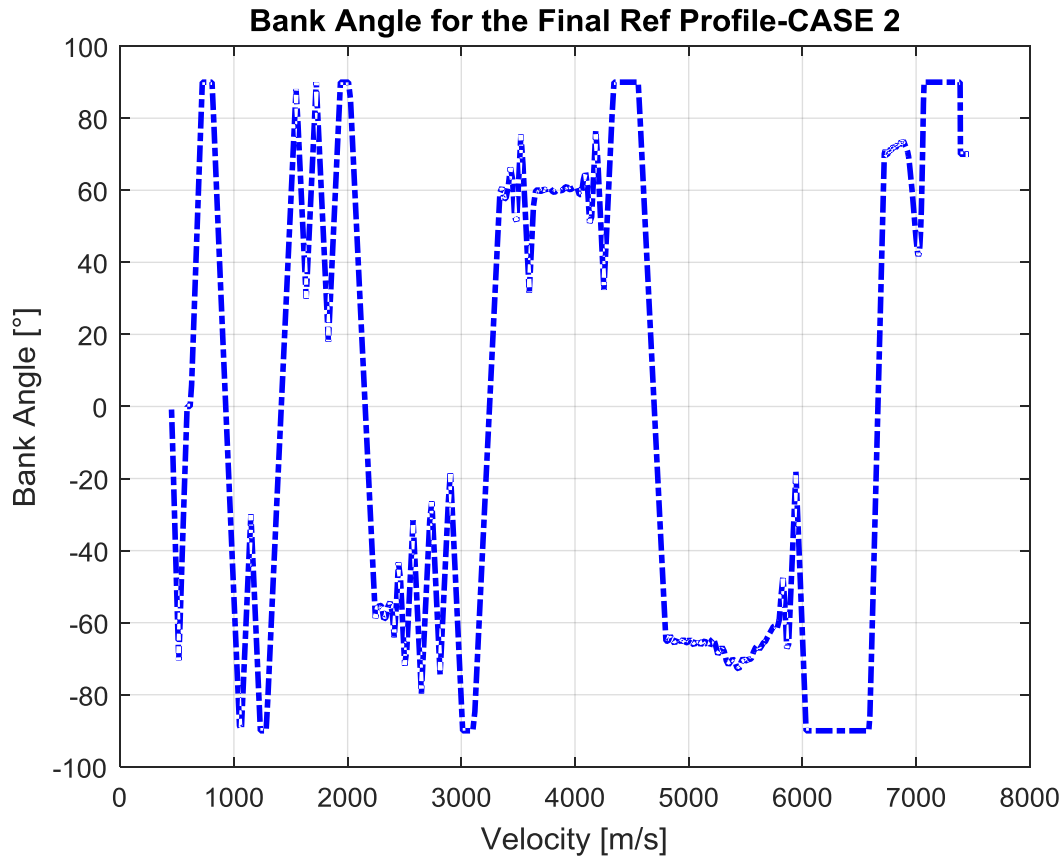


Figure 103: Bank Angle for the case2 and an initial position equal to $-1,7932^\circ$ as latitude and 195° as longitude, following the final reference profile obtained with the range correction.

Conditions	Nominal	Actual	Guidance Error
Velocity	448.5836 m/s	449.4476 m/s	0.1926%
Altitude	26 Km	26.8 Km	3 %
Latitude	3.2721°	3.2647°	0.2252%
Longitude	-123.1265°	-123.1605°	0.0276%
Range	4693.4	4689.9 Km	3.4856 Km

Table 35: Final values and errors for the case 2 in the first simulation.

The results in Table 36 respect the specifications about the maximum error, the vehicle is guided until the final point without violating the re-entry corridor constrains. Also in this case there are oscillations in the Bank Angle profile, the oscillations have a slightly lower amplitude but, also in this case, it's necessary a post processing in the Bank Angle profile or select a new PID gain law that better follows the dynamic at high dynamic pressure.

For the case 3 the results are the following:

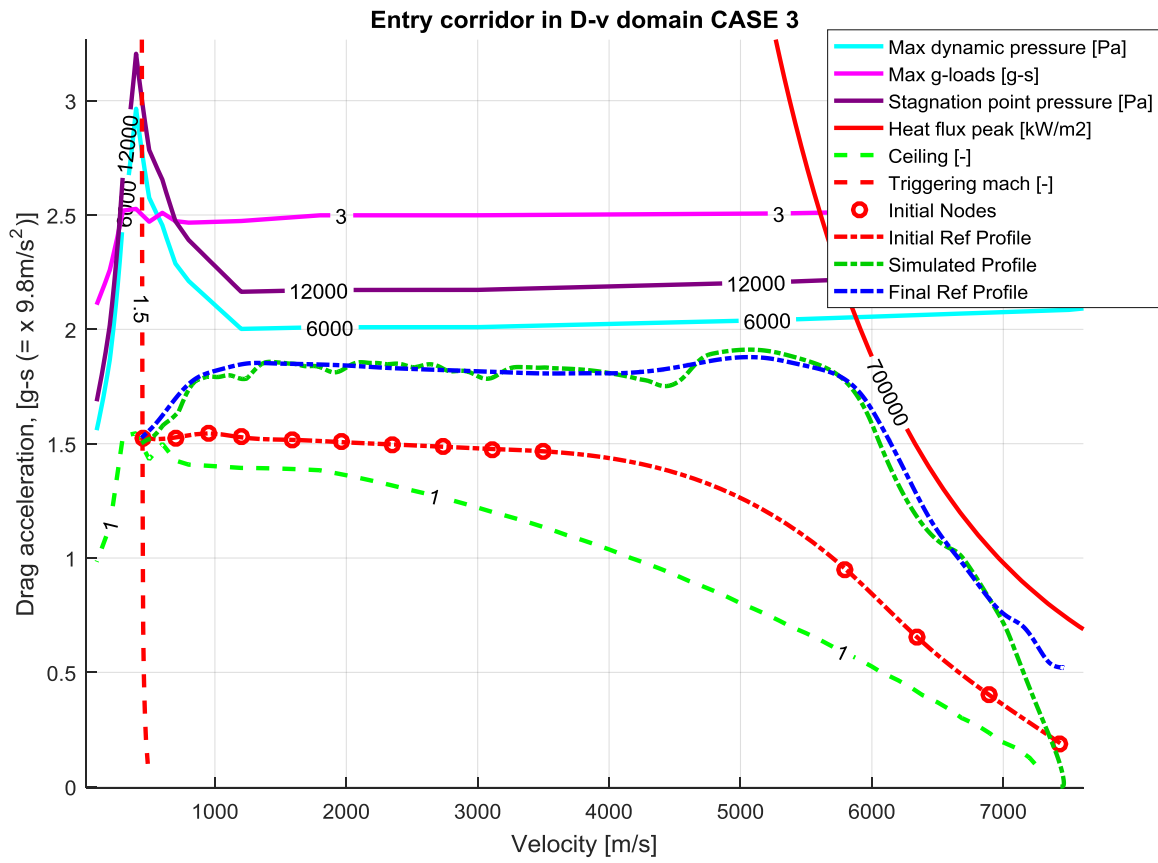


Figure 104: Simulation with range correction for the case 3 and an initial position equal to $-1,7932^\circ$ as latitude and 195° as longitude.

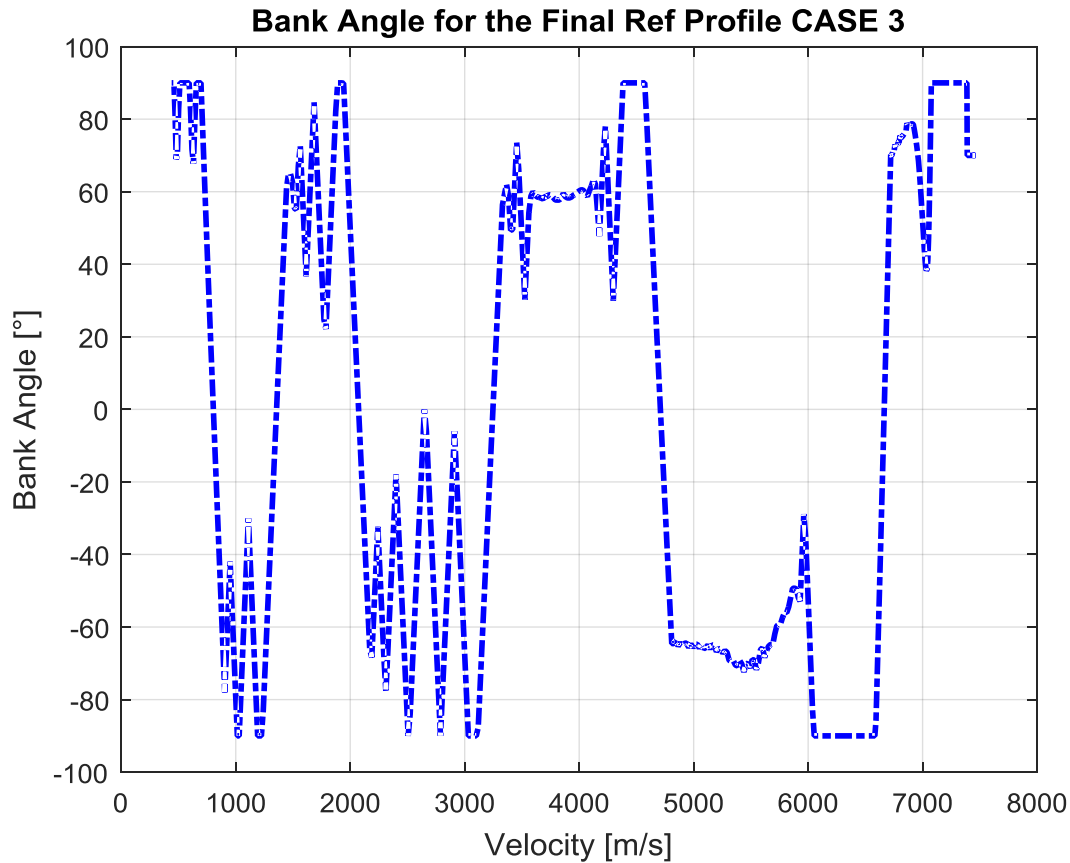


Figure 105: Bank Angle for the case 3 and an initial position equal to $-1,7932^\circ$ as latitude and 195° as longitude, following the final reference profile obtained with the range correction.

Conditions	Nominal	Actual	Guidance Error
Velocity	448.5836 m/s	448.6804 m/s	0.0216%
Altitude	26 Km	26.1 Km	0.3671%
Latitude	3.2721°	3.2859°	0.4216%
Longitude	-123.1265°	-123.0539°	0.0590%
Range	4693.4 Km	4710.9 Km	8.2152 Km

Table 36: Final values and errors for the case 3 in the first simulation.

The results in Table 37 respect the specifications about the maximum error, the vehicle is guided until the final point without violating the re-entry corridor constrains. Also in this case there are oscillations in the Bank Angle profile, especially in the final part of the profile.

For the case 4 the results are the following:

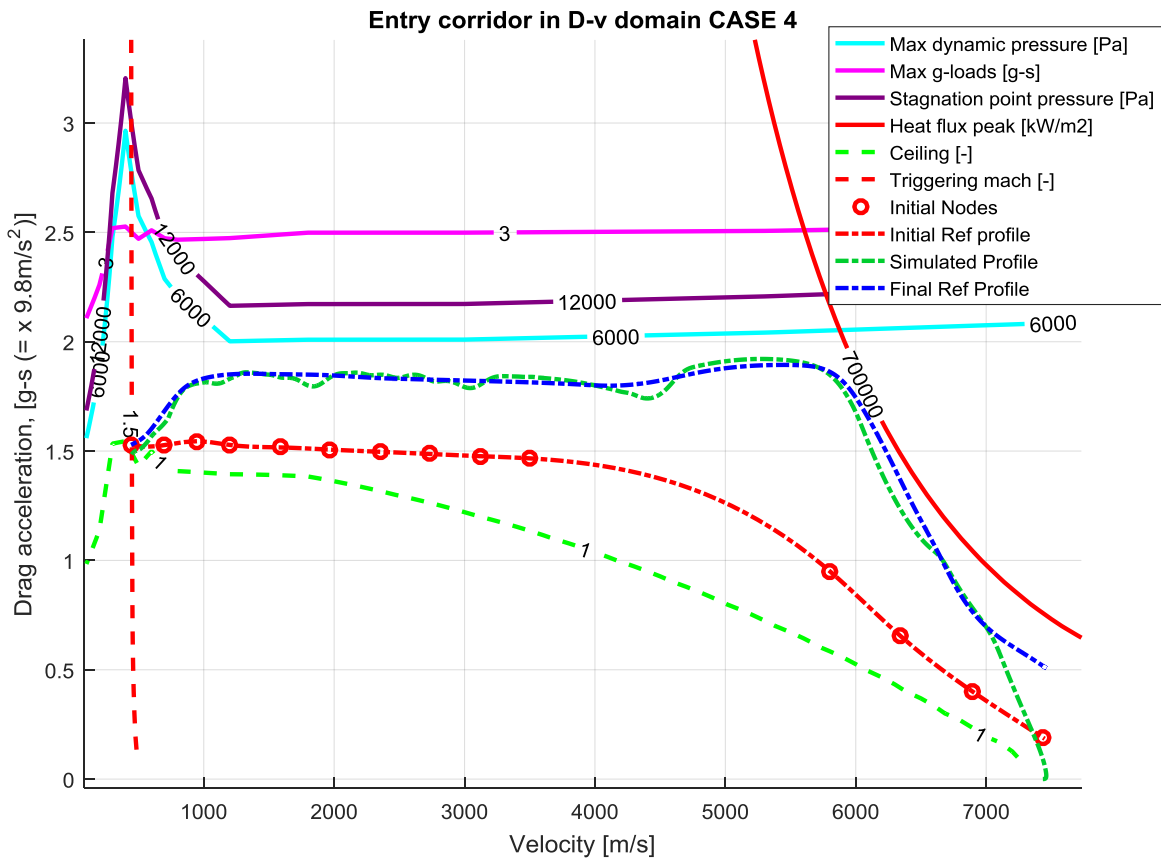


Figure 106: Simulation with range correction for the case 4 and an initial position equal to $-1,7932^\circ$ as latitude and 195° as longitude.

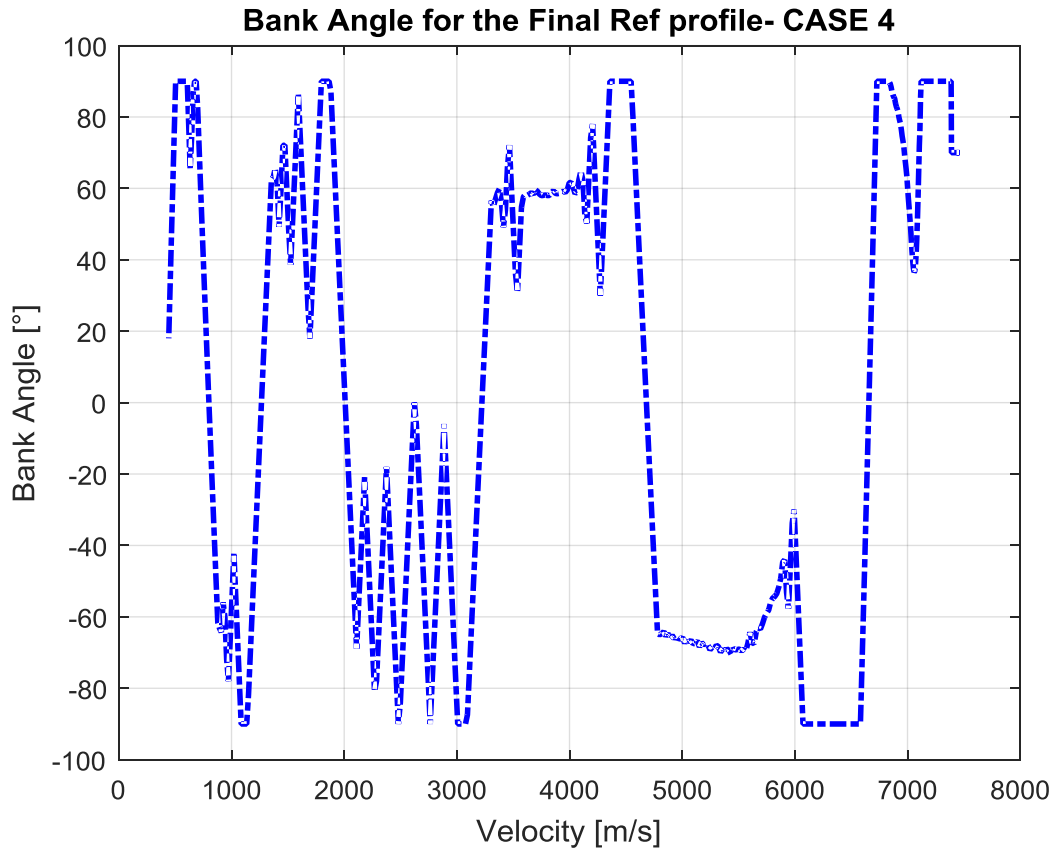


Figure 107: Bank Angle for the case 4 and an initial position equal to $-1,7932^\circ$ as latitude and 195° as longitude, following the final reference profile obtained with the range correction.

Conditions	Nominal	Actual	Guidance Error
Velocity	448.5836 m/s	448.7665 m/s	0.0408%
Altitude	26 Km	26.2 Km	0.6937%
Latitude	3.2721°	3.2696°	0.0762%
Longitude	-123.1265°	-123.116°	0.0085%
Range	4693.4 Km	4694.7 Km	1.1966 Km

Table 37: Final values and errors for the case 4 in the first simulation.

The results in Table 38 respect the specifications about the maximum error, the vehicle is guided until the final point without violating the re-entry corridor constrains. In this case the error is lower respect to the case 3, and as we can see the reference trajectory is closer to the dynamic pressure limit because, in this case, the upper limitation is less stringent (as we have explain in the chapter 4.1). Also in this case there are oscillations in the Bank Angle profile.

For the case 5 the results are the following:

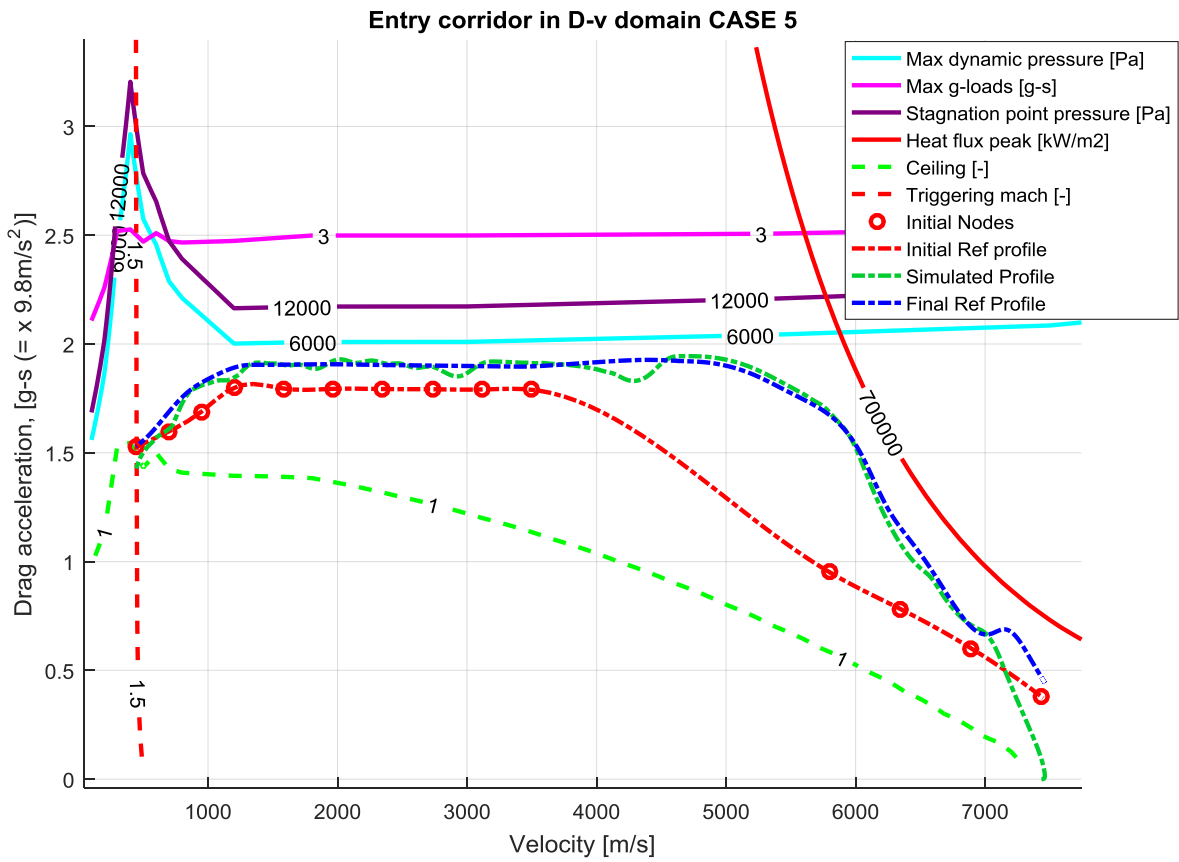


Figure 108: Simulation with range correction for the case 5 and an initial position equal to $-1,7932^\circ$ as latitude and $194,3^\circ$ as longitude.

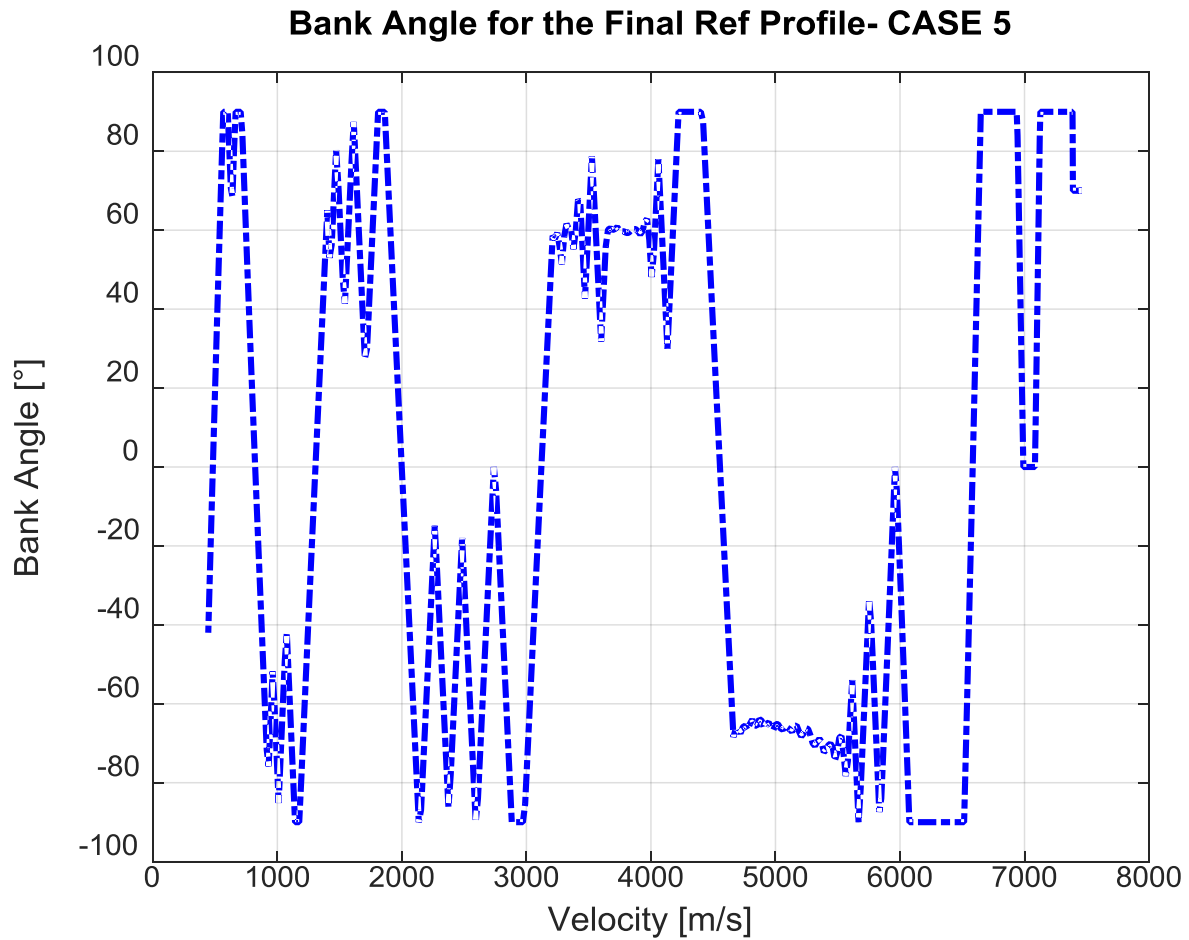


Figure 109: Bank Angle for the case 5 and an initial position equal to $-1,7932^\circ$ as latitude and $194,3^\circ$ as longitude, following the final reference profile obtained with the range correction.

Conditions	Nominal	Actual	Guidance Error
Velocity	448.5836 m/s	448.9966m/s	0.0921%
Altitude	26 Km	26.4 Km	1.5733%
Latitude	3.2721°	3.3635°	0.2636%
Longitude	-123.1265°	-123.1458°	0.0157
Range	4770.7 Km	4768.6 Km	2.2187Km

Table 38: Final values and errors for the case 5 in the first simulation.

The results in Table 39 respect the specifications, but the Bank Angle Profile presents oscillations also in the first part of the profile.

The second simulation wants to use the same initial point for all the cases. The initial desired range is really similar to the range of the initial reference profile. So we can guess that the final reference profile will only undergo a translation, without enter in the range correction made by the Simulink model.

The PID gains are chosen variable for all the five cases and N is equal to 1,2. The table for the gain is the following:

Dynamic Pressure [Pa]	K_P	K_D
0	120	$\frac{2400}{2}$
1505,233	119,9895	$\frac{2399,114}{2}$
2008,078	119,943	$\frac{2395,575}{2}$
2502,386	119,871	$\frac{2391,16}{2}$
3013,382	119,1325	$\frac{2356,232}{2}$
3513,389	$\frac{117,1894}{2}$	$\frac{2313,516}{2}$
4011,477	$\frac{115,4586}{2}$	$\frac{2006,827}{2}$
4503,342	$\frac{114,7672}{2}$	$\frac{1691,535}{2}$
5012,983	$\frac{110}{2}$	$\frac{1100}{2}$
5500	$\frac{110}{2}$	$\frac{1100}{2}$
5900	$\frac{110}{2}$	$\frac{1100}{2}$

Table 39: PID gains for the second simulation.

The gains, for a dynamic pressure higher than 3700 Pascal, are halved.

The integrative term is equal to $K_I = 1$. The basic idea is that if the reference curve has an high Drag Acceleration, to avoid oscillation, the integrative term must be reduced. For this reason in the previous case the integrative term was equal to 0,5.

The value of N is 0,7692.

During the Heat Flux Peak Phase range correction are used variable gains. The second constant gain in the Heat Flux Peak Phase range correction is equal to 1. The error Processing Parameters for the Straight Line

Drag Acceleration Phase correction during the Heat Flux Peak Phase range correction is set equal to 1/10. For all the cases is used the upper limitation described in Figure 90.

The error Processing Parameters for *S1, S2, S3* Phase correction during the Connection Phase range correction are chosen equal to 1/10. The error Processing Parameters for *C1, C2, C3* Phase correction during the Connection Phase range correction are chosen equal to 1/10, but if the phase is the current phase the gain is equal to 1/8.

The error Processing Parameters for *S1, S2, S3, S4, S5, S6* Phase correction during the Straight line Drag Acceleration Phase range correction are equal to 1/20.

The saturator for the range error is set equal to *inf*.

The initial point is the following:

Latitude [°]	Longitude [°]
-3,071	185

Table 40: Initial coordinates for the second simulation.

The final point is always the same:

	Latitude [°]	Longitude [°]
<i>Final Point</i>	3,2721	-123,1265

Table 41: Final coordinates for the second simulation.

For the case 1 the results are the following:

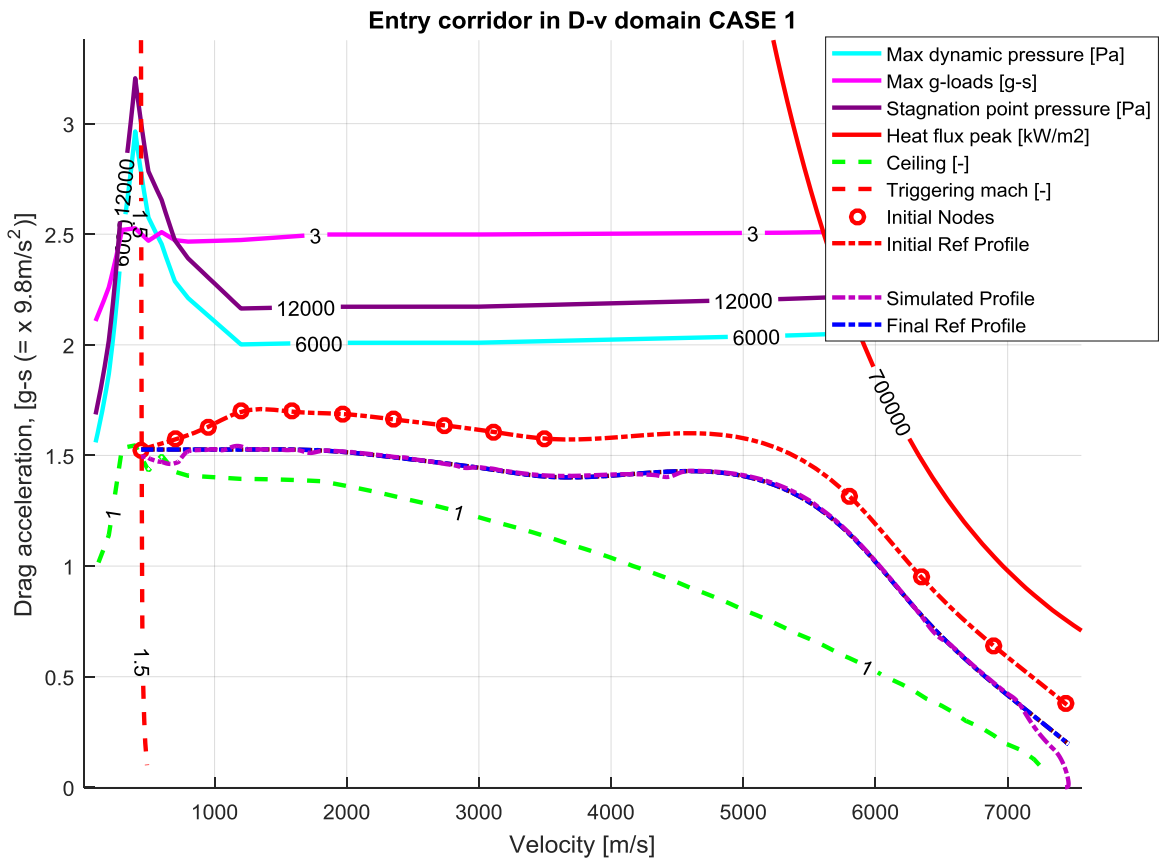


Figure 110: Simulation with range correction for the case 1 and an initial position equal to $-3,071^\circ$ as latitude and 185° as longitude.

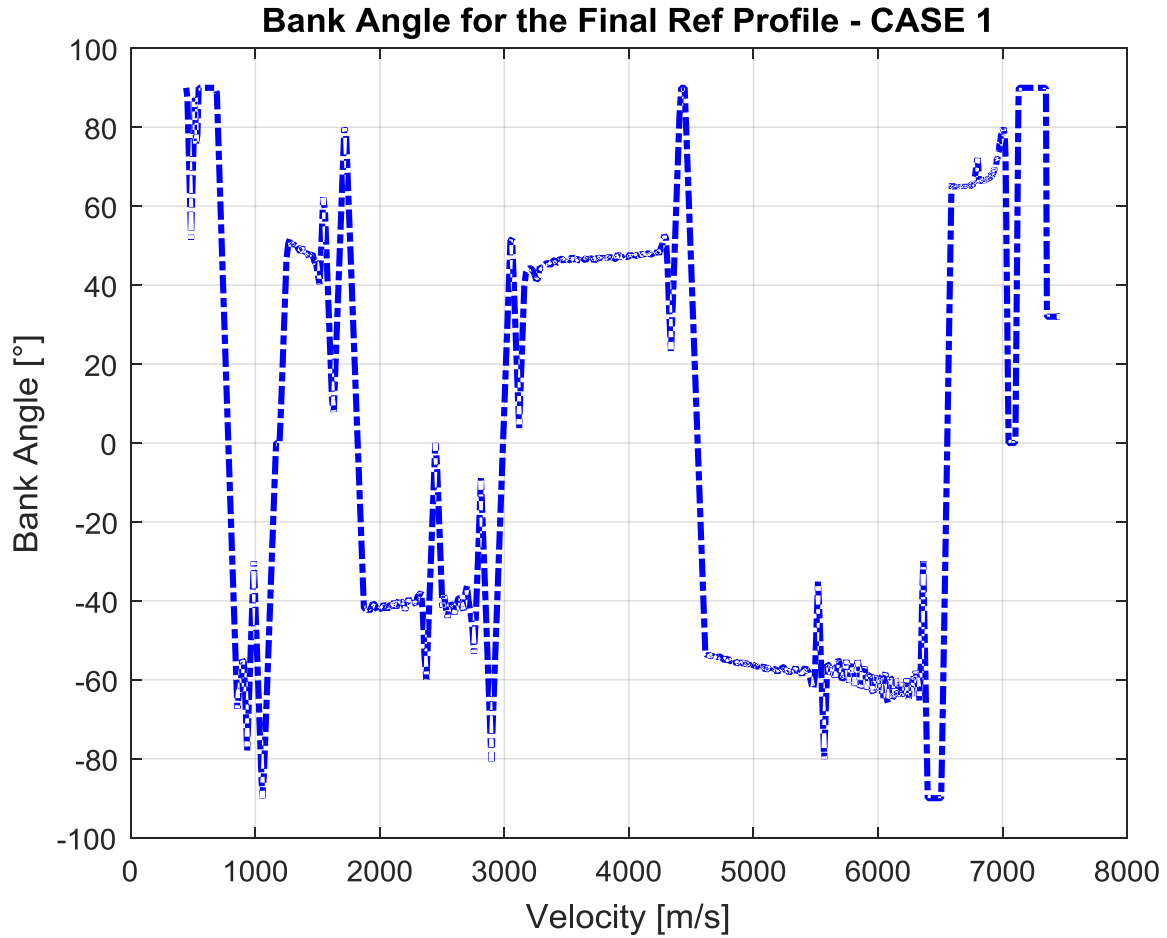


Figure 111: Bank Angle for the case 1 and an initial position equal to $-3,071^\circ$ as latitude and 185° as longitude., following the final reference profile obtained with the range correction.

Conditions	Nominal	Actual	Guidance Error
Velocity	448.5836 m/s	448.7334 m/s	0.0334%
Altitude	26 Km	26.1 Km	0.5671%
Latitude	3.2721°	3.2673	0.1764%
Longitude	-123.1265°	-123.0685°	0.0471%
Range	5814.6 Km	5821 Km	6.4823 Km

Table 42: Final values and errors for the case 1 in the second simulation.

The new reference profile, obtained with the range correction, is the translated reference profile, (this methodology is explained in Figure 73). All the results respect the specifications, with low oscillations in the Bank Angle Profile.

For the case 2 the results are the following:

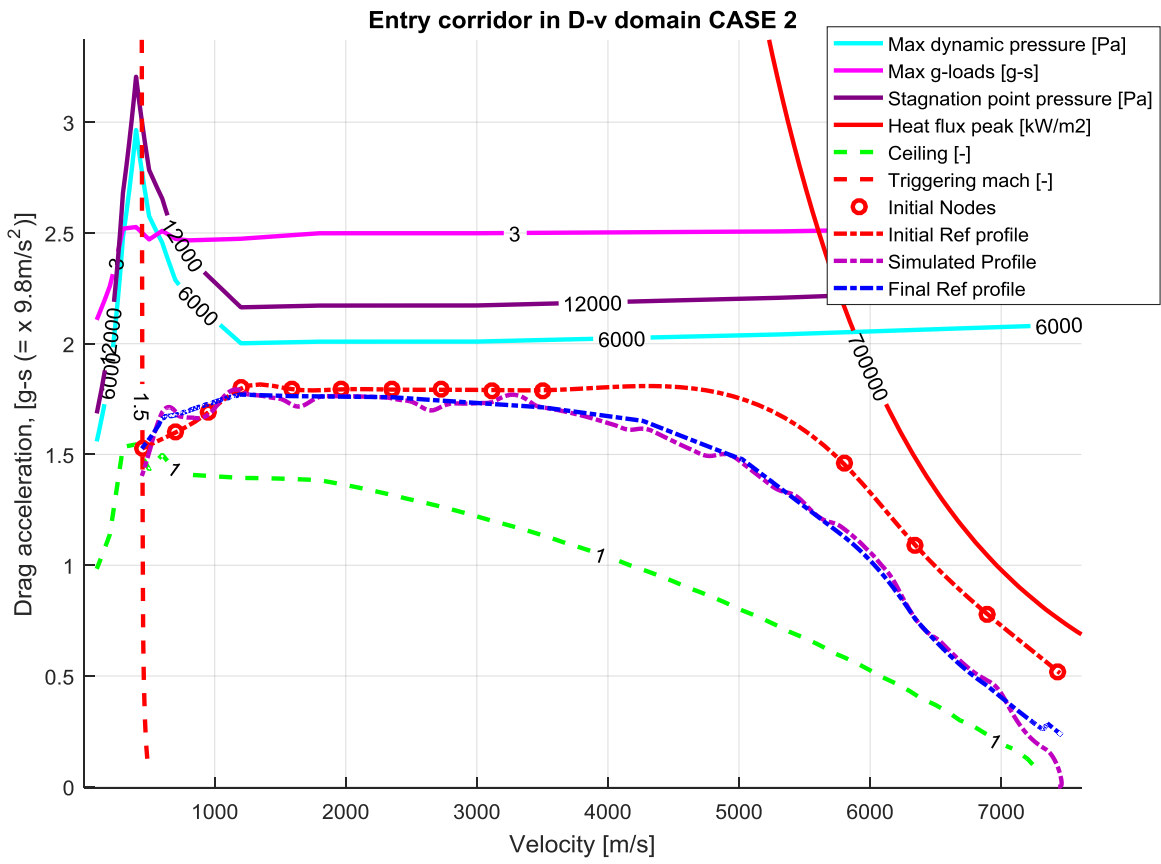


Figure 112: Simulation with range correction for the case 2 and an initial position equal to $-3,071^\circ$ as latitude and 185° as longitude.

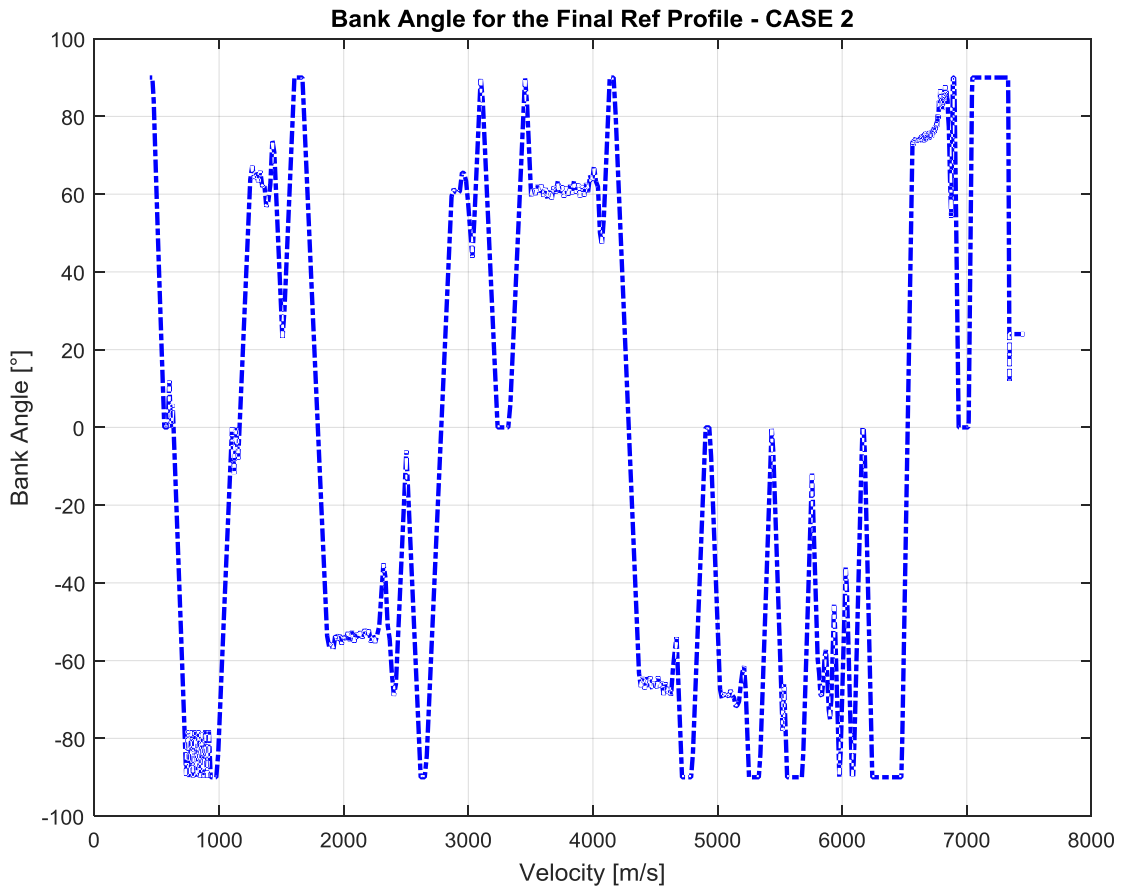


Figure 113: Bank Angle for the case 2 and an initial position equal to $-3,071^\circ$ as latitude and 185° as longitude., following the final reference profile obtained with the range correction.

Conditions	Nominal	Actual	Guidance Error
Velocity	448.5836 m/s	449.0995 m/s	0.1150%
Altitude	26 Km	26.5 Km	1.9661%
Latitude	3.2721°	3.2673	0.9810%
Longitude	-123.1265°	-123.0541°	0.0588%
Range	5814.6 Km	5823 Km	8.8008 Km

Table 43: Final values and errors for the case 2 in the second simulation.

In this case the new reference profile, after the translation, is also modified with the range correction procedure. The final error range is bigger respect to the others cases but the specification are always respected. In the Bank Angle Profile there are a lot of oscillations, so a post-processing will be necessary.

For the case 3 the results are the following:

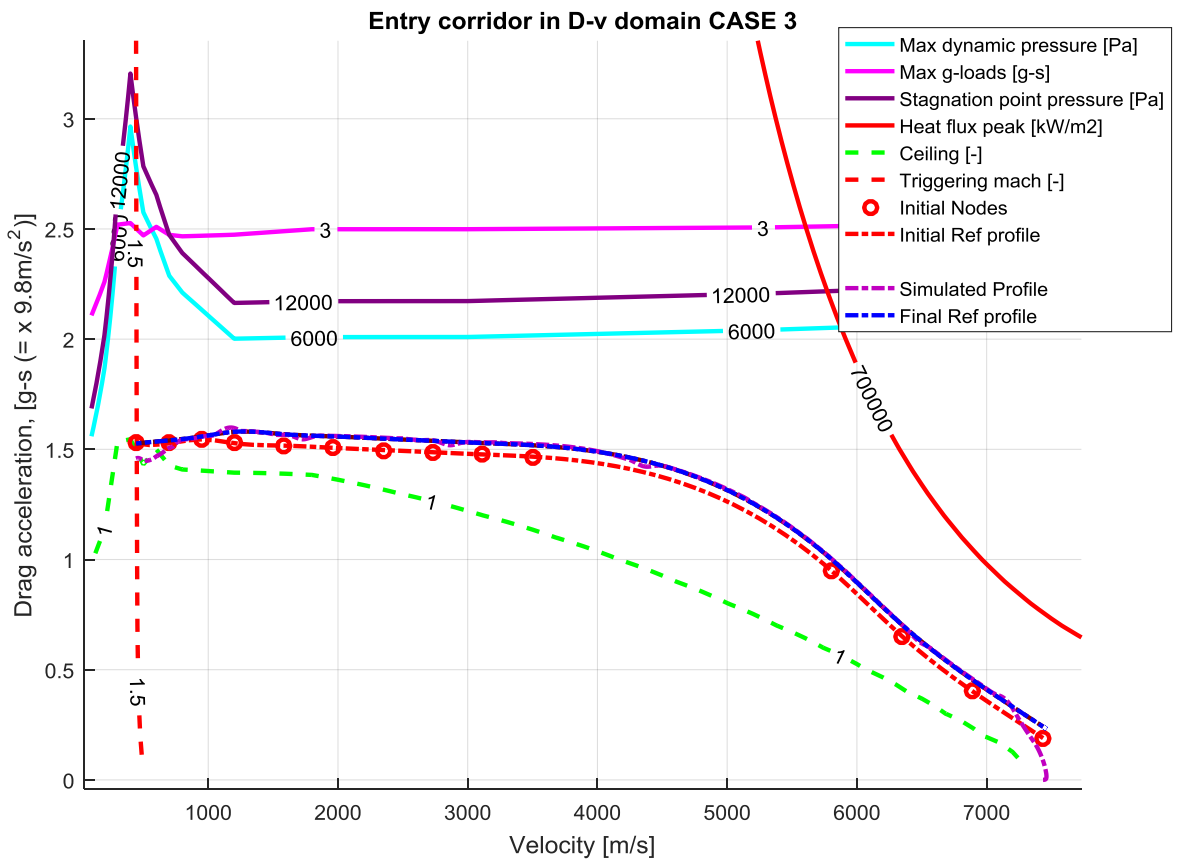


Figure 114: Simulation with range correction for the case 3 and an initial position equal to -3,071° as latitude and 185° as longitude.

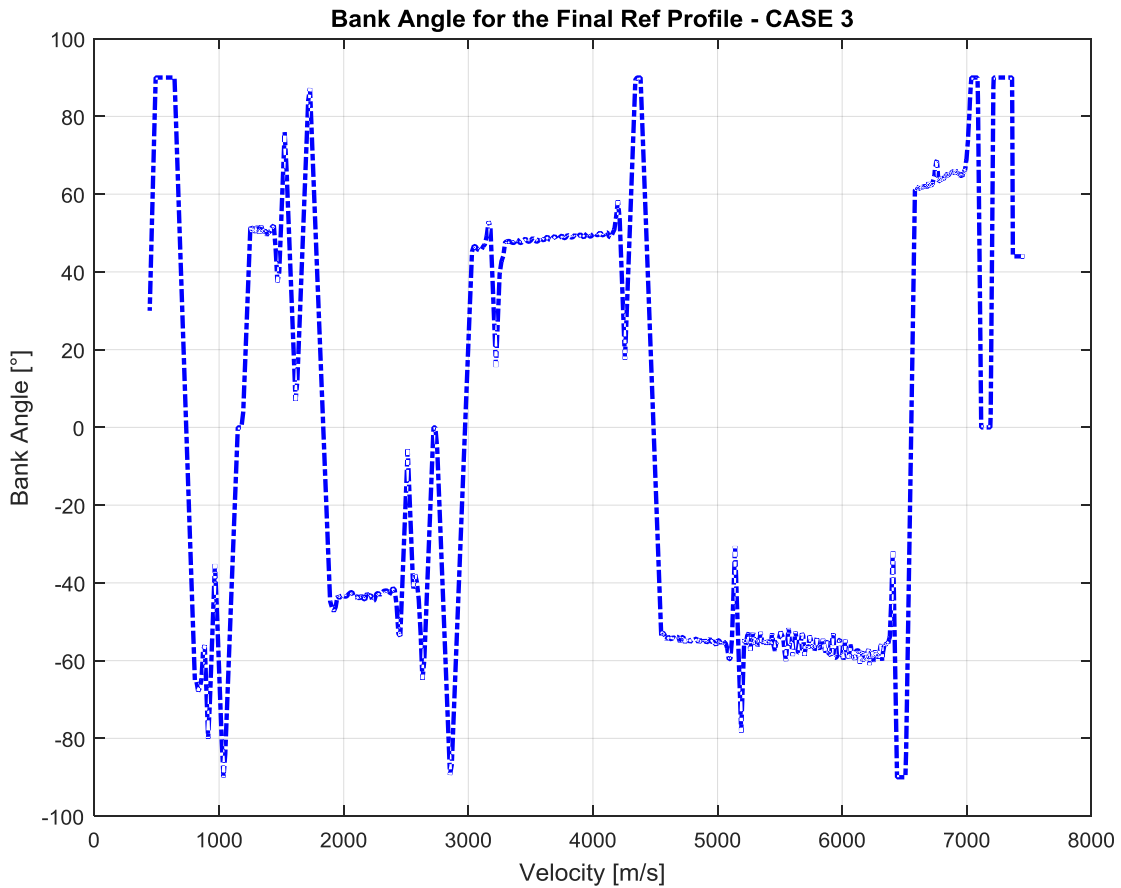


Figure 115: Bank Angle for the case 3 and an initial position equal to $-3,071^\circ$ as latitude and 185° as longitude, following the final reference profile obtained with the range correction.

Conditions	Nominal	Actual	Guidance Error
Velocity	448.5836 m/s	448.8825 m/s	0.0666%
Altitude	26 Km	26.3 Km	1.1368%
Latitude	3.2721°	3.2779°	0.1057%
Longitude	-123.1265°	-123.1466°	0.0163%
Range	5814.6 Km	5813 Km	2. 2644 Km

Table 44: Final values and errors for the case 3 in the second simulation.

The reference profile is obtained only with the translation, so the form doesn't change respect to the initial reference profile. All the errors are really small.

For the case 4 the results are the following:

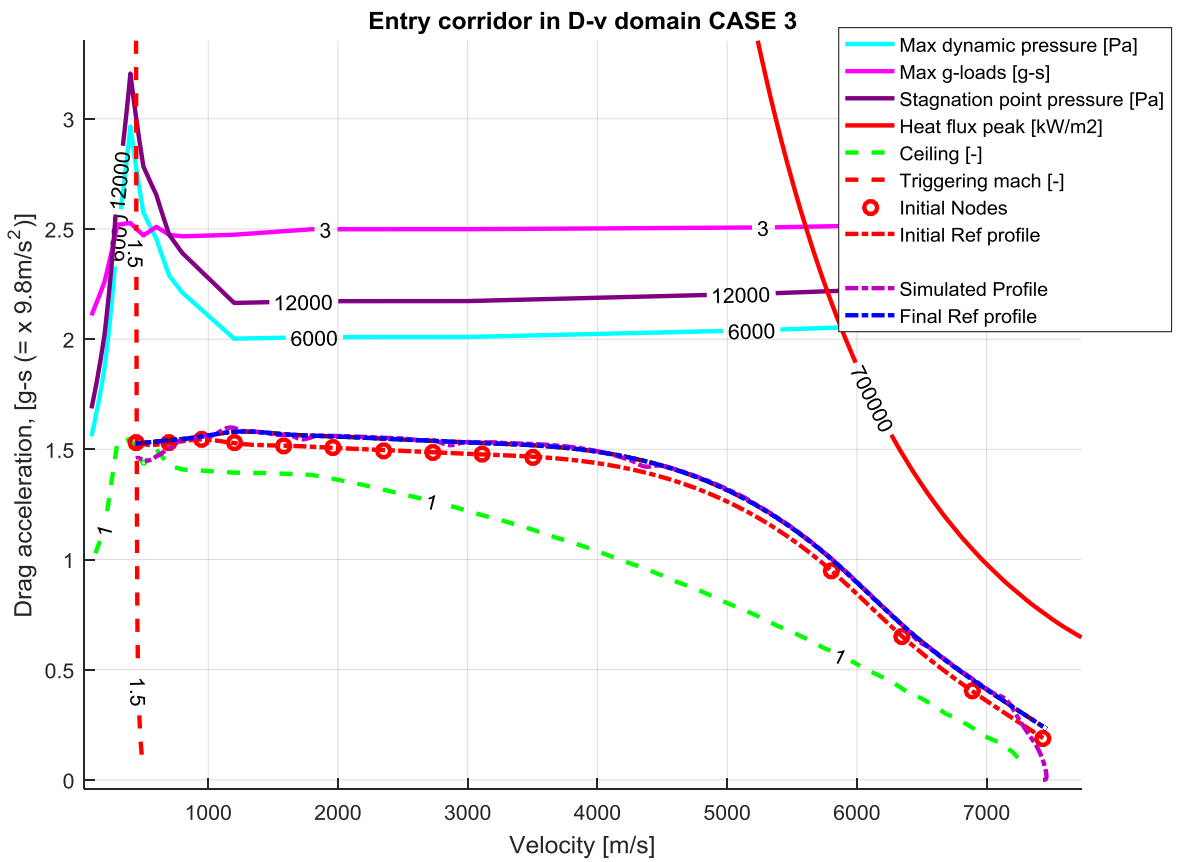


Figure 116: Simulation with range correction for the case 4 and an initial position equal to $-3,071^\circ$ as latitude and 185° as longitude.

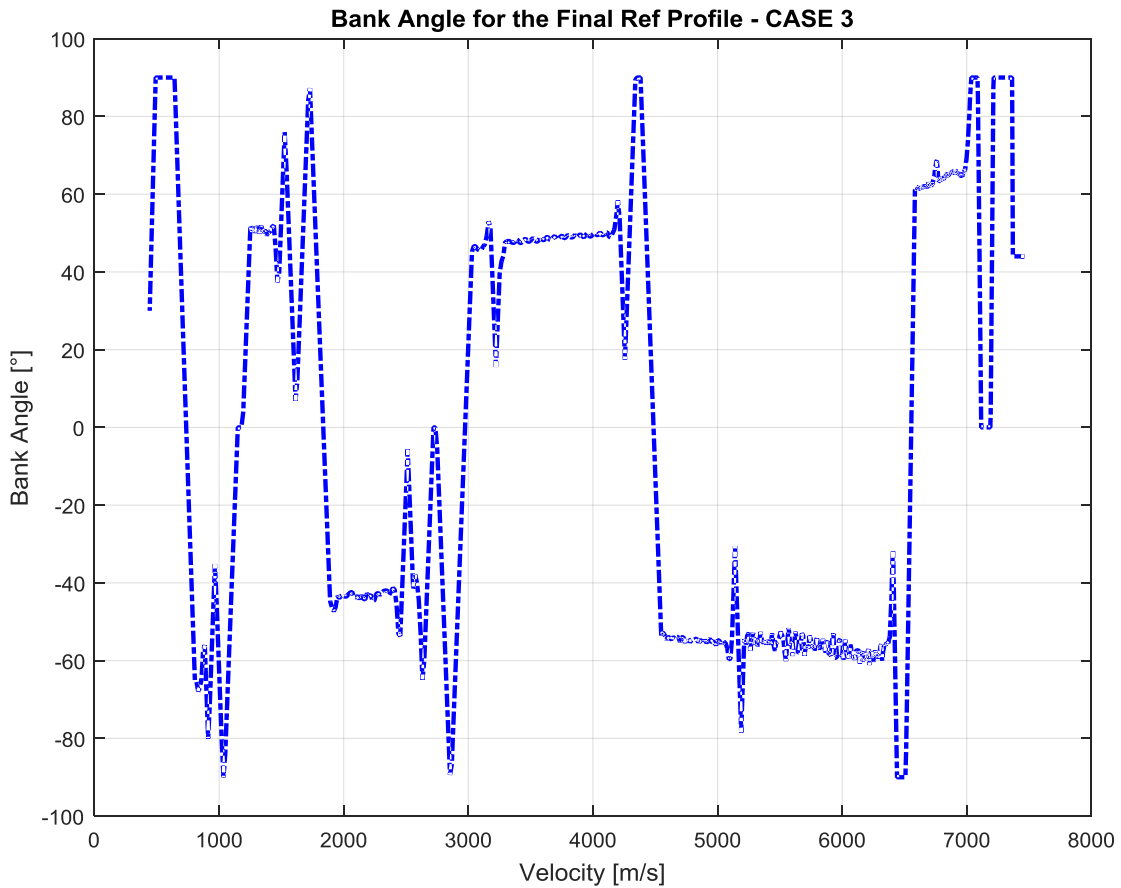


Figure 117: Bank Angle for the case 4 and an initial position equal to $-3,071^\circ$ as latitude and 185° as longitude, following the final reference profile obtained with the range correction.

Conditions	Nominal	Actual	Guidance Error
Velocity	448.5836 m/s	448.8825 m/s	0.0666%
Altitude	26 Km	26.3 Km	1.1368%
Latitude	3.2721°	3.2686°	0.1057%
Longitude	-123.1265°	-123.1446°	0.0163%
Range	5814.6 Km	5813 Km	2.2644 Km

Table 45: Final values and errors for the case 4 in the second simulation.

This case gives the same results of the case 3. In fact the reference profile is the same, there is only a change in the upper limitation position. But if the reference profile doesn't reach this limitation the obtained profile will be the same.

For the case 5 the results are the following:

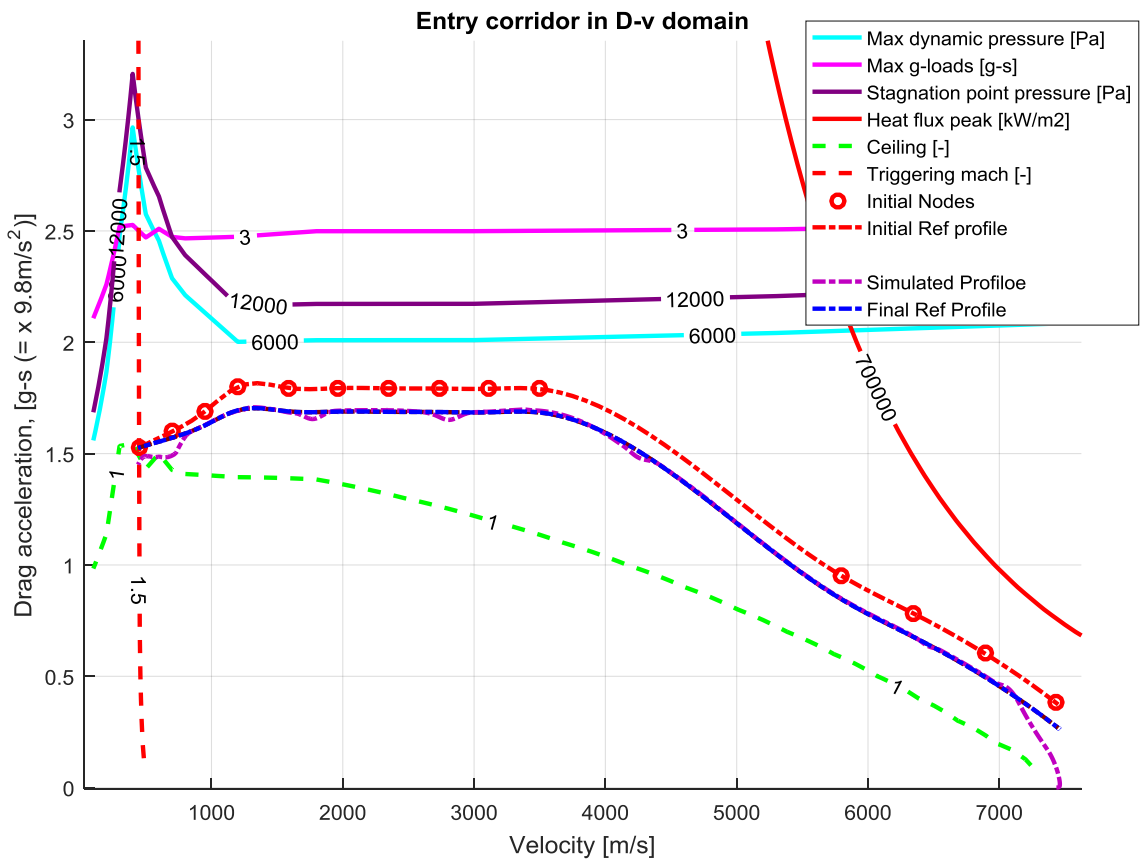


Figure 118: Simulation with range correction for the case 5 and an initial position equal to -3,071° as latitude and 185° as longitude.

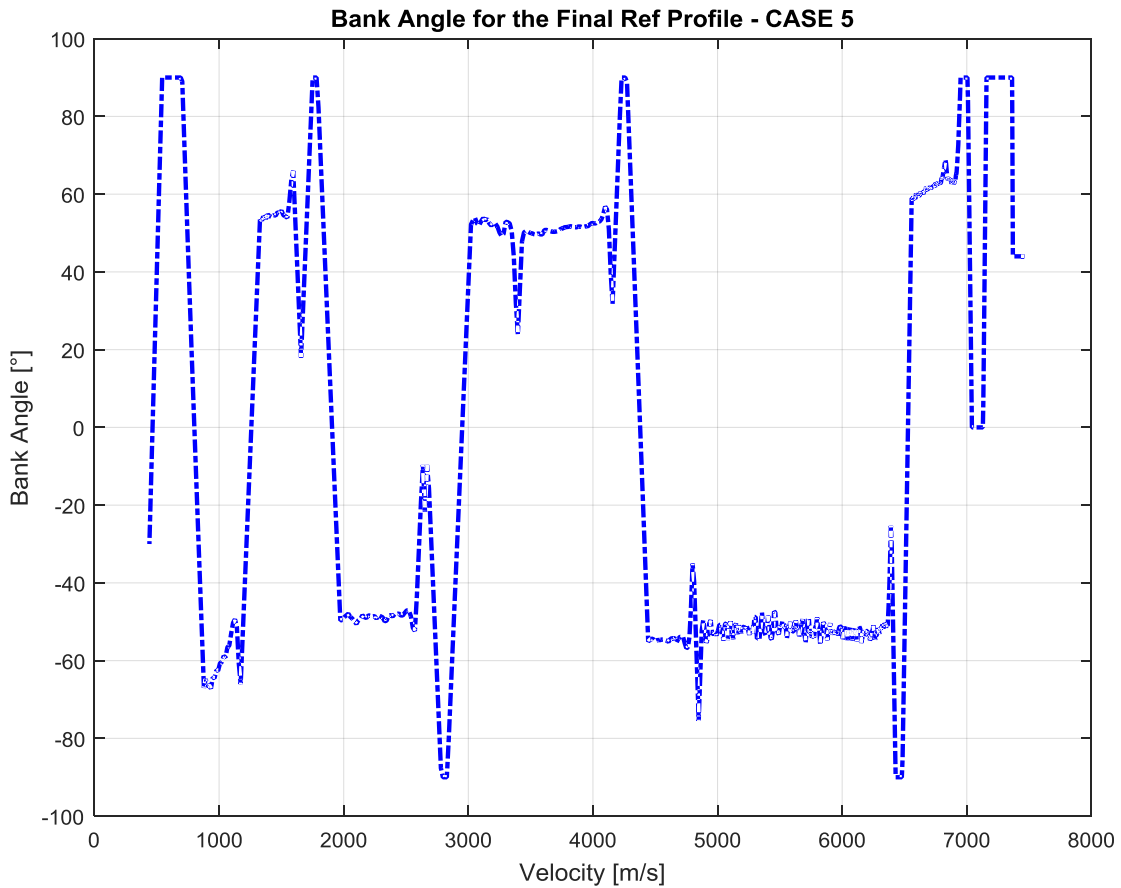


Figure 119: Bank Angle for the case 5 and an initial position equal to $-3,071^\circ$ as latitude and 185° as longitude, following the final reference profile obtained with the range correction.

Conditions	Nominal	Actual	Guidance Error
Velocity	448.5836 m/s	448.8768 m/s	1.1167%
Altitude	26 Km	26.3 Km	2.3567%
Latitude	3.2721°	3.2673°	0.1478%
Longitude	-123.1265°	-123.1281°	0.0013%
Range	5814.6 Km	5815 Km	0.5656 Km

Table 46: Final values and errors for the case 5 in the second simulation.

Also in this case the new reference profile is only the translated profile. This is the case with lower oscillations: the vehicle follows with small deviations the reference profile, so the final error range is really small.

In the third simulation are introduced the coordinates used for IXV. The PID gains are chosen variable, with the same law as the previous case. The integrative term is equal to $K_I = 2$ and the cut-off frequency is equal to $N = 1,2$.

The initial point is the following:

Latitude [°]	Longitude [°]
-4,47910691292286	173,484601053785

Table 47: Initial coordinates for the third simulation.

The final point is always the same:

	Latitude [°]	Longitude [°]
Final Point	3,2721	-123,1265

Table 48: Final coordinates for the third simulation.

In the case 2 the desired range is higher than the maximum range, so the simulation can't be done.

During the Heat Flux Peak Phase range correction are used constant gains. The constant gain in the Heat Flux Peak Phase range correction is equal to 0.1 for all the cases, except for the case 5 where, if the phase isn't the current phase, the gain is equal to 0.01. The second constant gain is equal to 0.1 for the case 3 and 4, equal to 0.2 for the case 1 and equal to 0.05 for the case 5. The error Processing Parameters for the Straight Line Drag Acceleration Phase correction during the Heat Flux Peak Phase range correction is set equal to 1/10. For the all the cases is used the upper limitation described in Figure 90.

The error Processing Parameters for $S1, S2, S3$ Phase correction during the Connection Phase range correction are chosen equal to 1/10 for all the case. The error Processing Parameters for $C1, C2, C3$ Phase correction during the Connection Phase range correction are chosen equal to 1/10, except for the phase 5 where the gain is equal to 1/5. But if the phase is the current phase, in the case 3 and 4, this gain is set equal to 1/8 and in the case 5 this gain is equal to 1/10.

The error Processing Parameters for $S1, S2, S3, S4, S5, S6$ Phase correction during the Straight line Drag Acceleration Phase range correction are equal to 1/30 for the case 1. In the case 3 and 4 this gain is equal to 1. For the case 5 the gain are equal to 1/30, except for the current phase where the gain is equal to 1/50.

The saturator for the range error is set equal to *inf*.

For the case 1 the results are the following:

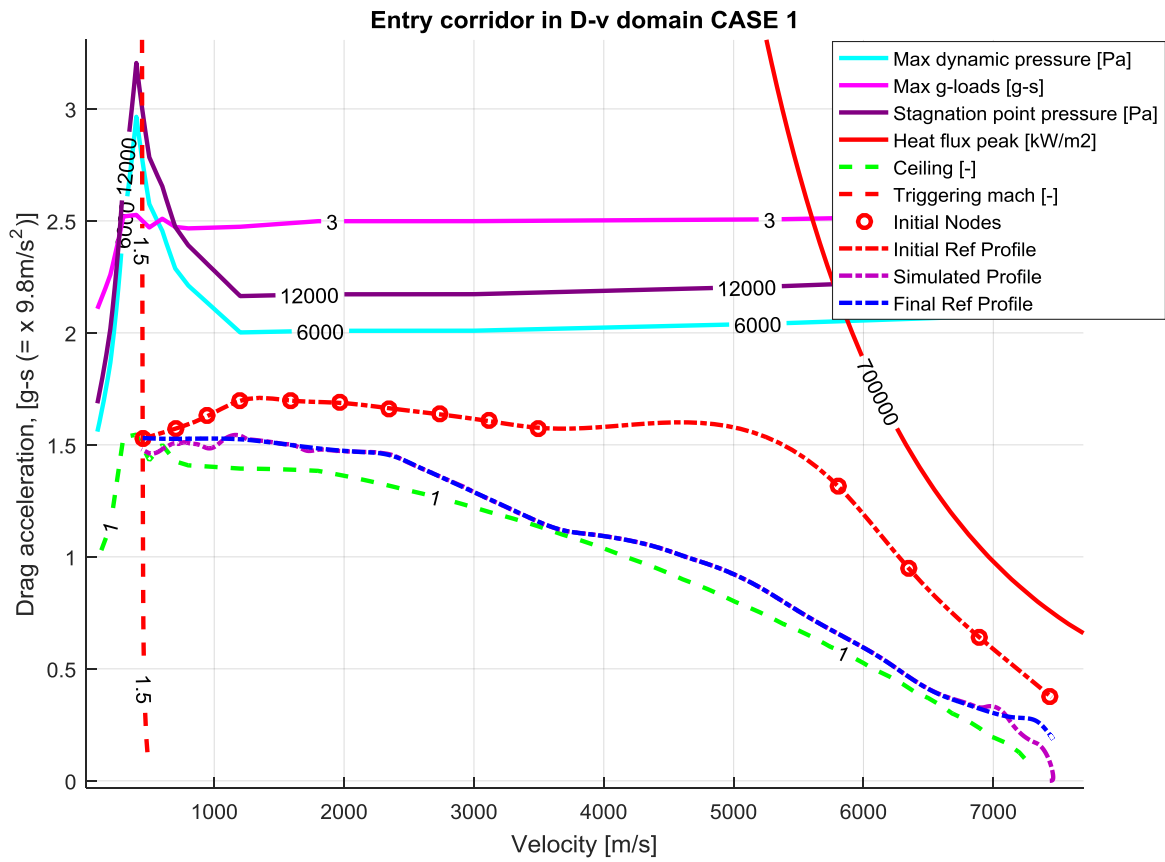


Figure 120: Simulation with range correction for the case 1 and an initial position equal to IXV latitude and longitude.

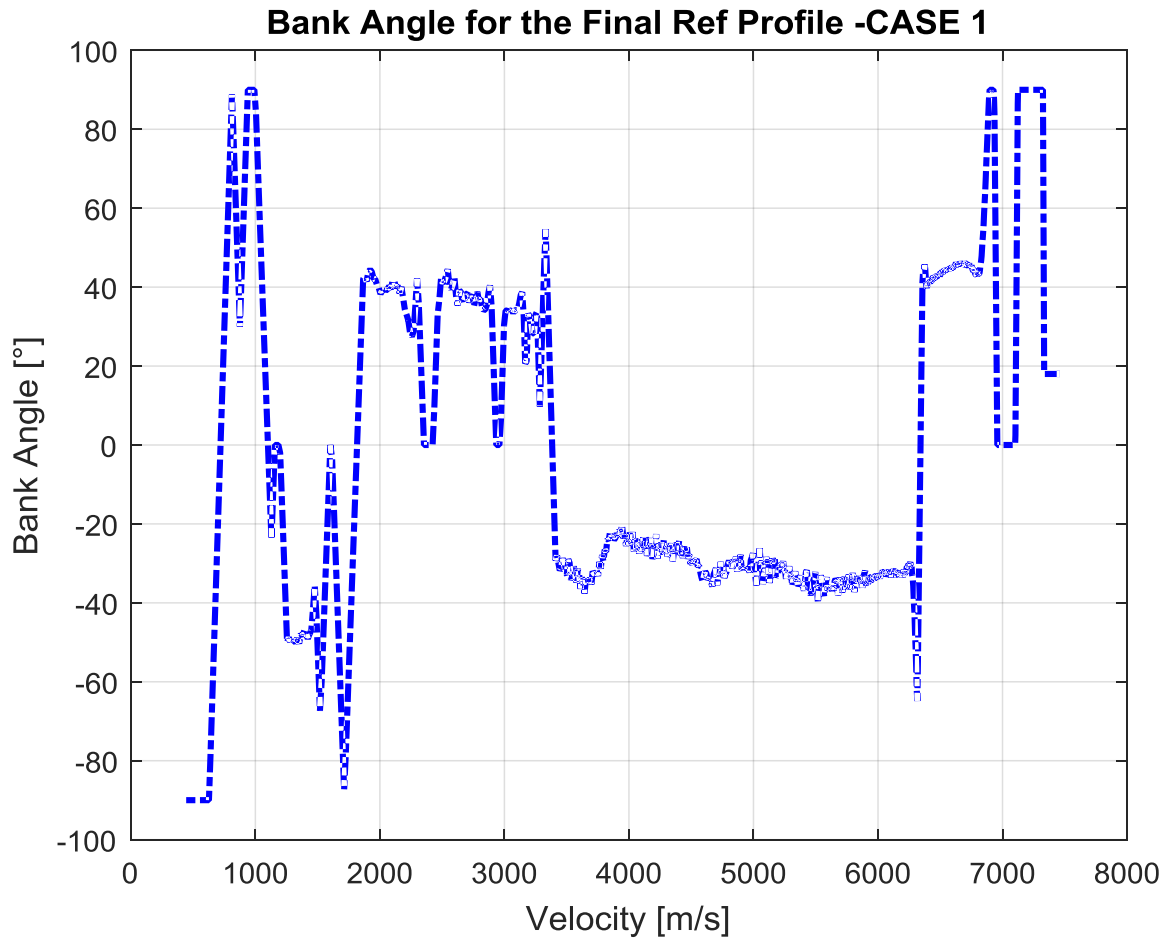


Figure 121: Bank Angle for the case 1 and an initial position equal to IXV latitude and longitude, following the final reference profile obtained with the range correction.

Conditions	Nominal	Actual	Guidance Error
Velocity	448.5836 m/s	448.7999 m/s	0.0482%
Altitude	26 Km	26.2 Km	0.8245%
Latitude	3.2721°	3.273°	0.0267%
Longitude	-123.1265°	-123.0873°	0.0319%
Range	7103.1 Km	7107.8 Km	4.3595 Km

Table 49: Final values and errors for the case 1 in the third simulation.

In this case the final reference profile isn't so regular. This problem can be solved changing the Error Processing Parameters. But despite the strange form of the reference profile, the vehicle is able to follow it, because the profile is a contoured profile (a countered profile is a profile where there are the continuity of first, second and third derivative), created with splines, after the procedure described in Figure 98. The errors respect the specifications.

For the case 3 the results are the following:

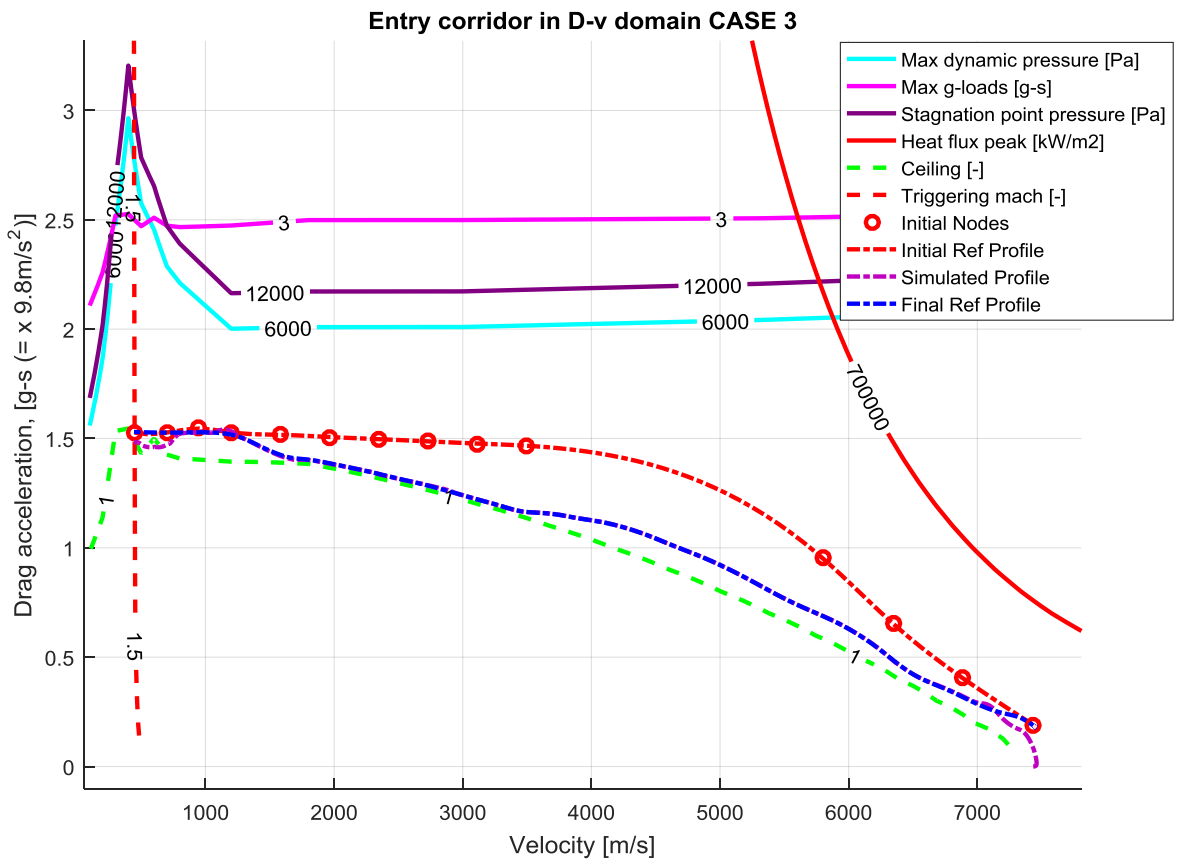


Figure 122: Simulation with range correction for the case 3 and an initial position equal to IXV latitude and longitude.

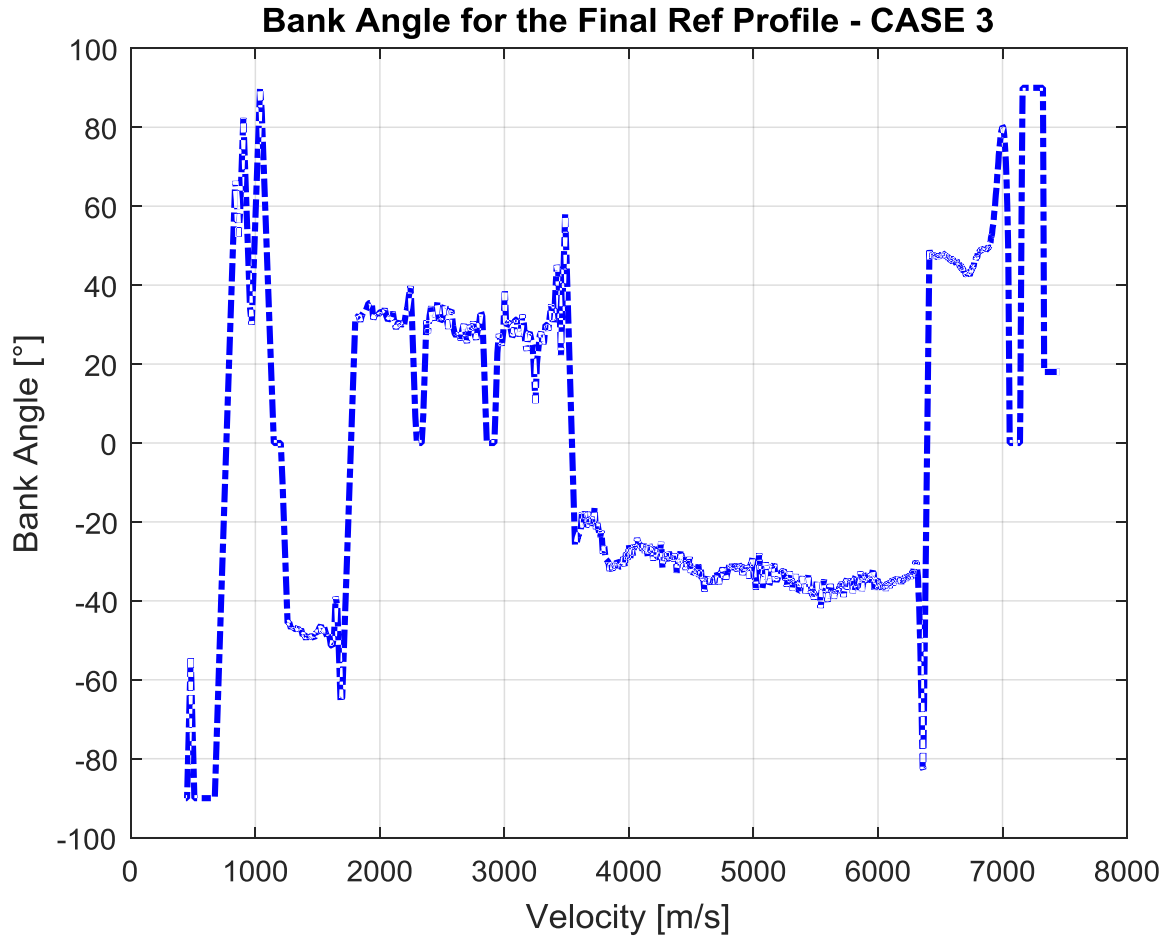


Figure 123: Bank Angle for the case 3 and an initial position equal to IXV latitude and longitude, following the final reference profile obtained with the range correction.

Conditions	Nominal	Actual	Guidance Error
Velocity	448.5836 m/s	448.7735 m/s	0.0423%
Altitude	26 Km	26.2 Km	0.7209%
Latitude	3.2721°	3.2789°	0.2077%
Longitude	-123.1265°	-123.0962°	0.0246%
Range	7103.1 Km	7106.8 Km	3.4479 Km

Table 50: Final values and errors for the case 3 in the third simulation.

For the case 4 the results are the following:

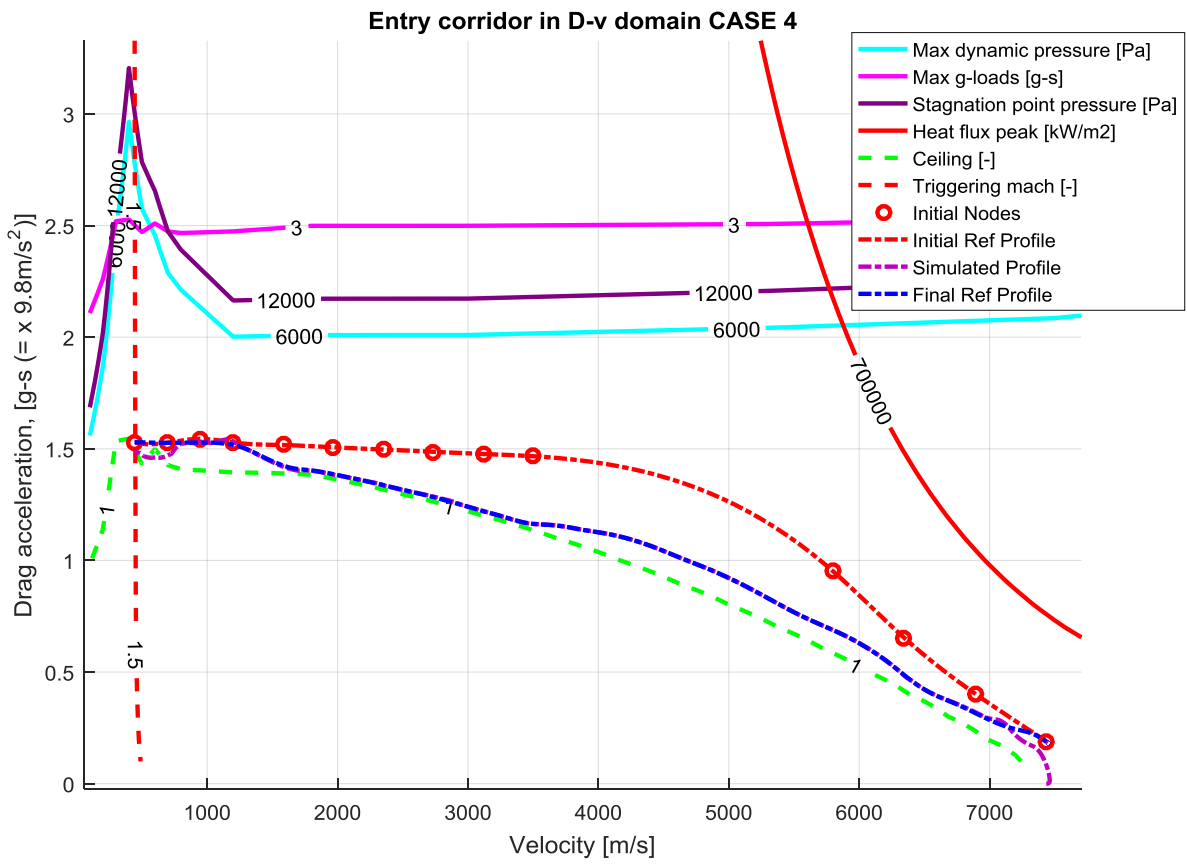


Figure 124: Simulation with range correction for the case 4 and an initial position equal to IXV latitude and longitude.

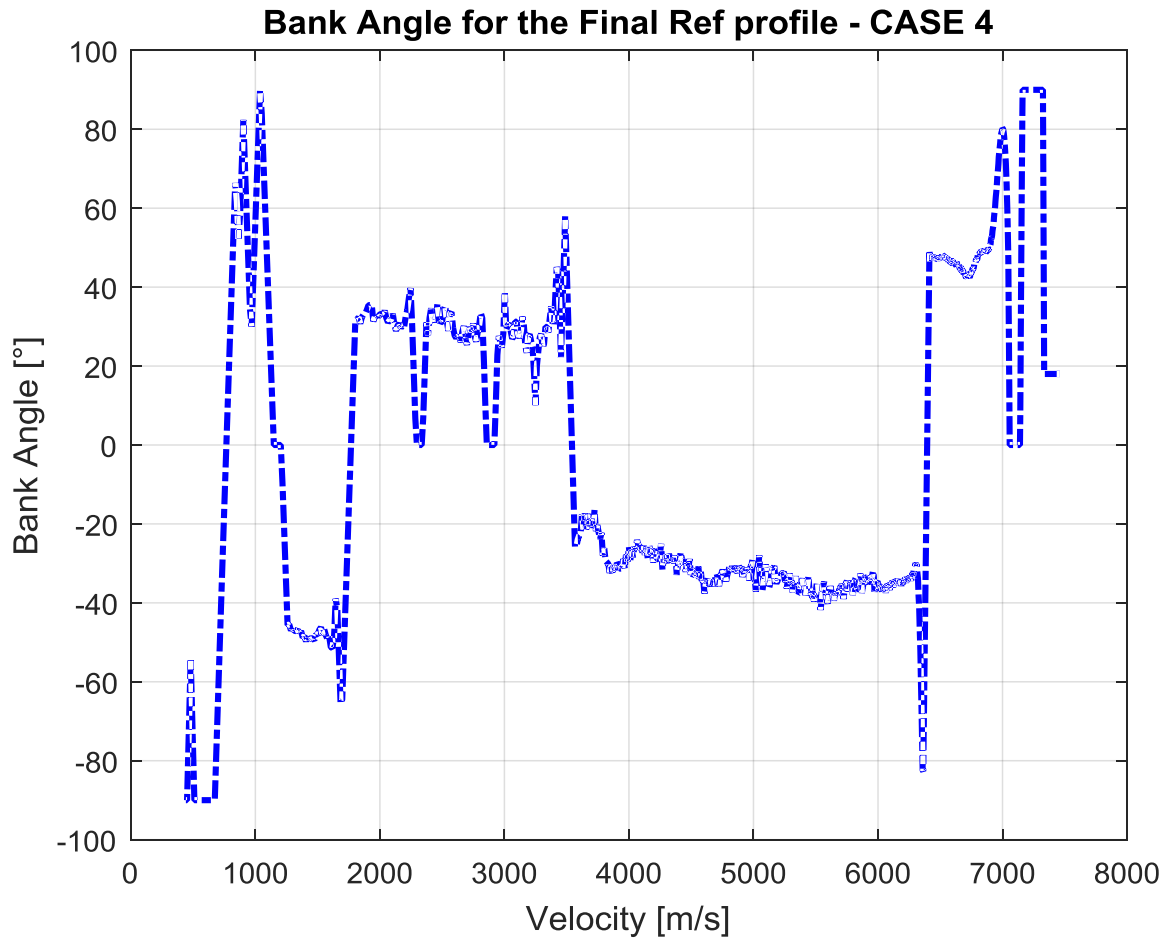


Figure 125: Bank Angle for the case 4 and an initial position equal to IXV latitude and longitude, following the final reference profile obtained with the range correction.

Conditions	Nominal	Actual	Guidance Error
Velocity	448.5836 m/s	448.7735 m/s	0.0423%
Altitude	26 Km	26.2 Km	0.7209%
Latitude	3.2721°	3.2789°	0.2077%
Longitude	-123.1265°	-123.0962°	0.0246%
Range	7103.1 Km	7106.8 Km	3.4479 Km

Table 51: Final values and errors for the case 4 in the third simulation.

The cases 3 and 4 give the same results for the new reference profile and for the guidance errors. The specifications are respected and the Bank Angle profile presents low oscillations.

For the case 5 the results are the following:

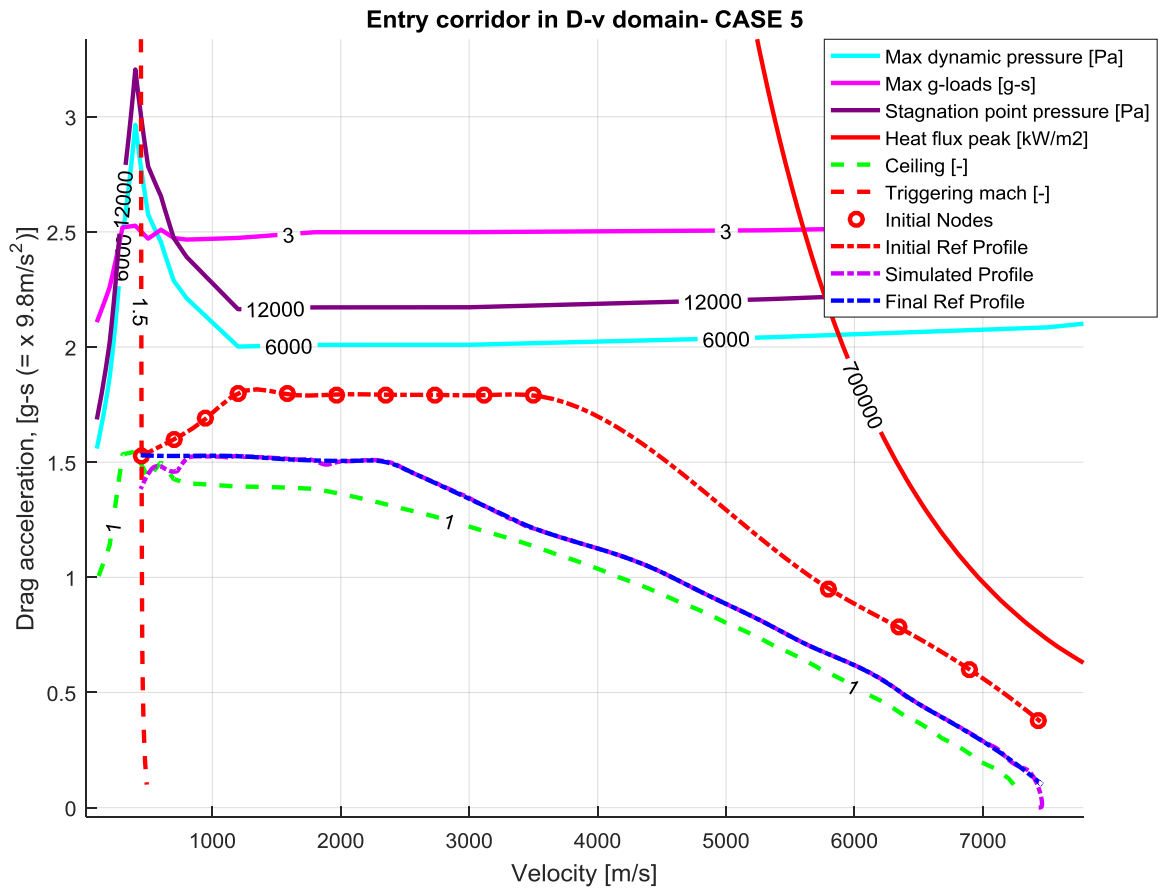


Figure 126: Simulation with range correction for the case 5 and an initial position equal to IXV latitude and longitude.

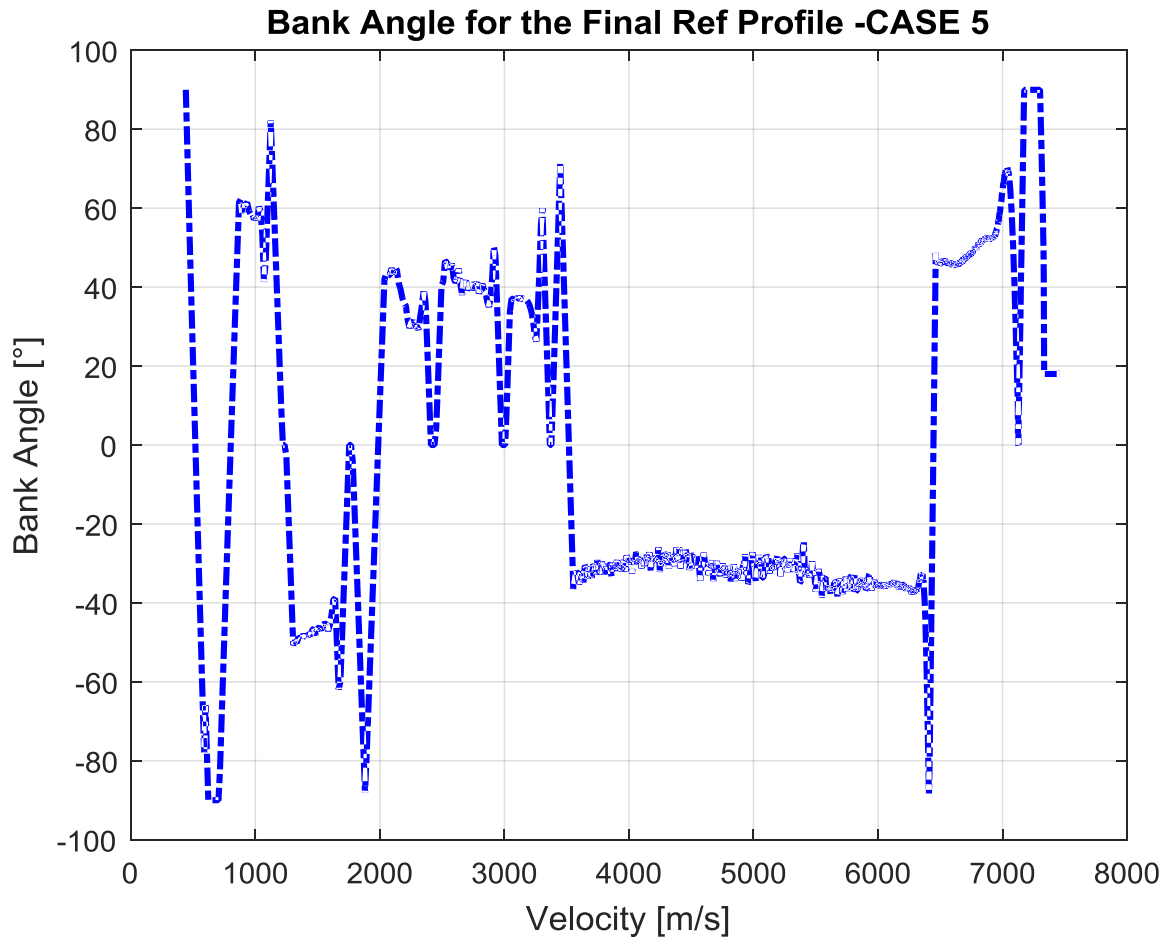


Figure 127: Bank Angle for the case 5 and an initial position equal to IXV latitude and longitude, following the final reference profile obtained with the range correction.

Conditions	Nominal	Actual	Guidance Error
Velocity	448.5836 m/s	449.1933 m/s	0.1359%
Altitude	26 Km	26.6 Km	2.3254%
Latitude	3.2721°	3.2625°	0.2921%
Longitude	-123.1265°	-123.2098°	0.0677%
Range	7103.1 Km	7094.1 Km	9.0112 Km

Table 52: Final values and errors for the case 5 in the third simulation.

The case 5 was the most difficult case to solve: a lot of iteration are been necessary to find the optimal error processing parameters that give a reference profile without elbow connections (elbow connections mean no continuity in the first, second and third derivative). In fact we must remember that if the reference profile has elbow connections the vehicle isn't able to follow it and the bank angle profile will present oscillations. Now the final reference profile hasn't elbow connections so the oscillation in the Bank Angle are reduced.

The last simulation has the aim to test if the algorithm is able to reach the lower limitation. The chosen initial coordinates are the coordinates that give a range really near to the maximum range. The PID gains are the same of the previous simulation because the IXV range and the maximum range aren't so different.

The initial point is the following:

	Latitude [°]	Longitude [°]
Case 1	-4,9786	169,4
Case 2	-4,2816	175,1
Case 3	-5,0764	168,6
Case 4	-5,0764	168,6
Case 5	-4,9786	169,4

Table 53: Initial coordinates for the fourth simulation.

The final point is always the same:

	Latitude [°]	Longitude [°]
Final Point	3,2721	-123,1265

Table 54: Final coordinates for the fourth simulation.

During the Heat Flux Peak Phase range correction are used constant gains. The constant gain in the Heat Flux Peak Phase range correction is equal to 0.05 for all the cases. The second constant gain is equal to 0.5 for all the cases, except when the phase is the current phase, in this situation the gain is equal to 1. The error Processing Parameters for the Straight Line Drag Acceleration Phase correction during the Heat Flux Peak Phase range correction is set equal to 1/10. For the all the cases is used the upper limitation described in Figure 90.

The error Processing Parameters for *S1*, *S2*, *S3* Phase correction during the Connection Phase range correction are chosen equal to 1/100 for all the case. The error Processing Parameters for *C1*, *C2*, *C3* Phase correction during the Connection Phase range correction are chosen equal to 1/10. When *C3* is the current phase, the gain for *C1* is equal to 1/15. For the case 5 the current phase has always a gain equal to 1/20.

The error Processing Parameters for *S1*, *S2*, *S3*, *S4*, *S5*, *S6* Phase correction during the Straight line Drag Acceleration Phase range correction are equal to 1/20 for all the cases.

The saturator for the range error is set equal to *inf*.

For the case 1 the results are the following:

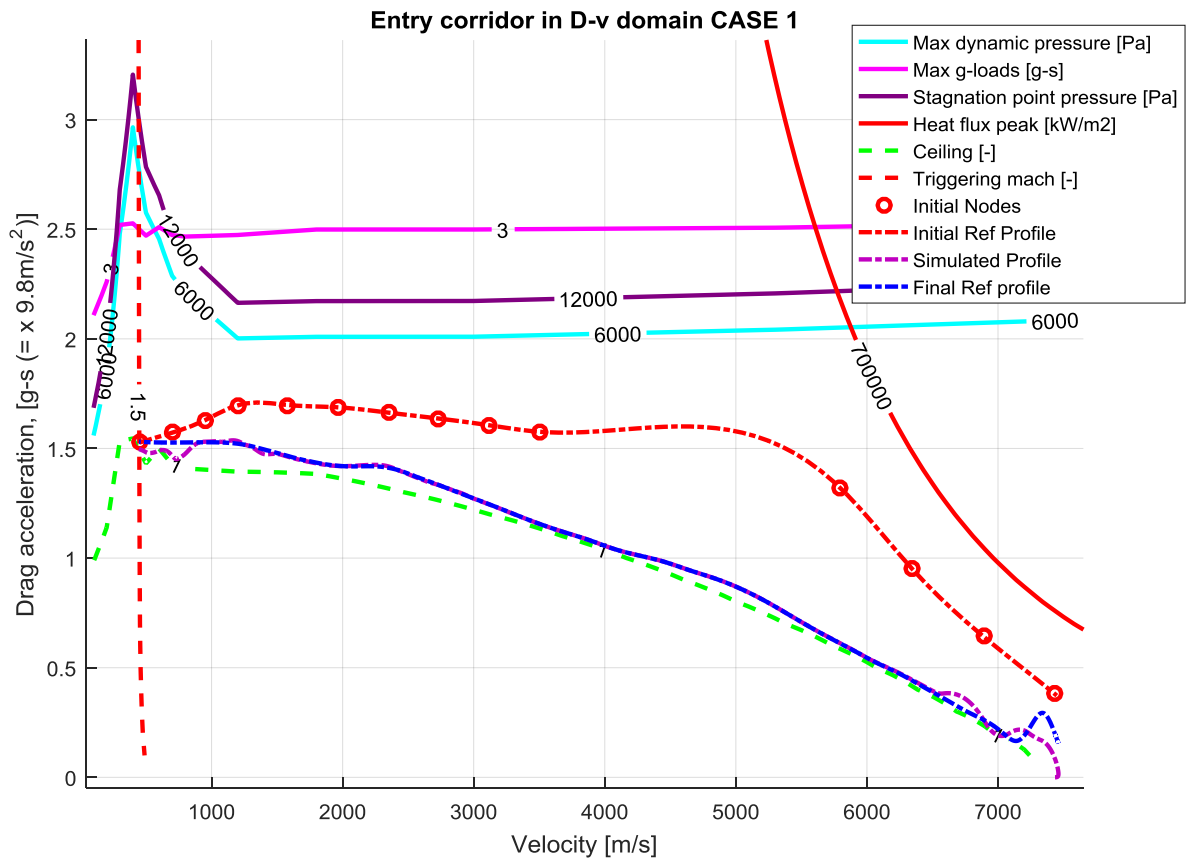


Figure 128: Simulation with range correction for the case 1 and an initial position equal to $-4,9786^\circ$ as latitude and 169° as longitude.

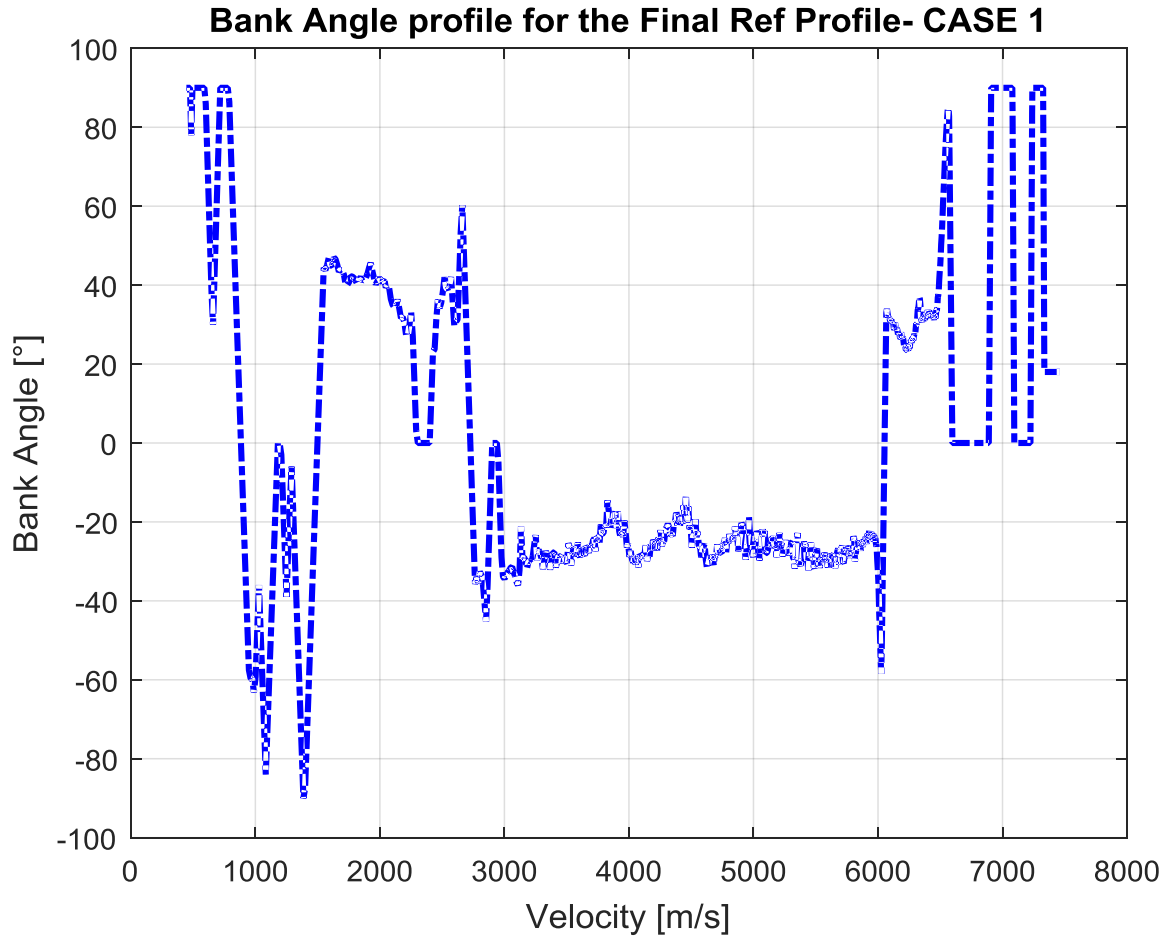


Figure 129: Bank Angle for the case 1 and an initial position equal to $-4,9786^\circ$ as latitude and 169° as longitude, following the final reference profile obtained with the range correction.

Conditions	Nominal	Actual	Guidance Error
Velocity	448.5836 m/s	448.7136 m/s	0.029%
Altitude	26 Km	26.1 Km	0.4923%
Latitude	3.2721°	3.2692°	0.0895%
Longitude	-123.1265°	-123.0724°	0.0439%
Range	7559.5 Km	7565.5 Km	6.1120 Km

Table 55: Final values and errors for the case 1 in the fourth simulation.

As we can see the oscillations in the Bank Angle profile are lesser respect to the others cases: that depends by the fact that the PID gains are optimal for the lower dynamic pressure, until a value of 4000 Pascal. All the errors respect the specifications

For the case 2 the results are the following:

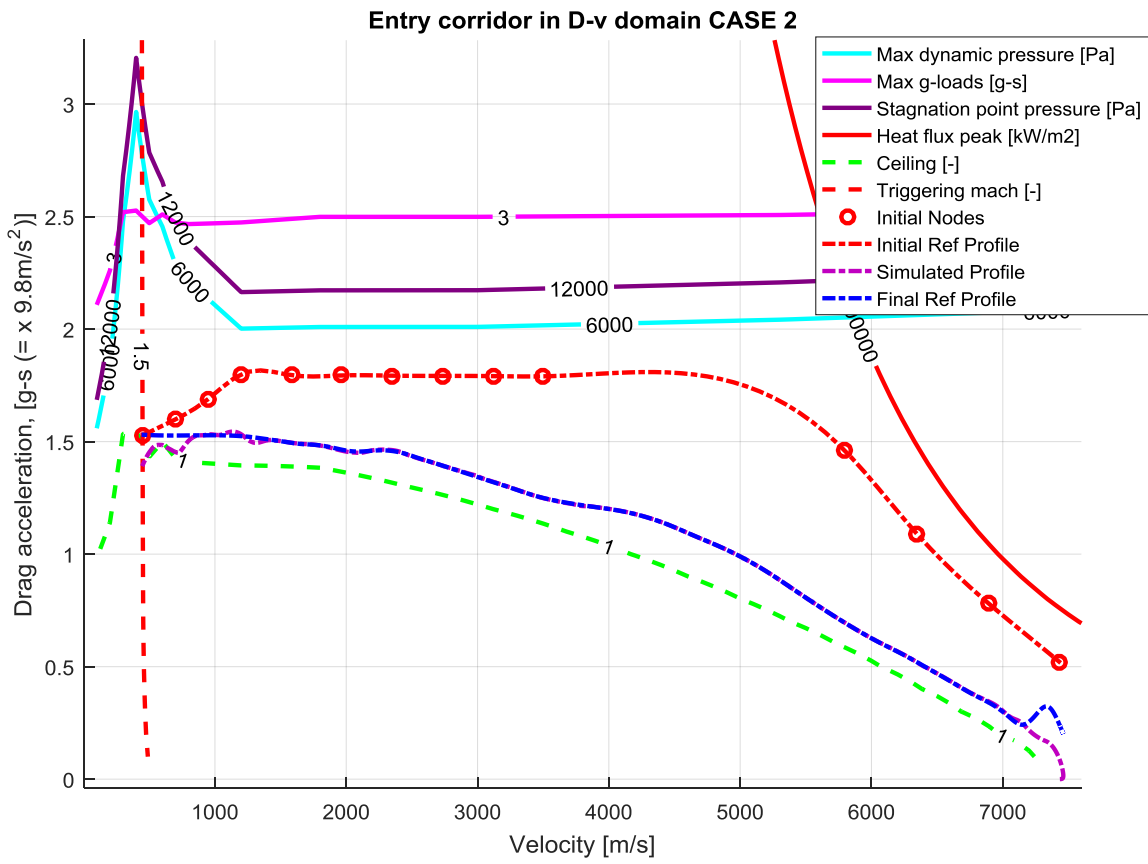


Figure 130: Simulation with range correction for the case 2 and an initial position equal to $-4,2816^\circ$ as latitude and $175,1^\circ$ as longitude.

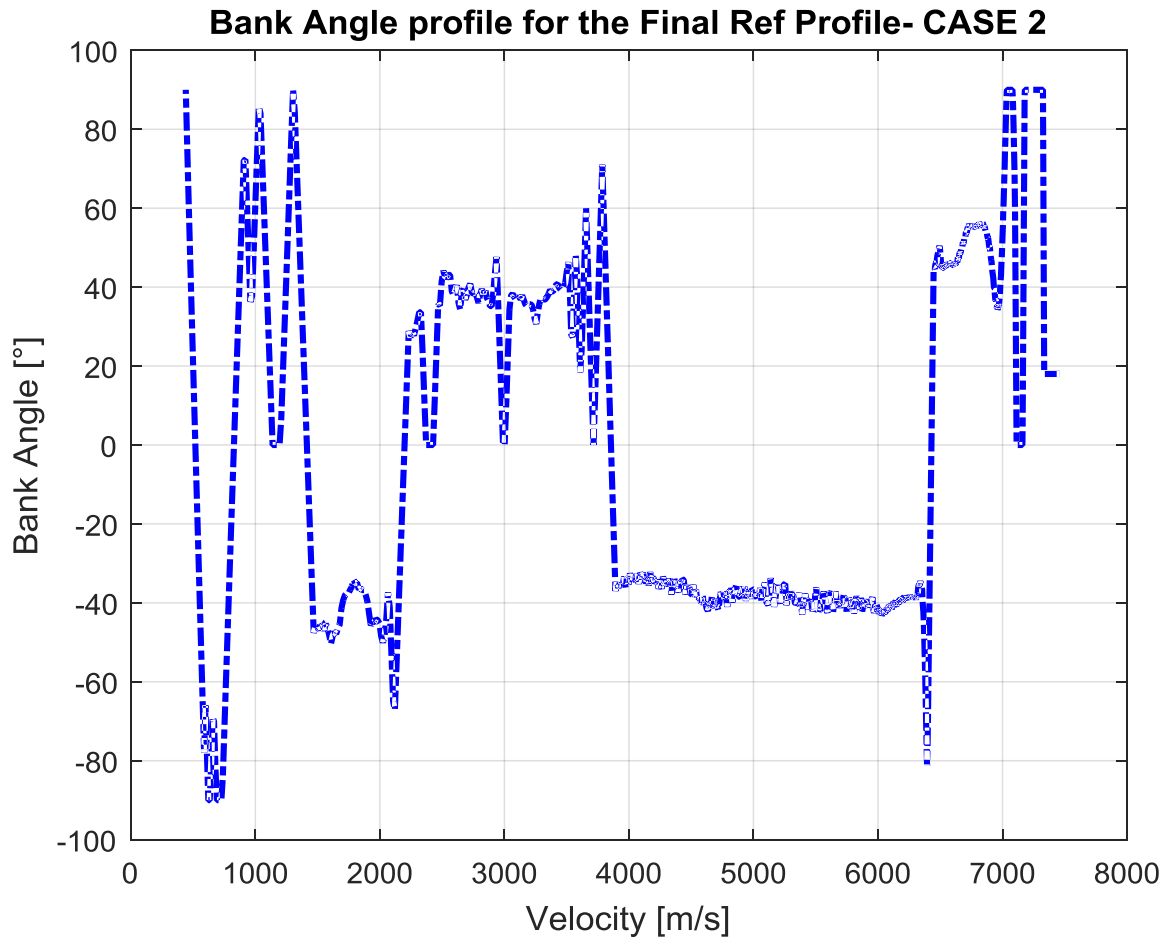


Figure 131: Bank Angle for the case 2 and an initial position equal to $-4,2816^\circ$ as latitude and $175,1^\circ$ as longitude, following the final reference profile obtained with the range correction.

Conditions	Nominal	Actual	Guidance Error
Velocity	448.5836 m/s	449.1811 m/s	0.1332%
Altitude	26 Km	26.6 Km	2.2792%
Latitude	3.2721°	3.267°	0.1551%
Longitude	-123.1265°	-123.1836°	0.0464%
Range	6922.5 Km	6916.4 Km	6.0472 Km

Table 56: Final values and errors for the case 1 in the fourth simulation.

In this case the oscillations have an amplitude a bit superior, but the specifications are respected. The profile is able to reach the lower limitation without problems.

For the case 3 the results are the following:

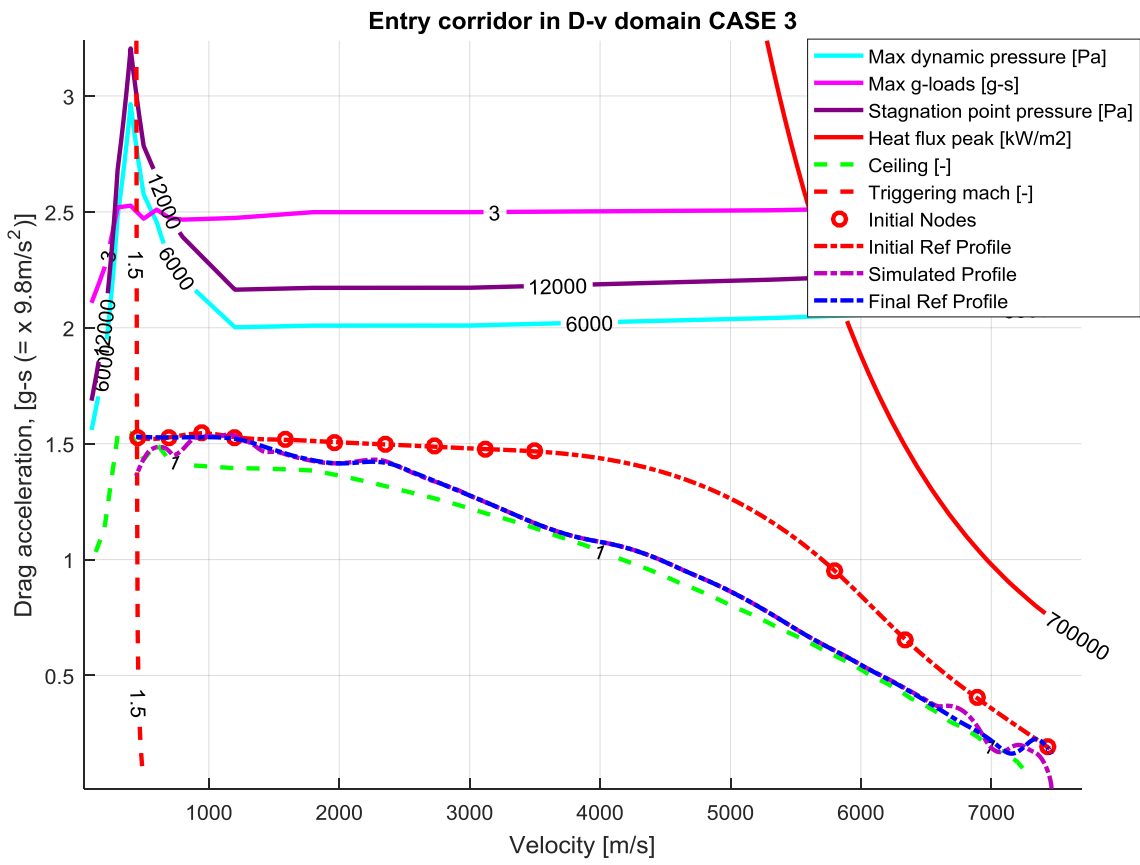


Figure 132: Simulation with range correction for the case 3 and an initial position equal to $-5,0764^\circ$ as latitude and $168,6^\circ$ as longitude.

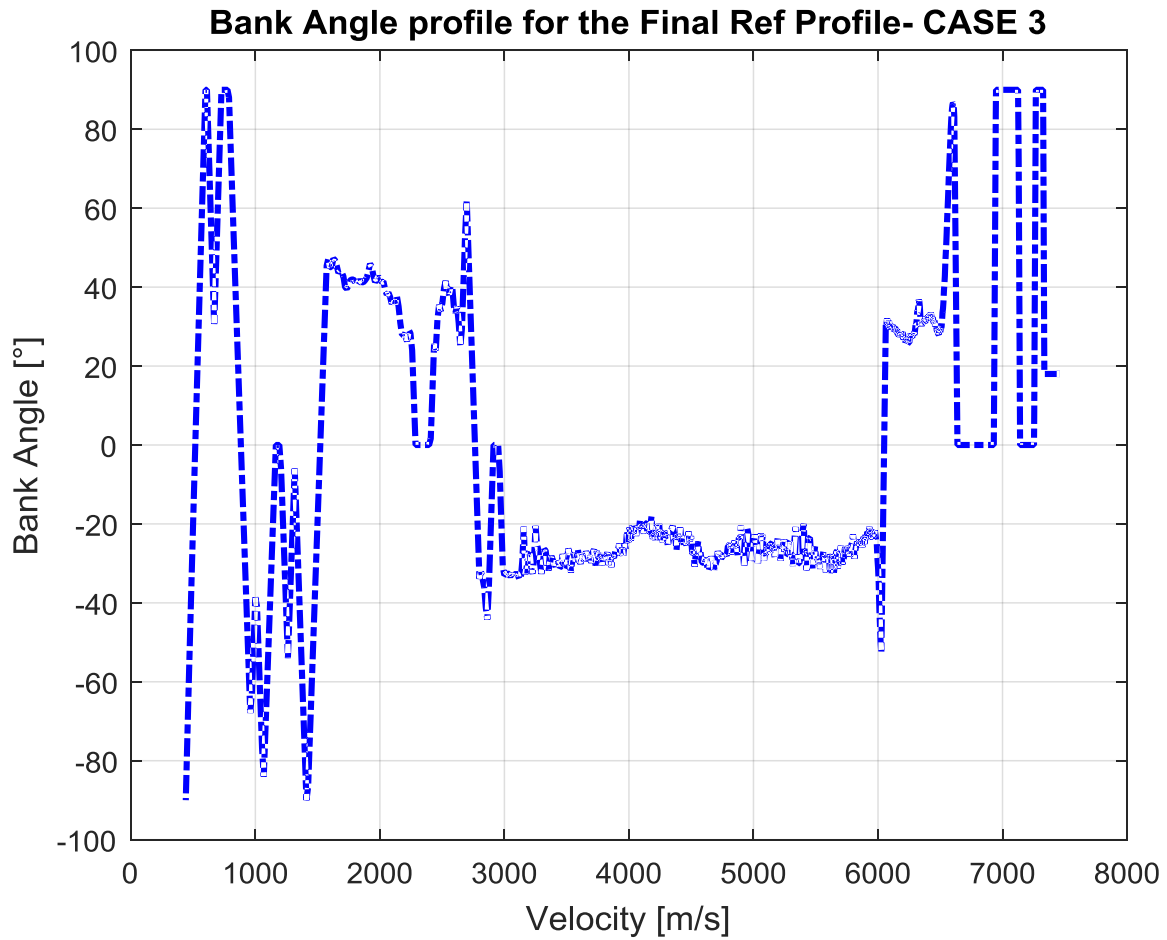


Figure 133: Bank Angle for the case 3 and an initial position equal to $-5,0764^\circ$ as latitude and $168,6^\circ$ as longitude, following the final reference profile obtained with the range correction.

Conditions	Nominal	Actual	Guidance Error
Velocity	448.5836 m/s	449.2963 m/s	0.1589%
Altitude	26 Km	26.7 Km	2.7197%
Latitude	3.2721°	3.2573°	0.4522%
Longitude	-123.1265°	-123.1703°	0.0356%
Range	7648.9 Km	7644.2 Km	5.1394 Km

Table 57: Final values and errors for the case 3 in the fourth simulation.

For the case 4 the results are the following:

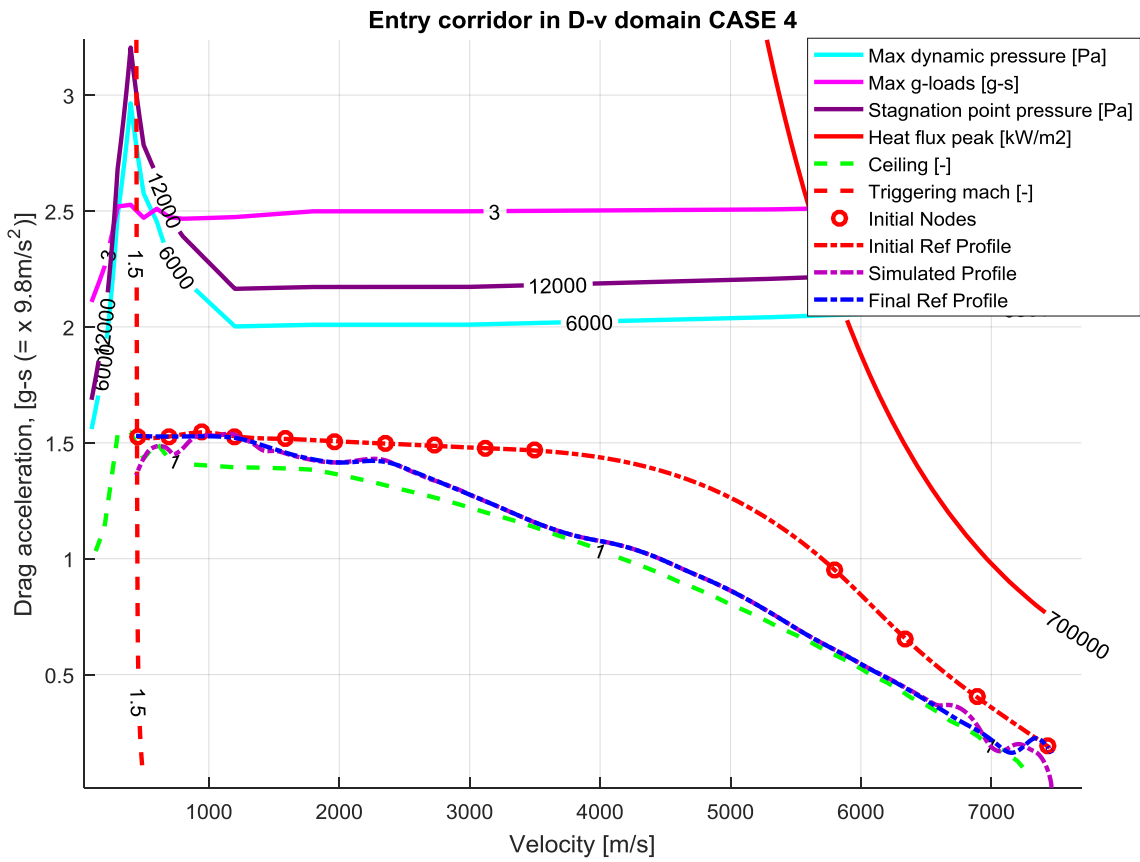


Figure 134: Simulation with range correction for the case 4 and an initial position equal to $-5,0764^\circ$ as latitude and $168,6^\circ$ as longitude.

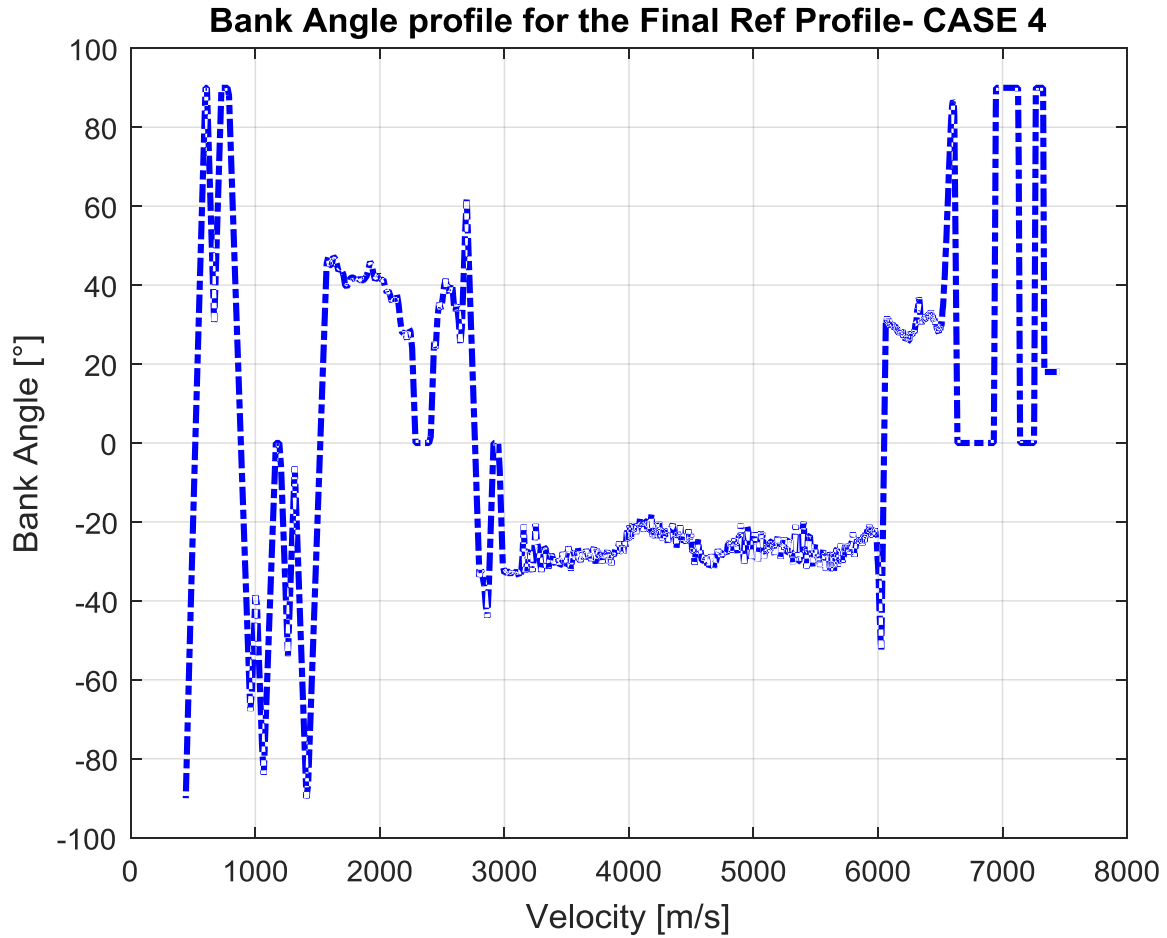


Figure 135: Bank Angle for the case 3 and an initial position equal to $-5,0764^\circ$ as latitude and $168,6^\circ$ as longitude, following the final reference profile obtained with the range correction.

Conditions	Nominal	Actual	Guidance Error
Velocity	448.5836 m/s	449.2963 m/s	0.1589%
Altitude	26 Km	26.7 Km	2.7197%
Latitude	3.2721°	3.2573°	0.4522%
Longitude	-123.1265°	-123.1703°	0.0356%
Range	7648.9 Km	7644.2 Km	5.1394 Km

Table 58: Final values and errors for the case 4 in the fourth simulation.

The case 3 and 4 give the same results, as expected, because the initial reference curve is the same. Also in this case the requirements are all respected. The final reference profile is a bit irregular but the problem can be solved changing the Error Processing Parameters.

For the case 5 the results are the following:

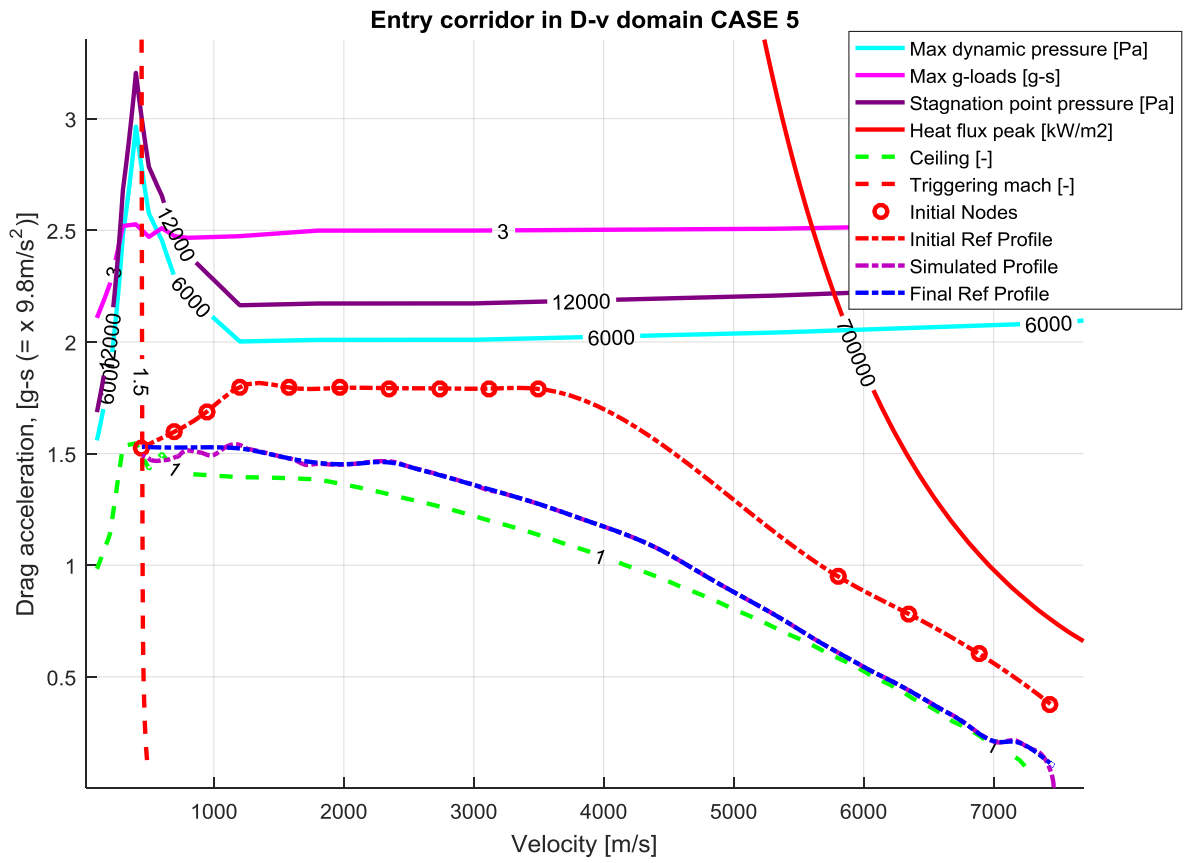


Figure 136: Simulation with range correction for the case 5 and an initial position equal to $-4,9786^\circ$ as latitude and 169° as longitude.

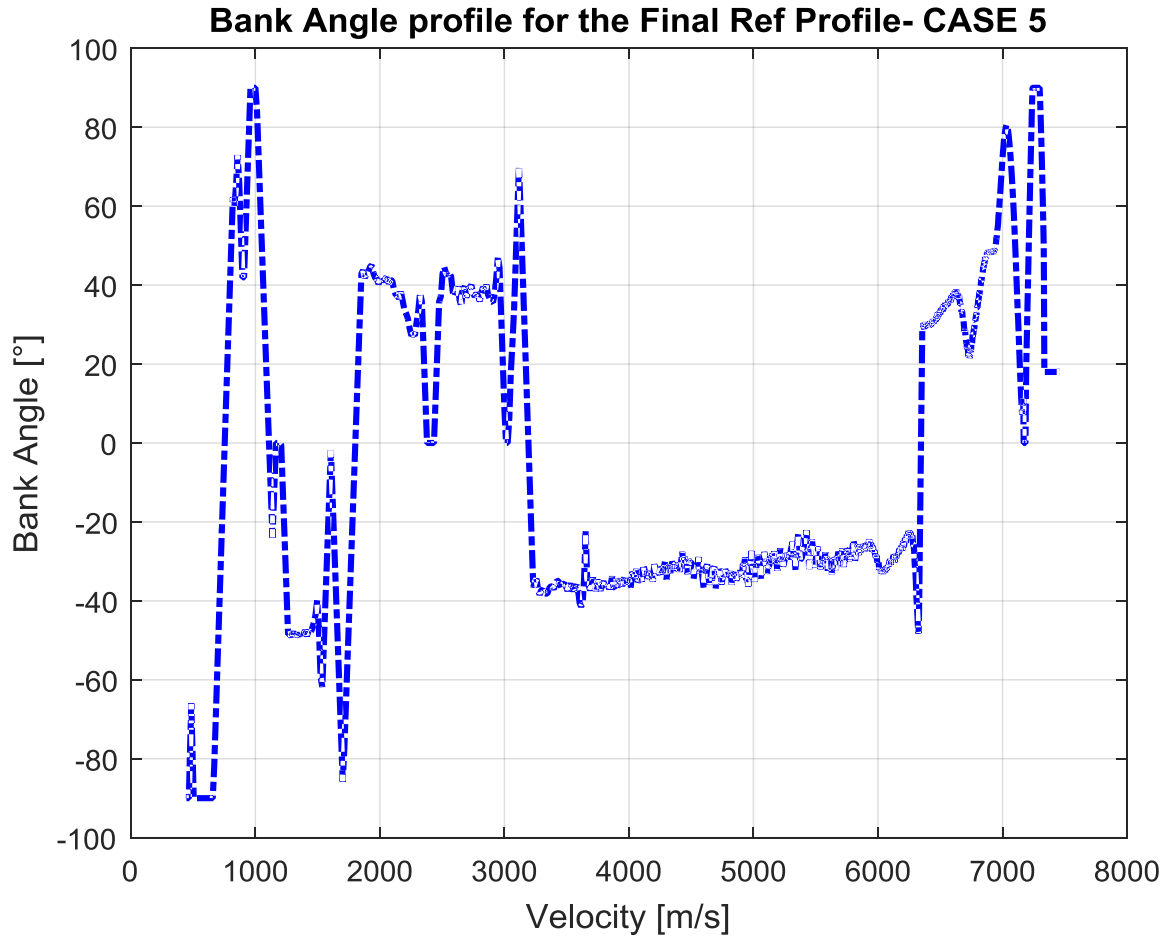


Figure 137: Bank Angle for the case 1 and an initial position equal to $-4,9786^\circ$ as latitude and 169° as longitude, following the final reference profile obtained with the range correction.

Conditions	Nominal	Actual	Guidance Error
Velocity	448.5836 m/s	448.7404 m/s	0.035%
Altitude	26 Km	26.2 Km	0.5953%
Latitude	3.2721°	3.2767°	0.1398%
Longitude	-123.1265°	-123.1177°	0.0072%
Range	7559.5 Km	7560.6 Km	1.1066 Km

Table 59: Final values and errors for the case 5 in the fourth simulation.

In this case it will be necessary to do a lot of iterations to find the correct Error Processing Parameters. The reference profile presents a good behavior, the errors respect the specifications and the Bank Angle profile has low oscillations.

6. Conclusions

As we can see, in all the simulations, choosing correctly the Error Processing Parameters and the PID gains, the final range error is less than 10 Km, the final velocity error is less than 0.2% and the final altitude error is less than 3%.

But this algorithm presents some inaccuracies that can be resolved with future improvements:

- In the final part of the trajectory the vehicle flies in ceiling. This behaviour probably is due to a low Lift to Drag Ratio. To avoid this problem a new control law for the final part can be implemented, creating also a PID variation law function of the aerodynamic. With this improvement the final altitude error can be reduced.
- The final profile isn't perfectly connected (there are discontinuities in the first, second or third derivatives). This behaviour probably is due to the fact that the range prediction formulations are approximate formulas, so the algorithm isn't able to correct perfectly the error range near the nodes, where the range of the current phase becomes really small. So the solution can be to divide the profile into fewer parts, reducing the nodes number.
- The PID gains aren't optimal for certain dynamic pressure: in fact in a lot of simulations we have to halve the PID gains values. This problem occurs because the system isn't a real linear system, so the optimal PID gains for the linear system are different respect to the optimal PID gain for the 3-Dof system. And also we must remember that the integrative gain isn't inserted in the linear system. For all these reasons can be necessary to find other states variables that better represent the system behaviour. With this procedure can be possible to write new scheduled PID gains.
- Another procedure can be finding a law function of the aerodynamic for the PID gains. The PID output is a Bank Angle, linked to the value of vertical lift. The vertical lift is linked to the control action. But if the aerodynamic coefficients are high, the lift force will have an high value, producing overcorrection. The aerodynamic coefficients can't change, so, to reduce the vertical lift force, is necessary to change the PID output. This operation can be done changing the PID gains as function of the aerodynamic.
- Another problem is identified by the profile of the bank angle obtained after the control action. This profile presents in a lot of case some oscillations that aren't physically permitted. The RCS can give these movements but the vehicle could suffers damage. These oscillations are caused by the PID gains that give an overcorrection. So the problem can be solved using a better optimized control law for the PID gains.
- These oscillations are also given by the obtained reference profile: if the reference profile has elbow connections (this happens because the reference profile is created with straight lines) the vehicle isn't able to follow them and, for this reason, the Drag Acceleration profile oscillates. If the Drag Acceleration profile oscillates that means that the Bank Angle profile presents rapid changes in values. To avoid this problem can be necessary, finished the error range correction phase, to create a contoured profile, using new nodes and Splines curves in all the phases and then translate the curve to adjust the error range. A second solution can be to represent from the beginning all the phases with a spline. The calculation and the algorithm probably will become more complex and the simulation time increases, but it will avoid the oscillations in the simulated profile and in the bank angle profile. Even without doing these two procedures this simulator can be used, but it's important to realize a post-processing on the Bank Angle profile to remove these oscillations. We must remember that, changing the error processing parameters, it's possible to find a contoured profile (Figure 97) that gives an error range less than the final reference profile found with the

range correction: the contoured profile in almost all cases has a Bank Angle profile that hasn't oscillations. This procedure is really long because there aren't any type of law to find in an unique moment all the gains. The basic idea is test the algorithm, and insert the error processing parameters to moves each phase.

- The last clarification to do is that the behavior changes every time, changing the initial point, the final point, the vehicle characteristics. But also the behavior of the system is always a function of what happens in the previous instant. So a sensitivity analysis can be necessary in every case to ameliorate the dynamic response if there will be oscillations or errors.

This simulator can be used to generate the optimal Reference Trajectory based on the re-entry corridor limitation, this trajectory varies depending on which limit you want to give more importance. Then the trajectory is modified trying to change the form of curve as little as possible, this modification is used to correct the final error range, that must be less than 10 Km. This operation is inserted in the vehicle dynamic loop, obtained a trajectory that the vehicle can follow with a low integral error. Near this control algorithm is inserted a guidance algorithm. The guidance algorithm is based on the PID controller that has the task to follow the trajectory to the vehicles, obtained a stable and damped dynamic.

The algorithm also gives as output the shallow trajectory, following the ceiling curve, and the steep trajectory, following the upper limitation. These two trajectory give the maximum and minimum range passable by the vehicle.

All these operations must be done without violating the re-entry corridor limits.

Bibliography

1. Aldo Bordano, Gerald LeBau, Lee Bryant, Michael Tigges, Charles Cambell, Thomas Horvath. *Aerodynamics and Flight Dynamics*. Engineering Innovations
2. Ashish Tewari. *Atmospheric and Space Flight Dynamic.*, Department of Aerospace Engineering, Indian Institute of Technology, Kanpur, India. 2007 Birkhauser, Boston
3. Axel J. Roenneke, Albert Markl. *Re-entry Control to a Drag-vs-Energy Profile*. University of Stuttgart, 70176 Stuttgart, Germany. Journal of Guidance, Control and Dynamics, Vol. 17, No. 5, September-October 1994
4. Axel J. Roenneke, Klaus H. Well. *Reentry Control of a Low-lift Maneuverable Spacecraft*. Institute of Flight Mechanics and Control, University of Stuttgart, Germany, 1992
5. Dean R. Chapman. *An Approximate Analytical Method For Studyng Entry into Planetary Atmospheres*. Ames Aureonatical Lboratory, Moffet Field, Calif. May 1958
6. Dennis J. McNabb. *Investigation of Atmospheric Reentry for the space maneuver vehicle*. Air Force Institute of Technology (USAF), Wright-Patterson AFB OH, March 2004
7. Derrick G. Tetzman. *Simulation and Optimization of Spacecraft Re-Entry Trajectory*. University of Minnesota, May 2010
8. Dr. Robert D. Braun. *Planetary Entry, Descent and Landing*. Georgia Institute of Technology, Jan 2005
9. Eleonora Botta. *A multidisciplinary tool for the combined optimization of manned atmospheric entry vehicles and their trajectory*. Politecnico di Milano, Facoltà di Ingegneria Industriale, Dipartimento di Scienze e Tecnologie Aerospaziali, 2012-2013
10. Evan Kontras. *Optimal Control of Apollo Space Capsule During Atmospheric Reentry*. Department of Mechanical And Aerospace Engineering. University of Missouri
11. Frank J. Regan, Satya M. Anandkrishnan. *Dynamics of Atmospheric Re-entry*. Naval Surface Warfare Center, Dahlgren Division, White Oak Center, Silver Spring, Maryland. AIAA Educational Series J.S. Przemieniecki/Series Editor-in-chief. Published by American Institue of Aeronautic and Astronautic, 1993
12. Greg A. Dukeman. *Profile-Following Entry Guidance using Linear Quadratic Regulator Theory*. NASA Marshall Space Flight Center, Huntsville, AL 35812. AIAA Guidance, Navigation and Control Conference and Exhibit, Monterey, California August 2002
13. <https://spaceflight.nasa.gov/shuttle/reference/shutref/events/entry/> Internet Site. Human Space Flight, National Aeronautics and Space Administration
14. Ir. E. Mooji. *Linear Quadratic Regulator design for an unpowered, winged re-entry vehicle*. TU University of Technology, Faculty of Aerospace Ingeeniring, Delf, February 1997
15. Jeng-Shing Chern, Nguyen Xuan Vinh *Optimum Reentry trajectories of a Lifting Vehicle*. University of Michigan, Ann Arbor, Michigan

16. Jon C. Harpold, Claude A. Graves. *Shuttle Entry Guidance*. Lyndon B Johnson Space Center (NASA), Huston, Texas, February 1979
17. Jon C. Harpold, Oliver Hill. *Shuttle Program. MCC level C Formulation Requirements. Entry Guidance and Entry Autopilot (Optimal TAEM Targeting)*. Mission Planning and Analysis Division. Lyndon B Johnson Space Center (NASA), Huston, Texas, April 1980
18. Jason L. Speyer, Arthur E. Bryson Jr. *A Neighboring optimum feedback control scheme based on estimated time-to-go with application to re-entry flight paths*. Office of Naval Research, National Aeronautics and Space Administrator, Division of Engineering and Applied Physics, Harvard University, Cambridge, Massachusetts June 1967
19. K. D. Mease, D. T Chen. Department of Mechanical and Aerospace Engineering, University of California, Irvine. S. Tandon, D.H. Young, S. Kim. The Boeing Company, Huntington Beach. *A three-Dimensional Predictive Entry Guidance Approach*. American Institute of Astronautic Paper 2000-3959
20. Luis André Carraca Guerreiro. *Development of a Guidance and Control Design Tool for Entry Space Vehicles with Different Lift-Over-Drag Ratio*. Universidade Técnica de Lisboa, July 2011
21. Manuela Battipede. *Guida e Controllo del Velivolo*. Politecnico di Torino, 2017/2018
22. Martins Sudars. *Numerical Flight Mechanics*. Master Course in Space Exploration and Development systems (SEEDS). Thale Alenia Space, 2016/2017
23. Michael H. Platt. *Full Lyapunov Exponent Placement in Reentry Trajectory*. Captain, USAF, Department of Air Force, Air University, Air Force Institute of Technology, Wright-Patterson Air Force Base, Ohio, December 1995
24. Nguyen X. Vinh, Adolf Busemann, Robert D. Culp. *Hypersonic and Planetary Entry Flight Mechanics*. Ann Arbor, The University of Michigan Press, 1980
25. R. Gifty Benjamin, Dr.U.P. Rajeev, Dr.V.R.Lalithambika, M.V.Dhekane. *Commanded Drag Guidance for the Entry Phase of Winged Entry Vehicles*. Vikram Sarabhai Space Center, Trivandrum 22, India
26. *Returning From Space: Re-entry*. Paper form Federal Aviation Administration
27. Rodney C. Wingrove. *A study of Guidance to Reference Trajectories for Lifting Reentry at Supercircular Velocity*. Ames Research Center, Moffett Field, Calif. December 1963